UNIVERSITY OF CALIFORNIA, MERCED

From the Cell to the Stand: Trait-Based Approaches to Understanding Forest Response to Climate Change

A dissertation submitted in partial satisfaction of the requirements for the degree of Doctor of Philosophy

In

Quantitative and Systems Biology

by

Jeffrey Daniel Lauder

Committee in Charge
Professor Stephen C. Hart, Chair
Professor Emily V. Moran, Research Advisor
Professor Roger Bales
Professor Jason Sexton

The Dissertation of Jeffrey Daniel Lauder, entitled “From the Cell to the Stand: Trait-Based Approaches to Understanding Forest Response to Climate Change,” is approved, and it is acceptable in quality and form for publication on microfilm and electronically:

Professor Roger Bales	Date
Professor Jason Sexton	Date
Professor Emily V. Moran, Advisor	Date
Professor Stephen C. Hart, Chair	Date

University of California
2020

Table of Contents

List of Tables

List of Figures

Acknowledgements

This research was only possible with funding from the National Science Foundation through the Southern Sierra Critical Zone Observatory (grant EAR-1331939) at the University of California, Merced and a National Geographic Society Early Career Grant (grant CP-062ER-17) and an NSF IOS grant (1925577). I personally thank Joe Rungee, Steve Hart, and Roger Bales for not only bringing the CZO funding to my attention, but actively assisting in funding me each in their own way. My research was also partially supported by funding from the Institute for the Study of Ecological and Evolutionary Climate Impacts (ISEECI), a Southern California Edison Fellowship at UCM, Quantitative Systems Biology (QSB) summer support, and a small CZO Science Across Virtual Institutes (SAVI) grant to get my research up and running. I'd like to acknowledge Ecologists Anonymous, a group of like-minded ecology students from the Environmental Systems and QSB graduate groups. While our group petered out in recent semesters, those bi-weekly meetings early during my grad school tenure were invaluable in preparing for quals, writing fellowship and grant applications, and in general feeling like a part of an ecology graduate student community. I'd like to personally thank Mengjun Shu, Robert Boria, Nate Fox, Danaan Deneve, Jackie Shay, Lillie Pennington, Laura Van Vranken, Daniel Toews, and Kinsey Brock for feedback, camaraderie, and for being a support system I never realized I needed. I owe a huge thanks to my entire committee of advisors. Roger Bales has always met whenever requested and shared data, contacts, and advice on how to proceed with research questions, as well as being actively involved in helping seek out career opportunities. Jay Sexton has been both a scientific and philosophical fountain of comfort; I thank him for involving me in interesting side projects, chatting about the philosophy of science and grad school, providing fuel for many discussions among grad students about "the Jay question" during an exam, and in general just being a huge rock to lean on in strange times. Steve Hart, my committee chair, has been an encouraging scientific force throughout my research. His genuine interest in my research questions has arguably spawned an entire chapter of this dissertation, and his own research in tree rings is what brought our labs together to share equipment, leading to other potential joint side projects. Finally, Emily Moran, my research advisor, has been the perfect combination of there when I'm stuck but supportive of my independent research. During times when things seemed to be going perfectly, she always asked the question that would lead down a deep but wholly relevant rabbit-hole. And when I have felt stuck at a dead-end, a 10 minute chat with Emily showed me multiple ways out. Lastly, I need to acknowledge my family. My interest in science almost entirely stems from my childhood, when we would go on extensive summer camping trips all over the West, exploring every national and state park we could get to. It was through these trips that my love of science, trees, and the Sierra was created and fostered. And Alicia, my wife, is the one who bore the brunt of my choice to live a scientist's life. From following me from Southern California to Chico and Nevada City, to living in a miner's cabin or an off-grid house in the woods, she has been nothing short of the definition of steadfast support. Grad school doesn't always afford financial or mental security, and without her support I truly don't know if I could have done this.

JEFFREY DANIEL LAUDER
PhD Candidate
School of Natural Sciences, University of California Merced
5200 North Lake Road, Merced, CA 95343
jlauder@ucmerced.edu

EDUCATION

Ph.D. Quantitative and Systems Biology Spring 2020 (Anticipated)
University of California, Merced
Thesis title: "From the Cell to the Stand: A Trait-Based Approach to Understanding Drought Tolerance and Fitness Tradeoffs in Sierra Nevada Conifers"

M.S. Environmental Science, Applied Ecology Spring 2015
California State University, Chico
Thesis title: "Forest Structure and Composition on New Britain Island, Papua New Guinea"

B.S. Environmental Science, Applied Ecology Winter 2011
California State University, Chico

POSITIONS HELD

Graduate Student Researcher Aug 2015-Present
University of California, Merced, Merced CA

Ecologist Jan 2011 – May 2015
Sierra Streams Institute, Nevada City CA

Forest Ecology Research Assistant Jun 2010 – Aug 2015
California State University, Chico, Chico CA

Wildlife Ecology Research Assistant Sep 2011 – Dec 2011
California State University, Chico, Chico CA

Ecology Intern May 2011 – Aug 2011
USGS, Western Ecological Research Center,
Yosemite Field Station, Wawona CA

GRANTS AND AWARDS

Current Research Funding

ISEECI (Inst. for Study of Ecol. And Evol. Climate Impacts) Summer Fellowship Summer 2019
$5000

Quantitative and Systems Biology Summer Fellow Summer 2019
UC Merced. *$5800*
Southern Sierra Critical Zone Obs. Graduate Fellowship Fall 2018-Spring 2019
UC Merced Southern Sierra Critical Zone Observatory.
$10636
ISEECI (Inst. for Study of Ecol. And Evol. Climate Impacts) Summer Fellowship Summer 2018
$6000
Quantitative and Systems Biology Summer Fellow Summer 2018
UC Merced. *$4000*
National Geographic Early Career Grant Summer 2017-2018
$4708
Southern California Edison Fellow Summer 2017
$12586
CZO Science Across Virtual Institutes (SAVI) Fellow Summer 2016
$2500
Quantitative and Systems Biology Summer Fellow Summer 2016
UC Merced. *$3000*

Prior Awards

Sally Casanova Pre-Doctoral Scholar 2014
California State University. *$3000*
Academic Excellence Award 2014
CSU Chico. *$1000*
Department Scholarship. Geol. And Env. Sciences Department 2014
CSU Chico. *$534*
Departmental Funding for Graduate Research 2013
Geological and Environmental Sciences Department, CSU Chico. *$400*
Terrestrial and Aquatic Sampling and Monitoring Equipment 2013
Norcross Wildlife Foundation. *$2,000*

Other Awards

Ford Foundation Pre-Doctoral Fellowship 2018
Honorable Mention

PUBLICATIONS

In preparation or revision

Lauder, J.D., Z. Malone, E. V. Moran. *In Review.* Assessing differences in lignin content between drought-killed and living pines using chemical and visual methods. *Invited manuscript in prep for Science of the Total Environment special issue on dendrochemistry.*

Lauder, J.D., C. Reynoso, M. Stephens, Y. Lommel, O. Moraes, A. Santos, T. Reyes, G. Dickman, T. Ghezzehei, J. Sexton. *In prep.* Small Beginnings: Implications of the giant sequoia (*Sequoiadendron giganteum*) seedling niche for post-fire conservation and management.

Lauder, J.D., D. J. Young, A. Latimer, E. V. Moran. *In prep.* How dry is dry? Comparison of drought metric predictive power of tree ring response.

Lauder, J.D., E. V. Moran. *In prep.* Simulating carbon allocation tradeoffs between wood hydraulic safety and tree fitness under drought.

Lauder, J.D., R. S. Senock. *In prep.* First documentation of tree species diversity and forest structure in the Lake Hargy Caldera, West New Britain, Papua New Guinea. *Biotropica.*

Peer-reviewed

Lauder, J.D. E. V. Moran, S. C. Hart. 2019. Fight or flight? Tradeoffs between drought defense and reproduction in conifers. *Tree Physiology*. tpz031. doi:10.1093/treephys/tpz031

Moran, E. V., **J. D. Lauder,** C. Musser, A. Stathos, and M. Shu. 2017. The genetics of drought tolerance in conifers. *New Phytol*. doi:10.1111/nph.14774

Lauder, J.D., O. Chafe, and J. Godfrey. 2017. Cadmium uptake and growth of three native California species grown in abandoned mine waste rock. *Ecological Rest*. 35: 210-213

Technical and Thesis

Lauder, J. D. 2015. Forest Structure and Composition on New Britain Island, Papua New Guinea. CSU, Chico Master's Thesis. CSUC

Wood, J. and **J.D. Lauder.** 2014. Ecosystem response to artificial gravel augmentation in a Western Sierra foothill Yuba River tributary. Sierra Streams Institute. Nevada City, CA.

Lauder, J.D. 2014. Patterns in Bird Communities at Woodpecker Reserve, Nevada City, CA, following mechanical forest thinning. Sierra Streams Institute. Nevada City, CA.

Lauder, J.D., 2013. Phytoremediation of Mine Waste: Feasibility Assessment. Sierra Streams Institute. Nevada City, CA.

Lauder, J.D., 2013. Physical Habitat Data Validation: Assessment of Citizen-Science Accuracy for Monitoring of Physical Habitat in Wadeable Streams. Sierra Streams Institute. Nevada City, CA.

PRESENTATIONS

Invited Lectures

Lauder, J. D. "The Role of Carbon Depletion in Conifer Physiological Resistance to Drought and Pests". Invited talk for California Forest Pest Council Meeting 2019. UC Davis. November 2019.

Lauder, J. D. "Drought, Tree Mortality, and Forest Management in a Changing World" UC Santa Barbara Ecology, Evolution, and Marine Biology Seminar. Cheadle Center for Biodiversity and Conservation. October 2019.

Lauder, J. D. "Sierra Conifers and Mega-drought: How do Trees Survive?" Invited seminar as part of Sierra Speaker Series. Sierra College. Grass Valley, CA. November 2017.

Contributed Talks

Lauder, J. D., E. V. Moran. "The Role of Carbon Depletion in Conifer Physiological Resistance to Drought" presented at Sierra Nevada Climate Change Symposium. Merced, CA. September 2019.

Lauder, J. D., D.J. Young., A. M. Latimer, E. V. Moran. "Biological Ground-truthing of Drought Metrics: Which metric predicts Sierra conifer growth?" poster presented at Southern Sierra Critical Zone Observatory Annual Meeting. Merced, CA. August 2019.

Lauder, J. D., E. V. Moran. "The Role of Carbon Depletion in Conifer Physiological Resistance to Drought" presented at North American Forest Ecology Workshop 2019. Flagstaff, AZ. June 2019.

Lauder, J. D., E. V. Moran. "How Conifers Cope with Drought: Differences in Growth and Wood Anatomy of Sierra Nevada Pines" presented at Southern Sierra Critical Zone Observatory Annual Meeting. Berkeley, CA. August 2018.

Lauder, J. D., E. V. Moran. "How Conifers Cope with Drought: Differences in Growth and Wood Anatomy of Sierra Nevada Pines" presented at ESA 2018. New Orleans, LA. August 2018.

Lauder, J. D., E. V. Moran. "Variation in Xylem Anatomy between Living and Drought-killed *Pinus ponderosa* and *P. jeffreyi* in the Sierra Nevada" poster presented at New Phytologist Biology of Wood Symposium. Lake Tahoe, CA. July 2018.

Lauder, J. D. "Hydraulic Architecture of Sierra Nevada Conifers: Varying Strategies of Drought Resilience" presented at ESA 2017. Portland, OR. August 2017

Lauder, J.D. "Exploring Drought Resilience in Conifers" presented at Sequoia National Park Centennial Science Symposium. Three Rivers, CA. November 2016.

Lauder, J.D., and R. Durben. "Integrating Physical Habitat into Bioassessment: A Case Study" presented at California Aquatic Bioassessment Workgroup. Davis, CA. November 2014.

Lauder, J.D. R. S. Senock. "Variation in Tropical Forest Structure and Diversity, New Britain Island, Papua New Guinea" presented at ESA 2014. Sacramento, CA. August 2014.

Wood, J., **J.D. Lauder.** "Ecosystem response to artificial gravel augmentation in a Yuba River tributary" presented at AFS 2014. Sacramento, CA. March 2014.

Durben, R., J. Wood, and **J.D. Lauder.** "Evaluating the Effects of Spawning Bed Enhancement on Water Quality and Benthic Communities in Deer Creek, Nevada County, California" presented at the California Aquatic Bioassessment Workshop. UC Davis, Davis, CA. October 2013.

Bell, A., **J.D. Lauder**. "Bioassessment on Deer Creek: Long Term and Case-specific Variation Using an IBI and Multivariate Methods" presented at the California Bioassessment Workshop. UC Davis, Davis, CA. November 2012.

OUTREACH

UC Merced RadioBio Spring 2017-Summer 2019

Founding Member, Content Producer, and Host

Planting Science Spring/Fall 2017
Scientist Mentor

MEMBERSHIPS AND AFFILIATIONS

American Association for the Advancement of Science, Program for Excellence in Science, Nominated Member
American Geophysical Union, Member
Society for Conservation Biology, Member
Society of American Foresters, Member
Ecological Society of America, Member
Sigma Xi Research Society, Associate Member

TEACHING EXPERIENCE

Courses taught

	Semester
ESS 130/BIO 130 - Plant Biology. UC Merced. Lab Section.	Spring 2016, 2017
Upper-division undergraduate and graduate students	
BIO 141 - Evolution. UC Merced. Lac Section.	Fall 2015, 2017
Upper-division undergraduate students	
GEOS 130 - Introduction to Environmental Science CSU Chico. Discussion Section.	Fall 2013-Spring 2015
First-year undergraduate students. Sustainability track course.	

TEACHING TRAINING

CSU Chico GEOS 606 TA Preparation, Fall 2013

UCM Center for Engaged Teaching and Learning (CETL) Internship Spring 2016-Fall 2017

CETL Course: Mastering the classroom with first generation college students Spring 2016

CETL Course: Developing Teaching Strategies Spring 2016

CETL Course: Improving Teaching by Assessing Learning Spring 2016

Guest Lectures

Flora of California. UC Merced. Spring 2019
"Abiotic Controls on Plant Growth"
Upper-division undergraduate students

Environmental Systems. UC Merced. Fall 2017
"The Biosphere"
Graduate students

Plant Biology. UC Merced. Spring 2017
"Semester Review"
Upper-division undergraduate and graduate students

California Naturalists. UCM and Sierra Streams Institute. Spring 2016-2018
"Forest Ecology"
Undergraduate, graduate students, and community members

Evolution. UC Merced. Fall 2015
"Sexual selection"
Upper-division undergraduate students

OTHER RELEVANT EXPERIENCE

Trip Leader, Adventure Outings. CSU Chico Fall 2009-Winter 2011
Trained leader in field expeditions that include climbing, caving, hiking, kayaking, and rafting.

Wilderness First Responder Certified Fall 2011

Abstract of the Dissertation

From the Cell to the Stand: A Trait-Based Approach to Understanding Drought Tolerance and Fitness Tradeoffs in Sierra Nevada Conifers

by

Jeffrey Daniel Lauder

Doctor of Philosophy in Quantitative Systems Biology

University of California, Merced
2020

Professor Stephen C. Hart, Chair
Professor Emily V. Moran, Research Advisor

Climate change is expected to drive shifts in forest species distribution to track ideal climatic conditions. The relative capacity for a tree species to persist under climatic stress is dependent on life history traits, such as growth, survival, and reproduction. Trees that produce large amounts of seed may be better able to colonize newly suitable habitats, while those that survive stress at current locations may persist longer than nearby competitors. These traits each represent distinct resource sinks, however. What remains unknown is how physiological modification in response to drought influences both survival and reproductive capacity. I analyzed growth, tree ring anatomy, and reproductive capacity in *Pinus ponderosa* and *P. jeffreyi* in the Sierra Nevada mountains of California, where the unprecedented 2012-2016 drought led to large-scale forest mortality. I found that trees that died during drought unexpectedly exhibited anatomical traits thought to confer drought tolerance, such as thicker walls in water-conducting xylem cells. Under drought, trees close stomata (pores in their leaf surface involved in gas exchange) to limit water loss, but at the expense of carbon (C) uptake. This leads to a theoretical expectation of C depletion in drought-stressed trees, particularly during prolonged (i.e., multi-year) drought. While direct evidence of this "C-starvation" has not been recorded in nature, my results point to a potential mechanism of the impact of C depletion on mortality. The sampled trees also experienced a high level of bark beetle (*Dendroctonus* spp.) attack, which is typically defended against in trees via the production of C-rich resin and other chemical defenses. Drought appears to have weakened sampled trees, and excessive allocation of available resources to drought defense may have depleted reserves necessary for fending off beetle attack. To quantify potential tradeoffs between drought defense and reproduction, I developed a novel technique to measure total lignin (a C-expensive material involved in xylem cell wall thickening) in tree rings, and found that trees that died had higher lignin content than living trees. To further explore these patterns, I modeled likelihood of tree mortality as a function of tree ring width (growth), xylem anatomy, competition, and climate. I first

compared multiple commonly used drought metrics with ring widths from >800 trees from across the Sierra Nevada and found that drought metric choice influences interpretation of drought impacts. I then showed that trees that grew not only thicker-walled xylem cells, but also more variable growth rings and variable cells between years were more likely to die. Trees that grew the same amount each year, or grew rings with relatively constant xylem cell diameters and wall thicknesses, were more likely to survive drought, counter to hypothesized tradeoffs between growth and reproduction during drought. Finally, cone counts of measured trees show that ring width (growth) was the primary determinant of reproductive capacity, with trees that grew more producing more cones. These results demonstrate that tree response to drought is a function of variation in xylem anatomy and ring width, with the mechanism of mortality being associated with C depletion. Trees that are less responsive to climate and maintain fairly constant growth appear to be most likely to survive prolonged drought, and trees that grow large rings (with low variance between years) are more likely to reproduce. These results improve our understanding of whole-forest response to future climate change by demonstrating the importance of both cellular scale (xylem anatomy) and forest-scale (drought metrics and competition) variation in influencing drought-induced forest mortality.

Chapter 1:
Introduction

1.1 Background

Globally, forest ecosystems cover approximately 4 billion hectares (ha) of land. This equates to 30% of the global ice-free land area or roughly 0.6 ha for every person on the planet (Keenan et al. 2015). These forests provide ecosystems services estimated at more than $4.7 trillion annually (Krieger 2001), including climatic regulation, provisioning services such as timber and food production, aesthetic and cultural services, and water storage and flow regulation (Seidl et al. 2016). Climate change threatens these services through altered precipitation, increased temperatures, and increasing likelihood of catastrophic fire (IPCC 2014). Current climate change projections include increasing temperatures and altered precipitation patterns in already arid and semi-arid environments. Understanding how forests may respond to future change depends on better understanding of both theoretical and mechanistic responses of forest trees to climate anomalies. The California drought of 2012-2016 was more severe than any observed in the previous 1200 years (Griffin and Anchukaitis 2014) and left an estimated 130 million standing dead trees in the Sierra Nevada (USDA). This "natural experiment" provides a unique opportunity to test hypotheses regarding drivers of tree mortality in a natural setting, and better quantify the range of potential responses to projected increases in aridity.

The mechanism of eventual tree death under extreme drought stress is still mostly unknown, and two theories are still debated. As water stress increases, trees close stomata (small openings on their leaf surface that facilitate movement of water and carbon), mitigating water loss but also limiting gas exchange. This may lead to eventual carbon (C) starvation as stressed trees are no longer assimilating sufficient C (McDowell et al. 2008). However, evidence of C starvation *in situ* is lacking (Sala 2009, Sala et al. 2012), and instead most trees are presumed to die of hydraulic failure. As drought stress rises, the pressure differential along the soil-plant-atmosphere continuum may eventually cause physical failure of tree xylem (water conducting tissues in trees) via either collapse or the formation of air bubbles (emboli) that break the water column (Sperry et al. 1988, Cochard 2006). Drought-killed conifers exhibit signatures of both hydraulic failure and C depletion (Adams et al. 2017), pointing to interactive effects of C limitation and xylem vulnerability to failure under drought stress. However, data on the mechanism of drought-induced mortality in conifers is primarily limited to arid southwestern US forest species. Further, no studies to date have directly tested how traits influencing likelihood of mortality scale from the individual cell to the tree and the whole forest stand, impacting whole-forest health. Such a scaling of traits from individual trees to the forest scale would allow better predictions of landscape-level change with increasing climate variability.

Trees are especially susceptible to the effects of climate due to their long life span and lack of mobility. Tree response to climatic stress may be tempered or exacerbated by both competition and individual physiology (D'Amato et al. 2013, Fernández-de-Uña et al. 2015). There is a long history of studies examining general climate response of forests (Allen and Breshears 1998, Dale et al. 2001, Millar et al. 2007, D'Amato et al. 2013, Clark et al. 2016), but we still do not fully understand how populations and species vary in their

drought-specific traits and how these traits scale from the individual to the forest stand (Clark et al. 2016). While interest in forest-scale responses to climate change merits studies at the stand level, species-level variation in traits are the primary drivers of those responses (Clark et al. 2011), and more scalable individual-based studies are needed (Clark et al. 2012). Analysis of functional traits has shown that models incorporating estimates of C assimilation and resource use may be more successful in explaining mortality than growth and related traits alone (Garcia-Forner et al. 2016). Using climate change as a natural experiment can allow us to test for the presence of a drought-resistant phenotype, or multiple phenotypes, using these trait-based approaches.

1.2 Objectives of this study

The mass-mortality events observed in the Sierra Nevada are primarily drought-induced but the likely cause of tree death may be bark beetle (*Dendroctonus* spp.) infestation (Hicke et al. 2016). Additionally, stand density in the Sierra is at a historic high (McIntyre et al. 2015), exacerbating climate and pest stress. My work seeks to understand how trees cope with mixed high-severity stressors such as drought, pest infestation, and increased crowding, and what strategies confer the highest degree of stress resilience. In this dissertation I: develop a new hypothesis of C allocation tradeoffs in drought-stressed trees; develop and test a new method for quantifying C allocation tradeoffs; assess the validity of current drought metrics for predicting growth responses of Sierra Nevada conifers; and model likelihood of tree mortality based on growth, hydraulic traits, competition, and climate.

In Chapter 2, I present a conceptual model of the C allocation tradeoffs associated with drought defense, pest defense, and reproduction during drought. Understanding how trees grow and reproduce is a key component of models of forest response to climate change. Tree response to climate stress is primarily a function of C budget (McDowell et al. 2008) and xylem hydraulic capacity (Sala 2009) as outlined above. Trees take in C through stomata, whose aperture is chemically controlled relative to the water and C status of the whole plant (Mansfield 1976). When water is unavailable, trees either slow stomatal gas exchange, slowing C uptake and potentially starving (Adams et al. 2013), or experience hydraulic failure, depending on tree ring anatomy (Sevanto et al. 2014). Reproduction may exacerbate drought-induced C limitation, as seeds and pollen also require C to be produced (Sánchez-Humanes et al. 2011). Stem growth itself also represents a tradeoff between hydraulic conductivity, drought or pest defense, and competitive dominance. This is because radial growth is a function of xylem anatomy, which directly influences drought and pest resistance. Because adults are non-mobile, tree populations can only "migrate" to track their ideal climate through successful reproduction and dispersal of seed. Thus, in stressful conditions there is a tradeoff between staying alive at current locations and producing enough seed to increase the likelihood that offspring can either find a more suitable area to germinate and grow, or successfully recruit and persist under current conditions. This relationship can potentially be described as a "fight" or "flight" response to drought. As trees change resource allocation and use under stress, they may focus primarily on growth and drought defense ("fight"), or hedge their bets on successful migration to track their climate niche by investing heavily in seed ("flight").

Chapter 3 expands on Chapter 2 by developing and testing a novel technique for quantifying the C cost of drought-resistant tree ring anatomy. Tree growth rings are made up almost entirely of xylem tracheids, the primary water-conducting cells of a plant. Wider tree rings are associated with larger or more numerous tracheids, which can move more water, but potentially at a higher risk of cavitation (via air embolism of the water column) or wall collapse (Pittermann et al. 2006). Drought stress, at both seasonal and long-term scales, is known to induce smaller tracheid diameters and thicker walls in conifers (Bryukhanova and Fonti 2012, Cuny et al. 2014, Fonti and Babushkina 2016). The "thickness to span" ratio is a ratio of xylem cell wall thickness to tracheid cell lumen diameter. Trees vary both within and between species in their threshold thickness to span ratio beyond which hydraulic failure occurs, with higher ratios being correlated with higher drought survival (Bouche et al. 2014). Thicker cell walls, however, are synthesized via deposition of lignin, a C-expensive aromatic polymer, into cell walls. Lignin costs 1.3-1.7 times the amount of C per unit volume of cellulose, the other primary component in tracheid cell formation (Amthor 2003). Quantifying total lignin content may thus provide a direct proxy of C allocation to hydraulic safety. However, current methods for measuring lignin are time-consuming, and require expensive and specialized laboratory apparatus. In Chapter 3, I present a novel technique using digital image quantification to estimate lignin concentrations in living and drought-killed conifers.

Chapter 4 asks: how do we define drought, and do current measures of drought accurately reflect tree response to water deficit? Simply defined, drought is the lack of water. But decreased water availability for plants can stem from decreased precipitation, increased temperature, or combinations of the two, as well as interactions of climate with stem density and rooting depth (Anderegg et al. 2013). Many of the currently widely available and used climate datasets include derived metrics of drought that attempt to combine raw climate variables into a biologically meaningful drought metric (Wang et al. 2011, Flint et al. 2013, Goulden and Bales 2014, Abatzoglou et al. 2018). While these metrics are widely used to quantify species response to drought, few of them have been directly compared to each other in terms of predictive performance of drought response. These metrics inherently vary due to differences in their underlying theory and modeling techniques, and comparisons of similar metrics in European trees have demonstrated significant differences in their predictive power of tree growth response (Bhuyan et al. 2017). In chapter 4, I use tree ring data—which provides a living, spatially explicit record of tree growth in response to climate—to test which of five widely used drought metrics best tracks tree growth in the Sierra Nevada. This chapter originally was conceived of as a simple methodological question to choose the preferred drought metric for inclusion in final models of tree mortality, but quickly spawned a discussion of the strengths and limitations of drought metrics that are often applied without in-depth consideration of their applicability.

Finally, Chapter 5 combines all of the concepts and techniques in the other chapters to ask: what cellular traits confer tree drought resilience, and how do these traits interact with each other across species and locations to influence likelihood of mortality during extreme drought? This chapter combines modeling techniques and drought metrics explored in Chapter 4 with the concepts and mechanisms outlined in Chapter 2 and 3. I

model mortality likelihood in Sierra Nevada conifers as a function of xylem anatomy, growth, growth variability, competition, drought, and estimates of C costs of each trait. I then use cone counts from target trees to assess the validity of the "fight or flight" hypothesis outlined in Chapter 2, and discuss how cellular traits can be scaled to the entire forest stand to better understand forest dynamics under projected climate change. I found that the most significant predictors of mortality during extreme drought were growth plasticity, xylem anatomy, and variation in xylem anatomy. Specifically, a high degree of interannual variation in growth and xylem anatomy were associated with higher likelihood of mortality. Unexpectedly, xylem anatomy thought to confer drought tolerance was also associated with mortality. These novel results demonstrate that growth alone does not predict mortality under severe drought, and that instead xylem anatomy and variation in growth and anatomy should be considered in current models of forest response to climate change.

1.3 References

Abatzoglou, J. T., S. Z. Dobrowski, S. A. Parks, and K. C. Hegewisch. 2018. TerraClimate, a high-resolution global dataset of monthly climate and climatic water balance from 1958–2015. Scientific Data 5:170191.

Adams, H. D., M. J. Germino, D. D. Breshears, G. A. Barron-Gafford, M. Guardiola-Claramonte, C. B. Zou, and T. E. Huxman. 2013. Nonstructural leaf carbohydrate dynamics of *Pinus edulis* during drought-induced tree mortality reveal role for carbon metabolism in mortality mechanism. New Phytologist 197:1142–1151.

Adams, H. D., M. J. B. Zeppel, W. R. L. Anderegg, H. Hartmann, S. M. Landhäusser, D. T. Tissue, T. E. Huxman, P. J. Hudson, T. E. Franz, C. D. Allen, L. D. L. Anderegg, G. A. Barron-Gafford, D. J. Beerling, D. D. Breshears, T. J. Brodribb, H. Bugmann, R. C. Cobb, A. D. Collins, L. T. Dickman, H. Duan, B. E. Ewers, L. Galiano, D. A. Galvez, N. Garcia-Forner, M. L. Gaylord, M. J. Germino, A. Gessler, U. G. Hacke, R. Hakamada, A. Hector, M. W. Jenkins, J. M. Kane, T. E. Kolb, D. J. Law, J. D. Lewis, J.-M. Limousin, D. M. Love, A. K. Macalady, J. Martínez-Vilalta, M. Mencuccini, P. J. Mitchell, J. D. Muss, M. J. O'Brien, A. P. O'Grady, R. E. Pangle, E. A. Pinkard, F. I. Piper, J. A. Plaut, W. T. Pockman, J. Quirk, K. Reinhardt, F. Ripullone, M. G. Ryan, A. Sala, S. Sevanto, J. S. Sperry, R. Vargas, M. Vennetier, D. A. Way, C. Xu, E. A. Yepez, and N. G. McDowell. 2017. A multi-species synthesis of physiological mechanisms in drought-induced tree mortality. Nature Ecology & Evolution 1:1285.

Allen, C. D., and D. D. Breshears. 1998. Drought-induced shift of a forest–woodland ecotone: Rapid landscape response to climate variation. Proceedings of the National Academy of Sciences 95:14839–14842.

Amthor, J. S. 2003. Efficiency of lignin biosynthesis: a quantitative analysis. Annals of Botany 91:673–695.

Anderegg, L. D. L., W. R. L. Anderegg, and J. A. Berry. 2013. Not all droughts are created equal: translating meteorological drought into woody plant mortality. Tree Physiology 33:672–683.

Bhuyan, U., C. Zang, and A. Menzel. 2017. Different responses of multispecies tree ring growth to various drought indices across Europe. Dendrochronologia 44:1–8.

Bouche, P. S., M. Larter, J.-C. Domec, R. Burlett, P. Gasson, S. Jansen, and S. Delzon. 2014. A broad survey of hydraulic and mechanical safety in the xylem of conifers. Journal of Experimental Botany 65:4419–4431.

Bryukhanova, M., and P. Fonti. 2012. Xylem plasticity allows rapid hydraulic adjustment to annual climatic variability. Trees 27:485–496.

Clark, J. S., D. M. Bell, M. H. Hersh, M. C. Kwit, E. Moran, C. Salk, A. Stine, D. Valle, and K. Zhu. 2011. Individual-scale variation, species-scale differences: inference needed to understand diversity. Ecology Letters 14:1273–1287.

Clark, J. S., D. M. Bell, M. Kwit, A. Stine, B. Vierra, and K. Zhu. 2012. Individual-scale inference to anticipate climate-change vulnerability of biodiversity. Philosophical Transactions of the Royal Society of London B: Biological Sciences 367:236–246.

Clark, J. S., L. Iverson, C. W. Woodall, C. D. Allen, D. M. Bell, D. C. Bragg, A. W. D'Amato, F. W. Davis, M. H. Hersh, I. Ibanez, S. T. Jackson, S. Matthews, N. Pederson, M. Peters, M. W. Schwartz, K. M. Waring, and N. E. Zimmermann. 2016. The impacts of increasing drought on forest dynamics, structure, and biodiversity in the United States. Global Change Biology 22:2329–2352.

Cochard, H. 2006. Cavitation in trees. Comptes Rendus Physique 7:1018–1026.

Cuny, H. E., C. B. K. Rathgeber, D. Frank, P. Fonti, and M. Fournier. 2014. Kinetics of tracheid development explain conifer tree-ring structure. New Phytologist 203:1231–1241.

Dale, V. H., L. A. Joyce, S. McNulty, R. P. Neilson, M. P. Ayres, M. D. Flannigan, P. J. Hanson, L. C. Irland, A. E. Lugo, C. J. Peterson, D. Simberloff, F. J. Swanson, B. J. Stocks, and B. M. Wotton. 2001. Climate Change and Forest Disturbances Climate change can affect forests by altering the frequency, intensity, duration, and timing of fire, drought, introduced species, insect and pathogen outbreaks, hurricanes, windstorms, ice storms, or landslides. BioScience 51:723–734.

D'Amato, A. W., J. B. Bradford, S. Fraver, and B. J. Palik. 2013. Effects of thinning on drought vulnerability and climate response in north temperate forest ecosystems. Ecological Applications 23:1735–1742.

Fernández-de-Uña, L., I. Cañellas, and G. Gea-Izquierdo. 2015. Stand Competition Determines How Different Tree Species Will Cope with a Warming Climate. PLoS ONE 10.

Flint, L. E., A. L. Flint, J. H. Thorne, and R. Boynton. 2013. Fine-scale hydrologic modeling for regional landscape applications: the California Basin Characterization Model development and performance. Ecological Processes 2:1–21.

Fonti, P., and E. A. Babushkina. 2016. Tracheid anatomical responses to climate in a forest-steppe in Southern Siberia. Dendrochronologia 39:32–41.

Garcia-Forner, N., A. Sala, C. Biel, R. Savé, and J. Martínez-Vilalta. 2016. Individual traits as determinants of time to death under extreme drought in *Pinus sylvestris* L. Tree Physiology 36:1196–1209.

Goulden, M. L., and R. C. Bales. 2014. Mountain runoff vulnerability to increased evapotranspiration with vegetation expansion. Proceedings of the National Academy of Sciences 111:14071–14075.

Griffin, D., and K. J. Anchukaitis. 2014. How unusual is the 2012–2014 California drought? Geophysical Research Letters 41:2014GL062433.

Hicke, J. A., A. J. H. Meddens, and C. A. Kolden. 2016. Recent Tree Mortality in the Western United States from Bark Beetles and Forest Fires. Forest Science 62:141–153.

IPCC. 2014. Climate Change 2014: Impacts,Adaptation, and Vulnerability. Part A: Global and Sectoral Aspects. Contribution of Working Group II to the Fifth Assessment Report of the Intergovernmental Panel on Climate Change. Page 1132. Cambridge University Press, Cambridge, UK and New York, USA.

Keenan, R. J., G. A. Reams, F. Achard, J. V. de Freitas, A. Grainger, and E. Lindquist. 2015. Dynamics of global forest area: Results from the FAO Global Forest Resources Assessment 2015. Forest Ecology and Management 352:9–20.

Krieger, D. 2001. Economic Value of Forest Ecosystem Services: A Review. The Wilderness Society.

Mansfield, T. A. 1976. Chemical Control of Stomatal Movements. Philosophical Transactions of the Royal Society of London. Series B, Biological Sciences 273:541–550.

McDowell, N., W. T. Pockman, C. D. Allen, D. D. Breshears, N. Cobb, T. Kolb, J. Plaut, J. Sperry, A. West, D. G. Williams, and E. A. Yepez. 2008. Mechanisms of plant survival and mortality during drought: why do some plants survive while others succumb to drought? New Phytologist 178:719–739.

McIntyre, P. J., J. H. Thorne, C. R. Dolanc, A. L. Flint, L. E. Flint, M. Kelly, and D. D. Ackerly. 2015. Twentieth-century shifts in forest structure in California: Denser forests, smaller trees, and increased dominance of oaks. Proceedings of the National Academy of Sciences of the United States of America 112:1458–1463.

Millar, C. I., R. D. Westfall, and D. L. Delany. 2007. Response of high-elevation limber pine (*Pinus flexilis*) to multiyear droughts and 20th-century warming, Sierra Nevada, California, USA. Canadian Journal of Forest Research 37:2508–2520.

Pittermann, J., J. S. Sperry, J. K. Wheeler, U. G. Hacke, and E. H. Sikkema. 2006. Mechanical reinforcement of tracheids compromises the hydraulic efficiency of conifer xylem. Plant, Cell & Environment 29:1618–1628.

Sala, A. 2009. Lack of direct evidence for the carbon-starvation hypothesis to explain drought-induced mortality in trees. Proceedings of the National Academy of Sciences of the United States of America 106:E68.

Sala, A., D. R. Woodruff, and F. C. Meinzer. 2012. Carbon dynamics in trees: feast or famine? Tree Physiology 32:764–775.

Sánchez-Humanes, B., V. L. Sork, and J. M. Espelta. 2011. Trade-offs between vegetative growth and acorn production in Quercus lobata during a mast year: the relevance of crop size and hierarchical level within the canopy. Oecologia 166:101–110.

Seidl, R., T. A. Spies, D. L. Peterson, S. L. Stephens, and J. A. Hicke. 2016. REVIEW: Searching for resilience: addressing the impacts of changing disturbance regimes on forest ecosystem services. Journal of Applied Ecology 53:120–129.

Sevanto, S., N. G. Mcdowell, L. T. Dickman, R. Pangle, and W. T. Pockman. 2014. How do trees die? A test of the hydraulic failure and carbon starvation hypotheses. Plant, Cell & Environment 37:153–161.

Sperry, J. S., J. R. Donnelly, and M. T. Tyree. 1988. A method for measuring hydraulic conductivity and embolism in xylem. Plant, Cell & Environment 11:35–40.

USDA, F. S. (n.d.). Region 5 - Forest & Grassland Health Aerial Detection Survey.

Wang, T., A. Hamann, D. L. Spittlehouse, and T. Q. Murdock. 2011. ClimateWNA—High-Resolution Spatial Climate Data for Western North America. Journal of Applied Meteorology and Climatology 51:16–29.

Chapter 2:

Fight or Flight? Potential tradeoffs between drought defense and reproduction in conifers[1]

[1]This chapter is a reproduction of a published article: Lauder, J. D., E. V. Moran, and S.C. Hart. 2019. Fight or Flight? Potential tradeoffs between drought defense and reproduction in conifers. Tree Physiology 39: 1071–1085

2.0 Abstract

Plants frequently exhibit tradeoffs between reproduction and growth when resources are limited, and often change these allocation patterns in response to stress. Shorter-lived plants such as annuals tend to allocate relatively more resources toward reproduction when stressed, while longer-lived plants tend to invest more heavily in survival and stress defense. However, severe stress may affect the fitness implications of allocating relatively more resources to reproduction versus stress defense. Increased drought intensity and duration have led to widespread mortality events in coniferous forests. In this review, we ask how potential tradeoffs between reproduction and survival influence the likelihood of drought-induced mortality and species persistence. We propose that trees may exhibit what we call “fight or flight” behaviors under stress. "Fight" behaviors involve greater resource allocation toward survival (e.g., growth, drought-resistant xylem, and pest defense). "Flight" consists of higher relative allocation of resources to reproduction, potentially increasing both offspring production and mortality risk for the adult. We hypothesize that flight behaviors increase as drought stress escalates the likelihood of mortality in a given location.

2.1 Introduction

Tradeoffs between reproduction and somatic investment have long been hypothesized (Williams 1966), and evidence of such tradeoffs has frequently been observed. For instance, perennial polycarpic plants often show a negative correlation between growth and reproduction (Harper 1977). The principle of allocation (Levins 1968) suggests that the cost of one resource sink can be quantified as the direct loss in potential allocation to a different sink. Different trait combinations, given such tradeoffs, may be optimal under different environmental conditions. For example, total lifetime fitness under non-stressful conditions may be positively correlated with growth and survival that increase future reproductive success, or with current reproductive effort at the expense of growth. Lifetime fitness is often maximized via intermediate investment in both growth and current reproductive effort. As stress intensifies or is prolonged, however, intermediate strategies may be less likely to maximize fitness as the overall pool of resources that is being divided between growth and reproduction shrinks.

Tradeoffs between radial growth rate, tree hydraulic efficiency and safety are well established in woody plants (Hacke et al. 2001, Pittermann et al. 2006b, Sperry et al. 2006), and there is increasing evidence of tradeoffs between growth and reproduction under drought stress (Woodward and Silsbee 1994, Climent et al. 2008, Hacket-Pain et al. 2017, Hacket-Pain et al. 2018). However, these tradeoffs are often explored

independently. Our aim in this paper is to briefly review what is known about these tradeoffs, and to present a conceptual model that synthesizes the tradeoffs between growth and hydraulic safety, and between growth and reproduction. Such a synthesis is necessary to move beyond simply predicting drought-induced mortality, to better model what that drought-induced mortality means for long-term forest dynamics including recruitment and overstory loss.

We propose that under extreme stress, trees may face a choice between two options. They may "fight" by allocating more carbon (C) resources to survival-enhancing features such as growth or defense at the expense of reproduction. Because perennial plants grow and reproduce over many seasons, greater survival is usually likely to increase lifetime reproductive output more than higher reproduction in any one year. Thus, this is the path one would expect trees to follow under most circumstances. Alternatively, by allocating more resources to reproduction, or not aborting reproductive structures already in various stages of production, they may increase the probability that offspring will successfully germinate in favorable sites locally or in a neighboring environment, achieving "flight." However, such a strategy could increase mortality risk if the resources diverted from growth decrease stress defenses. This strategy is commonly observed in annual plants (Wada and Takeno 2010, Suzuki et al. 2013) in which it often results in early death or senescence.

We propose that perennial polycarpic plants might also exhibit a similar shift in allocation if unfavorable conditions are sustained and the probability of adult mortality passes a critical threshold, as has been occurring during increasingly intense and frequent drought globally in recent years (Allen et al. 2015, Hartmann et al. 2018). For a tree, favoring growth and survival over reproduction when under stress would usually be expected to maximize lifetime fitness, as decades of potential future reproductive success become zero if a tree dies. However, because fitness is zero if no seed is produced, and there may be a threshold level of stress that will kill most trees in a population, under these conditions reproduction at the expense of increased mortality risk may maximize lifetime fitness.

While multiple types of stressors could induce these shifts in allocation, we will focus here on drought stress because closing stomata to reduce water loss (Tardieu and Simonneau 1998) decreases CO_2 uptake (Farquhar and Sharkey 1982) and availability of C for growth or reproduction (McDowell et al. 2008). Recent work has attempted to parse mechanisms of drought-induced mortality from both a physiological and C availability perspective (McDowell et al. 2008, McDowell 2011, Kerhoulas and Kane 2012, Anderegg et al. 2012, Sala et al. 2012, Anderegg and Anderegg 2013, Sevanto and Dickman 2015, Adams et al. 2017, Birami et al. 2018). However, there has been little synthesis across studies of drought-response physiology and life history tradeoffs, and several prominent unanswered questions remain. These include: How do climate and individual life history traits influence stress avoidance strategies?; Is there an optimal strategy of resource use that allows for both survival and the highest chance of successful reproduction under stressful conditions?; and what are the implications of tradeoffs between survival and reproduction for species persistence under climate change? Answering these questions requires a more robust scaling of mechanistic drought

responses from the individual cell to the whole tree with respect to both survival and reproduction.

In this paper, we focus on coniferous trees because they exhibit complex C dynamics, with drought-killed trees demonstrating both altered C storage patterns and hydraulic failure. In contrast, angiosperms primarily exhibit only hydraulic failure, with little evidence of C depletion (Adams et al. 2017). In addition, unlike most angiosperm fruits, conifer cones can take up to three years to mature following initiation (Mooney et al. 2011, Davi et al. 2016), potentially making reproductive allocation more risky in highly variable and unpredictable environments. However, though mechanisms involved may differ, similar tradeoffs are likely to occur in angiosperm trees as well.

We first review current understanding of C allocation to growth, tradeoffs between growth and hydraulic safety, and how drought modifies these allocation patterns. Tradeoffs between growth and hydraulic safety are well studied (Xu et al. 2014, Venturas et al. 2017, Barotto et al. 2018), but often only with respect to tree growth and survival. Here we place these tradeoffs into a fitness context by reviewing the C budget implications of growth, hydraulic safety, and the interaction of the two for reproductive capacity. Next, we discuss how drought influences reproductive patterns, and evidence of tradeoffs between growth and reproduction. We then present a new conceptual framework of C allocation under stress, and discuss both evolutionary and ecological implications of tradeoffs among growth, reproduction, and defense by distinguishing "fight" and "flight" strategies in stressed trees. Finally, we discuss opportunities for research and synthesis across C budget studies, climate change experiments, and analyses of tree physiology, with the aim of creating a more integrated understanding of tree response to stress.

2.2 Growth-survival relationships, as mediated by xylem hydraulic safety and carbon cost

Growth is often used as a proxy for drought response in forest trees, with rapid or prolonged periods of depressed growth suggesting an increased likelihood of mortality (Wyckoff and Clark 2002, Das et al. 2007, Cailleret et al. 2017). However, in some trees, growth plasticity under drought (Lloret et al. 2011) or overall slow growth (Moran et al. 2017) may in fact be a drought resistance strategy. Growing less during drought and then rapidly increasing ring width afterward may serve to conserve resources when water availability declines. This growth plasticity may simply be a by-product of shifts in allocation of growth resources belowground (Brunner et al. 2015, Hasibeder et al. 2015, Phillips et al. 2016), to carbohydrate storage pools (Chapin et al. 1990, Luxmoore et al. 1995), or to non-woody tissues or osmo-regulatory components (Gower et al. 1995). This relationship between growth plasticity and drought tolerance is likely due to the complex interactions between growth and xylem anatomy during times of C depletion.

Relationships among growth, xylem anatomy, and hydraulic safety are well established (Sperry et al. 2003, Xu et al. 2014, Venturas et al. 2017, Barotto et al. 2018). Hydraulic failure – breakage of the water column within xylem – can occur when air embolism blocks water flow (Sperry et al. 1988, Cochard 2006, Barotto et al. 2018), or when water potentials within the xylem become too negative and the xylem cell implodes (Hacke et al. 2001, Pittermann et al. 2006b). Drought increases the likelihood of either of

these mechanisms of hydraulic failure by decreasing water potentials within the soil and increasing the tension applied to the water column along the soil-plant-atmosphere continuum (Hacke et al. 2000, Sperry et al. 2003).

Conifer resistance to hydraulic failure is a function of anatomy of xylem cells (tracheids) and inter-tracheid pits (Hacke et al. 2001, Sperry 2003, Pittermann et al. 2006b, Sperry et al. 2006, Anderegg et al. 2015, Barotto et al. 2018). Trees with high resistance to hydraulic failure often have thickened xylem cell walls, high wood densities, lower xylem cell diameter (D), and lower inter-tracheid pit area than those that are less resistant (Hacke et al. 2001, Pittermann et al. 2006b, 2006a, Guet et al. 2015, Barotto et al. 2018). However, increases in wall thickness (t) and wood density represent multiple tradeoffs. First, trees with a high ratio of cell wall thickness to diameter (t/D) often have low hydraulic efficiency, as small xylem cells transport less water than larger cells (Hacke et al. 2001, Pittermann et al. 2006b). Additionally, thickened xylem cell walls have a higher C cost than thinner walls, potentially leading to tradeoffs among hydraulic safety and other potential C sinks such as radial growth (Figure 2.1).

Tracheid walls are mostly composed of cellulose and hemicellulose (primary cell wall) and lignin (secondary wall). In conifers, radial growth is often positively correlated with tracheid abundance and size, with larger ring widths being associated with more numerous and thinner-walled tracheids (Xu et al. 2014, Cuny et al. 2014). Tracheid wall thickness is positively correlated with lignin concentrations (Gindl 2001). Lignin contains, on average, 30% more energy (in the form of C) than cellulose (White 2007, Novaes et al. 2010). High negative correlations have been shown between total tree biomass and lignin concentrations (Novaes et al. 2010), demonstrating that decreased radial growth is often associated with increased relative lignin (and thus increased C cost) per unit volume of wood. Lignin concentration in gymnosperms is negatively correlated with Ψ50 (the water potential at which 50% of conductivity is lost, Figure 2.2). This is likely due to tracheid wall reinforcement, but there is also mixed evidence of lignin deposition into the various components of inter-tracheid pit membranes that may alter embolism resistance (Pereira et al. 2018). While the role of lignin in reducing likelihood of cavitation must be further explored, this data demonstrates that constructing drought-resistant xylem is lignin intensive. Thus, the tradeoffs among radial growth, xylem hydraulic safety, hydraulic efficiency, and the C cost of all three of these components show that growth and "type" of growth (i.e., high or low radial growth versus hydraulic safety) are only loosely dependent, and may be independent under drought stress. For example, two trees may grow rings of equal width, but with significantly different hydraulic safety and relative C investment; radial growth and hydraulic safety do not necessarily constrain each other, but may if resources are depleted.

The C costs of growth-related structures are further exacerbated by the multiple interactive stresses often placed on trees during drought. In many coniferous forests, for example, outbreaks of wood-boring insects and other pests coincide with drought stress due to weakened pest defenses and ideal conditions for pest proliferation (Hicke et al. 2016). Both chemical and physical defenses to pests represent a significant C cost (Franceschi et al. 2005). The quantity of resin ducts, which transport C-based defensive compounds, and the ratio of resin ducts to xylem cells, are both positively correlated with survival of bark beetle attack in conifers (Kane and Kolb 2010, Ferrenberg et al. 2014).

Tree growth and resin duct properties (including duct density) are also positively correlated, suggesting that conditions conducive to growth are also conducive to increased defenses (Kane and Kolb 2010, Ferrenberg et al. 2014), likely due to high availability of resources, including C. While resin duct formation tends to decrease under drought stress (Slack et al. 2017), allocation of resources to resin ducts can rise when trees are deprived of phosphorus (Ferrenberg et al. 2015), showing that different stresses can induce different changes in resource allocation to pest defense. Thus a tradeoff exists between stress defense (both drought and pest) and other resource sink demands, such as growth or reproduction.

2.3 Mast seeding and carbon costs

Average construction costs of seed vary and are not always significantly different from leaf and stem tissue, but maximum seed construction costs are often much higher than other tissues (Poorter et al. 2006). Reproductive structures can consume 6-10% of annual net canopy photosynthesis (Gower et al. 1995). Immature conifer cones can photosynthesize, but McDowell et al. (2000) reported that cone photosynthesis in *Pseudotsuga menziesii* can only provide about 27% of the C cost of cone production. The remaining C for cone formation must come from current photosynthetic activity or via drawing on C stores. Some data suggest potential C-limitation of reproduction. For instance, CO_2 fertilization of *P. taeda* induces larger cones and earlier seed production relative to tree size than under ambient conditions (Way et al. 2010). Similarly, *P. taeda* trees exposed to elevated CO_2 produced three times as many cones and were twice as likely to be reproductively mature as trees of the same size grown in ambient conditions (LaDeau and Clark 2001).

Masting, the production of large seed crops in synchrony across a population at semi-regular intervals, is a common reproductive strategy in trees (Kelly and Sork 2002). The advantages of this strategy are twofold. First, synchronous flowering/pollen production can increase successful ovule fertilization (Mooney et al. 2011, Rapp et al. 2013, Koenig et al. 2015, Bogdziewicz et al. 2017), perhaps especially in species that rely on wind to transport their pollen rather than the more directed dispersal services of animal pollinators. Second, synchronous seed production can satiate predators, reducing the proportion of seeds that get damaged or eaten (Mooney et al. 2011, Koenig et al. 2015). However, these reproductive flushes represent a significant potential resource expenditure at particular time intervals (Hacket-Pain et al. 2015, Pearse et al. 2016). Studying trees with this reproductive pattern allows direct measurement of plant status and resource investment before, during, and after a mast (Herrera et al. 1998).

Weather may affect particular stages of reproduction in different ways (Figure 2.3, Table 2.1). For instance, in species where the source of C for reproduction has been studied, spring reproductive structures (flower or immature female/pollen cones) tend to be built with stored C, while most of the C for developing fruits or cones comes from current-year assimilation (Hoch et al. 2003). Thus, weather conditions favorable for photosynthesis (relatively moist, moderately warm) during the seed development period are likely to be associated with larger seed crops (Keyes and González 2015, Guo et al. 2016b). However, the amount, synchrony, and effectiveness of pollen dispersal, which sets the stage for fruit/cone development, is often favored by dry, warm, or dry and warm

spring conditions (Koenig et al. 2015, Pearse et al. 2016, Bogdziewicz et al. 2017, Gallego Zamorano et al. 2018). The pollen dispersal stage in turn depends on the development of flower/cone primordia and the meiosis that produces the precursors of ovules and pollen. This is often favored by warm conditions in the previous spring and summer (Smaill et al. 2011, Bogdziewicz et al. 2017, Gallego Zamorano et al. 2018), though that is not universal (Mooney et al. 2011), and may depend on whether the species is more limited by cold or drought. Finally, in at least some species, the year prior to primordia formation seems to be important for "resource priming" (Buechling et al. 2016), and the uptake of nitrogen (N) and other nutrients incorporated at this stage is often favored by moist, cool, or moist and cool conditions (Mooney et al. 2011, Smaill et al. 2011).

There are tradeoffs evident in resource allocation to different stages of reproduction. In pines, which develop cones over two to three years, the cone maturation period that will result in seed dispersal in the fall of year one overlaps with two years of cone primordia initiation and one year of pollen production and dispersal (Figure 2.3). Any resources devoted to one of these stages cannot be allocated to the others, likely resulting in masting periods that approximate a 3 year cycle (Guo et al. 2016b). Even in trees with a shorter seed development period, years of high seed production tend to be followed by years of low seed production, even if favorable weather conditions persist. This may account for patterns such as warm spring weather in the year of flowering and two years prior being positively associated with seed production, but warm spring weather one year prior being negatively associated with seed production (Keyes and González 2015, Pearse et al. 2016, Gallego Zamorano et al. 2018).

There is mixed evidence for tradeoffs among growth and reproduction during drought (Table 2.1). Tree growth is often decreased both during mast years and one year following masts (Hacket-Pain et al. 2017, Hacket-Pain et al. 2018). While positive correlations between growth and reproduction in non-masting years have been observed in *Pinus halepensis* (Santos et al. 2010, Ayari et al. 2012, Ayari and Khouja 2014), *P. pinaster* (Santos et al. 2010), *P. banksiana* (Despland and Houle 1997), and *Abies sachinelensis* (Hisamoto and Goto 2017), none of these studies explicitly assessed the growth-reproduction relationship in mast years versus non-mast years. Woodward and Silsbee (1994) found that both *A. lasiocarpa* and *Tsuga mertensiana* showed positive correlations between growth and reproduction overall, but that large cone crops (i.e., mast years) were associated with decreased radial growth. Koenig and Knops (1998) found negative correlations between vegetative growth and reproductive output over multiple years in both *Picea* and *Pinus* spp., and argue that this is direct evidence of a “switch” in C allocation between mast events. Eis et al. (1965) found that ring widths in *P. menziesii* over a 28-year period were only depressed during years of large cone crop production. Finally, a recent experimental study found that pines from which developing cones were removed grew marginally more immediately after the treatment, and also produced 70% more cones the year after, compared to control trees (Santos-del-Blanco et al. 2012). This suggests that resources may be mostly or entirely allocated to reproduction but re-allocated following cone removal.

2.4 Drought impacts on reproduction

Reproductive response of conifers to drought stress varies widely (Table 2.1). Direct evidence of drought-induced reproduction in conifers is mixed, and often difficult to directly assess (Davi et al. 2016). In part, this may be because, as mentioned above, climatic conditions can influence reproductive allocation during cone initiation, growth, and maturation differently. Consistent with the favorable impacts of dry conditions on pollination, several studies in conifers have found either negative correlations between initial male and female cone production and precipitation (Roland et al. 2014), or positive associations between water stress and initial female cone production (Greenwood 1981, Riemenschneider 1985). On the other hand, wet years are better for C assimilation, and have been found to be positively associated with the initiation of cone primordia (Mooney et al. 2011) or the development of fertilized cones (Roland et al. 2014, Keyes and González 2015, Guo et al. 2016b).

Because cone production is usually a multi-year process, a switch in C allocation toward greater relative investment in growth than reproduction during a low-resource year would likely result in abortion of currently developing cones. Cone abortion in conifers does appear to be higher in subdominant trees than dominant trees under ambient conditions (Goubitz et al. 2002). This may be the result of decreased CO_2 under light limitation (Berdanier and Clark 2016), leading to abortion of cones whose development cannot be safely supported. Thus, one potential direct indicator of altering C allocation to reproduction or growth under drought stress would be drought-induced increases in cone abortion rates, as trees shunt resources from cone production back into growth, drought defense, or pest defense.

2.5 Fight or Flight

2.5.1 Tradeoffs between growth, defenses, and reproduction

If there are tradeoffs between growth and hydraulic safety, as well as between growth and reproduction, the C depletion experienced by trees under drought stress may further exacerbate the impacts of these tradeoffs. This may lead to one strategy (i.e. allocation to hydraulic safety, allocation to rapid radial growth, allocation to storage, or allocation to reproduction) becoming dominant. If trees exhibit significant tradeoffs between xylem construction and reproductive patterns, they may be displaying variations on classic "fight or flight" behaviors (Cannon 1915). If a stressed tree invests more of an available resource into defenses (against drought, pests, or competition) at the xylem anatomy, growth, or C storage levels, then this may be considered a "fight" behavior. Fight behaviors include numerous actions currently categorized under such terms as drought avoidance, drought tolerance, and drought resilience (Heschel and Riginos 2005, Lloret et al. 2011, Moran et al. 2017). Fight behaviors may increase likelihood of survival, potentially at the expense of reproductive success in the current or next year but allowing for later reproduction. If a tree instead invests more available resources into reproduction, either through maintenance of investment in previously initiated cones or through new cone initiation, this may be considered a "flight" behavior. Such a reproductive pulse could increase the risk of tree death under low resource conditions, but may also maximize lifetime fitness if mortality risk is already high and investment in reproduction increases the probability that offspring will reach suitable sites for establishment.

No current conceptual models of C allocation partition growth apportionment into sub-categories, such as hydraulic architecture versus radial growth. While radial growth produces new xylem, the anatomy of the xylem that makes up that radial growth can vary widely from year-to-year or tree-to-tree, affecting hydraulic safety. Few models of C allocation distinguish "types" of radial growth, such as the C cost of high radial growth with low wood density (and associated low hydraulic safety) versus the cost of low radial growth with high wood density. Such partitioning is important to fully understand the fitness implications of C allocation. Low stem radial growth is often predictive of mortality (Das et al. 2007), but lack of growth cannot be deemed drought intolerance if the tree is re-partitioning available resources to other "fight" behaviors that increase survival probabilities (e.g., decreased growth as a function of increased tracheid lignification, increased defensive chemicals, or increased root growth). Tradeoffs may occur not only between reproduction and growth, but also between growth of different tissues (i.e., stem, leaf, or root), and between different components of tissue growth, such as tracheid widening versus thickening.

2.5.2 Physiological mechanisms of tradeoffs

The density of sapwood, the zone of active xylem transport in a tree stem, is negatively correlated with whole plant hydraulic conductance (*K*; Mencuccini 2003) and xylem cell enlargement (Cuny et al. 2014), and positively correlated with tracheid wall thickness (Pittermann et al. 2006b). High *K* is also associated with high photosynthetic capacity and general plant vigor (Mencuccini 2003), and leaf area often scales linearly with sapwood conductive area (Luxmoore et al. 1995, Trugman et al. 2018). Thus, we can consider tracheid diameter (which is positively correlated with *K*), wall thickness, and number—in terms of their effects on whole plant hydraulics, stem sapwood growth, and C acquisition at the leaf level—and further parse the responses of these components to drought.

Under drought, high *K* does not always increase survival. In fact, high *K* relative to hydraulic safety (i.e., low xylem wall thickness or inter-tracheid pit resistance to cavitation) may increase risk of mortality (Pittermann et al. 2006b). Drought stress will likely lead to increased investment in wall thickening in newly grown tracheids, and to decreases in *K*. Turgor-limited cell expansion provides a mechanism for this shift. Cellular radial growth is constrained by the amount of water present, which drives tracheid cell enlargement prior to wall lignification and cell death (Woodruff et al. 2004). Cell lumen diameter is highly dependent on how long turgor can be maintained; the longer the expansion phase, the larger the lumen diameters and the smaller the t/D of the cell (Anfodillo et al. 2012). If a plant is drought stressed, cell turgor tends to be reduced, leading to drought-induced decreases in new xylem cell diameters and a relative increase in wall thickness (Cuny et al. 2014). This would result in a decrease in *K*, which may signal defoliation and thus reduced photosynthetic capacity. Further, a decrease in *K* via decreased tracheid lumen diameters and increased wall thickness would result in an increase in the relative C cost per unit volume of wood produced. Thus, the relationship between *K*, photosynthetic capacity, and hydraulic safety represents a positive feedback loop; drought would induce smaller tracheids with a higher hydraulic safety and higher relative C cost, which is further exacerbated by decreased C uptake potential.

Unlike growth, which contains further allocation tradeoffs, reproduction represents only one significant tradeoff to the tree - the potential net loss of resources to reproduction from all other processes. However, as mentioned above, there may be tradeoffs in allocation between developing fertilized cones and cone primordia that results in negative correlations of current year seed production with reproduction in the year or two prior. Additionally, reproduction may reduce photosynthetic capacity, as cones take up branch area that may normally be covered in needle tissue (Luxmoore et al. 1995). However, surrounding photosynthetic tissues may compensate for decreased leaf area, at least to some degree. Carbon assimilation dynamics are increasingly being shown to be sink-controlled (Luxmoore et al. 1995, Sala et al. 2012, Hayat et al. 2017). That is, as C demand at sinks increases, photosynthesis may be up-regulated. Yet, in the context of drought, if C sink demand increases photosynthetic activity, we may expect increased water loss due to increased stomatal conductance. This would increase the likelihood of hydraulic failure or lead to stomatal closure to mitigate water loss, counter-acting any potential cone-driven increases in C assimilation via photosynthesis.

2.5.3 Conceptual model of C allocation tradeoffs

By incorporating these various components of growth—radial growth, xylem anatomy, and the tradeoffs between hydraulic safety and hydraulic capacity—into a new conceptual model of C allocation, we can examine the implications of multiple tradeoffs in the C allocation pathway for masting conifer species in drought-prone environments (Figure 2.4). Under stressful conditions, we would expect the uppermost tradeoff in the allocation hierarchy to be exacerbated, if the C cost of both growth and reproduction is too high for the stressed tree. As discussed above, we would expect conifers in most situations to exhibit “fight” responses to stress (Figure 2.4A), with increased relative investment in components of growth, including induced defenses. This will maximize their potential to survive the stress and reproduce in subsequent years, even if current year reproduction is suppressed. However, if drought is prolonged or reaches an intensity threshold beyond which survival is unlikely, flight may be more beneficial.

Two potential fight responses are possible if direct tradeoffs exist between C allocation to belowground versus aboveground growth (Figure 2.4A). The first possibility is investment primarily in root growth, which could enable trees to reduce drought stress by accessing more water. Some studies in seedlings have found increased root allocation early in drought, though roots can die as drought intensifies or lengthens (Brunner et al. 2015). There is some evidence of enhanced root non-structural carbohydrate (NSC) allocation during drought in many taxa (Hagedorn et al. 2016, Kannenberg et al. 2017, Piper et al. 2017), though other studies have found no significant change in C mobilization belowground (Kerhoulas and Kane 2012, Blessing et al. 2015), or decreased root NSC and increased stem NSC (Birami et al. 2018, Li et al. 2018). Changes in strategy from passive to active root C storage instead of growth may represent in-season switches in C allocation that serve to build up C reserves and shorten stress recovery time (Hagedorn et al. 2016).

The second possible C allocation pathway associated with a fight response would be to aboveground growth or chemical pest defenses. Aboveground C allocation can result in either increased radial growth, increased hydraulic safety, or increased chemical

defenses. Turgor-limited cell expansion would be expected to lead to decreased tracheid diameter and increased relative wall thickness. Maximizing radial growth may increase susceptibility to hydraulic failure, but will also increase competitive ability, particularly if a tree survives the drought. However, growing small rings in order to maintain hydraulic safety does not preclude a tree from maintaining a large sapwood area and post-drought competitive ability. Theoretically, if a "fighting" tree does not maximize growth increment but instead grows larger numbers of smaller tracheids, *K* per unit area of wood (and associated canopy leaf area) can be maintained with little change in hydraulic safety, but at a higher C cost than small rings or large rings with large tracheids. Such a pattern has been demonstrated in nature; *Picea crassifolia* grew larger rings when more numerous smaller tracheids were produced and smaller rings were associated with less numerous larger tracheids (Xu et al. 2014). While this study did not directly assess C or lignin content of measured rings, we would expect these larger, tracheid-dense rings to be more C-expensive than the smaller rings, demonstrating fight behavior. Finally, drought stress may induce increased production of C-rich chemical defenses against pests that attack drought-weakened trees, such as terpenoids and phenolic compounds (Turtola et al. 2003), or resin (Franceschi et al. 2005). The production of these chemicals may preclude other C-expensive processes, thus representing fight behavior.

Flight responses would be demonstrated by maintained or increased relative allocation to reproduction (Figure 2.4B). Due to the relationship between growth, tracheid diameter, and sapwood conductance (Mencuccini 2003, Pittermann et al. 2006b), if a switch in C allocation leads to decreased growth and increased reproduction, we would expect a decrease in *K* and total photosynthetic capacity in subsequent years relative to average climatic conditions, as well as decreased C availability for pest defenses. Thus, a stress-induced mast is likely only a viable strategy if risk of mortality is already high or if tree resource pools are sufficient. Another potential flight response in conifers would simply be continued development during drought years of cones that formed in prior years, but measurable decreases in survival-enhancing traits such as resin ducts or growth of xylem with high hydraulic safety.

A switch to a flight response need not require mortality after reproduction or initiation of reproductive structures—only a shift to greater relative investment in reproduction. The terminal investment hypothesis, which argues that organisms may allocate resources preferentially to reproduction immediately prior to death or senescence (Clutton-Brock 1984) may not apply directly to long-lived perennial polycarpic trees. Koenig et al. (2017) present one of the first direct assessments of terminal investment in polycarpic trees, and find little support for it in Valley Oak (*Quercus lobata*). This conclusion is based on there being no tradeoff between growth and reproduction, and no change in seed production at the stand scale prior to mortality. However, this study did not examine tradeoffs between reproduction and growth in geographically constrained populations undergoing a stress-induced mass mortality event. Instead, only 0.7% of observed trees died "apparently of natural causes" across a large geographic range, and the lack of observable tradeoffs may be a result of natural patterns of senescence versus switches in resource allocation in terminally stressed trees. Thus terminal investment may still apply in highly stressed tree populations, but evidence is limited. More likely, trees

that increase C allocation to reproduction under drought stress may be somewhat reducing allocation to survival traits, but not to the point of ensuring their own death. Differential rates of continued investment of resources into reproduction that was initiated prior to stressful conditions can be categorized as fight or flight. If a tree invests resources into cone initiation and then resource availability drops, then we would expect an increase in cone abortion rates as trees switch resource allocation toward survival as part of a fight strategy (Figure 2.5A). A lack of increased abortion would then be indicative of continued resource allocation to reproductive output (Figure 2.5B). If coupled with a decrease in investment in fight responses, this would indicate a relative shift toward flight. If cone initiation and development are triggered by a drought at the expense of growth, survival probability, or both (Figure 2.5C), this would be a flight strategy tipping toward terminal investment.

2.6 Evolutionary Implications

From an evolutionary perspective, the effect of either of these behaviors on fitness depends on climatic and competitive conditions. If a tree species experiences rapid climate change, it must "migrate" via seed dispersal into newly favorable areas or adapt to new conditions. If a tree cannot migrate or adapt, the species may experience a decrease in population size or range (Aitken et al. 2008). This may reduce the relative fitness benefit of fight responses when climatic stresses increase, as sexual reproduction generates new genetic combinations on which natural selection can act locally, while dispersal enables migration to less climatically stressful areas (Figure 2.6).

Investment in seed production does not guarantee successful recruitment of new individuals into a population, let alone a successful range expansion or shift (Case and Taper 2000, Aitken et al. 2008). Recent work has demonstrated that reproductive effort in *P. ponderosa* is expected to increase under climate change, but that the same conditions that benefit reproductive output may reduce seedling recruitment, leading to a net decrease in *P. ponderosa* range (Petrie et al. 2017). Increased reproduction does, however, increase adaptive potential in long-lived plants. Climent et al. (2008) show that early investment in reproduction may be an ideal strategy for trees that have serotinous cones, as building an early aerial seedbank can increase overall fitness in areas prone to stand-replacing fires. Reproductive investment at an earlier age than most *Pinus* species has been observed in both *P. halepensis* and *P. pinaster* (Climent et al. 2008, Santos-del-Blanco et al. 2012), which both live in fire-prone landscapes with high-severity burns, demonstrating potential selection for high reproductive output in a disturbance-prone landscape. Tree species can exhibit "adaptation lag," whereby the rate of genetic change is much slower than that of climate change (Aitken et al. 2008). Modeling studies have shown that increased adult mortality could potentially reduce this adaptation lag by allowing better-adapted seedling genotypes to regenerate more quickly in the resulting gaps (Kuparinen et al. 2010). Further, increased allocation of C and N to seeds has been shown to increase germination potential, demonstrating the simultaneous benefit of increased seed output and potential recruitment in trees investing more resources in seed (Caliskan and Makineci 2015). Thus, flight strategies may increase adaptive potential in stressful environments.

One caveat of the framework presented here is the response of a tree to stress may be affected by pre-stress growth patterns. Trees that grew vigorously when immature may be more susceptible to stress when mature, because fast growing trees may be more likely to be attacked by wood-boring insects and defoliators (Ruel and Whitham 2002). A tree can thus exhibit drought avoidance strategies in the current year and still be at risk of drought stress due to prior growth patterns. If a tree has already grown "safe" xylem (i.e. tracheids with high t/D), then decreased overall growth may actually be the best strategy. Such a strategy may then allow a tree to store more C in pools for later use. If a tree has inefficient or unsafe xylem, then rapid growth of safe xylem or root tissue may be the most beneficial strategy, depending on current leaf area. If leaf area is high, then high *K* must be maintained—potentially at the expense of hydraulic safety—in order to maintain canopy hydration (Pittermann, personal communication). Regardless, we hypothesize that as drought intensity or length increases, the fitness benefit of a reproductive flush is increased.

2.7 Implications for Future Research

The tradeoffs discussed above (reproduction-growth and growth-hydraulic safety) are not new concepts. Nor is the idea of tradeoffs between various survival-enhancing tree traits under stress (Ferrenberg et al. 2015). However, no research to date has synthesized both sets of tradeoffs into an integrative C budget model for trees under stress. The conceptual framework presented here identifies multiple targets for future research. If conifer populations do exhibit stress-induced flight behaviors, this would represent a significant shift in our understanding of the implications of drought stress on tree populations. We hypothesize that the tradeoffs inherent in wood growth in coniferous trees are exacerbated by drought in ways that can have counterintuitive effects on cellular physiology and reproductive output. We propose that "flight" strategies may increase fitness in stressful environments. To test this hypothesis, we must examine models of C allocation with the context of extreme environmental gradients. Recent and current studies continue to provide new insights into formation, concentration, and mobilization of NSC storage pools (Oberhuber et al. 2011, Aaltonen et al. 2016, Guo et al. 2016a, Birami et al. 2018, Li et al. 2018), which will greatly increase understanding of conifer C storage dynamics.

Seed production and seed quality are areas in need of continued research. Comprehensive models of seed production that incorporate data from simple field methods (Clark et al. 1999, Sánchez et al. 2011) should be employed in studies of C dynamics to scale from individual tree physiology to patterns of seed production. Additional research is needed to quantify C investment in cone and seed tissue, as well as what variation in investment to cones and seeds means for germination success. Thus, future studies of forest drought response should incorporate cone and seed collections or counts as well as adult tree physiology. The greatest opportunity for integration of multi-scale measurements of tree responses to climate change is in the joining of wood anatomy and tree ecology (Locosselli and Buckeridge 2017). Recent advances in the fields of tracheid anatomy and phenology demonstrate the temporal information that can be gathered from observing xylem production relative to climate stress in situ, including timing of xylem formation, tracheid widening, and wall thickening (Rossi et al. 2012,

Ziaco and Biondi 2016). These kinds of observational studies can be paired with reproductive surveys, ^{13}C pulse-labeling experiments (Heinrich et al. 2015), and further chemical partitioning of wood (i.e., measurement of lignin concentrations) to understand the xylem-level tradeoffs that may occur under stress. Modern instrumentation can also be leveraged to measure everything from growth dynamics to sap flow and NSC concentrations all on a single tree in an automated fashion. Steppe et al. 2015) outline an idealized study system utilizing instrument clusters to pair ecophysiological and anatomical measurement, allowing a high-resolution, real-time tracking of growth dynamics along with potential C allocation patterns. These kinds of studies could then be used to further test for evidence of fight or flight behavior by incorporating simple reproductive surveys. Finally, hierarchical modeling techniques can use the conceptual model presented here as a foundation for building trait-based predictions of whole-forest or species-level range shifts in response to climate change (Rehfeldt et al. 2015, Garcia-Forner et al. 2016, O'Brien et al. 2017).

Climate change-induced mortality in forests can be leveraged as a "natural experiment" to evaluate differences between living and stress-killed trees (Gleason et al. 2017). The widespread, drought-induced mortality of conifers in Western North America (Hicke et al. 2016, Young et al. 2017) provides an ideal system for examining drivers of differential mortality and survival at small scales. Such drivers may include variation in the cellular components of growth (e.g., variation in xylem anatomy) relative to reproductive output, as well as the degree of tradeoff between hydraulic architecture and seed production. As climate change continues to apply novel stresses to tree populations, forest ecologists and tree physiologists must develop methods to test not only current response to stress, but also how responses at multiple spatial scales affect whole-forest response. Some species and individuals may fight, and invest all available resources into survival at the risk of succumbing to long-term or permanent climatic stress. Others may exhibit flight behavior, putting resources toward seed, which may increase migration or adaptation potential. Our understanding of these responses can be enhanced by not only developing conceptual and numeric models of C allocation within a tree, but also how that allocation affects future C allocation, tradeoffs, and feedbacks among tree processes. Fine-scale mechanistic studies of tree physiology continue to use novel approaches that should now be combined into integrative models of tree response to changing climate.

2.8 Acknowledgments

This article was first developed in a Global Change Biology course taught by EVM and further refined in Advanced Topics in Ecology, taught by SCH at UCM. We would like to acknowledge the Southern Sierra Critical Zone Observatory (CZO), Sequoia National Park, and the USDA Forest Service for facilitating fieldwork that supported conception of the hypotheses presented here. We thank Melaine Aubry-Kientz, Mengjun Shu, and anonymous reviewers for helpful comments on this manuscript.

2.9 References

Aaltonen, H., A. Lindén, J. Heinonsalo, C. Biasi, and J. Pumpanen. 2016. Effects of prolonged drought stress on Scots pine seedling carbon allocation. Tree Physiology:1–10.

Adams, H. D., M. J. B. Zeppel, W. R. L. Anderegg, H. Hartmann, S. M. Landhäusser, D. T. Tissue, T. E. Huxman, P. J. Hudson, T. E. Franz, C. D. Allen, L. D. L. Anderegg, G. A. Barron-Gafford, D. J. Beerling, D. D. Breshears, T. J. Brodribb, H. Bugmann, R. C. Cobb, A. D. Collins, L. T. Dickman, H. Duan, B. E. Ewers, L. Galiano, D. A. Galvez, N. Garcia-Forner, M. L. Gaylord, M. J. Germino, A. Gessler, U. G. Hacke, R. Hakamada, A. Hector, M. W. Jenkins, J. M. Kane, T. E. Kolb, D. J. Law, J. D. Lewis, J.-M. Limousin, D. M. Love, A. K. Macalady, J. Martínez-Vilalta, M. Mencuccini, P. J. Mitchell, J. D. Muss, M. J. O'Brien, A. P. O'Grady, R. E. Pangle, E. A. Pinkard, F. I. Piper, J. A. Plaut, W. T. Pockman, J. Quirk, K. Reinhardt, F. Ripullone, M. G. Ryan, A. Sala, S. Sevanto, J. S. Sperry, R. Vargas, M. Vennetier, D. A. Way, C. Xu, E. A. Yepez, and N. G. McDowell. 2017. A multi-species synthesis of physiological mechanisms in drought-induced tree mortality. Nature Ecology & Evolution 1:1285.

Aitken, S., S. Yeaman, J. Holliday, T. Wang, and S. Curtis-McLane. 2008. Adaptation, migration or extirpation: climate change outcomes for tree populations. Evolutionary Applications 1:95–111.

Allen, C. D., D. D. Breshears, and N. G. McDowell. 2015. On underestimation of global vulnerability to tree mortality and forest die-off from hotter drought in the Anthropocene. Ecosphere 6:1–55.

Anderegg, W. R. L., and L. D. L. Anderegg. 2013. Hydraulic and carbohydrate changes in experimental drought-induced mortality of saplings in two conifer species. Tree Physiology 33:252–260.

Anderegg, W. R. L., J. A. Berry, D. D. Smith, J. S. Sperry, L. D. L. Anderegg, and C. B. Field. 2012. The roles of hydraulic and carbon stress in a widespread climate-induced forest die-off. Proceedings of the National Academy of Sciences 109:233–237.

Anderegg, W. R. L., A. Flint, C. Huang, L. Flint, J. A. Berry, F. W. Davis, J. S. Sperry, and C. B. Field. 2015. Tree mortality predicted from drought-induced vascular damage. Nature Geoscience 8:367–371.

Anfodillo, T., A. Deslauriers, R. Menardi, L. Tedoldi, G. Petit, and S. Rossi. 2012. Widening of xylem conduits in a conifer tree depends on the longer time of cell expansion downwards along the stem. Journal of Experimental Botany 63:837–845.

Ayari, A., and M. L. Khouja. 2014. Ecophysiological variables influencing Aleppo pine seed and cone production: a review. Tree Physiology 34:426–437.

Ayari, A., A. Zubizarreta-Gerendiain, M. Tome, J. Tome, S. Garchi, and B. Henchi. 2012. Stand, tree and crown variables affecting cone crop and seed yield of Aleppo pine forests in different bioclimatic regions of Tunisia. Forest Systems 21:128–140.

Barotto, A. J., S. Monteoliva, J. Gyenge, A. Martinez-Meier, and M. E. Fernandez. 2018. Functional relationships between wood structure and vulnerability to xylem cavitation in races of Eucalyptus globulus differing in wood density. Tree Physiology 38:243–251.

Berdanier, A. B., and J. S. Clark. 2016. Divergent reproductive allocation trade-offs with canopy exposure across tree species in temperate forests. Ecosphere 7:n/a-n/a.

Birami, B., M. Gattmann, A. G. Heyer, R. Grote, A. Arneth, and N. K. Ruehr. 2018. Heat Waves Alter Carbon Allocation and Increase Mortality of Aleppo Pine Under Dry Conditions. Frontiers in Forests and Global Change 1.

Blessing, C. H., R. A. Werner, R. Siegwolf, and N. Buchmann. 2015. Allocation dynamics of recently fixed carbon in beech saplings in response to increased temperatures and drought. Tree Physiology 35:585–598.

Bogdziewicz, M., J. Szymkowiak, I. Kasprzyk, Ł. Grewling, Z. Borowski, K. Borycka, W. Kantorowicz, D. Myszkowska, K. Piotrowicz, M. Ziemianin, and M. B. Pesendorfer. 2017. Masting in wind-pollinated trees: system-specific roles of weather and pollination dynamics in driving seed production. Ecology 98:2615–2625.

Brunner, I., C. Herzog, M. A. Dawes, M. Arend, and C. Sperisen. 2015. How tree roots respond to drought. Frontiers in Plant Science 6.

Buechling, A., P. H. Martin, C. D. Canham, W. D. Shepperd, and M. A. Battaglia. 2016. Climate drivers of seed production in Picea engelmannii and response to warming temperatures in the southern Rocky Mountains. Journal of Ecology 104:1051–1062.

Cailleret, M., S. Jansen, E. M. R. Robert, L. Desoto, T. Aakala, J. A. Antos, B. Beikircher, C. Bigler, H. Bugmann, M. Caccianiga, V. Čada, J. J. Camarero, P. Cherubini, H. Cochard, M. R. Coyea, K. Čufar, A. J. Das, H. Davi, S. Delzon, M. Dorman, G. Gea-Izquierdo, S. Gillner, L. J. Haavik, H. Hartmann, A.-M. Hereş, K. R. Hultine, P. Janda, J. M. Kane, V. I. Kharuk, T. Kitzberger, T. Klein, K. Kramer, F. Lens, T. Levanic, J. C. L. Calderon, F. Lloret, R. Lobo-Do-Vale, F. Lombardi, R. L. Rodríguez, H. Mäkinen, S. Mayr, I. Mészáros, J. M. Metsaranta, F. Minunno, W. Oberhuber, A. Papadopoulos, M. Peltoniemi, A. M. Petritan, B. Rohner, G. Sangüesa-Barreda, D. Sarris, J. M. Smith, A. B. Stan, F. Sterck, D. B. Stojanović, M. L. Suarez, M. Svoboda, R. Tognetti, J. M. Torres-Ruiz, V. Trotsiuk, R. Villalba, F. Vodde, A. R. Westwood, P. H. Wyckoff, N. Zafirov, and J. Martínez-Vilalta. 2017. A synthesis of radial growth patterns preceding tree mortality. Global Change Biology 23:1675–1690.

Caliskan, S., and E. Makineci. 2015. Effects of carbon and nitrogen content on seed germination of calabrian pine *(Pinus brutia*) populations. Bosque (Valdivia) 36:435–443.

Cannon, W. B. Walter B. 1915. Bodily changes in pain, hunger, fear and rage, an account of recent researches into the function of emotional excitement. New York and London, D. Appleton and Co.

Case, T. J., and M. L. Taper. 2000. Interspecific Competition, Environmental Gradients, Gene Flow, and the Coevolution of Species' Borders. The American Naturalist 155:583–605.

Chapin, F. S., E.-D. Schulze, and H. A. Mooney. 1990. The Ecology and Economics of Storage in Plants. Annual Review of Ecology and Systematics 21:423–447.

Clark, J. S., M. Silman, R. Kern, E. Macklin, and J. HilleRisLambers. 1999. Seed Dispersal near and Far: Patterns across Temperate and Tropical Forests. Ecology 80:1475–1494.

Climent, J., M. A. Prada, R. Calama, M. R. Chambel, D. S. de Ron, and R. Alía. 2008. To grow or to seed: ecotypic variation in reproductive allocation and cone production by young female Aleppo pine (*Pinus halepensis*, Pinaceae). American Journal of Botany 95:833–842.

Clutton-Brock, T. H. 1984. Reproductive Effort and Terminal Investment in Iteroparous Animals. The American Naturalist 123:212–229.

Cochard, H. 2006. Cavitation in trees. Comptes Rendus Physique 7:1018–1026.

Cuny, H. E., C. B. K. Rathgeber, D. Frank, P. Fonti, and M. Fournier. 2014. Kinetics of tracheid development explain conifer tree-ring structure. New Phytologist 203:1231–1241.

Das, A. J., J. J. Battles, N. L. Stephenson, and P. J. van Mantgem. 2007. The relationship between tree growth patterns and likelihood of mortality: a study of two tree species in the Sierra Nevada. Canadian Journal of Forest Research 37:580–597.

Davi, H., M. Cailleret, G. Restoux, A. Amm, C. Pichot, and B. Fady. 2016. Disentangling the factors driving tree reproduction. Ecosphere 7:n/a-n/a.

Despland, E., and G. Houle. 1997. Climate influences on growth and reproduction of *Pinus banksiana* (Pinaceae) at the limit of the species distribution in eastern North America. American Journal of Botany 84:928–928.

Eis, S., E. H. Garman, and L. F. Ebell. 1965. Relation between cone production and diameter increment of Douglas Fir (*Pseudotsuga menziesii* (mirb.) Franco), Grand Fir (*Abies grandis* (dougl.) Lindl.), and Western White Pine (*Pinus monticola* Dougl.). Canadian Journal of Botany 43:1553–1559.

Farquhar, G. D., and T. D. Sharkey. 1982. Stomatal conductance and photosynthesis. Annual review of plant physiology 33:317–345.

Ferrenberg, S., J. M. Kane, and J. M. Langenhan. 2015. To grow or defend? Pine seedlings grow less but induce more defences when a key resource is limited. Tree Physiology 35:107–111.

Ferrenberg, S., J. M. Kane, and J. B. Mitton. 2014. Resin duct characteristics associated with tree resistance to bark beetles across lodgepole and limber pines. Oecologia 174:1283–1292.

Franceschi, V. R., P. Krokene, E. Christiansen, and T. Krekling. 2005. Anatomical and chemical defenses of conifer bark against bark beetles and other pests. New Phytologist 167:353–376.

Gallego Zamorano, J., T. Hokkanen, and A. Lehikoinen. 2018. Climate-driven synchrony in seed production of masting deciduous and conifer tree species. Journal of Plant Ecology 11:180–188.

Garcia-Forner, N., A. Sala, C. Biel, R. Savé, and J. Martínez-Vilalta. 2016. Individual traits as determinants of time to death under extreme drought in *Pinus sylvestris* L. Tree Physiology 36:1196–1209.

Gindl, W. 2001. Cell-wall lignin content related to tracheid dimensions in drought-sensitive austrian pine (*Pinus nigra*). IAWA Journal 22:113–120.

Gleason, K. E., J. B. Bradford, A. Bottero, A. W. D'Amato, S. Fraver, B. J. Palik, M. A. Battaglia, L. Iverson, L. Kenefic, and C. C. Kern. 2017. Competition amplifies drought stress in forests across broad climatic and compositional gradients. Ecosphere 8:n/a-n/a.

Goubitz, S., M. J. A. Werger, A. Shmida, and G. Ne'eman. 2002. Cone abortion in *Pinus halepensis*: the role of pollen quantity, tree size and cone location. Oikos 97:125–133.

Gower, S. T., J. G. Isebrands, and D. W. Sheriff. 1995. 7 - Carbon Allocation and Accumulation in Conifers. Pages 217–254 *in* W. K. Smith and T. M. Hinckley, editors. Resource Physiology of Conifers. Academic Press, San Diego.

Greenwood, M. S. 1981. Reproductive development in Loblolly Pine II. The Effect of age, gibberellin plus water stress and out-of-phase dormancy on long shoot growth behavior. American Journal of Botany 68:1184–1190.

Guet, J., R. Fichot, C. Lédée, F. Laurans, H. Cochard, S. Delzon, C. Bastien, and F. Brignolas. 2015. Stem xylem resistance to cavitation is related to xylem structure but not to growth and water-use efficiency at the within-population level in Populus nigra L. Journal of Experimental Botany 66:4643–4652.

Guo, Q., J. Li, Y. Zhang, J. Zhang, D. Lu, H. Korpelainen, and C. Li. 2016a. Species-specific competition and N fertilization regulate non-structural carbohydrate contents in two Larix species. Forest Ecology and Management 364:60–69.

Guo, Q., S. J. Zarnoch, X. Chen, and D. G. Brockway. 2016b. Life cycle and masting of a recovering keystone indicator species under climate fluctuation. Ecosystem Health and Sustainability 2:e01226.

Hacke, U. G., J. S. Sperry, and J. Pittermann. 2000. Drought experience and cavitation resistance in six shrubs from the Great Basin, Utah. Basic and Applied Ecology 1:31–41.

Hacke, U. G., J. S. Sperry, W. T. Pockman, S. D. Davis, and K. A. McCulloh. 2001. Trends in wood density and structure are linked to prevention of xylem implosion by negative pressure. Oecologia 126:457–461.

Hacket-Pain, A. J., D. Ascoli, G. Vacchiano, F. Biondi, L. Cavin, M. Conedera, I. Drobyshev, I. D. Liñán, A. D. Friend, M. Grabner, C. Hartl, J. Kreyling, F. Lebourgeois, T. Levanič, A. Menzel, E. van der Maaten, M. van der Maaten-Theunissen, L. Muffler, R. Motta, C.-C. Roibu, I. Popa, T. Scharnweber, R. Weigel, M. Wilmking, and C. S. Zang. 2018. Climatically controlled reproduction drives interannual growth variability in a temperate tree species. Ecology Letters.

Hacket-Pain, A. J., A. D. Friend, J. G. A. Lageard, and P. A. Thomas. 2015. The influence of masting phenomenon on growth–climate relationships in trees: explaining the influence of previous summers' climate on ring width. Tree Physiology 35:319–330.

Hacket-Pain, A. J., J. G. A. Lageard, and P. A. Thomas. 2017. Drought and reproductive effort interact to control growth of a temperate broadleaved tree species (*Fagus sylvatica*). Tree Physiology 37:744–754.

Hagedorn, F., J. Joseph, M. Peter, J. Luster, K. Pritsch, U. Geppert, R. Kerner, V. Molinier, S. Egli, M. Schaub, J.-F. Liu, M. Li, K. Sever, M. Weiler, R. T. W. Siegwolf, A. Gessler, and M. Arend. 2016. Recovery of trees from drought depends on belowground sink control. Nature Plants 2:16111.

Harper, J. L. 1977. Population biology of plants. Blackburn Press, Caldwell, New Jersey.

Hartmann, H., C. F. Moura, W. R. L. Anderegg, N. K. Ruehr, Y. Salmon, C. D. Allen, S. K. Arndt, D. D. Breshears, H. Davi, D. Galbraith, K. X. Ruthrof, J. Wunder, H. D.

Adams, J. Bloemen, M. Cailleret, R. Cobb, A. Gessler, T. E. E. Grams, S. Jansen, M. Kautz, F. Lloret, and M. O'Brien. 2018. Research frontiers for improving our understanding of drought-induced tree and forest mortality. New Phytologist 218:15–28.

Hasibeder, R., L. Fuchslueger, A. Richter, and M. Bahn. 2015. Summer drought alters carbon allocation to roots and root respiration in mountain grassland. The New Phytologist 205:1117–1127.

Hayat, A., A. J. Hacket-Pain, H. Pretzsch, T. T. Rademacher, and A. D. Friend. 2017. Modeling Tree Growth Taking into Account Carbon Source and Sink Limitations. Frontiers in Plant Science 8.

Heinrich, S., M. A. Dippold, C. Werner, G. L. B. Wiesenberg, Y. Kuzyakov, and B. Glaser. 2015. Allocation of freshly assimilated carbon into primary and secondary metabolites after in situ 13C pulse labelling of Norway spruce (*Picea abies*). Tree Physiology 35:1176–1191.

Herrera, C. M., P. Jordano, J. Guitián, and A. Traveset. 1998. Annual variability in seed production by woody plants and the masting concept: reassessment of principles and relationship to pollination and seed dispersal. The American Naturalist 152:576–594.

Heschel, M. S., and C. Riginos. 2005. Mechanisms of selection for drought stress tolerance and avoidance in *Impatiens capensis* (Balsaminaceae). American Journal of Botany 92:37–44.

Hicke, J. A., A. J. H. Meddens, and C. A. Kolden. 2016. Recent Tree Mortality in the Western United States from Bark Beetles and Forest Fires. Forest Science 62:141–153.

Hisamoto, Y., and S. Goto. 2017. Genetic control of altitudinal variation on female reproduction in *Abies sachalinensis* revealed by a crossing experiment. Journal of Forest Research 22:195–198.

Hoch, G., A. Richter, and Ch. Körner. 2003. Non-structural carbon compounds in temperate forest trees. Plant, Cell & Environment 26:1067–1081.

Jost, L. 2008. G_{ST} and its relatives do not measure differentiation. Molecular Ecology 17:4015–4026.

Kane, J. M., and T. E. Kolb. 2010. Importance of resin ducts in reducing ponderosa pine mortality from bark beetle attack. Oecologia 164:601–609.

Kannenberg, S. A., K. A. Novick, and R. P. Phillips. 2017. Coarse roots prevent declines in whole-tree non-structural carbohydrate pools during drought in an isohydric and an anisohydric species. Tree Physiology:1–9.

Kelly, D., and V. L. Sork. 2002. Mast Seeding in Perennial Plants: Why, How, Where? Annual Review of Ecology and Systematics 33:427–447.

Kerhoulas, L. P., and J. M. Kane. 2012. Sensitivity of ring growth and carbon allocation to climatic variation vary within ponderosa pine trees. Tree Physiology 32:14–23.

Keyes, C. R., and R. M. González. 2015. Climate-influenced ponderosa pine (*Pinus ponderosa*) seed masting trends in western Montana, USA. Forest Systems 24:021.

Koenig, W. D., and J. M. H. Knops. 1998. Scale of mast-seeding and tree-ring growth. Nature 396:225–226.

Koenig, W. D., J. M. H. Knops, W. J. Carmen, and I. S. Pearse. 2015. What drives masting? The phenological synchrony hypothesis. Ecology 96:184–192.

Koenig, W. D., J. M. H. Knops, W. J. Carmen, and M. B. Pesendorfer. 2017. Testing the Terminal Investment Hypothesis in California Oaks. The American Naturalist 189:564–569.

Kuparinen, A., O. Savolainen, and F. M. Schurr. 2010. Increased mortality can promote evolutionary adaptation of forest trees to climate change. Forest Ecology and Management 259:1003–1008.

LaDeau, S., and J. S. Clark. 2001. Rising CO2 levels and the fecundity of forest trees. Science 292:95–98.

Levins, R. 1968. Evolution in Changing Environments: Some Theoretical Explorations. Princeton University Press, Princeton, New Jersey.

Li, W., H. Hartmann, H. D. Adams, H. Zhang, C. Jin, C. Zhao, D. Guan, A. Wang, F. Yuan, and J. Wu. 2018. The sweet side of global change–dynamic responses of non-structural carbohydrates to drought, elevated CO2 and nitrogen fertilization in tree species. Tree Physiology 38:1706–1723.

Lloret, F., E. G. Keeling, and A. Sala. 2011. Components of tree resilience: effects of successive low-growth episodes in old ponderosa pine forests. Oikos 120:1909–1920.

Locosselli, G. M., and M. S. Buckeridge. 2017. Dendrobiochemistry, a missing link to further understand carbon allocation during growth and decline of trees. Trees:1–14.

Luxmoore, R. J., R. Oren, D. W. Sheriff, and R. B. Thomas. 1995. Source–Sink–Storage Relationships of Conifers. Pages 179–216 Resource Physiology of Conifers: Acquisition, Allocation, and Utilization. Academic Press, San Diego.

McDowell, N. G. 2011. Mechanisms linking drought, hydraulics, carbon metabolism, and vegetation mortality. Plant Physiology 155:1051–1059.

McDowell, N., W. T. Pockman, C. D. Allen, D. D. Breshears, N. Cobb, T. Kolb, J. Plaut, J. Sperry, A. West, D. G. Williams, and E. A. Yepez. 2008. Mechanisms of plant survival and mortality during drought: why do some plants survive while others succumb to drought? New Phytologist 178:719–739.

McDowell, S. C. L., N. G. McDowell, J. D. Marshall, and K. Hultine. 2000. Carbon and nitrogen allocation to male and female reproduction in Rocky Mountain Douglas-fir (*Pseudotsuga menziesii* var. glauca, Pinaceae). American Journal of Botany 87:539–546.

Mencuccini, M. 2003. The ecological significance of long-distance water transport: short-term regulation, long-term acclimation and the hydraulic costs of stature across plant life forms. Plant, Cell & Environment 26:163–182.

Mooney, K. A., Y. B. Linhart, and M. A. Snyder. 2011. Masting in ponderosa pine: comparisons of pollen and seed over space and time. Oecologia 165:651–661.

Moran, E., J. Lauder, C. Musser, A. Stathos, and M. Shu. 2017. The genetics of drought tolerance in conifers. New Phytologist 216:1034–1048.

Novaes, E., M. Kirst, V. Chiang, H. Winter-Sederoff, and R. Sederoff. 2010. Lignin and Biomass: A Negative Correlation for Wood Formation and Lignin Content in Trees1. Plant Physiology 154:555–561.

Oberhuber, W., I. Swidrak, D. Pirkebner, and A. Gruber. 2011. Temporal dynamics of nonstructural carbohydrates and xylem growth in *Pinus sylvestris* exposed to drought. Canadian Journal of Forest Research 41:1590–1597.

O'Brien, M. J., B. M. J. Engelbrecht, J. Joswig, G. Pereyra, B. Schuldt, S. Jansen, J. Kattge, S. M. Landhäusser, S. R. Levick, Y. Preisler, P. Väänänen, and C. Macinnis-Ng. 2017. A synthesis of tree functional traits related to drought-induced mortality in forests across climatic zones. Journal of Applied Ecology:10.1111/1365-2664.12874.

Pearse, I. S., W. D. Koenig, and D. Kelly. 2016. Mechanisms of mast seeding: resources, weather, cues, and selection. New Phytologist 212:546–562.

Pereira, L., A. P. Domingues-Junior, S. Jansen, B. Choat, and P. Mazzafera. 2018. Is embolism resistance in plant xylem associated with quantity and characteristics of lignin? Trees 32:349–358.

Petrie, M. D., J. B. Bradford, R. M. Hubbard, W. K. Lauenroth, C. M. Andrews, and D. R. Schlaepfer. 2017. Climate change may restrict dryland forest regeneration in the 21st century. Ecology 98:1548–1559.

Phillips, R. P., I. Ibáñez, L. D'Orangeville, P. J. Hanson, M. G. Ryan, and N. G. McDowell. 2016. A belowground perspective on the drought sensitivity of forests: Towards improved understanding and simulation. Forest Ecology and Management 380:309–320.

Piper, F. I., A. Fajardo, and G. Hoch. 2017. Single-provenance mature conifers show higher non-structural carbohydrate storage and reduced growth in a drier location. Tree Physiology 37:1001–1010.

Pittermann, J., J. S. Sperry, U. G. Hacke, J. K. Wheeler, and E. H. Sikkema. 2006a. Inter-tracheid pitting and the hydraulic efficiency of conifer wood: the role of tracheid allometry and cavitation protection. American Journal of Botany 93:1265–1273.

Pittermann, J., J. S. Sperry, J. K. Wheeler, U. G. Hacke, and E. H. Sikkema. 2006b. Mechanical reinforcement of tracheids compromises the hydraulic efficiency of conifer xylem. Plant, Cell & Environment 29:1618–1628.

Poorter, H., S. Pepin, T. Rijkers, Y. de Jong, J. R. Evans, and C. Körner. 2006. Construction costs, chemical composition and payback time of high- and low-irradiance leaves. Journal of Experimental Botany 57:355–371.

Rapp, J. M., E. J. B. McIntire, and E. E. Crone. 2013. Sex allocation, pollen limitation and masting in whitebark pine. Journal of Ecology 101:1345–1352.

Rehfeldt, G. E., J. J. Worrall, S. B. Marchetti, and N. L. Crookston. 2015. Adapting forest management to climate change using bioclimate models with topographic drivers. Forestry 88:528–539.

Riemenschneider, D. E. 1985. Water Stress Promotes Early Flowering in Jack Pine.

Roland, C. A., J. H. Schmidt, and J. F. Johnstone. 2014. Climate sensitivity of reproduction in a mast-seeding boreal conifer across its distributional range from lowland to treeline forests. Oecologia 174:665–677.

Rossi, S., H. Morin, and A. Deslauriers. 2012. Causes and correlations in cambium phenology: towards an integrated framework of xylogenesis. Journal of Experimental Botany 63:2117–2126.

Ruel, J., and T. G. Whitham. 2002. Fast-Growing Juvenile Pinyons Suffer Greater Herbivory When Mature. Ecology 83:2691–2699.

Sala, A., D. R. Woodruff, and F. C. Meinzer. 2012. Carbon dynamics in trees: feast or famine? Tree Physiology 32:764–775.

Sánchez, J. M. C., D. F. Greene, and M. Quesada. 2011. A field test of inverse modeling of seed dispersal. American Journal of Botany 98:698–703.

Santos, L., E. Notivol, R. Zas, M. R. Chambel, J. Majada, and J. Climent. 2010. Variation of early reproductive allocation in multi-site genetic trials of Maritime pine and Aleppo pine. Forest Systems 19:381–392.

Santos-del-Blanco, L., J. Climent, S. C. González-Martínez, and J. R. Pannell. 2012. Genetic differentiation for size at first reproduction through male versus female functions in the widespread Mediterranean tree *Pinus pinaster*. Annals of Botany 110:1449–1460.

Sevanto, S., and L. T. Dickman. 2015. Where does the carbon go?—Plant carbon allocation under climate change. Tree Physiology 35:581–584.

Slack, A., J. Kane, E. Knapp, and R. Sherriff. 2017. Contrasting impacts of climate and competition on large sugar pine growth and defense in a fire-excluded forest of the Central Sierra Nevada. Forests. 8(7): 244 8.

Smaill, S. J., P. W. Clinton, R. B. Allen, and M. R. Davis. 2011. Climate cues and resources interact to determine seed production by a masting species: Climatic cues, resources and seed production. Journal of Ecology 99:870–877.

Sperry, J. S. 2003. Evolution of water transport and xylem structure. International Journal of Plant Sciences 164:s115–s127.

Sperry, J. S., J. R. Donnelly, and M. T. Tyree. 1988. A method for measuring hydraulic conductivity and embolism in xylem. Plant, Cell & Environment 11:35–40.

Sperry, J. S., U. G. Hacke, and J. Pittermann. 2006. Size and function in conifer tracheids and angiosperm vessels. American Journal of Botany 93:1490–1500.

Sperry, J. S., V. Stiller, and U. G. Hacke. 2003. Xylem Hydraulics and the Soil–Plant–Atmosphere Continuum. Agronomy Journal 95:1362–1370.

Steppe, K., F. Sterck, and A. Deslauriers. 2015. Diel growth dynamics in tree stems: linking anatomy and ecophysiology. Trends in Plant Science 20:335–343.

Suzuki, N., G. Miller, H. Sejima, J. Harper, and R. Mittler. 2013. Enhanced seed production under prolonged heat stress conditions in Arabidopsis thaliana plants deficient in cytosolic ascorbate peroxidase 2. Journal of Experimental Botany 64:253–263.

Tardieu, F., and T. Simonneau. 1998. Variability among species of stomatal control under fluctuating soil water status and evaporative demand: modelling isohydric and anisohydric behaviours. Journal of Experimental Botany 49:419–432.

Trugman, A. T., M. Detto, M. K. Bartlett, D. Medvigy, W. R. L. Anderegg, C. Schwalm, B. Schaffer, and S. W. Pacala. 2018. Tree carbon allocation explains forest drought-kill and recovery patterns. Ecology Letters 21:1552–1560.

Venturas, M. D., J. S. Sperry, and U. G. Hacke. 2017. Plant xylem hydraulics: What we understand, current research, and future challenges. Journal of Integrative Plant Biology 59:356–389.

Wada, K. C., and K. Takeno. 2010. Stress-induced flowering. Plant Signaling & Behavior 5:944–947.

Way, D. A., S. L. Ladeau, H. R. Mccarthy, J. S. Clark, R. Oren, A. C. Finzi, and R. B. Jackson. 2010. Greater seed production in elevated CO2 is not accompanied by reduced seed quality in *Pinus taeda* L. Global Change Biology 16:1046–1056.

White, R. H. 2007. Effect of Lignin Content and Extractives on the Higher Heating Value of Wood. Wood and Fiber Science 19:446–452.

Williams, G. C. 1966. Natural Selection, the Costs of Reproduction, and a Refinement of Lack's Principle. The American Naturalist 100:687–690.

Woodruff, D. R., B. J. Bond, and F. C. Meinzer. 2004. Does turgor limit growth in tall trees? Plant, Cell & Environment 27:229–236.

Woodward, A., and D. Silsbee. 1994. Influence of climate on radial growth and cone production in the subalpine fir (*Abies lasiocarpa*) and mountain hemlock (*Tsuga mertensiana*). Canadian Journal of Forest Research 24:1133–1143.

Wyckoff, P. H., and J. S. Clark. 2002. The relationship between growth and mortality for seven co-occurring tree species in the southern Appalachian Mountains. Journal of Ecology 90:604–615.

Xu, J., J. Lu, R. Evans, and G. M. Downes. 2014. Relationship between ring width and tracheid characteristics In *Picea crassifolia*: implication in dendroclimatology. BioResources 9:2203–2213.

Young, D. J. N., J. T. Stevens, J. M. Earles, J. Moore, A. Ellis, A. L. Jirka, and A. M. Latimer. 2017. Long-term climate and competition explain forest mortality patterns under extreme drought. Ecology Letters 20:78–86.

Ziaco, E., and F. Biondi. 2016. Tree growth, cambial phenology, and wood anatomy of limber pine at a Great Basin (USA) mountain observatory. Trees:1–15.

Table 2.1: Reported positive (+) or negative (-) relationships between growth and cone production or drought and cone production in studies directly assessing reproduction in conifer species. Spearman ρ and Pearson r correlation coefficients or estimated β values from original fitted models are reported where present or calculated from published data, and were re-calculated as a species average if values were from multiple plots in one location. Correlations between final cone production and climatic values in the inferred year of initiation, pollination, or maturation, if specified, are presented. Total R = total cone production. Values in parentheses are S.D.

Species	Growth: Total R	Drought: Initiation	Drought: Pollination	Drought: Maturation	Drought: Total R	Reference
Abies sachinelensis	+					Hisamoto and Goto 2017
Pinus banksiana	+0.05 (0.02)[a]	0.32[a]	0.05[a]	-0.16[a]		Riemenschneider 1985, Despland and Houle 1997
Picea engelmanii	+				+	Buechling et al. 2016
Pinus pinea	+					Gonçalves and Pommerening 2012
Pinus sylvestris	0.355[b]				-	Vilà-Cabrera et al. 2014
Abies alba	-0.14[b]	0.55[b]	-0.53[b]	-		Davi et al. 2016
Abies lasiocarpa	-	-0.1(0.45)[c]	0.05 (2.95)[c]	-0.1(0.45)[c]		Woodward and Silsbee 1994
Tsuga mertensiana	-/+	-0.075 (0.575)[c]	0.075 (0.375)[c]	-0.075 (0.575)[c]		Woodward and Silsbee 1994
Pseudotsuga menziensii	-				+	Ebell 1967, Eis et al. 1965
Pinus edulis		≤ -0.51[c*]				Redmond et al. 2012
Picea glauca		-0.29[b]	0.47[b]	-0.25[b]	+	Roland et al. 2014
Pinus palustris					+	Guo et al. 2016
Pinus pinea		-0.01[b]				Calama et al. 2011
Pinus ponderosa		≤ -0.35[c]			-0.61[b]	Mooney et al. 2011, Keyes and González 2015
Pinus taeda		+				Greenwood 1981
Pinus halepensis			-(female) +(male)	+(Spring) - (Summer)		Girard et al. 2012, Thabeet et al. 2009

[a]Spearman's ρ, [b]β estimate for reproduction term in fitted model (see reference for model), [c]Pearson's r
[*]Temperature stress only

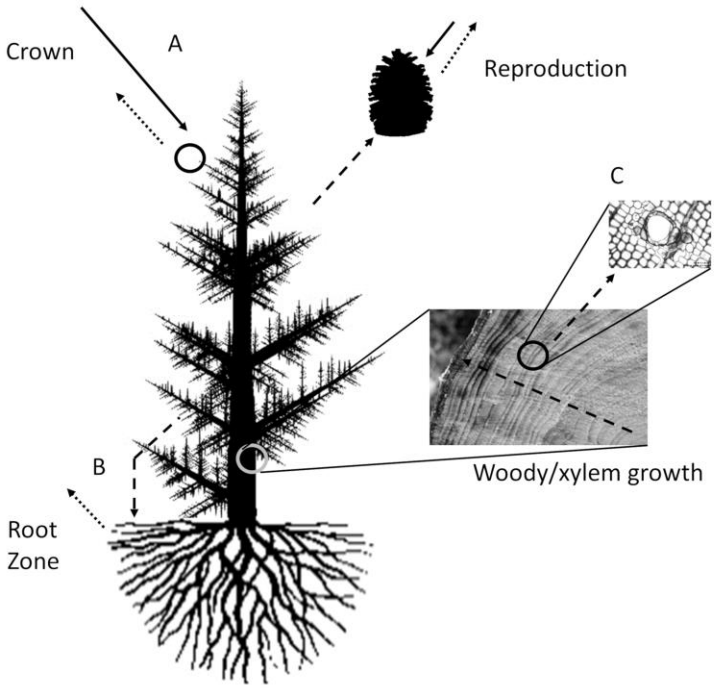

Figure 2.1. Conceptual diagram depicting potential tradeoffs in carbon (C) allocation in coniferous trees. Solid arrows represent C uptake (photosynthesis), dotted arrows represent C loss (respiration), and dashed arrows represent C allocation pathways. If C is allocated to seed production, that C is no longer available for leaf production (and associated photosynthesis, A), root production (B), or radial growth, which itself influences hydraulic conductivity and resistance to pests (as a function of tracheid size and resin duct formation, C).

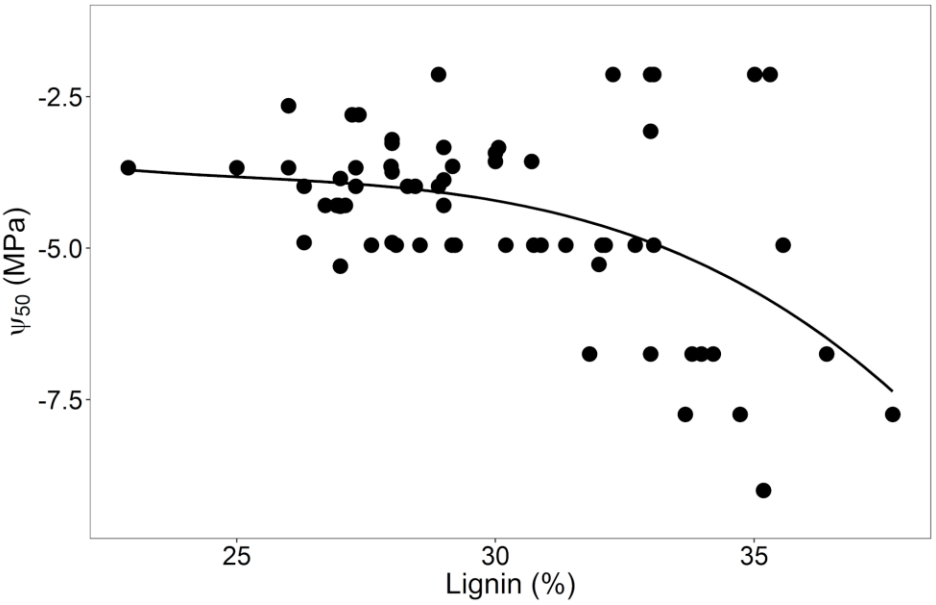

Figure 2.2. Relationship between total wood lignin concentration (%) and Ψ_{50}, the water potential at which 50% of conductivity is lost, in 25 gymnosperm species distributed globally. R^2 = 0.20, P = 0.0007. Data from (Pereira *et al.*, 2018) and (Choat *et al.*, 2012). Lignin data from multiple wood sources (branch or stem), and is assumed to scale linearly between sampled organs (see Pereira et al. 2018 for sample inclusion criteria).

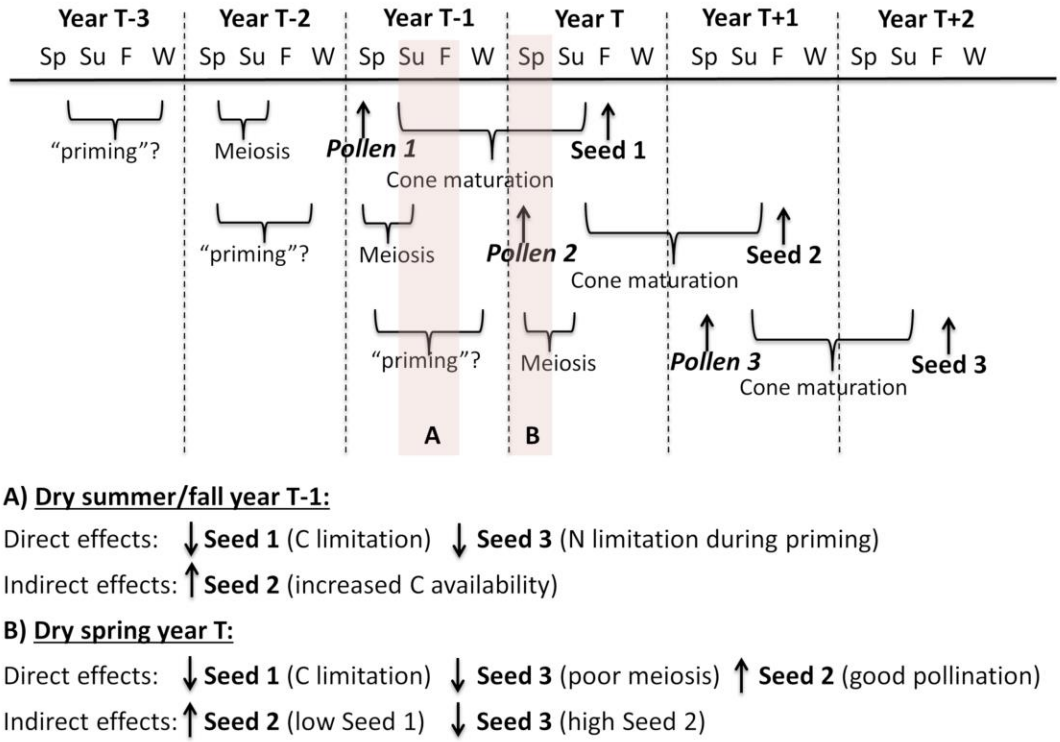

Figure 2.3. Potential effects of two given drought events (shaded boxes A and B) on reproductive output in masting conifers relative to a given year (T). Conifer cone production occurs over two to three years, and the effects of drought on resource availability for masting can have both direct effects (e.g., decreased reproduction in a year of drought) or indirect effects (e.g., increased reproduction in subsequent years due to increased C storage) depending on the reproductive stage. Arrows in figure represent timing of each reproductive stage. Arrows below figure represent relative change in each reproductive stage, with the expected mechanism of this change given in parentheses.

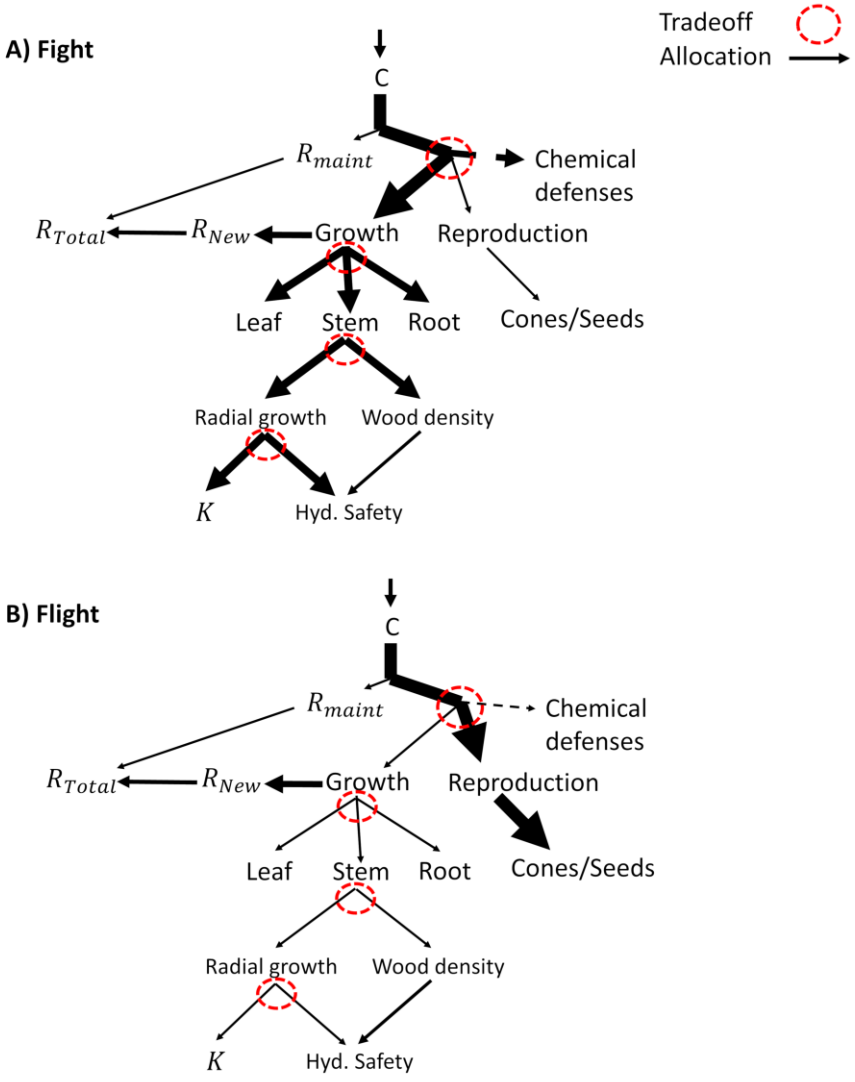

Figure 2.4. Theoretical expectations of a "fight" response (A) or a "flight" response (B) in conifers under drought stress. Line weight represents the relative magnitude of carbon (C) allocation to that particular plant pool following a tradeoff induced by drought stress. Fight responses are demonstrated by allocation of available resources to growth or drought or pest defenses at the expense of reproductive allocation. Flight responses occur when a tree allocates C to cone and seed production at the expense of growth and drought defense or pest defense. C = carbon pool, R = respiration, Hyd. Safety = hydraulic safety, K = sapwood conductance.

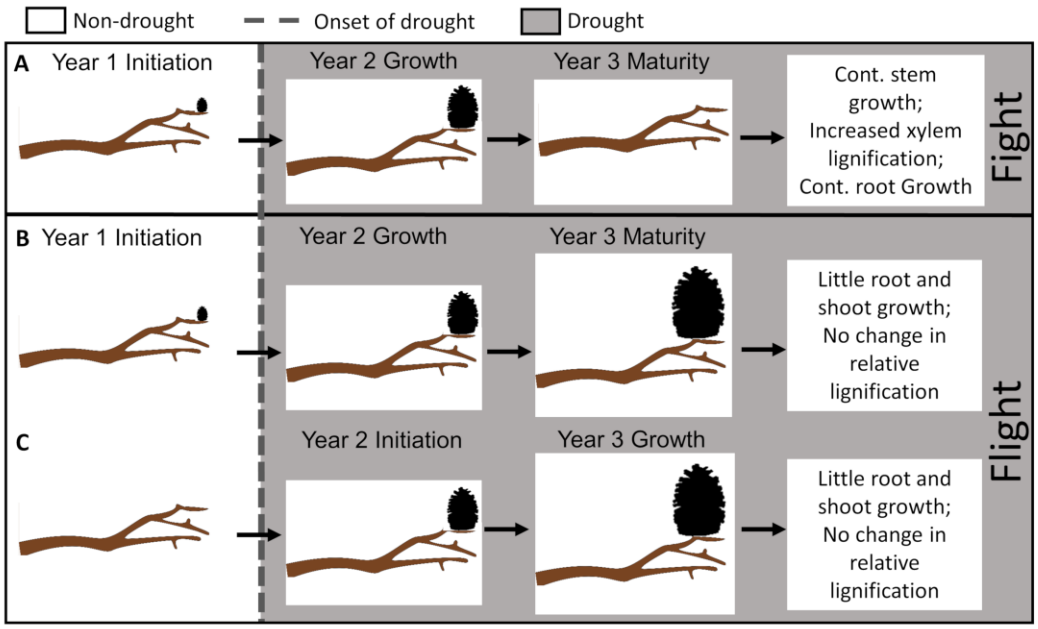

Figure 2.5. Multiple strategies for "flight" behaviors relative to prior reproductive investment. If a drought occurs after cone initiation, cone abortion and re-allocation of resources to growth and drought defense is an indicator of "fight" behaviors (A). On the other hand, if cones are not aborted but maintained through their maturation under drought stress, this can be considered a flight behavior (B). The final observable flight behavior is drought-induced reproduction (C), which may or may not be associated with terminal investment prior to mortality.

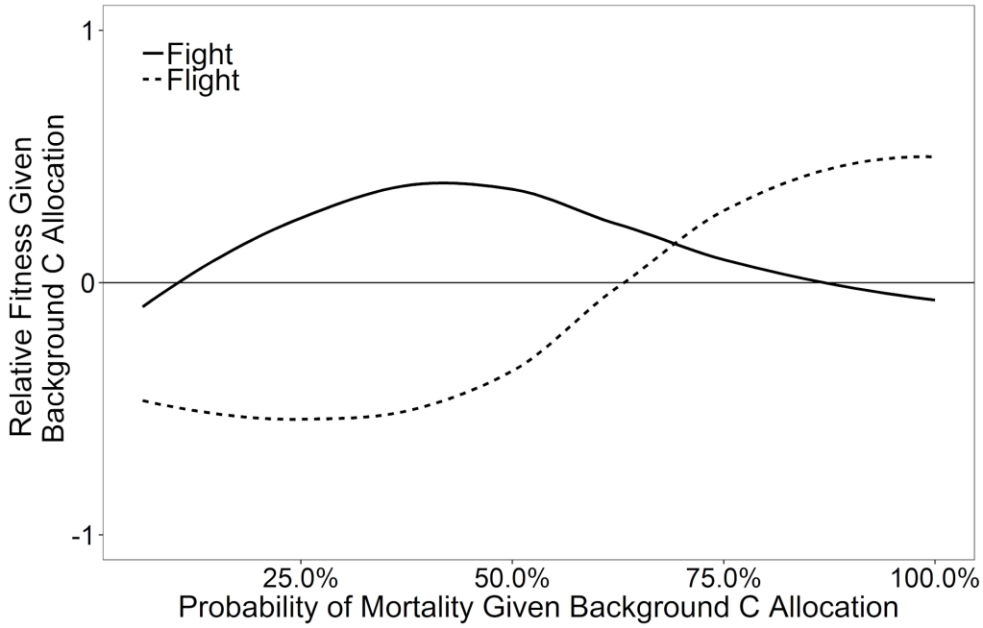

Figure 2.6. Hypothetical increase or decrease in fitness versus expected "background" fitness of "fight" or "flight" behaviors relative to the likelihood of mortality under drought stress. As likelihood of drought-induced mortality increases (e.g., with increased drought intensity and duration), the relative benefit of fight behaviors may decrease as drought defenses fail and trees die without reproducing. Flight behaviors provide little increased fitness benefit when the probability of mortality is low, but provide significantly higher fitness increases as probability of mortality increases. This is because flight behaviors increase potential future recruitment of new seedlings and capacity for adaptation to a drier climate or migration to track a more optimal climate.

Chapter 3:
Assessing differences in lignin content between drought-killed and living pines using chemical and visual methods

3.0 Abstract: Current climate models predict increasing drought intensity, frequency, and duration in semi-arid forests globally. Tree drought resilience is a function of physiological resistance to hydraulic stress and management of carbon (C) reserves. Physiological resistance to drought-induced damage is partially conferred via deposition of lignin, a polymer that strengthens cell walls at a high C expense. Measuring lignin content in tree rings allows us to track the physiological response of trees to drought relative to C cost, but conventional lignin quantification methods can be expensive and time-consuming. We test a novel lignin quantification technique based on digital image analysis of stained wood cross sections that approximates lignin concentrations derived from conventional methods in living and dead trees from the drought-stricken Sierra Nevada mountains. Contrary to our initial hypothesis, living trees did not have higher lignin concentrations than dead trees, and dead trees had higher average and more variable lignin concentrations, suggesting that excessive lignification may lead to C depletion and mortality risk. Our rapid quantification method detects these differences, though it tends to exaggerate them, and can be combined with xylem anatomy analyses for little cost beyond that of thin-sectioning techniques. The visual method tracked traditional chemically derived lignin concentrations better for living than for dead trees, most likely due to differences in decomposition rates of cell walls versus all cell contents in wood of dead trees. It therefore has potential to aid assessments of C allocation, particularly in studies focusing on cell anatomy of live trees.

3.1 Introduction

Lignin is a complex aromatic polymer deposited in plant cell walls that serves many important roles. These include resistance to both drought stress (Pereira et al. 2018) and insect attack (McKay et al. 2003, Franceschi et al. 2005) via reinforcement of tissues for transporting water and chemical defenses. Lignification also provides the mechanical strength necessary for woody plants to achieve an erect growth habit (Hacke and Sperry 2001, Sperry 2003, Sperry et al. 2006, Vanholme et al. 2010) as it confers resistance to bending stress (Voelker et al. 2011) and supports long-distance vertical water transport (Mencuccini 2003, Sperry 2003). However, lignin is carbon-expensive (Amthor 2003, Novaes et al. 2010); it has even been estimated to constitute up to 30% of all terrestrial biosphere carbon (Boerjan et al. 2003), although this is primarily due to its slow decomposition rate. Under increasing aridity expected to be associated with projected climate change, we may expect the interactions among wood lignification and total carbon (C) budgets to become more significant and play an important role in forest response to drought.

Greater lignification of xylem cells (tracheids) seems to reduce likelihood of hydraulic failure under drought stress (Pereira et al. 2018). Xylem wall thickness is positively correlated with lignin concentrations (Gindl 2001) and this wall thickening may reduce likelihood of conduit collapse during drought (Hacke et al. 2001, Pittermann

et al. 2006). Lignification may also play a role in inter-tracheid pit membrane resistance to embolism (Pereira et al. 2018). This is important because drought intensity and frequency are expected to increase under projected climate change (IPCC 2014). Indeed, drought-induced forest die-offs are already occurring (Allen et al. 2010, 2015). A major goal of current forest ecophysiology research is to parse the interactions and tradeoffs among physiological traits that confer drought resistance and tree C budgets (Sala et al. 2012, Sevanto and Dickman 2015, Adams et al. 2017). Comparing relative lignin concentrations between stressed and unstressed trees may be one avenue to further evaluate the C cost of growth and survival under extreme drought.

Quantification of annual variation in lignification in trees is an important step in tracking C budget implications of drought stress in forests. Lignin quantification is notoriously time-intensive, requires unique laboratory apparatus, and is often very sensitive to materials or methods used. Questions remain regarding the ability of any lignin measurement method to accurately quantify true lignin concentration (Hatfield and Fukushima 2005). Current methods in lignin chemistry can be broken down into gravimetric methods versus noninvasive methods, and are extensively reviewed elsewhere (Hatfield and Fukushima 2005, Lupoi et al. 2015). Gravimetric methods are primarily based on the measurement of Klason lignin, or the lignin left over after complete dissolution of all non-lignin materials in 64-72% H_2SO_4 (Browning 1967, Nakano and Meshitsuka 1992). Noninvasive methods include the measurement of ultraviolet absorbance (Fukushima and Hatfield 2004), fluorescence or interference microscopy (Donaldson et al. 1999, Bond et al. 2008), near infrared (NIR, Gidh et al. 2006, Li et al. 2015) and Fourier-transformed infrared (FTIR, Liu et al. 2010, Schwanninger et al. 2011) spectroscopy, and nuclear magnetic resonance (NMR) imaging (Martin-Sampedro et al. 2011). All of these noninvasive methods utilize physical properties of lignin, such as reflectance of specific wavelengths of light, to estimate lignin content. Finally, hybrid methods involve the use of UV spectroscopy to quantify lignin in solution. Each of these methods requires highly specialized equipment.

As a potential alternative, we tested digital image analysis using histologically stained wood thin sections and a standard compound light microscope. Quantification of stain intensity in laboratory-stained thin sections of tissues is standard practice in histology (Jensen 2013, Ursache et al. 2018), and is gaining increasing traction among plant physiological studies (Bond et al. 2008, Pradhan Mitra and Loqué 2014). However, studies that do use histological staining of plant cells still primarily use it as a qualitative tool (Pradhan Mitra and Loqué 2014) or to assess spatial deposition of materials or quantitative change in lignification over time (e.g., lignin during xylogenesis, Rossi et al. 2012). Little work has used it to explicitly quantify total lignin concentration differences between samples or across multiple annual growth rings. We have only identified one study to date that used histological staining and standard light microscopy to measure lignin content quantitatively, in which the authors were able to discern quantitative spatial variability in maize stem lignin content (Zhang et al. 2013).

Plant physiologists studying hydraulic traits often obtain thin sections from selected individuals and cross-stain them to differentiate lignin and cellulose for improved visualization of cellular anatomy (Kutscha and R. Gray 1972, Kraus et al. 1998, Bond et al. 2008). Here, we test the hypothesis that trees that survive drought will

have a higher total lignin content in annual rings during and after drought due to increased C allocation to hydraulic safety when stressed. We compare stain intensity of thin sections of living and dead conifers from drought-stricken locations in the Sierra Nevada in California with lignin concentrations measured using conventional methods to test for differences in lignin content between trees that lived and died as a result of the historic 2012-2016 California drought (Griffin and Anchukaitis 2014).

3.2 Methods

3.2.1 Field Sampling

We extracted increment cores from living and drought-killed *Pinus ponderosa* and *P. jeffreyi* in six permanent sampling plots in California's Sierra Nevada (Figure 3.1). These plot locations experienced high tree mortality as a result of the 2012-2016 drought. Sites were at 1905 m (SP), 2170 m (SJP), 1172m (SR), 878m (TP), and 1667m (TJP) elevation, spanning the middle elevation distribution of *P. ponderosa* to the middle elevation distribution of *P. jeffreyi* in the region. Where possible, we cored ten randomly selected living and dead trees of each species in each plot, with only recently killed (needles brown but not yet completely defoliated) trees cored. All selected trees were either dominant or sub-dominant trees ranging from 22 cm to 147 cm diameter at breast height (DBH). Reaction wood is the growth of thicker rings and more woody biomass on the uphill ("tension wood" in angiosperms) and downhill ("compression wood" in gymnosperms) sides of trees growing on steep slopes that helps maintain an upright growth position. We extracted cores in two perpendicular directions (from positions perpendicular and parallel to the slope) to mediate effects of potential reaction wood (Speer 2010). This allowed accurate annual ring dating, as well as ensured lignin concentration measurements were not biased toward reaction wood, which often has higher lignin concentrations (Yamashita et al. 2007).

We used standard dendrochronology methods to ensure lignin concentrations were compared between the same years across all cores (Speer 2010). We stabilized cores in wooden mounts, surfaced them using consecutively finer grades of sandpaper until individual cells were visible, and then scanned them at 800 dpi. Ring widths were automatically measured in the winDENDRO tree ring software package (Regent Instruments Canada Inc. 2017). We cross-dated cores visually within winDENDRO, and checked final annual ring dates using the cross-dating statistical package COFECHA (Grissino-Mayer 2001). We adjusted dates manually under a stereo microscope if necessary. Trees were dropped from further analysis if robust cross-dating likelihood (assessed via correlation among chronologies in COFECHA) was not achieved. Thus, final cores were only analyzed if sample tree ring years were positively identified.

3.2.2 Thin Section Preparation

After rings were properly dated, we took 10-16 µm radial thin sections from each core using a GSL-1 tree core microtome (Gärtner et al. 2014). The thin sectioning process also removed any transferred wood powder that may have settled in non-current year rings during sanding. In lieu of stabilization of tree cores in paraffin, we brushed prepared core surfaces with a corn starch solution to facilitate non-destructive wood sectioning (von

Arx et al. 2016). We cleaned sections of all starch using deionized water and ethanol and cross-stained them using a 1% safranin and 1% astra blue solution (1:1 v/v).

We chose to use safranin after preliminary trials identified it as the most efficient stain for our wood tissues. Cresyl violet acetate and phloroglucinol have higher lignin affinity (Perdih and Perdih 2011), and recent advances in studies of cambial phenology have utilized cresyl violet acetate (Deslauriers et al. 2008, Rossi et al. 2012), while phloroglucinol has a rich history in lignin visualization. However, cresyl violet does not provide enough of a color distinction between violet and blue to quantitatively assess total lignin content digitally. Phloroglucinol, while providing optimal staining of soft tissues, did not stain our wood thin sections consistently, and resulted in large variance in stain efficiency between thin sections from the same sample. Safranin avoided these problems.

All thin sections were stained for approximately 15 seconds with sufficient stain to fully cover the section and then thoroughly washed using deionized water and ethanol until runoff ran clear. We permanently fixed thin sections to slides using Euparal, placed them under a weight, and allowed them to dry for a minimum of 48 hours. Following drying, all slides were cleaned of excess mounting media using a razor blade and photographed at 100x magnification using a Leica DME compound microscope equipped with a Leica DFC290 digital camera.

3.2.3 Lignin Quantification

We analyzed lignin concentrations in annual rings via a modified acetyl bromide method (Barnes and Anderson 2017). We chose this method as it has been shown to provide the highest recovery of lignin in small sample sizes when compared to gravimetric methods (Fukushima and Hatfield 2004, Moreira-Vilar et al. 2014). We first removed individual annual rings using a razor blade as close to the ring boundary as possible under a stereo microscope. Effort was made to err on the side of the current year ring where ring boundaries were hard to see so that any sampling error would result in a loss of low-lignin earlywood rather than inclusion of lignin-rich latewood from the previous year. We ground resulting wood wafers with mortar and pestle using liquid nitrogen, then further homogenized them in 2-mL safeseal tubes with three stainless steel grinding balls using a mini-g tissue lyser for approximately 3 minutes at 1800 RPM.

Interfering extraneous substances (e.g., soluble fats, waxes, simple sugars, and low-molecular soluble phenolics) were removed in four successive two-day extractions with acetone. After each extraction, we centrifuged samples and replaced supernatant acetone. After the final extraction, we aspirated supernatant acetone and left all tubes open to air dry in a fume hood. The resulting structural biomass (plant cell wall) was used to quantify total lignin.

We added one mL of freshly prepared 25% (w/w) acetyl bromide/glacial acetic acid solution to approximately 1 mg (+/- 0.2) air-dry, extractive-free wood powder in 2-mL polypropylene micro-tubes and placed them in a water bath for 30 min with repeated mixing at 70 ˚C and stopped the reaction by submerging in ice. We transferred 100 µL of the reaction mixture into a 2 mL UV quartz cuvette containing 200 µL of 2.0 M sodium hydroxide, and filled to 2 mL with 1.7 mL of glacial acetic acid. The UV absorbance of the solution was determined at 280 nm against a blank solution on a Tecan M200 Pro UV

spectrophotometer (Tecan Trading AG, Switzerland). Total lignin was calculated from measured absorbance using the equation:

$$ABSL = \left(\frac{A^{280}}{\varepsilon L}\right) * \left(\frac{D}{m}\right) * 100,$$

where ABSL = acetyl bromide-soluble lignin (%), A^{280} = absorbance at 280 nm, L = path length (2 cm for the cuvette), D = dilution factor of final solution (1 = no dilution for our samples), m = mass of the sample prior to acetyl bromide mixing, and ε = the extinction coefficient of a known lignin standard. For this analysis, we used ε = 23.3 (Barnes and Anderson 2017). After final sample preparation, due to some samples being unmeasurable, we were left with n = 165 total ring samples broken down as follows: 52 rings from 7 living *P. ponderosa*, 66 rings from 7 living *P. jeffreyi*, 35 rings from 7 dead *P. ponderosa, and* 12 rings from 2 dead *P. jeffreyi*,.

We also created a lignin standard curve using kraft alkali lignin (Sigma Aldrich 370959) and compared our standard curve-derived lignin estimates with those calculated using the above equation. Because of a robust standard curve (R^2 = 0.99, Figure S3.1), we elected to calculate lignin content relative to our lignin standard (i.e., by using the regression equation of our standard curve), hereafter referred to as acetyl bromide lignin.

3.2.4 Image Analysis

We performed all image analyses in ImageJ (Schindelin 2015), following a modified version of the protocol for analysis of stained plant thin sections outlined by (Zhang et al. 2013). Our three-step protocol (Figure 3.2) consisted of: (1) background bright-field correction of all images to account for dust, debris, mounting media blurring, and other imaging aberrations; (2) splitting of each image into red, green, and blue channels; and (3) selection of target areas in the red channel image, with an attempt to exclude areas of smudging, out-of-focus regions, and folded or broken wood that may significantly alter stain concentrations, followed by calculation of red intensity. For each image, we calculated Mean Red Density (mean gray value of the red channel image), Integrated Density (Mean Red Density x image area), and Raw Integrated Density (sum of all gray values in the red channel). Preliminary regressions of each of these metrics against acetyl bromide lignin found Mean Red Density had the best fit (Table 3.1), leading us to use this metric for all subsequent analyses.

We measured tracheid dimensions using the automated image analysis program winCELL, a sub-package of the winDENDRO suite of tree ring analysis software (Regent Instruments Canada Inc. 2017). We used winCELL to automatically detect cell walls and lumina, and manually corrected images with excessive torn walls or faint wall boundaries. We measured lumen diameter and wall thickness in all cells that were automatically detectable within a given thin section image. Data were then pooled and used to calculate within-ring average thickness-to-span (T-S, the ratio of tracheid wall thickness to cell lumen diameter), an indicator of hydraulic safety. Here, we use T-S as a final check of all methods of lignin detection, as tree rings with higher ratios of wall to lumen theoretically contain more lignin.

3.2.5 Statistical Analysis

Prior to all analyses, we assessed acetyl bromide lignin and stain-derived metrics for age effects, as prior work in tropical trees has demonstrated higher lignin and lower

holocellulose in younger trees (Martin et al. 2013). While our sampling scheme did not target especially young trees, our range of tree diameters included both small and large trees, and thus warranted checking for age effects. Linear regression of acetyl bromide lignin versus tree age found no significant age effect (p >0.5) and analyzed all trees together with no age term.

Because our main focus here is on how lignin content differs between living and dead trees and whether stain-derived estimates of lignin approximate these differences, we conducted two-sample t-tests to compare all living trees to dead trees, living to dead *P. ponderosa*, and living *P. ponderosa* to living *P. jeffreyi* using each metric (stain-derived lignin versus acetyl bromide lignin) individually. Due to sample size limitations on dead *P. jeffreyi*, we limited analyses to comparisons of living versus dead entirely, living *P. ponderosa* versus living *P. jeffreyi*, and living versus dead *P. ponderosa* only, avoiding analyses of dead *P. jeffreyi* versus live *P. jeffreyi*.

We then assessed correlations between stain-derived metrics, T-S, and acetyl bromide lignin using linear regressions. Lignin concentrations in dead trees may change significantly due to wood rot after tree death (Pandey and Pitman 2004). We therefore tested for a "decay" effect by removing samples with greater than 50% acetyl bromide lignin (outliers >1.5 sd from mean lignin) and re-running models. We chose to use stain-derived metrics as responses instead of predictors due to the basic assumption that stain intensity is itself a function of lignin, and not vice versa. To assess final model fit, we assessed p-values and adjusted R^2. Data were assessed for homoscedasticity, and log-transformed prior to final regressions, with residual inspection used to confirm assumptions were met. We also evaluated the ability of stain-derived estimates of lignin to track acetyl bromide lignin over time via 3-factor analysis of variance (ANOVA) with lignin concentration as a response and species, year, and survival status as factors, ignoring dead *P. jeffreyi*.

Finally, we assessed the sensitivity of our stain-derived metrics to methodological error by comparing model results from final runs with those from models using discarded thing sections. Thin sections dropped from final analyses were discarded due to an inability to distinguish xylem cell lumen from wall, or general thin section quality issues such as section thickness and mounting media smudging. This allowed an assessment of the effects of "user error." All analyses were carried out in base R version 3.5.1 (R Development Core Team 2020).

3.3 Results

Dead trees had higher acetyl bromide lignin than living trees on average (Figure 3.3A), but the difference was not statistically significant (p = 0.484, Table 3.1). Dead *P. ponderosa* had higher average acetyl bromide lignin content than dead *P. ponderosa*, but again, the difference was not statistically significant (p = 0.622). A high proportion of dead *P. ponderosa* lignin samples had lower lignin content than living *P. ponderosa*, but dead trees showed much higher variance in lignin content than living trees and higher content on average (Figure 3.4A).

Mean Red Density approximated the same differences in average lignin concentration shown by acetyl bromide lignin (Table 3.1), but exaggerated differences, finding statistically significant differences not detected in acetyl bromide lignin. Mean

Red Density was weakly positively correlated with acetyl bromide lignin across all samples (Figure 3.6, Table 3.2), and had very low fit ($p = 0.092$, $R^2 = 0.013$, $n = 165$). Separating living and dead trees improved significance and fit for both living ($p = 0.008$, $R^2 = 0.062$, $n = 118$) and dead trees ($p = <0.001$, $R^2 = 0.261$, $n = 47$, Figure 3.7). When further separating samples by species and status, the relationship improved for dead *P. ponderosa* ($p < 0.001$, $R^2 = 0.290$, $n = 35$), and living *P. jeffreyi* ($p = 0.001$, $R^2 = 0.179$, $n = 66$), but not living *P. ponderosa* ($p = 0.523$, $R^2 = 0.013$, $n = 52$).

Variation in thin section quality slightly modified results. Removal of "low quality" thin sections caused species differences to no longer be significant in ANOVAs, but all other differences remained similar (Table S3.1). Relationships between Mean Red Density and acetyl bromide lignin in all dead trees and only dead *P. ponderosa* were no longer significant after removal of "low quality" thin sections (Table S3.2). Our test for a "decay" effect by removing samples with more than 50% acetyl bromide lignin resulted in ANOVA results that were no longer significant for any variable in the acetyl bromide models, demonstrating that high lignin samples may significantly influence results (Table S3.3). Removal of high lignin samples had a similar effect on regressions as removal of "low quality" thin sections, with dead tree-only models no longer being significant (Table S3.4). Stain-derived estimates of lignin continued to uncover more extreme differences between living and dead trees than acetyl bromide lignin even with high lignin dead trees removed (Table S3.3).

Models of lignin concentrations that included year, species, and status improved fits dramatically over regressions with no year effect (Table 3.2, $p < 0.001$, < 0.001, and $= 0.001$, $R^2 = 0.222$, 0.246, 0.211, and $n = 165$, 87, 66 for all samples, *P. ponderosa* only, and living *P. jeffreyi* only, respectively). Lignin concentrations over time were more variable in dead trees than living trees (Figure 3.8). Mean Red Density did not track acetyl bromide lignin over time particularly well in dead trees. However, in living trees, both methods provide similar estimates of change over time (Figure 3.9), particularly after drought onset in 2012.

Thickness-to-span (T-S) was only correlated with acetyl bromide lignin across all samples or when accounting for tree status (Table 3.2, Figure 3.10), but did not track differences by species. The model comparing T-S to acetyl bromide overall was significant ($p = 0.016$), unlike the overall model for mean Red Density, but fit was very low ($R^2 = 0.0690$).

3.4 Discussion

We found that the hypothesis that living trees exposed to drought stress would exhibit higher lignin concentrations was not supported. Instead, dead trees had higher and more variable lignin content, on average, and that lignin content varied substantially over time after drought onset, while living trees appeared to have more constant interannual lignin concentrations. We also found that our stain-derived proxy of lignin content varied in its consistency with conventional lignin measures. Stain-derived estimates of lignin may be viable for predicting change in lignin content over time, primarily in living trees. However, we also found that the relationship between stain-derived lignin and acetyl bromide lignin switched from positive to negative in dead trees.

More samples are needed to confirm differences in living and dead tree lignin content, but the higher variability in dead than living trees, higher lignin content on average in dead than living trees, and higher lignin in *P. ponderosa* than *P. jeffreyi* warrant further exploration. While numerous studies have assessed the effects of drought and other abiotic stressors on lignin biosynthesis and associated adjustments in wood traits (Gindl 2001, Deslauriers et al. 2014), this is the first study to document patterns in lignin concentrations in living and dead trees affected by drought with results that are counter to expectations. On-going research continues to elucidate the significance of C budgets and resource allocation in drought-stressed trees. Our results demonstrate that the concentration of lignin, a C-intensive material, in wood may not vary as significantly as previously predicted between living and dead trees, and in fact may vary more in dead trees. We note that the ultimate cause of mortality of target trees was likely a result of drought stress combined with bark beetle attack (Hicke et al. 2016, Das et al. 2016). Drought may reduce C uptake as a result of stomatal closure to limit water loss, limiting total C reserves over prolonged droughts (Adams et al., 2017). Our sampled trees were additionally under intense bark beetle pressure (Hicke et al. 2016), and production of defensive compounds may further stress C reserves (Franceschi et al. 2005, Ferrenberg et al. 2014). The C cost of lignin may lead to potential tradeoffs among mechanical strength, hydraulic safety, pest defense, and resource availability for other processes such as growth or reproduction (Lauder et al. 2019). For example, lignin concentration is negatively correlated with biomass and radial growth (Novaes et al. 2010).

One potential explanation for the observed higher lignin in dead trees than expected is a greater sensitivity to drought at the cellular level in the dead trees. Drought may induce decreased xylem cell diameters and shortened cell growth times via turgor-limited cell expansion (Woodruff et al. 2004). Earlier cell death as a result of this shortened expansion time is often associated with increases in lignification time (Anfodillo et al. 2012). Likelihood of mortality does appear to be greater in trees with greater general drought sensitivity (Cailleret et al. 2017, 2019), and our sample dead trees appear to have higher average cell wall thicknesses and smaller cell diameters than living trees (Chapter 5). Our results may point to drought-induced increases in cell lignification and associated depletion of C resources as a mechanism of mortality in drought-sensitive trees, but that this drought-induced cell lignification varies from individual to individual, with some trees that eventually died allocating far more C to lignification and some allocating far less.

Future work could incorporate stain-derived estimates of lignification into direct comparisons of lignification, hydraulic traits, and mortality relative to total C reserves such as non-structural carbohydrates (NSC; Hoch et al. 2003, Piper 2011, Oberhuber et al. 2011). Drought may reduce C availability for construction of new structures in the stem (Deslauriers et al. 2014), as non-structural carbohydrates (NSC) are preferentially allocated to maintenance of other drought defenses such as osmotic potential or shunted to roots (Piper 2011, Hasibeder et al. 2015, Hagedorn et al. 2016) and branches (Kannenberg et al. 2017). Our finding of increased lignification in drought-stressed trees prior to mortality demonstrates that if trees with altered NSC dynamics allocate C to lignification of cell walls to resist hydraulic stress, they may further deplete already stressed C stores.

We demonstrated that histological staining can be used to detect differences in tree lignin content across years and living vs. dead individuals. However, caution is needed in quantifying the degree of difference, as the method is sensitive to outliers in measured lignin concentration, and species and survival status need to be taken into account. While values do not quantitatively track acetyl bromide lignin across samples precisely enough to be used as a direct substitute for chemical measurement methods, we found that Mean Red Density may provide a reasonable proxy for comparison between annual rings over time once species and survival status are accounted for.

Assessing lignin in 50 ring samples with the Acetyl Bromide method costs approximately $50 per sample for sample preparation, and analysis requires a UV Spectrophotometer (price range $1200-$15000). Once such initial measurements are used to build a calibration curve, if thin sections and xylem anatomy are already being analyzed, there is no additional monetary cost to assess lignin concentration using the stain method. Further, the amount of time needed dropped from an average of 110 minutes per sample for the acetyl bromide method to 23 minutes (only 3 if thin sections are already being created) when digital image assessment with an automated script was used (Table 3.3). The stain method facilitates rapid, high-throughput analysis of a previously time-intensive trait to measure. However, if the project would not otherwise utilize thin sections, it would be more time-efficient to use standard lignin quantification methods.

Interestingly, stain-derived estimates of lignin concentrations were positively correlated with acetyl bromide lignin in living trees overall, but negatively correlated in *P. ponderosa*. This relationship was more negative in dead *P. ponderosa* than in living *P. ponderosa*. We hypothesize that this change in relationship according to tree status is due to changing lignin structure, distribution, and composition as trees die and wood decays. Our highest measured acetyl bromide lignin concentration was 71% in a dead tree. Although this value is higher than expected average values in conifers, it is consistent with Pandey and Pitman (2004), who found lignin concentrations in *Pinus sylvestris* in excess of 80% in wood that had experienced 64% decrease in weight via degradation of carbohydrates after 12 weeks of exposure to the brown-rot fungus *Coniophora puteana*.

We sampled target trees at the same time at each site, and although dating of tree rings allows us to track year of mortality, we were unable to discern when during the year trees died. Dead trees thus could have been exposed to rot for up to six months prior to sampling. This raises the significance of outlier scrutiny; we removed trees with impossible acetyl bromide lignin concentration estimates (i.e., >100%) from final analyses and attributed results to user or instrument error. We elected to keep high-lignin (i.e., > 40%) samples in final analyses after checking for decay effects, however, to include the natural range of variation that would be expected when comparing living and partially decayed dead trees. Our findings of a higher degree of difference between living and dead samples in stain-derived lignin than acetyl bromide may reflect this decay-induced change in lignin estimates. Carbohydrate degradation may be accounted for in total acetyl bromide lignin because final lignin is expressed as % dry weight; as carbohydrates degrade, total sample mass also declines, and the relative lignin concentration increases. However, carbohydrate degradation would not necessarily be captured in stain-derived metrics when using a stain with a high lignin affinity; stain

intensity may be the same for one sample with high total biomass (no rot) and low biomass (significant carbohydrate degradation and decay), whereas measured (% dry weight) lignin will vary significantly. This is consistent with our observations of higher but much less variable stain-derived lignin than acetyl bromide lignin in dead trees. This may point to stain-derived estimates of lignin providing a more robust means of estimating dead tree lignin content when time since mortality cannot be accounted for (i.e., there may be lower absolute quantities of lignin in decaying wood than % by weight methods predict), but this hypothesis must be tested directly. Further complicating interpretation of our lignin estimates is the uncertainty surrounding all lignin measurement methods. Although more traditional methods (including acetyl bromide extraction) have been accepted as standard, debate remains on if these methods themselves are accurately quantifying lignin content, likely due to the inherent variation in lignin structure (Hatfield and Fukushima, 2005). Thus, we cannot rule out the possibility that our stain-derived estimates of higher lignin in dead trees across both species is more accurately picking up differences in lignin content than acetyl bromide lignin.

Our observations that T-S did not perfectly predict acetyl bromide lignin was unexpected, as wall thickness, and thus T-S, is expected to covary with total lignin content (Gindl 2001, Zhang et al. 2013). We hypothesize three potential explanations; variance in individual tree lignification with respect to wall thickness, measurement error not accounted for in our assessment of thin section quality effects, and inaccuracy and imprecision in the acetyl bromide lignin measurement process. Wall thickness and lignin content are predicted to covary based on the primary mechanism of cell wall thickening. Lignification occurs from the middle lamella (the zone between two adjacent cell walls) inward toward the center of the cell lumen via ordered deposition and buildup of three distinct cell wall layers, known as the S1, S2, and S3 layers (moving from middle lamella inward; Boudet et al. 1995, Wagner et al. 2012). There can be substantial variation in lignin content of these three layers due to variation in fiber orientation. Further, tension wood in angiosperms (wood formed on uphill sides of stems to keep them upright) and compression wood in conifers (wood formed on downhill side of stems) has been shown to have significantly increased S2 lignin content (Boudet et al. 1995, Yoshinaga et al. 2012, Barros et al. 2015). Here, we sampled stems from mixed topographical conditions, but mitigated influence of compression wood by coring trees from positions perpendicular to the slope, and only taking compression wood samples to assist in cross-dating. However, we did not directly characterize middle lamella lignin versus wall lignin, nor did we compare lignin chemistry using other analysis methods such as Nuclear Magnetic Resonance (NMR) imaging, which would allow further separation of lignin by type and location within the cell wall. Thus, it is likely that there is variation in cell wall lignin content entirely unexplained by wall thickness. Another potential explanation for our lack of observed correlation between T-S and acetyl bromide lignin is measurement error. While we controlled for image quality, there is inherent variation between images in wall-detection fidelity.

Overall, we found that stain-derived estimates of lignin content are applicable to living trees, and may in fact predict lignin concentrations in dead trees as a function of cell wall lignification more realistically than methods based on % dry weight when wood

decay is expected. Nevertheless, this needs to be tested further, as we cannot definitively say that our stain-derived estimates or acetyl bromide-derived estimates are true measurements of total lignin. Our findings of higher lignin concentrations in dead trees, on average, demonstrate that the method outlined here can be used to rapidly extrapolate the C implications of hydraulic safety from physiological datasets to scale up from individual cells to whole tree C budgets. Here we analyzed lignin content in trees from three distinct forest transects from across the Sierra Nevada, but whether our observation of higher lignin in dead trees is a genetic characteristic of certain trees, a local site or population effect, or due to an interaction of these things is unknown and an important future research question. Further work is needed to calibrate stain-derived estimates of lignin, but this study presents a new method for high-throughput, low-cost estimates of lignin in samples that are already being examined for xylem anatomical variation. If using a stain with a high lignin affinity as well as standardized thin section thickness, stain times, and microscope light intensities, stain-derived estimates of lignin concentration appear relatively robust. A second line of evidence, T-S ratios, may help to confirm presence of higher or lower lignin concentrations between living and dead trees. Future work can assess further the quantitative relationships among xylem cell anatomy, lignin content, and tree survival to attribute differences in lignification to mechanisms of drought resilience. Such an effort would greatly improve our ability to forecast future drought-induced mortality across forest stands.

3.5 Acknowledgements

This work was performed in part at the University of California Natural Reserve System (Sierra Nevada Research Institute-Yosemite Field Station) Reserve DOI: 10.21973/N3V36C. We appreciate use of the cabin facilities for field sampling. We would like to thank Stephen C. Hart for helpful comments on how decay effects lignin content and for use of laboratory equipment.

3.6 References

Adams, H. D., M. J. B. Zeppel, W. R. L. Anderegg, H. Hartmann, S. M. Landhäusser, D. T. Tissue, T. E. Huxman, P. J. Hudson, T. E. Franz, C. D. Allen, L. D. L. Anderegg, G. A. Barron-Gafford, D. J. Beerling, D. D. Breshears, T. J. Brodribb, H. Bugmann, R. C. Cobb, A. D. Collins, L. T. Dickman, H. Duan, B. E. Ewers, L. Galiano, D. A. Galvez, N. Garcia-Forner, M. L. Gaylord, M. J. Germino, A. Gessler, U. G. Hacke, R. Hakamada, A. Hector, M. W. Jenkins, J. M. Kane, T. E. Kolb, D. J. Law, J. D. Lewis, J.-M. Limousin, D. M. Love, A. K. Macalady, J. Martínez-Vilalta, M. Mencuccini, P. J. Mitchell, J. D. Muss, M. J. O'Brien, A. P. O'Grady, R. E. Pangle, E. A. Pinkard, F. I. Piper, J. A. Plaut, W. T. Pockman, J. Quirk, K. Reinhardt, F. Ripullone, M. G. Ryan, A. Sala, S. Sevanto, J. S. Sperry, R. Vargas, M. Vennetier, D. A. Way, C. Xu, E. A. Yepez, and N. G. McDowell. 2017. A multi-species synthesis of physiological mechanisms in drought-induced tree mortality. Nature Ecology & Evolution 1:1285.

Allen, C. D., D. D. Breshears, and N. G. McDowell. 2015. On underestimation of global vulnerability to tree mortality and forest die-off from hotter drought in the Anthropocene. Ecosphere 6:1–55.

Allen, C. D., A. K. Macalady, H. Chenchouni, D. Bachelet, N. McDowell, M. Vennetier, T. Kitzberger, A. Rigling, D. D. Breshears, E. H. (Ted) Hogg, P. Gonzalez, R. Fensham, Z. Zhang, J. Castro, N. Demidova, J.-H. Lim, G. Allard, S. W. Running, A. Semerci, and N. Cobb. 2010. A global overview of drought and heat-induced tree mortality reveals emerging climate change risks for forests. Forest Ecology and Management 259:660–684.

Amthor, J. S. 2003. Efficiency of lignin biosynthesis: a quantitative analysis. Annals of Botany 91:673–695.

Anfodillo, T., A. Deslauriers, R. Menardi, L. Tedoldi, G. Petit, and S. Rossi. 2012. Widening of xylem conduits in a conifer tree depends on the longer time of cell expansion downwards along the stem. Journal of Experimental Botany 63:837–845.

von Arx, G., A. Crivellaro, A. L. Prendin, K. Čufar, and M. Carrer. 2016. Quantitative Wood Anatomy—Practical Guidelines. Frontiers in Plant Science 7.

Barnes, W., and C. Anderson. 2017. Acetyl Bromide Soluble Lignin (ABSL) Assay for Total Lignin Quantification from Plant Biomass. BIO-PROTOCOL 7.

Barros, J., H. Serk, I. Granlund, and E. Pesquet. 2015. The cell biology of lignification in higher plants. Annals of Botany 115:1053–1074.

Boerjan, W., J. Ralph, and M. Baucher. 2003. Lignin Biosynthesis. Annual Review of Plant Biology 54:519–546.

Bond, J., L. Donaldson, S. Hill, and K. Hitchcock. 2008. Safranine fluorescent staining of wood cell walls. Biotechnic & Histochemistry: Official Publication of the Biological Stain Commission 83:161–171.

Boudet, A. M., C. Lapierre, and J. Grima-Pettenati. 1995. Biochemistry and molecular biology of lignification. New Phytologist 129:203–236.

Browning, B. L. 1967. Methods of wood chemistry. Interscience Publishers, New York,.

Cailleret, M., V. Dakos, S. Jansen, E. M. R. Robert, T. Aakala, M. M. Amoroso, J. A. Antos, C. Bigler, H. Bugmann, M. Caccianaga, J.-J. Camarero, P. Cherubini, M. R. Coyea, K. Čufar, A. J. Das, H. Davi, G. Gea-Izquierdo, S. Gillner, L. J. Haavik, H. Hartmann, A.-M. Hereş, K. R. Hultine, P. Janda, J. M. Kane, V. I. Kharuk, T. Kitzberger, T. Klein, T. Levanic, J.-C. Linares, F. Lombardi, H. Mäkinen, I. Mészáros, J. M. Metsaranta, W. Oberhuber, A. Papadopoulos, A. M. Petritan, B. Rohner, G. Sangüesa-Barreda, J. M. Smith, A. B. Stan, D. B. Stojanovic, M.-L. Suarez, M. Svoboda, V. Trotsiuk, R. Villalba, A. R. Westwood, P. H. Wyckoff, and J. Martínez-Vilalta. 2019. Early-Warning Signals of Individual Tree Mortality Based on Annual Radial Growth. Frontiers in Plant Science 9.

Cailleret, M., S. Jansen, E. M. R. Robert, L. Desoto, T. Aakala, J. A. Antos, B. Beikircher, C. Bigler, H. Bugmann, M. Caccianiga, V. Čada, J. J. Camarero, P. Cherubini, H. Cochard, M. R. Coyea, K. Čufar, A. J. Das, H. Davi, S. Delzon, M. Dorman, G. Gea-Izquierdo, S. Gillner, L. J. Haavik, H. Hartmann, A.-M. Hereş, K. R. Hultine, P. Janda, J. M. Kane, V. I. Kharuk, T. Kitzberger, T. Klein, K. Kramer, F. Lens, T. Levanic, J. C. L. Calderon, F. Lloret, R. Lobo-Do-Vale, F. Lombardi, R. L. Rodríguez, H. Mäkinen, S. Mayr, I. Mészáros, J. M. Metsaranta, F. Minunno, W. Oberhuber, A. Papadopoulos, M. Peltoniemi, A. M. Petritan, B.

Rohner, G. Sangüesa-Barreda, D. Sarris, J. M. Smith, A. B. Stan, F. Sterck, D. B. Stojanović, M. L. Suarez, M. Svoboda, R. Tognetti, J. M. Torres-Ruiz, V. Trotsiuk, R. Villalba, F. Vodde, A. R. Westwood, P. H. Wyckoff, N. Zafirov, and J. Martínez-Vilalta. 2017. A synthesis of radial growth patterns preceding tree mortality. Global Change Biology 23:1675–1690.

Das, A. J., N. L. Stephenson, and K. P. Davis. 2016. Why do trees die? Characterizing the drivers of background tree mortality. Ecology 97:2616–2627.

Deslauriers, A., M. Beaulieu, L. Balducci, A. Giovannelli, M. J. Gagnon, and S. Rossi. 2014. Impact of warming and drought on carbon balance related to wood formation in black spruce. Annals of Botany 114:335–345.

Deslauriers, A., S. Rossi, T. Anfodillo, and A. Saracino. 2008. Cambial phenology, wood formation and temperature thresholds in two contrasting years at high altitude in southern Italy. Tree Physiology 28:863–871.

Donaldson, L. A., A. P. Singh, A. Yoshinaga, and K. Takabe. 1999. Lignin distribution in mild compression wood of *Pinus radiata*. Canadian Journal of Botany 77:41–50.

Ferrenberg, S., J. M. Kane, and J. B. Mitton. 2014. Resin duct characteristics associated with tree resistance to bark beetles across lodgepole and limber pines. Oecologia 174:1283–1292.

Franceschi, V. R., P. Krokene, E. Christiansen, and T. Krekling. 2005. Anatomical and chemical defenses of conifer bark against bark beetles and other pests. New Phytologist 167:353–376.

Fukushima, R. S., and R. D. Hatfield. 2004. Comparison of the Acetyl Bromide Spectrophotometric Method with Other Analytical Lignin Methods for Determining Lignin Concentration in Forage Samples. Journal of Agricultural and Food Chemistry 52:3713–3720.

Gärtner, H., S. Lucchinetti, and F. H. Schweingruber. 2014. New perspectives for wood anatomical analysis in dendrosciences: The GSL1-microtome. Dendrochronologia 32:47–51.

Gidh, A. V., S. R. Decker, C. H. See, M. E. Himmel, and C. W. Williford. 2006. Characterization of lignin using multi-angle laser light scattering and atomic force microscopy. Analytica Chimica Acta 555:250–258.

Gindl, W. 2001. Cell-wall lignin content related to tracheid dimensions in drought-sensitive austrian pine (*Pinus nigra*). IAWA Journal 22:113–120.

Griffin, D., and K. J. Anchukaitis. 2014. How unusual is the 2012–2014 California drought? Geophysical Research Letters 41:2014GL062433.

Grissino-Mayer, H. D. 2001. Evaluating Crossdating Accuracy: A Manual and Tutorial for the Computer Program COFECHA. Tree-Ring Research.

Hacke, U. G., and J. S. Sperry. 2001. Functional and ecological xylem anatomy. Perspectives in Plant Ecology, Evolution and Systematics 4:97–115.

Hacke, U. G., J. S. Sperry, W. T. Pockman, S. D. Davis, and K. A. McCulloh. 2001. Trends in wood density and structure are linked to prevention of xylem implosion by negative pressure. Oecologia 126:457–461.

Hagedorn, F., J. Joseph, M. Peter, J. Luster, K. Pritsch, U. Geppert, R. Kerner, V. Molinier, S. Egli, M. Schaub, J.-F. Liu, M. Li, K. Sever, M. Weiler, R. T. W.

Siegwolf, A. Gessler, and M. Arend. 2016. Recovery of trees from drought depends on belowground sink control. Nature Plants 2:16111.

Hasibeder, R., L. Fuchslueger, A. Richter, and M. Bahn. 2015. Summer drought alters carbon allocation to roots and root respiration in mountain grassland. The New Phytologist 205:1117–1127.

Hatfield, R., and R. S. Fukushima. 2005. Can Lignin Be Accurately Measured? Crop Science 45:832–839.

Hicke, J. A., A. J. H. Meddens, and C. A. Kolden. 2016. Recent Tree Mortality in the Western United States from Bark Beetles and Forest Fires. Forest Science 62:141–153.

Hoch, G., A. Richter, and Ch. Körner. 2003. Non-structural carbon compounds in temperate forest trees. Plant, Cell & Environment 26:1067–1081.

IPCC. 2014. Climate Change 2014: Impacts,Adaptation, and Vulnerability. Part A: Global and Sectoral Aspects. Contribution of Working Group II to the Fifth Assessment Report of the Intergovernmental Panel on Climate Change. Page 1132. Cambridge University Press, Cambridge, UK and New York, USA.

Jensen, E. C. 2013. Quantitative Analysis of Histological Staining and Fluorescence Using ImageJ. The Anatomical Record 296:378–381.

Kannenberg, S. A., K. A. Novick, and R. P. Phillips. 2017. Coarse roots prevent declines in whole-tree non-structural carbohydrate pools during drought in an isohydric and an anisohydric species. Tree Physiology:1–9.

Kraus, J. E., H. C. de Sousa, M. H. Rezende, N. M. Castro, C. Vecchi, and R. Luque. 1998. Astra Blue and Basic Fuchsin Double Staining of Plant Materials. Biotechnic & Histochemistry 73:235–243.

Kutscha, N., and J. R. Gray. 1972. TB53: The Suitability of Certain Stains for Studying Lignification in Balsam Fir, *Abies balsamea* (L.) Mill.

Lauder, J. D., E. V. Moran, and S. C. Hart. 2019. Fight or Flight? Potential tradeoffs between drought defense and reproduction in conifers. Tree Physiology tpz031.

Li, X., C. Sun, B. Zhou, and Y. He. 2015. Determination of Hemicellulose, Cellulose and Lignin in Moso Bamboo by Near Infrared Spectroscopy. Scientific Reports 5:17210.

Liu, L., X. P. Ye, A. R. Womac, and S. Sokhansanj. 2010. Variability of biomass chemical composition and rapid analysis using FT-NIR techniques. Carbohydrate Polymers 81:820–829.

Lupoi, J. S., S. Singh, R. Parthasarathi, B. A. Simmons, and R. J. Henry. 2015. Recent innovations in analytical methods for the qualitative and quantitative assessment of lignin. Renewable and Sustainable Energy Reviews 49:871–906.

Martin, A. R., S. C. Thomas, and Y. Zhao. 2013. Size-dependent changes in wood chemical traits: a comparison of neotropical saplings and large trees. AoB Plants 5.

Martin-Sampedro, R., E. A. Capanema, I. Hoeger, J. C. Villar, and O. J. Rojas. 2011. Lignin Changes after Steam Explosion and Laccase-Mediator Treatment of Eucalyptus Wood Chips. Journal of Agricultural and Food Chemistry 59:8761–8769.

McKay, S. A. B., W. L. Hunter, K.-A. Godard, S. X. Wang, D. M. Martin, J. Bohlmann, and A. L. Plant. 2003. Insect Attack and Wounding Induce Traumatic Resin Duct Development and Gene Expression of (—)-Pinene Synthase in Sitka Spruce. Plant Physiology 133:368–378.

Mencuccini, M. 2003. The ecological significance of long-distance water transport: short-term regulation, long-term acclimation and the hydraulic costs of stature across plant life forms. Plant, Cell & Environment 26:163–182.

Moreira-Vilar, F. C., R. de C. Siqueira-Soares, A. Finger-Teixeira, D. M. de Oliveira, A. P. Ferro, G. J. da Rocha, M. de L. L. Ferrarese, W. D. dos Santos, and O. Ferrarese-Filho. 2014. The Acetyl Bromide Method Is Faster, Simpler and Presents Best Recovery of Lignin in Different Herbaceous Tissues than Klason and Thioglycolic Acid Methods. PLOS ONE 9:e110000.

Nakano, J., and G. Meshitsuka. 1992. The Detection of Lignin. Pages 23–32 *in* D. S. Y. Lin and P. E. D. C. W. Dence, editors. Methods in Lignin Chemistry. Springer Berlin Heidelberg.

Novaes, E., M. Kirst, V. Chiang, H. Winter-Sederoff, and R. Sederoff. 2010. Lignin and Biomass: A Negative Correlation for Wood Formation and Lignin Content in Trees1. Plant Physiology 154:555–561.

Oberhuber, W., I. Swidrak, D. Pirkebner, and A. Gruber. 2011. Temporal dynamics of nonstructural carbohydrates and xylem growth in *Pinus sylvestris* exposed to drought. Canadian Journal of Forest Research 41:1590–1597.

Pandey, K. K., and A. J. Pitman. 2004. Examination of the lignin content in a softwood and a hardwood decayed by a brown-rot fungus with the acetyl bromide method and Fourier transform infrared spectroscopy. Journal of Polymer Science Part A: Polymer Chemistry 42:2340–2346.

Perdih, F., and A. Perdih. 2011. Lignin selective dyes: quantum-mechanical study of their characteristics. Cellulose 18:1139–1150.

Pereira, L., A. P. Domingues-Junior, S. Jansen, B. Choat, and P. Mazzafera. 2018. Is embolism resistance in plant xylem associated with quantity and characteristics of lignin? Trees 32:349–358.

Piper, F. I. 2011. Drought induces opposite changes in the concentration of non-structural carbohydrates of two evergreen Nothofagus species of differential drought resistance. Annals of Forest Science 68:415–424.

Pittermann, J., J. S. Sperry, J. K. Wheeler, U. G. Hacke, and E. H. Sikkema. 2006. Mechanical reinforcement of tracheids compromises the hydraulic efficiency of conifer xylem. Plant, Cell & Environment 29:1618–1628.

Pradhan Mitra, P., and D. Loqué. 2014. Histochemical Staining of Arabidopsis thaliana Secondary Cell Wall Elements. Journal of Visualized Experiments : JoVE.

R Development Core Team. 2020. R: A language and environment for statistical computing. R Foundation for Statistical Computing, Vienna, Austria.

Regent Instruments Canada Inc. 2017. winDENDRO for Tree-ring Analysis.

Rossi, S., H. Morin, and A. Deslauriers. 2012. Causes and correlations in cambium phenology: towards an integrated framework of xylogenesis. Journal of Experimental Botany 63:2117–2126.

Sala, A., D. R. Woodruff, and F. C. Meinzer. 2012. Carbon dynamics in trees: feast or famine? Tree Physiology 32:764–775.

Schindelin, J. 2015. The ImageJ ecosystem: An open platform for biomedical image analysis.

Schwanninger, M., J. C. Rodrigues, N. Gierlinger, and B. Hinterstoisser. 2011. Determination of Lignin Content in Norway Spruce Wood by Fourier Transformed near Infrared Spectroscopy and Partial Least Squares Regression. Part 1: Wavenumber Selection and Evaluation of the Selected Range. Journal of Near Infrared Spectroscopy 19:319–329.

Sevanto, S., and L. T. Dickman. 2015. Where does the carbon go?—Plant carbon allocation under climate change. Tree Physiology 35:581–584.

Speer, J. 2010. Fundamentals of Tree Ring Research. University of Arizona Press.

Sperry, J. S. 2003. Evolution of water transport and xylem structure. International Journal of Plant Sciences 164:s115–s127.

Sperry, J. S., U. G. Hacke, and J. Pittermann. 2006. Size and function in conifer tracheids and angiosperm vessels. American Journal of Botany 93:1490–1500.

Tecan Trading AG. Tecan M200 Pro UV Spectrophotometer. Switzerland.

Ursache, R., T. G. Andersen, P. Marhavý, and N. Geldner. 2018. A protocol for combining fluorescent proteins with histological stains for diverse cell wall components. The Plant Journal 93:399–412.

Vanholme, R., B. Demedts, K. Morreel, J. Ralph, and W. Boerjan. 2010. Lignin Biosynthesis and Structure. Plant Physiology 153:895–905.

Voelker, S. L., B. Lachenbruch, F. C. Meinzer, P. Kitin, and S. H. Strauss. 2011. Transgenic poplars with reduced lignin show impaired xylem conductivity, growth efficiency and survival. Plant, Cell & Environment 34:655–668.

Wagner, A., L. Donaldson, and J. Ralph. 2012. Chapter 2. Lignification and Lignin Manipulations in Conifers. Pages 37–76 Advances in Botanical Research.

Woodruff, D. R., B. J. Bond, and F. C. Meinzer. 2004. Does turgor limit growth in tall trees? Plant, Cell & Environment 27:229–236.

Yamashita, S., M. Yoshida, S. Takayama, and T. Okuyama. 2007. Stem-righting Mechanism in Gymnosperm Trees Deduced from Limitations in Compression Wood Development. Annals of Botany 99:487–493.

Yoshinaga, A., H. Kusumoto, F. Laurans, G. Pilate, and K. Takabe. 2012. Lignification in poplar tension wood lignified cell wall layers. Tree Physiology 32:1129–1136.

Zhang, Y., S. Legay, Y. Barrière, V. Méchin, and D. Legland. 2013. Color quantification of stained maize stem section describes lignin spatial distribution within the whole stem. Journal of Agricultural and Food Chemistry 61:3186–3192.

Table 3.1. Results of comparisons of ABSL and Mean density by tree species and survival status. Mean density = mean red intensity by thin section area (total red density divided by total number of image pixels), ABSL = acetyl bromide soluble lignin. T-tests were used for comparisons with only two groups, while 3-factor analysis of variance (ANOVA) was used to test for year effects. Bold values represent significance at α =0.05.

Variable	Factor	n	Test	*p*
ABSL	Survival Status	165	T-test	0.484
ABSL	Survival Status, PIPO only	87	T-test	0.622
ABSL	**Species, Living only**	118	T-test	**0.005**
Mean density	**Survival Status**	165	T-test	**<0.001**
Mean density	**Survival Status, PIPO only**	87	T-test	**<0.001**
Mean density	**Species, Living only**	118	T-test	**0.017**
ABSL	**Year**	165	ANOVA	**0.036**
	Survival Status	165	ANOVA	0.065
	Species	165	ANOVA	**0.002**
Mean density	**Year**	165	ANOVA	**0.04**
	Survival Status	165	ANOVA	**<0.001**
	Species	165	ANOVA	**0.055**

Table 3.2. Results of linear models comparing stain-derived lignin concentration estimates to acetyl bromide soluble lignin measurements. Mean density = mean red intensity by thin section area (total red density divided by total number of image pixels), ABSL = acetyl bromide soluble lignin, T-S = "thickness-to-span", the ratio of tracheid wall thickness to lumen diameter. Bold values represent significance at α = 0.05.

Model	*n*	*p*	R^2
Mean density ~ ABSL	165	0.092	0.013
Mean density ~ ABSL, living only	**118**	**0.008**	**0.062**
Mean density ~ ABSL, dead only	**47**	**<0.001**	**0.261**
Mean density ~ ABSL, living PIPO only	52	0.523	0.01
Mean density ~ ABSL, dead PIPO only	**35**	**<0.001**	**0.290**
Mean density ~ ABSL, living PIJE only	**66**	**0.001**	**0.179**
Mean density ~ ABSL + Year + SPP + Status	**165**	**<0.001**	**0.222**
Mean density ~ ABSL + Year + Status, PIPO only	**87**	**<0.001**	**0.246**
Mean density ~ ABSL + Year, living PIJE only	**66**	**0.001**	**0.211**
T-S ~ ABSL	**165**	**0.016**	**0.069**
T-S ~ ABSL + Status	**165**	**0.050**	**0.059**
T-S ~ ABSL, living only	118	0.062	0.075
T-S ~ ABSL, dead only	47	0.128	0.041

Model notation: Response ~ predictors

Table 3.3. Approximate average time per sample (minutes) necessary for each activity associated with Acetyl Bromide-derived (ABSL) and stain-derived (Stain) lignin concentration estimates.

Method	Active Analysis	Time	Passive Analysis	Time	Hazards	Total Time
ABSL	Removal of rings	1.00			Low	110.77
	Grinding	5.00			Low	
	Homogenizing	5.33			Low	
	Acetone Extraction	1.50	Acetone Extraction	90.00	Medium	
	Acetyl Bromide Extraction	4.00		0.94	High	
	Final Sample Dilution	1.00			Medium	
	UV Absorbance	2.00			Low	
Stain	Thin Section Preparation[1]	20.00			Low	23.23
	Image Collation	3.00			None	
	Script preparation[2]	0.00	Running of Script	0.23	None	

[1]Optional depending on other analyses (e.g., only necessary if thin sections are not already being taken)
[2]See Appendix A for pre-packaged script

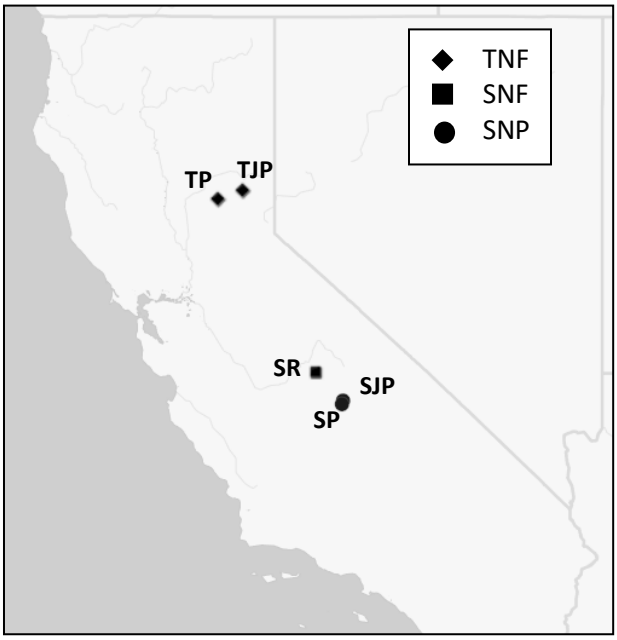

Figure 3.1. Sample site locations. SP = "Sequoia Ponderosa", SJP = "Sequoia Jeffrey Ponderosa" in Sequoia National Park (SNP). SR = "Soaproot Ponderosa" in Sierra National Forest (SNF). TP = "Tahoe Ponderosa", TJP = "Tahoe Jeffrey Ponderosa" in Tahoe National Forest (TNF).

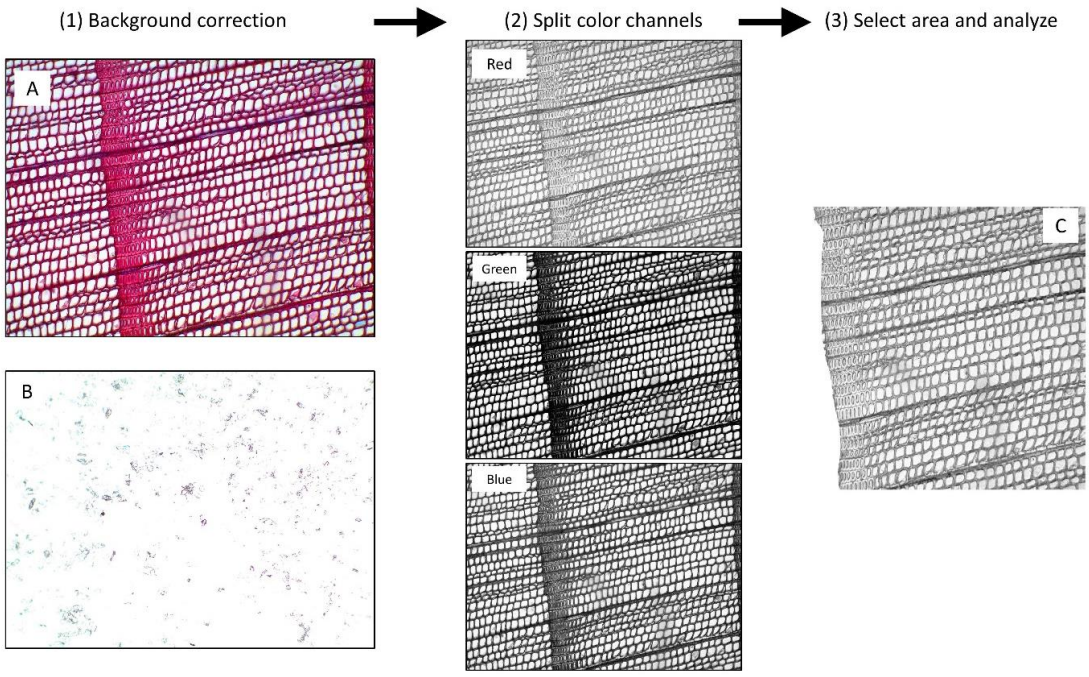

Figure 3.2. Steps involved in lignin quantification via stain intensity measurement. The imageJ script (Appendix A) first applies a background correction to the raw stained thin section image (A) to correct for microscope slide noise from dust, excess mounting medium, etc. (B). The script then splits the image into RGB channels, and selects the red channel. Finally, the script prompts the user to outline the region of interest for final image quantification (C).

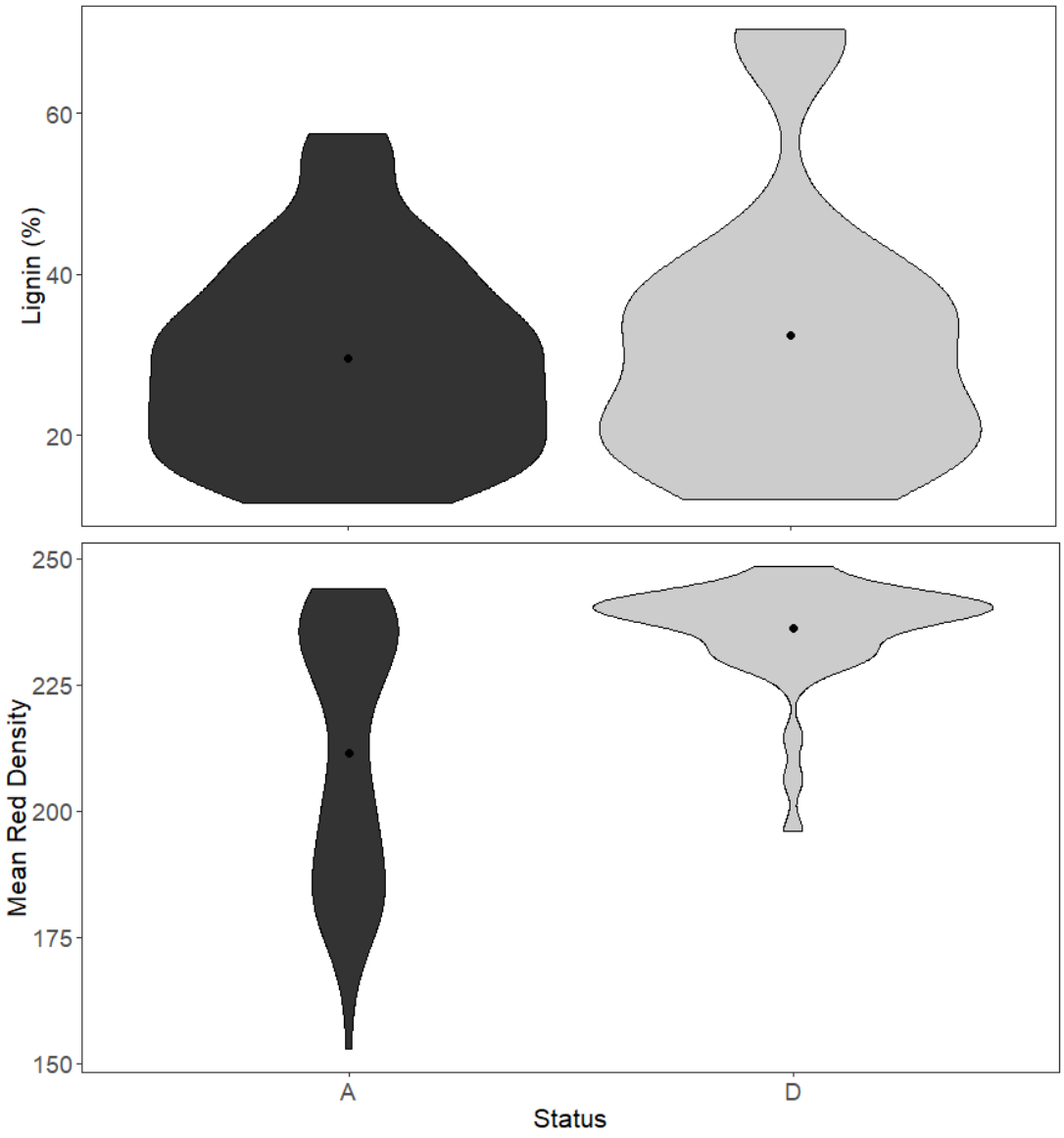

Figure 3.3. Violin plots of lignin concentration in living (A) and dead (D) tree ring samples from *Pinus ponderosa* and *P. jeffreyi* in the Sierra Nevada over 2011-2018. Width of figure represents number of samples with a given lignin value. Black dots represent mean values. Lignin concentrations were measured using a modified Acetyl Bromide extraction method (top) and a stain-derived estimate of lignin content (bottom).

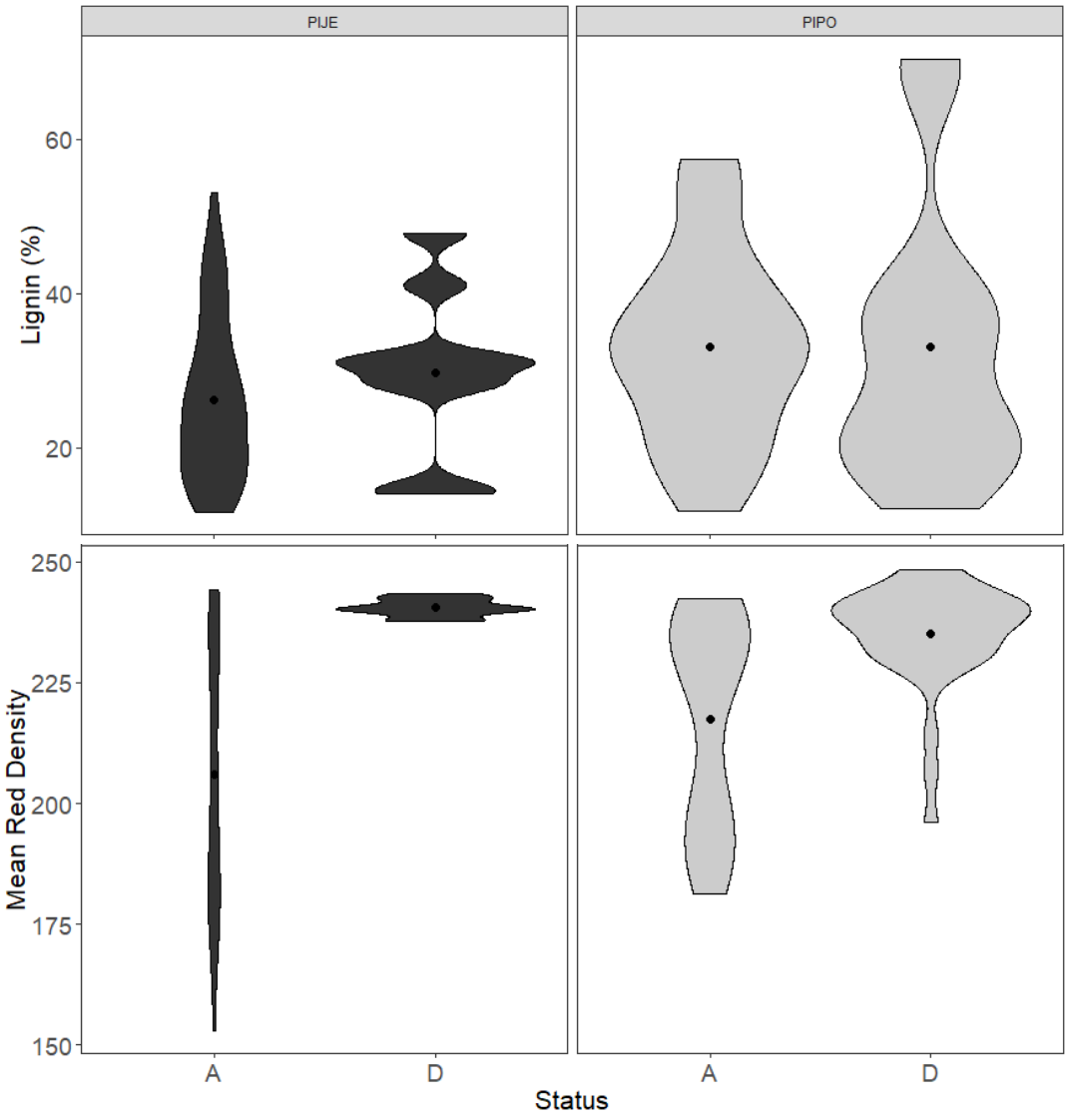

Figure 3.4. Violin plots of lignin concentrations by species and tree status. A = Alive, D = Dead, PIJE = *Pinus jeffreyi*, PIPO = *P. ponderosa.* Width of figure represents number of samples with a given lignin value. Black dots represent mean values. Lignin concentrations were measured using a modified Acetyl Bromide extraction method (top) and a stain-derived estimate of lignin content (bottom).

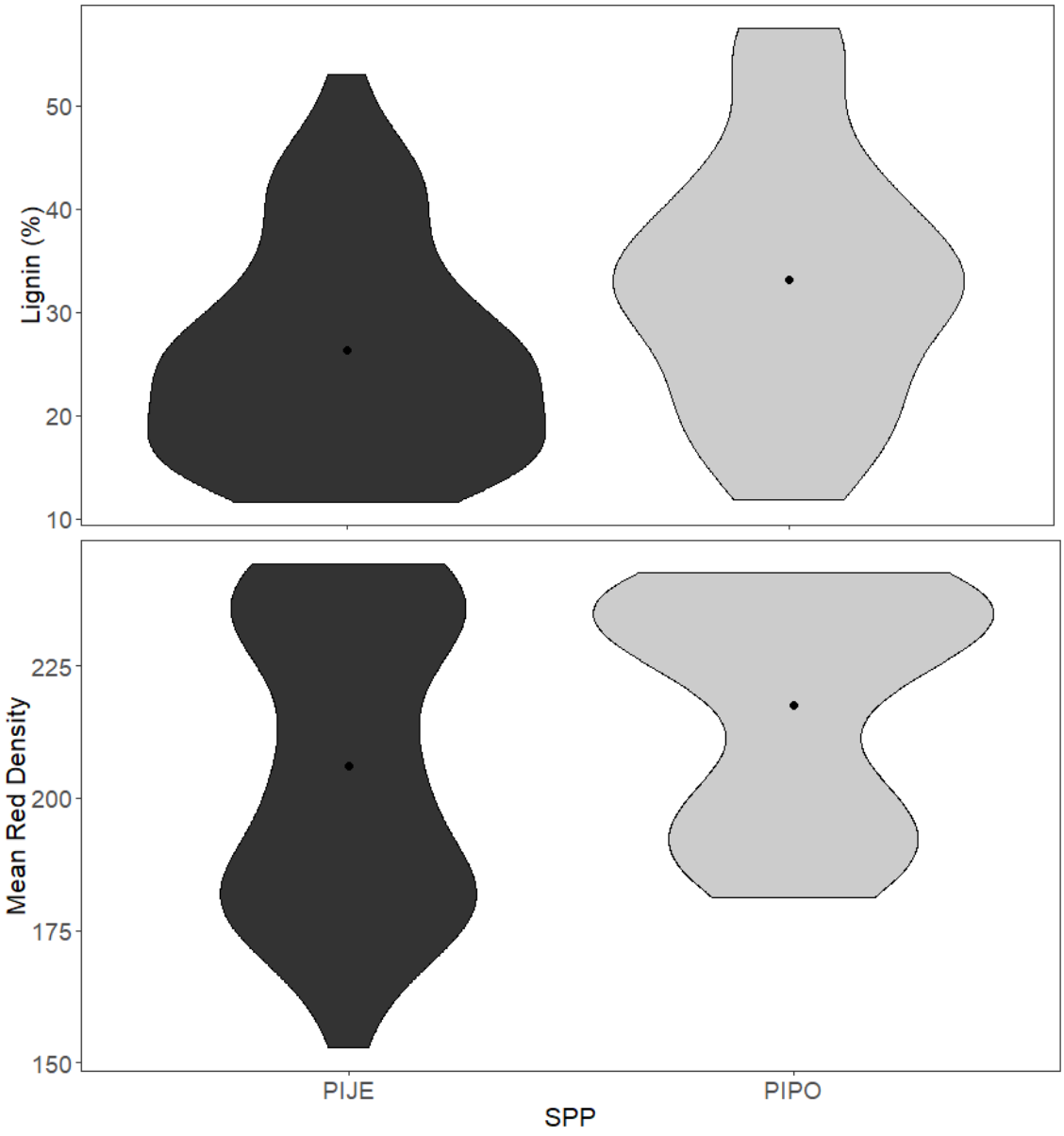

Figure 3.5. Violin plots of lignin concentrations by species in living *Pinus jeffreyi* (PIJE) and *P. ponderosa* (PIPO) trees only. Width of figure represents number of samples with a given lignin value. Black dots represent mean values. Lignin concentrations were measured using a modified Acetyl Bromide extraction method (top) and a stain-derived estimate of lignin content (bottom).

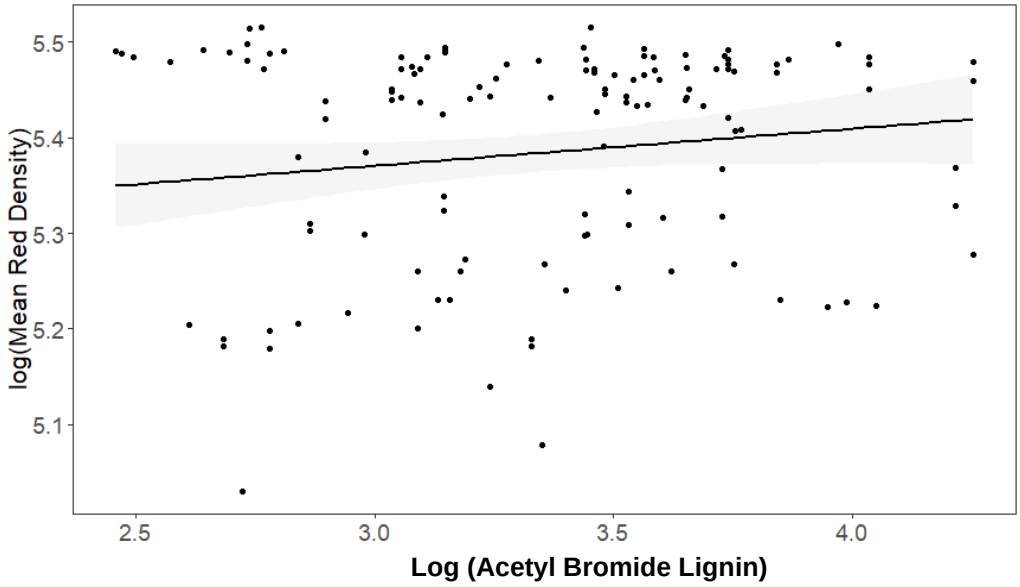

Figure 3.6. Linear regression of Mean Red Density against acetyl bromide-derived lignin concentrations. Both variables were log-transformed due to heteroscedasticity (heavy left skew for red density, and right skew for % Lignin, respectively). R^2 = 0.013, p = 0.092, n = 165). Shaded region represents 95% confidence interval of regression line.

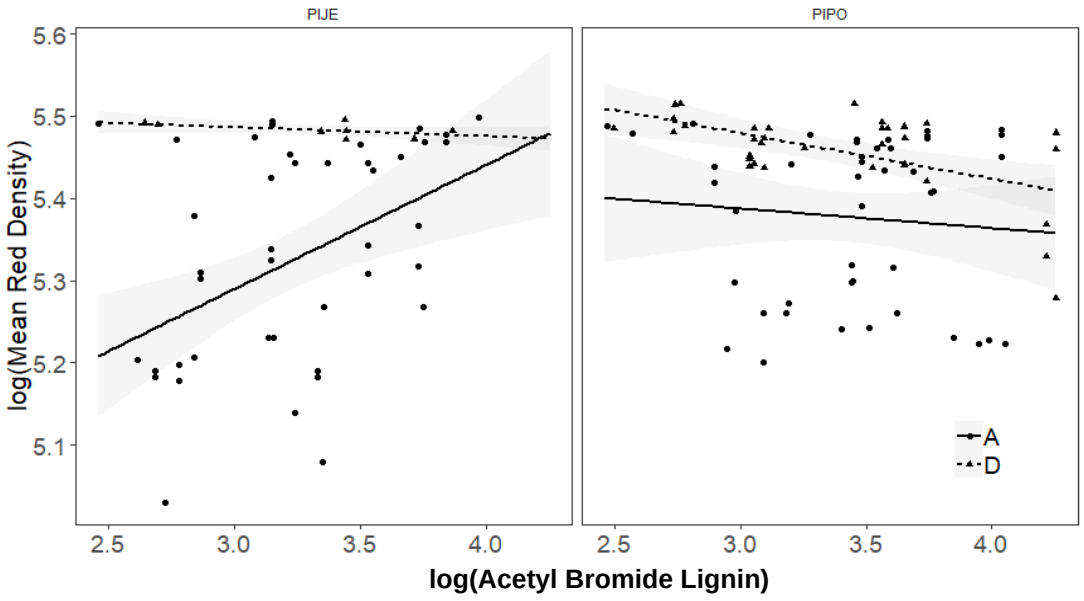

Figure 3.7. Linear regression of Mean Red Density again chemically measured lignin concentrations by status. A = Alive, D = Dead. R^2 = 0.062 and = 0.261 , p = 0.008 and <0.001 for living and dead trees, respectively. Shaded region represents 95% confidence interval of regression line.

Figure 3.8. Lignin concentration z-scores over time in living (A) and dead (D) tree ring samples. Z-scores were used to place estimated lignin concentrations on comparable scales. Solid lines with dark shaded areas represent Acetyl Bromide-derived lignin, while dashed lines with light grey shaded area represent mean red density. Shaded areas represent 95% confidence intervals.

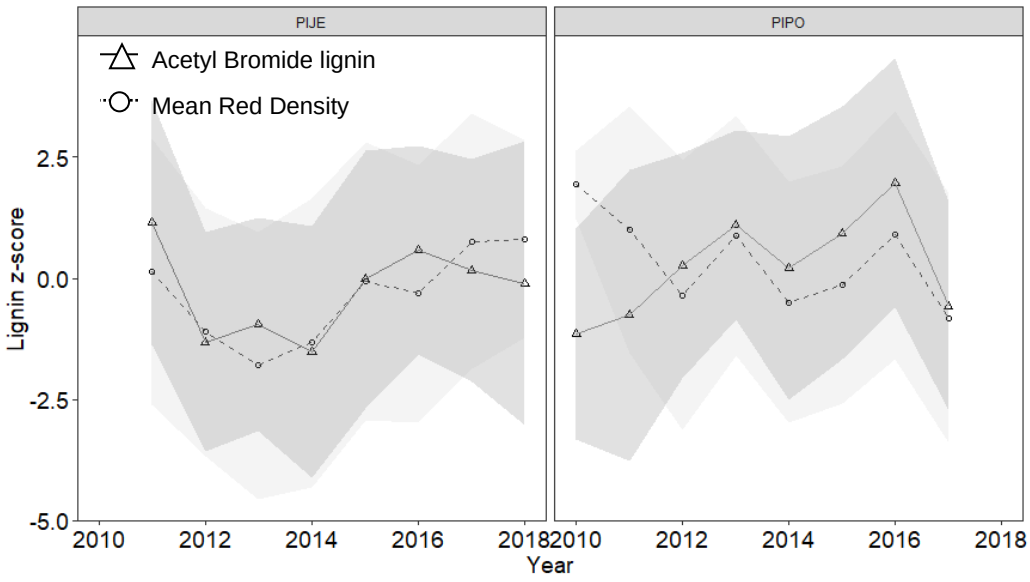

Figure 3.9. Lignin concentration z-scores over time in living *Pinus jeffreyi* (PIJE) and *P. ponderosa* (PIPO) tree ring samples. Z-scores were used to place estimated lignin concentrations on comparable scales. Solid lines with dark shaded areas represent Acetyl Bromide-derived lignin, while dashed lines with light grey shaded area represent mean red density. Shaded areas represent 95% confidence intervals.

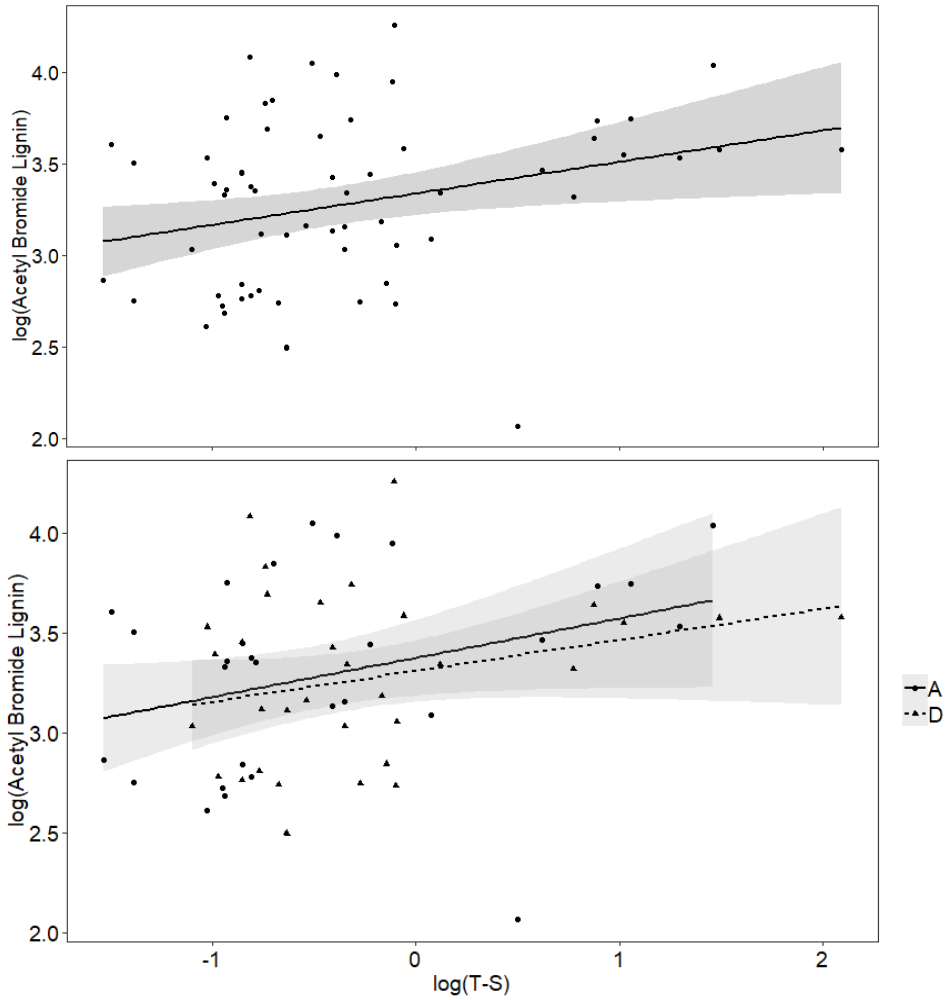

Figure 3.10. Relationship between Acetyl Bromide lignin and thickness-to-span (T-S, the ratio of tracheid wall thickness to lumen diameter) in all measured trees (top, R^2 = 0.069, p = 0.016), and when separating living and dead (R^2 = 0.075 and 0.041, p = 0.062 and 0.128, n = 165, respectively). Species effects were not significant.

Supplementary Material

Table S3.1. Results of t-tests and ANOVA when including "low quality" thin sections with potentially artificially inflated stain intensities.

Variable	Factor	Test	*p*
ABSL	Survival Status	T-test	0.1955
ABSL	Survival Status, PIPO only	T-test	0.535
ABSL	**Species, Living only**	T-test	**0.006**
Mean density	**Survival Status**	T-test	**<0.001**
Mean density	**Survival Status, PIPO only**	T-test	**0.013**
Mean density	**Species, Living only**	T-test	**0.006**
ABSL	**Year**	ANOVA	**0.030**
	Survival Status	ANOVA	0.397
	Species	ANOVA	**0.007**
Mean density	**Year**	ANOVA	**0.011**
	Survival Status	ANOVA	**0.003**
	Species	*ANOVA*	*0.255*

Table S3.2. Model results when using "low quality" thin sections. Bold values represent significance at $\alpha = 0.05$. Italicized values represent models that changed from significant to not significant following inclusion of low quality sections.

Model	*p*	R^2
Mean density ~ ABSL	0.072	0.0145
Mean density ~ ABSL, living only	**0.008**	**0.058**
Mean density ~ ABSL, dead only	*0.8481*	*0.004*
Mean density ~ ABSL, living PIPO only	0.5398	0.010
Mean density ~ ABSL, dead PIPO only	*0.755*	*0.019*
Mean density ~ ABSL, living PIJE only	**0.017**	**0.071**
Mean density ~ ABSL + Year + SPP + Status	**<0.001**	**0.092**
Mean density ~ ABSL + Year + Status, PIPO only	**<0.001**	**0.119**
Mean density ~ ABSL + Year, living PIJE only	**0.039**	**0.069**

Table S3.3. Results of t-tests and ANOVA after removing dead tree samples with > 50% lignin content to test for a "decay" effect.

Variable	Factor	Test	*p*
ABSL	Survival Status	T-test	0.993
ABSL	Survival Status, PIPO only	T-test	0.211
ABSL	**Species, Living only**	T-test	**0.045**
Mean density	**Survival Status**	T-test	**<0.001**
Mean density	**Survival Status, PIPO only**	T-test	**<0.001**
Mean density	**Species, Living only**	T-test	**0.007**
ABSL	*Year*	ANOVA	*0.530*
	Survival Status	ANOVA	0.843
	Species	ANOVA	*0.122*
Mean density	**Year**	ANOVA	**0.025**
	Survival Status	ANOVA	**<0.001**
	Species	ANOVA	**0.013**

Table S3.4. Model results when excluding high lignin outliers in dead trees to test for "decay effect." Bold values represent significance at $\alpha = 0.05$. Italic values represent models that changed from significant to not significant following inclusion of outliers.

Model	*p*	R^2
Mean density ~ ABSL	**0.031**	**0.029**
Mean density ~ ABSL, living only	**0.006**	**0.072**
Mean density ~ ABSL, dead only	*0.126*	*0.038*
Mean density ~ ABSL, living PIPO only	0.745	0.02
Mean density ~ ABSL, dead PIPO only	*0.1392*	*0.045*
Mean density ~ ABSL, living PIJE only	**0.003**	**0.151**
Mean density ~ ABSL + Year + SPP + Status	**<0.001**	**0.298**
Mean density ~ ABSL + Year + Status, PIPO only	**<0.001**	**0.311**
Mean density ~ ABSL + Year, living PIJE only	**0.002**	**0.202**

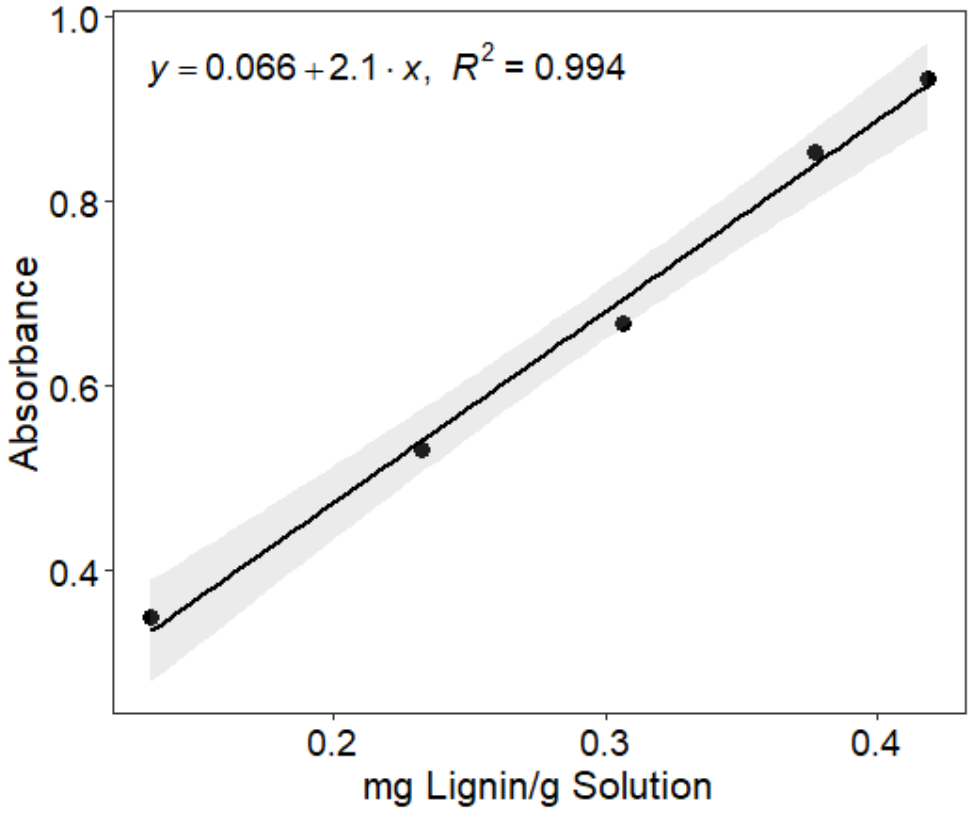

Figure S3.1. Standard curve derived from UV-absorbance measurements of kraft lignin (Sigma Aldrich 370959) digested in acetyl bromide and acetic acid and measured at 280nm.

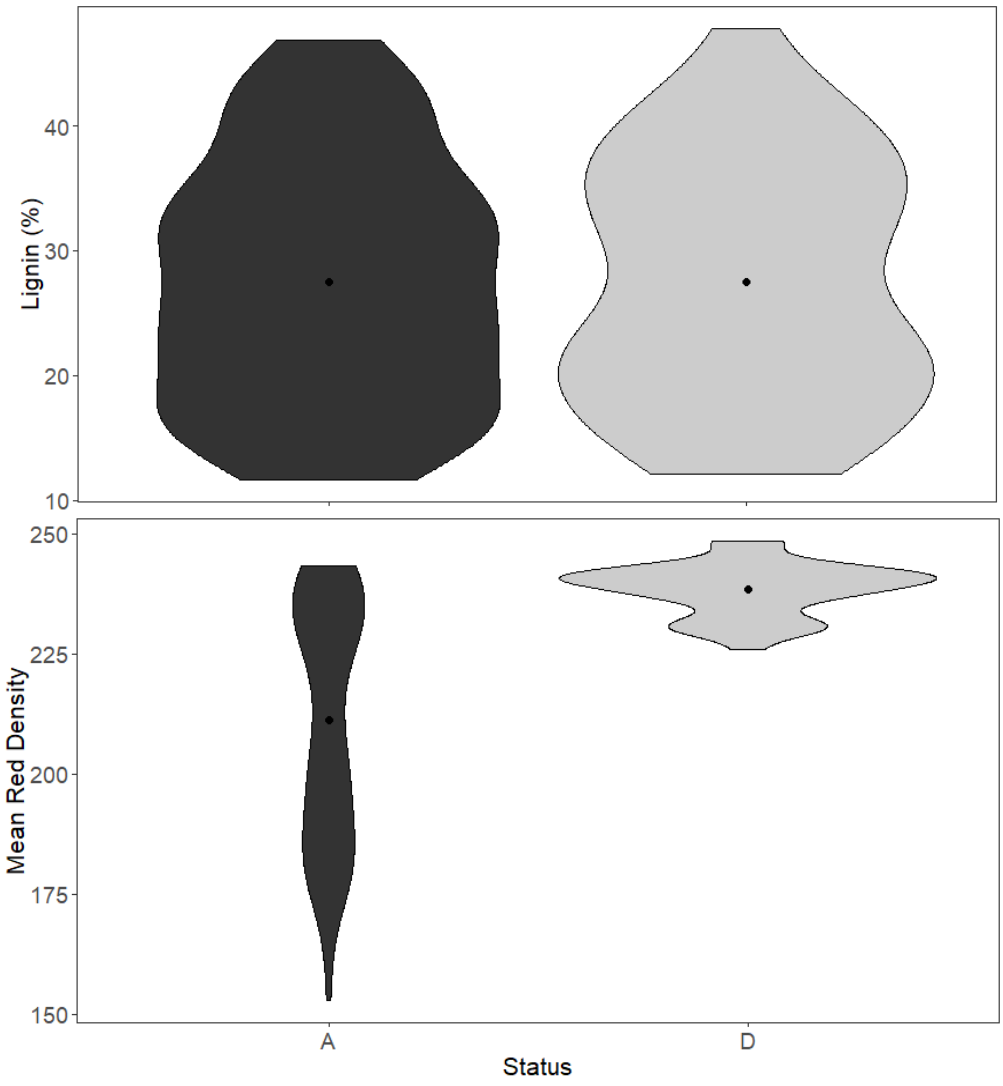

Figure S3.2. Violin plots of lignin concentration in living (A, left side) and dead (D, right side) *P. ponderosa* and *P. jeffreyi*, separated by species after removal of high lignin concentration outliers. Width of figure represents number of samples with a given lignin value. Black dots represent mean values. Lignin concentrations were measured using a modified Acetyl Bromide extraction method (top) and a stain-derived estimate of lignin content (bottom).See text for rationale behind outlier use in final analyses.

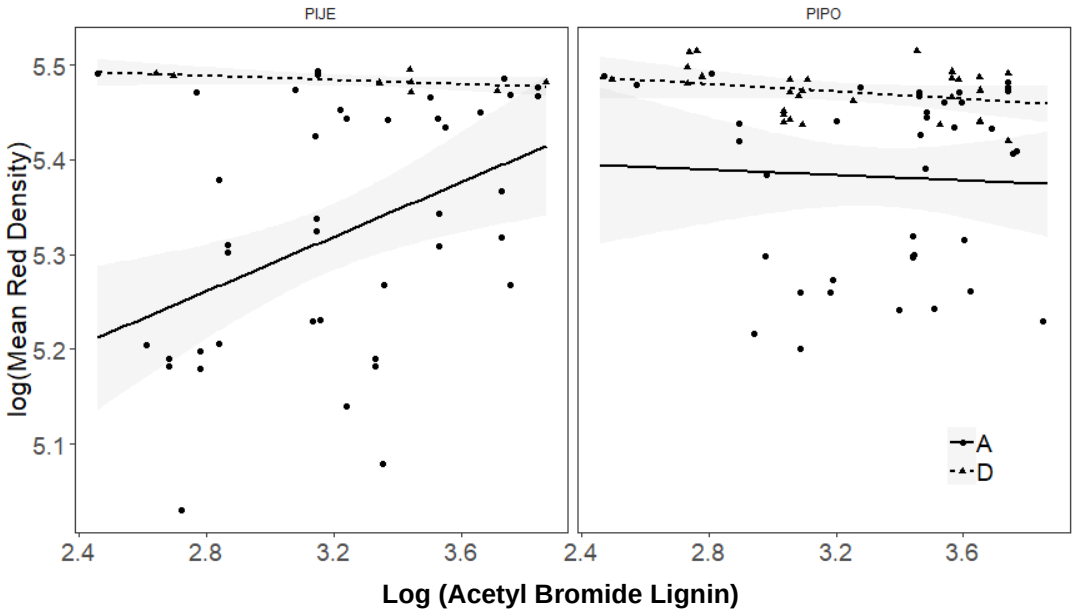

Figure S3.3. Mean Red Density (red intensity, which ranges from 0-255) of thin sections versus Lignin % measured via the acetyl bromide method across all trees, separated by species, after removal of high lignin outliers. A = Alive, D = Dead. See text for rationale behind outlier use in final analyses.

Chapter 4:
How dry is dry? Comparison of drought metric ability to predict tree growth

4.0 Abstract

Global climate models predict increasing temperatures and more variable precipitation in already arid and semi-arid forests. Our ability to model forest response to climatic change depends on reducing uncertainty in relationships between forest health and climate. Many current, widely used climate models incorporate derived drought metrics—measures of water deficit based on relationships between temperature and precipitation—into their projections. However, the ability of these drought metrics to predict biological response to water deficit is often justified based on theory and not direct measurements. Here, we use tree rings from 866 trees sampled from across the Sierra Nevada of California to ask which of five widely available drought metrics best predicts measured ring width. We discuss spatial variability and sensitivity of each metric to wet and dry years, and applicability of each metric to projections of forest response to future drought. We show that Palmer Drought Severity Index (PDSI) and a measure of precipitation minus evapotranspiration (P-ET) derived from eddy flux tower-calibrated remotely sensed ET measurements are the best predictors of changes in ring width. We also show that P-ET shows large differences between locations, while climatic moisture deficit (CMD) from the ClimateNA model shows the smallest differences between locations. We find that PDSI is most sensitive to dry years, while climatic water deficit (CWD) is most sensitive to wet years.

4.1 Introduction

Current climate projections include increased temperatures and precipitation variability in drought-prone forests (Cook et al. 2010, IPCC 2014). Increasing drought frequency and intensity is predicted to lead to declines in forest productivity and increased large-scale tree mortality events (Allen et al. 2010), with greater than 50% loss of needleleaf evergreen trees in arid areas like the desert southwest of North America by 2100 (McDowell et al. 2016). Quantifying tree response to drought has implications for forest management (Clark et al. 2016, Vose et al. 2016), water resources (Adams et al. 2012, Goulden and Bales 2014), fire risk (Dale et al. 2001, Westerling et al. 2006), and carbon sequestration (Powers et al. 2013). However, considerable uncertainty remains in current large-scale drought metric datasets and their ability to accurately quantify biologically meaningful changes in water availability.

"Drought" as a concept is superficially simple, yet it can be challenging to quantify and the proper definition of drought can depend on the question at hand (Palmer 1965). For instance, should it be defined in terms of the total amount of precipitation, the amount of moisture potentially available to plants given runoff or evaporation, or the degree of moisture stress experienced by the plants themselves? Some of the drought metrics that aim to represent water availability include climatic water deficit (CWD, Stephenson 1990, 1998), climatic moisture deficit (CMD, Wang et al. 2011), Palmer Drought Severity Index (PDSI, Palmer 1965), and hydrothermal deficit (HTD, Clark et

al. 2016). The basis for these metrics is the frequent observation of increased plant water stress as precipitation and/or soil moisture decrease and temperature increases.

The majority of drought metrics are derived using simplified modeling frameworks that make potentially unrealistic assumptions about hydrologic and plant physiological processes, or use calculations that are not biologically meaningful. For example, PDSI assumes that the top (arbitrarily defined, typically ~150 mm) layer of soil contains 1 inch (2.54 cm) of water at field capacity (Palmer 1965), limiting its ability to capture spatial variability in drought extremes outside of its calibration source in the Midwestern United States (Alley 1984). In highly topographically diverse landscapes, soil depth and water holding capacity can vary widely. This can lead to drastic over-predictions of drought at large spatial scales (Sheffield and Wood 2008, Seneviratne et al. 2012). Similarly, CWD relies on soil water holding capacity values derived from soil maps describing the upper 1.5 (Cal-BCM) or 2.5 (Dobrowski et al. 2013) m of soil. Nevertheless, biologically important water storage may occur at up to 20 m depth in some ecosystems, including the Sierra Nevada of California (Klos et al. 2018). Analyses of vegetation sensitivity to drought across time and/or space may lead to inaccurate inferences if the drought metrics they are based on do not accurately reflect the hydrologic environment experienced by plants. Given that each metric has its own nuances, it is unclear which is most useful for understanding the sensitivity of plants to drought.

Tree response to drought stress is often a function of aboveground tree physiology (McDowell et al. 2008b, McDowell 2011, Adams et al. 2017) relative to belowground access to water (Chitra-Tarak et al. 2018, Bales et al. 2018, Goulden and Bales 2019, Love et al. 2019). Variability in annual tree ring width can track water availability (Graumlich 1993, Cook et al. 2007, Boucher et al. 2014, Mokria et al. 2017), and provide a unique record of tree productivity as well as likelihood of mortality. Rapid and prolonged declines in growth often predict mortality following drought stress (Das et al. 2007, Cailleret et al. 2017, 2019), and trees that show greater sensitivity of growth to precipitation variation tend to be more likely to die due to drought (McDowell et al. 2009).

Tree rings are often used to reconstruct past conditions such as climate (Boucher et al. 2014, Mokria et al. 2017) or streamflow. Yet this fundamental principle of dendroclimatology has not yet been used to ground-truth widely used drought metrics; one exception is a study on variations of PDSI across Europe (Bhuyan et al. 2017). Further, over-reliance on tree ring records from the international tree ring database—which by design only includes trees sampled from semi-arid environments on rocky outcrops or otherwise climate-sensitive locations—can lead to biased interpretations and overall high predictions of drought impacts on vegetation (Klesse et al. 2018, Zhao et al. 2019).

Here, we use tree ring records from across the Sierra Nevada of California to assess drought metric utility for predicting tree growth. We focus on the Sierra Nevada due to its Mediterranean climate and seasonal drought, as well as to leverage knowledge gained during the 2012-2016 California drought. The first half of this drought was the most intense experienced by the region in approximately 1200 years (Griffin and Anchukaitis 2014). As a result, this four-year period was associated with widespread tree

mortality driven by drought, competition and bark beetle infestation (Hicke et al. 2016, Young et al. 2017). We ask how responsive five widely available and popular drought metrics are to known dry and wet years, and which metrics best match annual tree growth in dominant Sierra Nevada conifers.

4.2 Methods

4.2.1 Dendrochronology

We sampled 866 trees from across the Sierra Nevada of California (Figure 4.1) from two tree-core datasets: (1) randomly selected dominant trees within 11 permanent 0.8 ha sampling plots in Sequoia National Park, Sierra National Forest, and Tahoe National Forest selected to fall within the ranges of ponderosa pine (*Pinus ponderosa*), Jeffrey pine (*P. jeffreyi*),, or their overlap; and (2) dominant (>20 cm diameter at breast height, DBH) trees and co-dominant competitors at point locations across the Sierra Nevada, randomly placed within the Douglas fir (*Pseudotsuga menziesii*) range in sites stratified by aspect. The species included in this analysis were the three target species - *Pseudotsuga mensziessii, Pinus ponderosa,* and *P. jeffreyi* - plus *P. sabiniana* (grey pine), *P. lambertiana* (sugar pine), *Abies concolor* (white fir), and *A. magnifica* (red fir). Unlike the many dendroclimatology studies, which target trees expected to be more climate-sensitive than average, this approach should yield a more typical range of responses for adult trees.

All trees were cored at breast height using a Haglof 4.37 mm diameter increment borer (Haglof, Sweden). We transported cores to the laboratory for standard dendrochronological sample preparation (Speer 2010); we surfaced them using progressively finer grits of sandpaper and scanned them at 600 dpi for ring width measurement.

Cores were analyzed using winDENDRO (Regent Instruments Canada Inc. 2017) and cooRecorder (Cybis Electronic 2013) tree ring software; two software packages were used due to differences in sampling times and laboratory software availability among the authors. Rings were automatically detected in winDENRO and corrected manually by two observers to confirm ring boundary locations, while samples analyzed in cooRecorder had ring boundaries manually identified. Ring widths were measured to the nearest 0.01 mm. We cross-dated cores to confirm ring years in multiple ways. Cores in cooRecorder were assessed for overall correlation among cores, with cores with low correlation manually checked and removed from analysis if cross-dating was not possible. Cores in winDENDRO were both visually and statistically cross-dated within winDENDRO and adjusted to note missing or false rings or incorrect outer year dates, then checked using the COFECHA statistical cross-dating program. Cores flagged by COFECHA were manually checked, and dropped from analysis if adjustments were not possible given evidence from the cores. Finally, winDENDRO cores and cooRecorder cores were visually cross-dated using the "list" method. We visually ensured that marker years (e.g. the dry 1967/1977 period) matched across chronologies to ensure consistency across both core datasets, and found marker years were consistently represented.

We converted ring widths to unit-less ring-width indices (RWI) by detrending with a 20-year smoothing spline. A 20-year spline was first calculated for each core, and then raw ring width was divided by this spline value, yielding large values for years of

rapid growth and small values for years of slow growth. This removes low-frequency climate variability (such as ENSO or long-term trends), as well as age-based declines in growth, leaving only annual variability due to annual climatic variation or biological impacts (Speer 2010, Sullivan et al. 2016).

4.2.2 Climate Data

We selected five drought metrics from among popular drought metrics used to model forest drought, particularly in western North American and California forests. We performed a brief meta-analysis to identify the most frequently used drought metrics in California (Figure S4.1), as well as two relatively recent models of drought based on measured evapotranspiration (ET). We focused on selecting at least one model from this final set that uses each of the predominant ET estimation methods. This allowed us to account for variation in ET calculations (Table 4.1). The drought metrics examined were:

1. Climatic moisture deficit (CMD) from ClimateNA (Wang et al. 2011, 2016)
2 & 3. Palmer Drought Severity Index (PDSI) and water deficit (DEF) extracted from TerraClim (Abatzoglou et al. 2018)
4.Climatic Water Deficit (CWD) from Cal-BCM (Flint et al. 2013)
5. A metric of precipitation minus ET (P-ET) using ET calculated from LandSat-derived Normalized Differential Vegetation Index (NDVI) and eddy flux tower-measured ET (Goulden et al. 2012, Bales et al. 2018).

We extracted climate data from each of the target climate models using ArcGIS version 10.6 (ESRI 2018) and the R package "raster" for each site over the length of the climate dataset. Lengths of each climate dataset vary significantly. For example, the longest dataset is CWD, with values available from 1896-2016, but the shortest dataset, P-ET, only has data available since 1980 due to its reliance on LandSat imagery. Thus final models employed climate datasets trimmed to their common time period: 1980-2016.

4.2.3 Analysis

We conducted our analysis in three main steps: direct comparison of climate models to each other, sensitivity of climate models to wet and dry years, and comparison of models to tree ring width in trees throughout the Sierra Nevada. We assessed spatial and temporal variation in each drought metric with respect to known wet and dry periods. Year 2011 was the wettest and coldest period on record for the 1986-2016 period, whereas 2015 and 2016 were the warmest and driest (Figure 4.2). These years were used as indicator years to examine sensitivity of drought metrics to extreme years. Assessments of sensitivity to indicator years were conducted by comparing z-scores of each metric across the common period to examine temporal variability and sensitivity to extreme years. We also examined coefficients of variation (CV) for each year for each metric from the 2011-2016 period as a measure of spatial variability (variation between sample locations) during wet and dry years; higher average within-year CVs indicate higher variability across the sampling area. Finally, the ability of each drought metric to predict tree ring width was assessed using hierarchical regressions.

Ring width was modeled as a function of each drought metric individually within a Bayesian framework using Stan (Gelman et al. 2015) within the "brms" (Bürkner 2017) package for R version 3.6.2 (R Development Core Team 2020). Each tree ring was compared to drought metrics, with each drought metric nested within individual trees, each with an independent intercept:

$$RWI_{ij} \sim N(\beta_{0j} + \beta_{1j} Drought_{ij}, \sigma_y^2)$$
$$\beta_{0j} \sim N(\gamma_{00} + u_{0j}, \sigma_\beta^2)$$
$$\beta_{1j} \sim N(\gamma_{10} + u_{1j}, \sigma_\beta^2),$$

where RWI_{ij} is the logarithm of RWI of annual tree ring *i* within tree *j*; β_{0j} is the intercept for tree *j*, allowing trees to vary in their average growth; β_{1j} is the slope of the relationship between tree *j* ring width and drought metric; $Drought_{ij}$ is the scaled (z-score) drought metric value for tree ring (year) *i* at the tree *j* location; and σ_y^2 is unexplained variance in the distribution of RWI_{ij} not explained by this model. Drought metrics were nested within trees, as individual trees may differ in their drought responses for various reasons. We used the same weakly informative priors for all models after assessing visual relationships between RWI and scaled drought metrics and after considering expected relationships; priors were broad normal distributions with a mean of 0 and a standard deviation of 1. Species effects were omitted from these models because preferential sampling of *P. ponderosa, P. jeffreyi,* and *P. mensziessii* not allowing robust comparison of species effects with the other species. However, while a few species (particularly *Pinus sabiniana*) have slightly different responses, the overall response across species was fairly constant (Figure S4.1). Moreover, the goal here was to identify drought metrics that predict growth across trees in general.

In order to account for variation in sample location climate biasing our results, we removed trees sampled from locations with higher than average precipitation for each species according to their current distributions within the Sierra Nevada. This resulted in 12 chronologies being removed from further analysis. Thus, final analyses represent assessment of drought metric predictive power for ring widths in drier than average sites for each species, except for *P. ponderosa* and *P. jeffreyi*. Due to the difficulty of accurately distinguishing smaller individuals of *P. ponderosa* and *P. jeffreyi* in their zones of range overlap and differences in species identification in the two datasets used here, we calculated climate thresholds for each species individually as well as the distribution of both species, lumped here as "Yellow Pine". All 12 removed individuals were identified as "Yellow Pine" from two sites that had higher than average precipitation for both species individually and for "Yellow Pine". Thus, trees from sites with high precipitation for both species were removed from further analyses, but trees from sites that have higher than average precipitation for *P. ponderosa* but not higher than average for "Yellow Pine" may still be retained.

To examine whether a linear or non-linear model was required, we assessed linearity of models visually using spline regressions, and found that relationships between scaled drought metrics and RWI were mostly linear when species effects were not included (Figure S4.2). To assess model fit, we used posterior predictive checks and leave-one-out posterior integral transformed (LOO-PIT) predictive checks in lieu of

model information criteria. The LOO-PIT method converts response values to a uniform distribution via integral transformation, and allow visual interpretation of modeled responses to observed responses (Gabry et al. 2019). Posterior predictive checks compare raw observations with successive draws from the model posterior distribution and are often a better indicator of model fit than simple comparison of information criteria among models.

We ran each model for 10000 iterations of four chains with 3000 iterations discarded as "burn-in" (Gelman et al. 2015). Model convergence was assessed visually using trace plots, and statistically using the scale reduction factor ($\hat{R}$), with values >1.02 indicating non-convergence (Gelman et al. 2015). Predictive power of drought metrics was finally assessed by comparing credible intervals and fit from each model, and identifying parameters that converged and had credible intervals not overlapping 0, indicating that there is at least a 95% chance of a non-zero correlation between the variable and the response.

4.3 Results

We found that differences between individual drought metrics were greatest in wet and dry years. Ring width index (RWI) did not track any single drought metric over short time periods but tracked longer duration drought or wet periods (Figure 4.3). Meanwhile, PDSI and CWD were highly sensitive to specific drought and wet years, respectively. CWD was most sensitive to wet years, with its lowest value in 2011, the wettest year in the sample period. PDSI as most sensitive to dry years, with high values in 2009 and 2014. The DEF, P-ET, and CMD models all appeared to track dry and wet periods well but were not as sensitive to extreme years as CWD and PDSI. P-ET also demonstrated a rapid "recovery" period following dry years, with z-scores declining more rapidly following a dry year than the other metrics. Interestingly, all five metrics were in almost complete agreement during the 2001-2004 period and were particularly well correlated with RWI during this time. Use of PDSI may over-emphasize dry years, while use of CWD may over-emphasize wet years.

We found interesting patterns in spatial variability (as demonstrated by high within-year variation across sites) that do not match expectations relative to model resolution. Whereas CMD is calculated at the highest resolution of the models compared here, P-ET (the second highest resolution dataset) was the most spatially variable drought metric across all years, while CWD (the third highest resolution dataset) is the most spatially variable in anomalously dry years. Spatial variability was highest in P-ET and lowest in CMD and DEF (Figure 4.4). Spatial variability in CWD was low in drought years but high in a wet year (2011). Spatial variability in P-ET was very high in dry years, but low in 2011, and spatial variability in PDSI was higher in wet years than dry years. Use of P-ET may over-estimate drought spatial variability, while the other metrics may under-estimate it. Further comparisons of each model with direct measurements of soil moisture are needed to compare these sensitivities with real-world values as opposed to the intermodal comparison presented here.

We found that the drought metrics compared here vary somewhat in their ability to predict tree growth. Bayesian models all achieved convergence ($1.00 < \hat{R} < 1.01$ for all predictors). Those using PDSI and P-ET as the drought metric had the best fit according

to LOO-PIT comparisons, although no model had a notably poor fit. Posterior predictive checks (Figure 4.5) and LOO-PIT comparisons (Figure S4.3) demonstrated that no models had extreme deviations between model predictions and raw data. PDSI and P-ET also had the greatest effects on RWI among all models, though the effect sizes were rather small for all drought metrics (Figure 4.6, Table 4.2). The posterior estimate of the effect of CMD on RWI was the lowest of the drought metrics (Figure 4.6, Figure 4.7), but also had the smallest credible interval (variance, Figure 4.6), demonstrating less uncertainty in posterior predictions. Credible intervals of PDSI and P-ET overlapped, but the posterior probability for PDSI was slightly higher, indicating PDSI may be most correlated with RWI, but not significantly different from the effect of P-ET on RWI. These results demonstrate that choice of drought metric can influence modeled ring width, particularly in anomalously wet or dry years.

4.4 Discussion

Here we evaluated the ability of widely used drought metrics to predict tree ring width (RWI) and found that drought metrics do vary in their ability to predict tree growth. Our observation that each metric varies in its sensitivity to wet versus dry years, as well as in their ability to predict tree growth overall, may reflect inherent differences in the underlying method of calculation for each metric. Further, the assumptions implicated in each metric calculation may not always reflect true hydrologic processes in a natural landscape. For example, Climatic moisture deficit (CMD) is computed as annual potential evapotranspiration (PET) – annual precipitation (Wang et al. 2016). This lacks biological meaning because it does not account for water storage in soil and snow or the seasonal interactions of energy and water (Stephenson and Das 2011). Climatic water deficit (CWD) is interpreted to represent unrealized evaporative demand (Stephenson 1998). It is computed as PET minus actual evapotranspiration (AET). AET represents the amount of water evaporated and transpired from a site given actual water availability, whereas PET represents the amount of evapotranspiration expected given unlimited water supply, and therefore purely reflects available energy (Stephenson 1990). Although AET is mechanistically related to important plant processes, particularly transpiration and photosynthesis (Rosenzweig 1968), CWD is not.

Different vegetation types can differ substantially in the amount of solar radiation, heat, and/or water limitation they experience, as well as in their response to that stress. This change in response can then shift estimates of ET in ways that may not reflect actual shifts in plant-available soil moisture. Many species exhibit dormancy or persistence as seeds through hot and/or dry periods (Volaire and Norton 2006). Some species reduce photosynthesis, stomatal conductance, and thus transpiration when water availability declines in order to conserve water and/or reduce physiological damage (McDowell et al. 2008a, West et al. 2012, Nardini et al. 2014, Skelton et al. 2015), and others store water in succulent leaves and stems for continued relatively normal photosynthesis when the surrounding environment is dry (Bartlett et al. 2012). A reduction in ET and increase in CWD as water availability declines is thus not necessarily associated with water stress or environmental (un)suitability.

Further complicating interpretation and use of drought metrics is their inclusion of parameters that difficult to accurately measure. Computing CWD requires modeling PET

and AET values across a landscape based on temperature and precipitation and simplified hydrological processes (e.g., Willmott et al. 1985, Dobrowski et al. 2013, Flint et al. 2013). Despite the potential value of metrics such as CWD for understanding drought sensitivity of plants, it is difficult to tell the degree to which current methods reflect biologically meaningful water availability and stress. Direct measurement of AET requires lysimeters or eddy flux towers (Dingman 2002), and measurement of PET would require thoroughly watering the site(s) of interest first, or extensive sampling when water is not limiting. Because of the difficulty of obtaining values empirically, water balance values used in ecology (Willmott et al. 1985, Dobrowski et al. 2013, Flint et al. 2013) are usually derived from models parameterized for agricultural crops, short green grass, or simple modifications thereof, for which relationships have been more thoroughly studied and validated (e.g. PDSI, Alley 1984). The reliability of such models for plot-level estimates in natural ecosystems has not been evaluated. The physiological and hydrological assumptions inherent in these models affect not only the absolute estimates of AET and CWD (e.g., comparison of values derived by Stephenson 1998, Lutz et al. 2010, and Flint et al. 2013), but also their relative variation across a landscape and, by extension, through time (Derek Young, University of California Davis, unpublished data).

The variability in the ability of each metric to predict tree growth may partly reflect variability in soil moisture storage. The ability of trees to resist ongoing drought stress is dependent on below ground hydrologic 'refugia' (McDowell et al. 2019). Increasing evidence points to the importance of deep rooting for drought tolerance (Brunner et al. 2015), and that bedrock-depth water availability buffers drought stress (Goulden and Bales 2014, 2019, Bales et al. 2018). In fact, simulations of tree response to drought incorporating evaporative demand and deep soil rooting showed that removal of deep roots led to significantly reduced stem water potential (an indicator of drought stress) and led to rapid increases in tree mortality (Millar et al. 2017). However, Chitra-Tarak et al. (2018) also found that trees classified as rooting in deep bedrock zones were more likely to die during prolonged drought as their rooting zone had slower recharge than trees rooted in more shallow soils. Only P-ET has been explicitly modeled and tested as a measure of deep soil water capacity (Bales et al. 2018), while PDSI, CWD, and DEF all only assume 1.5 m soil depth. Soil porosity in PDSI, CWD, and DEF are all parameterized using regionally-specific field measurements, with only CWD being parameterized for California. However, a preliminary analysis of ring width, P-ET and CWD at the heavily instrumented Southern Sierra Critical Zone Observatory (SSCZO) showed that both metrics appear to be correlated with soil moisture down to 90 cm, which predicted ring width in a small subsample of trees (Lauder, unpublished data).

Differences in spatial resolution can potentially impact predictive ability of each drought metric. The metrics tested here represent a wide range of spatial resolutions: CMD is estimated as a scale-less point-measurement using elevation-corrected downscaling, P-ET is measured at 30 m resolution, CWD is measured at 270 m resolution, and DEF and PDSI are measured at 4 km resolution. If resolution played a significant role in differences in measured drought, we would predict higher spatial variability in higher-resolution metrics. Spatial variability was higher in P-ET than CMD across all years, even though CMD is calculated at a higher resolution. Further, in wet

years, DEF and PDSI were more spatially variable than CMD and CWD. Although this is not a direct test of the impact of spatial resolution on ring width predictive power, it does demonstrate that across our sampled sites, resolution alone does not explain differences in measured drought variability. Future studies, however, should scale each metric to a common resolution and assess differences in model output.

An important driver of drought stress and its impacts is forest density. Many reconstructions of past climate using dendrochronological records focus on tree rings measured in climate-sensitive trees, little influenced by plant competition for resources like soil water. In western forests that have experienced intensive drought-induced die-off, competition amplifies drought stress and is a significant covariate in models of drought susceptibility (Young et al. 2017, Asner et al. 2016). We did not include competition in our model due to incompatibility in the methods used for calculating competition in each dataset. This analysis combined data from cores extracted from target trees sampled over a wide range with competition estimated using Voronoi polygons with data from cores extracted from trees sampled in intensively sampled plots with full forest inventories. Voronoi polygons are derived using neighboring trees as vertices of a polygon centered on the sampled tree, with area of the polygon used as a proxy for the region of tree influence (an inverse proxy of competition). While we were able to calculate Voronoi polygons for trees sampled in forest inventory plots, the polygons for trees in the wide-ranging dataset derived from measurements taken from nearby dominant neighbors along bearing lines. We were able to roughly approximate similar estimates for our plot-based trees, but edge effects from trees sampled near a plot edge did not allow estimation of a truly comparable Voronoi polygon. However, future models aiming to predict forest growth based on correlations between ring width and climate should still attempt to incorporate competition where possible.

A caveat to drought metric comparisons is that correlation between ring width and climate is an imperfect indicator of drought metric utility. Decoupling of ring width and climate in highly drought-stressed populations has been shown to predict eventual mortality (Cailleret et al. 2017, 2019). Thus, caution is warranted when interpreting high correlation as justification for use of a particular drought metric; low correlation can mean low predictive power, or simply that sampled trees have stopped responding to climate and may die soon after sampling. However, in this study, we only used living trees, rather than those that died during the drought, and conducted analyses across all tree rings for every tree since 1980. This reflects average growth response to climate over a 36-year period across individual years and individual trees. Decoupling of tree ring width from climate would not be reflected in this calculation, as it would ostensibly only decrease correlations in recent years in trees that may eventually succumb to drought. Future work should incorporate lagged effects and time-series correlations to detect degree of growth variation in direct response to climatic variation and further test for this decoupling effect.

Our results demonstrate that the capacity of widely employed drought metrics to track spatial and temporal extremes in drought as well as tree growth response to those extremes varies. By using tree ring chronologies to compare drought metrics, we were able to show that spatial resolution alone does not predict degree of spatial sensitivity to drought, but instead that the method of drought metric derivation may drive differences in

predictive power. Understanding the inherent variation and biases in each of these metrics is an important component of future models of forest response to climate change. On-going research into both the reconstruction of past climate and how current forests may respond to future conditions should carefully consider the drought metric of choice, and how well the theoretical framework underlying that drought metric reflects biologically meaningful water availability and thus true drought experienced by natural forests.

4.5 Acknowledgements

We thank John Abatzgalou for helpful comments about PDSI and TerraClim model output. We also thank Julia Morocco, Madisen Hinkley, Aubrey Hayes, Pedro Garcia, and Veronica Magana-Buie for assistance with tree core preparation and analysis. This work was financially supported by the National Science Foundation through the Southern Sierra Critical Zone Observatory (grant EAR-1331939) at the University of California, Merced and the National Geographic Society (grant CP-062ER-17), and an NSF IOS grant (1925577).

4.6 References

Abatzoglou, J. T., S. Z. Dobrowski, S. A. Parks, and K. C. Hegewisch. 2018. TerraClimate, a high-resolution global dataset of monthly climate and climatic water balance from 1958–2015. Scientific Data 5:170191.

Adams, H. D., C. H. Luce, D. D. Breshears, C. D. Allen, M. Weiler, V. C. Hale, A. M. S. Smith, and T. E. Huxman. 2012. Ecohydrological consequences of drought- and infestation- triggered tree die-off: insights and hypotheses. Ecohydrology 5:145–159.

Adams, H. D., M. J. B. Zeppel, W. R. L. Anderegg, H. Hartmann, S. M. Landhäusser, D. T. Tissue, T. E. Huxman, P. J. Hudson, T. E. Franz, C. D. Allen, L. D. L. Anderegg, G. A. Barron-Gafford, D. J. Beerling, D. D. Breshears, T. J. Brodribb, H. Bugmann, R. C. Cobb, A. D. Collins, L. T. Dickman, H. Duan, B. E. Ewers, L. Galiano, D. A. Galvez, N. Garcia-Forner, M. L. Gaylord, M. J. Germino, A. Gessler, U. G. Hacke, R. Hakamada, A. Hector, M. W. Jenkins, J. M. Kane, T. E. Kolb, D. J. Law, J. D. Lewis, J.-M. Limousin, D. M. Love, A. K. Macalady, J. Martínez-Vilalta, M. Mencuccini, P. J. Mitchell, J. D. Muss, M. J. O'Brien, A. P. O'Grady, R. E. Pangle, E. A. Pinkard, F. I. Piper, J. A. Plaut, W. T. Pockman, J. Quirk, K. Reinhardt, F. Ripullone, M. G. Ryan, A. Sala, S. Sevanto, J. S. Sperry, R. Vargas, M. Vennetier, D. A. Way, C. Xu, E. A. Yepez, and N. G. McDowell. 2017. A multi-species synthesis of physiological mechanisms in drought-induced tree mortality. Nature Ecology & Evolution 1:1285.

Allen, C. D., A. K. Macalady, H. Chenchouni, D. Bachelet, N. McDowell, M. Vennetier, T. Kitzberger, A. Rigling, D. D. Breshears, E. H. (Ted) Hogg, P. Gonzalez, R. Fensham, Z. Zhang, J. Castro, N. Demidova, J.-H. Lim, G. Allard, S. W. Running, A. Semerci, and N. Cobb. 2010. A global overview of drought and heat-induced tree mortality reveals emerging climate change risks for forests. Forest Ecology and Management 259:660–684.

Alley, W. M. 1984. The Palmer Drought Severity Index: Limitations and Assumptions. Journal of Climate and Applied Meteorology 23:1100–1109.

Asner, G. P., P. G. Brodrick, C. B. Anderson, N. Vaughn, D. E. Knapp, and R. E. Martin. 2016. Progressive forest canopy water loss during the 2012–2015 California drought. Proceedings of the National Academy of Sciences 113:E249–E255.

Bales, R. C., M. L. Goulden, C. T. Hunsaker, M. H. Conklin, P. C. Hartsough, A. T. O'Geen, J. W. Hopmans, and M. Safeeq. 2018. Mechanisms controlling the impact of multi-year drought on mountain hydrology. Scientific Reports 8.

Bartlett, M. K., C. Scoffoni, and L. Sack. 2012. The determinants of leaf turgor loss point and prediction of drought tolerance of species and biomes: a global meta-analysis. Ecology Letters 15:393–405.

Belmecheri, S., F. Babst, E. R. Wahl, D. W. Stahle, and V. Trouet. 2016. Multi-century evaluation of Sierra Nevada snowpack. Nature Climate Change 6:2–3.

Bhuyan, U., C. Zang, and A. Menzel. 2017. Different responses of multispecies tree ring growth to various drought indices across Europe. Dendrochronologia 44:1–8.

Boucher, É., J. Guiot, C. Hatté, V. Daux, P.-A. Danis, and P. Dussouillez. 2014. An inverse modeling approach for tree-ring-based climate reconstructions under changing atmospheric CO2 concentrations. Biogeosciences 11:3245–3258.

Brunner, I., C. Herzog, M. A. Dawes, M. Arend, and C. Sperisen. 2015. How tree roots respond to drought. Frontiers in Plant Science 6.

Bürkner, P.-C. 2017. brms: An R Package for Bayesian Multilevel Models Using Stan. Journal of Statistical Software 80:1–28.

Cailleret, M., V. Dakos, S. Jansen, E. M. R. Robert, T. Aakala, M. M. Amoroso, J. A. Antos, C. Bigler, H. Bugmann, M. Caccianaga, J.-J. Camarero, P. Cherubini, M. R. Coyea, K. Čufar, A. J. Das, H. Davi, G. Gea-Izquierdo, S. Gillner, L. J. Haavik, H. Hartmann, A.-M. Hereş, K. R. Hultine, P. Janda, J. M. Kane, V. I. Kharuk, T. Kitzberger, T. Klein, T. Levanic, J.-C. Linares, F. Lombardi, H. Mäkinen, I. Mészáros, J. M. Metsaranta, W. Oberhuber, A. Papadopoulos, A. M. Petritan, B. Rohner, G. Sangüesa-Barreda, J. M. Smith, A. B. Stan, D. B. Stojanovic, M.-L. Suarez, M. Svoboda, V. Trotsiuk, R. Villalba, A. R. Westwood, P. H. Wyckoff, and J. Martínez-Vilalta. 2019. Early-Warning Signals of Individual Tree Mortality Based on Annual Radial Growth. Frontiers in Plant Science 9.

Cailleret, M., S. Jansen, E. M. R. Robert, L. Desoto, T. Aakala, J. A. Antos, B. Beikircher, C. Bigler, H. Bugmann, M. Caccianiga, V. Čada, J. J. Camarero, P. Cherubini, H. Cochard, M. R. Coyea, K. Čufar, A. J. Das, H. Davi, S. Delzon, M. Dorman, G. Gea-Izquierdo, S. Gillner, L. J. Haavik, H. Hartmann, A.-M. Hereş, K. R. Hultine, P. Janda, J. M. Kane, V. I. Kharuk, T. Kitzberger, T. Klein, K. Kramer, F. Lens, T. Levanic, J. C. L. Calderon, F. Lloret, R. Lobo-Do-Vale, F. Lombardi, R. L. Rodríguez, H. Mäkinen, S. Mayr, I. Mészáros, J. M. Metsaranta, F. Minunno, W. Oberhuber, A. Papadopoulos, M. Peltoniemi, A. M. Petritan, B. Rohner, G. Sangüesa-Barreda, D. Sarris, J. M. Smith, A. B. Stan, F. Sterck, D. B. Stojanović, M. L. Suarez, M. Svoboda, R. Tognetti, J. M. Torres-Ruiz, V. Trotsiuk, R. Villalba, F. Vodde, A. R. Westwood, P. H. Wyckoff, N. Zafirov, and

J. Martínez-Vilalta. 2017. A synthesis of radial growth patterns preceding tree mortality. Global Change Biology 23:1675–1690.

Charney, N. D., F. Babst, B. Poulter, S. Record, V. M. Trouet, D. Frank, B. J. Enquist, and M. E. K. Evans. 2016. Observed forest sensitivity to climate implies large changes in 21st century North American forest growth. Ecology Letters 19:1119–1128.

Chitra-Tarak, R., L. Ruiz, H. S. Dattaraja, M. S. M. Kumar, J. Riotte, H. S. Suresh, S. M. McMahon, and R. Sukumar. 2018. The roots of the drought: Hydrology and water uptake strategies mediate forest-wide demographic response to precipitation. Journal of Ecology 106:1495–1507.

Clark, J. S., L. Iverson, C. W. Woodall, C. D. Allen, D. M. Bell, D. C. Bragg, A. W. D'Amato, F. W. Davis, M. H. Hersh, I. Ibanez, S. T. Jackson, S. Matthews, N. Pederson, M. Peters, M. W. Schwartz, K. M. Waring, and N. E. Zimmermann. 2016. The impacts of increasing drought on forest dynamics, structure, and biodiversity in the United States. Global Change Biology 22:2329–2352.

Cook, E. R., R. Seager, M. A. Cane, and D. W. Stahle. 2007. North American drought: Reconstructions, causes, and consequences. Earth-Science Reviews 81:93–134.

Cook, E. R., R. Seager, R. R. Heim, R. S. Vose, C. Herweijer, and C. Woodhouse. 2010. Megadroughts in North America: placing IPCC projections of hydroclimatic change in a long-term palaeoclimate context. Journal of Quaternary Science 25:48–61.

Cybis Electronic. 2013. CDendro and CooRecorder V.7.7.

Dale, V. H., L. A. Joyce, S. McNulty, R. P. Neilson, M. P. Ayres, M. D. Flannigan, P. J. Hanson, L. C. Irland, A. E. Lugo, C. J. Peterson, D. Simberloff, F. J. Swanson, B. J. Stocks, and B. M. Wotton. 2001. Climate Change and Forest Disturbances Climate change can affect forests by altering the frequency, intensity, duration, and timing of fire, drought, introduced species, insect and pathogen outbreaks, hurricanes, windstorms, ice storms, or landslides. BioScience 51:723–734.

Das, A. J., J. J. Battles, N. L. Stephenson, and P. J. van Mantgem. 2007. The relationship between tree growth patterns and likelihood of mortality: a study of two tree species in the Sierra Nevada. Canadian Journal of Forest Research 37:580–597.

Dingman, S. L. 2002. Physical hydrology. Prentice-Hall Inc. USA.

Dobrowski, S. Z., J. Abatzoglou, A. K. Swanson, J. A. Greenberg, A. R. Mynsberge, Z. A. Holden, and M. K. Schwartz. 2013. The climate velocity of the contiguous United States during the 20th century. Global Change Biology 19:241–251.

ESRI. 2018. ArcGIS. Environmental Systems Research Institute, Redlands, CA.

Fisher, J. B., T. A. DeBiase, Y. Qi, M. Xu, and A. H. Goldstein. 2005. Evapotranspiration models compared on a Sierra Nevada forest ecosystem. Environmental Modelling & Software 20:783–796.

Flint, L. E., A. L. Flint, J. H. Thorne, and R. Boynton. 2013. Fine-scale hydrologic modeling for regional landscape applications: the California Basin Characterization Model development and performance. Ecological Processes 2:1–21.

Gabry, J., D. Simpson, A. Vehtari, M. Betancourt, and A. Gelman. 2019. Visualization in Bayesian workflow. Journal of the Royal Statistical Society. Series A (Statistics in Society) 182:389–402.

Gelman, A., D. Lee, and J. Guo. 2015. Stan: A Probabilistic Programming Language for Bayesian Inference and Optimization. Journal of Educational and Behavioral Statistics 40:530–543.

Goulden, M. L., R. G. Anderson, R. C. Bales, A. E. Kelly, M. Meadows, and G. C. Winston. 2012. Evapotranspiration along an elevation gradient in California's Sierra Nevada. Journal of Geophysical Research: Biogeosciences 117:G03028.

Goulden, M. L., and R. C. Bales. 2014. Mountain runoff vulnerability to increased evapotranspiration with vegetation expansion. Proceedings of the National Academy of Sciences 111:14071–14075.

Goulden, M. L., and R. C. Bales. 2019. Regional forest die-off during warm drought is linked to mult-year deep soil drying. Nature Geoscience.

Graumlich, L. J. 1993. A 1000-Year Record of Temperature and Precipitation in the Sierra Nevada. Quaternary Research 39:249–255.

Griffin, D., and K. J. Anchukaitis. 2014. How unusual is the 2012–2014 California drought? Geophysical Research Letters 41:2014GL062433.

Hicke, J. A., A. J. H. Meddens, and C. A. Kolden. 2016. Recent Tree Mortality in the Western United States from Bark Beetles and Forest Fires. Forest Science 62:141–153.

IPCC. 2014. Climate Change 2014: Impacts,Adaptation, and Vulnerability. Part A: Global and Sectoral Aspects. Contribution of Working Group II to the Fifth Assessment Report of the Intergovernmental Panel on Climate Change. Page 1132. Cambridge University Press, Cambridge, UK and New York, USA.

Klesse, S., R. J. DeRose, C. H. Guiterman, A. M. Lynch, C. D. O'Connor, J. D. Shaw, and M. E. K. Evans. 2018. Sampling bias overestimates climate change impacts on forest growth in the southwestern United States. Nature Communications 9:1–9.

Klos, P. Z., M. L. Goulden, C. S. Riebe, C. L. Tague, A. T. O'Geen, B. A. Flinchum, M. Safeeq, M. H. Conklin, S. C. Hart, A. A. Berhe, P. C. Hartsough, W. S. Holbrook, and R. C. Bales. 2018. Subsurface plant-accessible water in mountain ecosystems with a Mediterranean climate. Wiley Interdisciplinary Reviews: Water 5:e1277.

Love, D. M., M. D. Venturas, J. S. Sperry, P. D. Brooks, J. L. Pettit, Y. Wang, W. R. L. Anderegg, X. Tai, and D. S. Mackay. 2019. Dependence of Aspen Stands on a Subsurface Water Subsidy: Implications for Climate Change Impacts. Water Resources Research 55:1833–1848.

Lutz, J. A., J. W. van Wagtendonk, and J. F. Franklin. 2010. Climatic water deficit, tree species ranges, and climate change in Yosemite National Park. Journal of Biogeography 37:936–950.

McDowell, N. G. 2011. Mechanisms linking drought, hydraulics, carbon metabolism, and vegetation mortality. Plant Physiology 155:1051–1059.

McDowell, N. G., C. D. Allen, and L. Marshall. 2009. Growth, carbon-isotope discrimination, and drought-associated mortality across a *Pinus ponderosa* elevational transect. Global Change Biology 16:399–415.

McDowell, N. G., C. Grossiord, H. D. Adams, S. Pinzón-Navarro, D. S. Mackay, D. D. Breshears, C. D. Allen, I. Borrego, L. T. Dickman, A. Collins, M. Gaylord, N. McBranch, W. T. Pockman, A. Vilagrosa, B. Aukema, D. Goodsman, and C. Xu. 2019. Mechanisms of a coniferous woodland persistence under drought and heat. Environmental Research Letters 14:045014.

McDowell, N. G., A. P. Williams, C. Xu, W. T. Pockman, L. T. Dickman, S. Sevanto, R. Pangle, J. Limousin, J. Plaut, D. S. Mackay, J. Ogee, J. C. Domec, C. D. Allen, R. A. Fisher, X. Jiang, J. D. Muss, D. D. Breshears, S. A. Rauscher, and C. Koven. 2016. Multi-scale predictions of massive conifer mortality due to chronic temperature rise. Nature Climate Change 6:295–300.

McDowell, N., W. T. Pockman, C. D. Allen, D. D. Breshears, N. Cobb, T. Kolb, J. Plaut, J. Sperry, A. West, D. G. Williams, and E. A. Yepez. 2008a. Mechanisms of plant survival and mortality during drought: why do some plants survive while others succumb to drought? New Phytologist 178:719–739.

McDowell, N., W. T. Pockman, C. D. Allen, D. D. Breshears, N. Cobb, T. Kolb, J. Plaut, J. Sperry, A. West, D. G. Williams, and E. A. Yepez. 2008b. Mechanisms of plant survival and mortality during drought: why do some plants survive while others succumb to drought? New Phytologist 178:719–739.

Millar, D. J., B. E. Ewers, D. S. Mackay, S. Peckham, D. E. Reed, and A. Sekoni. 2017. Improving ecosystem-scale modeling of evapotranspiration using ecological mechanisms that account for compensatory responses following disturbance. Water Resources Research 53:7853–7868.

Mokria, M., A. Gebrekirstos, A. Abiyu, M. Van Noordwijk, and A. Bräuning. 2017. Multi-century tree-ring precipitation record reveals increasing frequency of extreme dry events in the upper Blue Nile River catchment. Global Change Biology 23:5436–5454.

Nardini, A., M. A. Lo Gullo, P. Trifilò, and S. Salleo. 2014. The challenge of the Mediterranean climate to plant hydraulics: Responses and adaptations. Environmental and Experimental Botany 103:68–79.

Palmer, W. C. 1965. Meteorological Drought. Page 58. U.S. Weather Bureau.

Powers, E. M., J. D. Marshall, J. Zhang, and L. Wei. 2013. Post-fire management regimes affect carbon sequestration and storage in a Sierra Nevada mixed conifer forest. Forest Ecology and Management 291:268–277.

R Development Core Team. 2020. R: A language and environment for statistical computing. R Foundation for Statistical Computing, Vienna, Austria.

Regent Instruments Canada Inc. 2017. winDENDRO for Tree-ring Analysis.

Rosenzweig, M. L. 1968. Net primary productivity of terrestrial communities: prediction from climatological data. American Naturalist:67–74.

Seneviratne, S. I., N. Nicholls, D. Easterling, C. M. Goodess, S. Kanae, J. Kossin, Y. Luo, J. Marengo, K. Mc Innes, M. Rahimi, M. Reichstein, A. Sorteberg, C. Vera, X. Zhang, M. Rusticucci, V. Semenov, L. V. Alexander, S. Allen, G. Benito, T. Cavazos, J. Clague, D. Conway, P. M. Della-Marta, M. Gerber, S. Gong, B. N. Goswami, M. Hemer, C. Huggel, B. Van den Hurk, V. V. Kharin, A. Kitoh, A. M. G. Klein Tank, G. Li, S. Mason, W. Mc Guire, G. J. Van Oldenborgh, B. Orlowsky, S. Smith, W. Thiaw, A. Velegrakis, P. Yiou, T. Zhang, T. Zhou, and F.

W. Zwiers. 2012. Changes in climate extremes and their impacts on the natural physical environment. Pages 109–230 Managing the Risks of Extreme Events and Disasters to Advance Climate Change Adaptation. Cambridge University Press, Cambridge.

Sheffield, J., and E. F. Wood. 2008. Projected changes in drought occurrence under future global warming from multi-model, multi-scenario, IPCC AR4 simulations. Climate Dynamics 31:79–105.

Skelton, R. P., A. G. West, and T. E. Dawson. 2015. Predicting plant vulnerability to drought in biodiverse regions using functional traits. Proceedings of the National Academy of Sciences 112:5744–5749.

Speer, J. 2010. Fundamentals of Tree Ring Research. University of Arizona Press.

Stephenson, N. 1998. Actual evapotranspiration and deficit: biologically meaningful correlates of vegetation distribution across spatial scales. Journal of Biogeography 25:855–870.

Stephenson, N. L. 1990. Climatic Control of Vegetation Distribution: The Role of the Water Balance. The American Naturalist 135:649–670.

Stephenson, N. L., and A. J. Das. 2011. Comment on "Changes in Climatic Water Balance Drive Downhill Shifts in Plant Species' Optimum Elevations". Science 334:177–177.

Sullivan, P. F., R. R. Pattison, A. H. Brownlee, S. M. P. Cahoon, and T. N. Hollingsworth. 2016. Effect of tree-ring detrending method on apparent growth trends of black and white spruce in interior Alaska. Environmental Research Letters 11:114007.

Volaire, F., and M. Norton. 2006. Summer Dormancy in Perennial Temperate Grasses. Annals of Botany 98:927–933.

Vose, J. M., J. S. Clark, and C. H. Luce. 2016. Introduction to drought and US forests: Impacts and potential management responses. Forest Ecology and Management 380:296–298.

Wang, T., A. Hamann, D. Spittlehouse, and C. Carroll. 2016. Locally Downscaled and Spatially Customizable Climate Data for Historical and Future Periods for North America. PLOS ONE 11:e0156720.

Wang, T., A. Hamann, D. L. Spittlehouse, and T. Q. Murdock. 2011. ClimateWNA—High-Resolution Spatial Climate Data for Western North America. Journal of Applied Meteorology and Climatology 51:16–29.

Wells, N., S. Goddard, and M. J. Hayes. 2004. A Self-Calibrating Palmer Drought Severity Index. Journal of Climate 17:2335–2351.

West, A. G., T. E. Dawson, E. C. February, G. F. Midgley, W. J. Bond, and T. L. Aston. 2012. Diverse functional responses to drought in a Mediterranean-type shrubland in South Africa. New Phytologist 195:396–407.

Westerling, A. L., H. G. Hidalgo, D. R. Cayan, and T. W. Swetnam. 2006. Warming and Earlier Spring Increase Western U.S. Forest Wildfire Activity. Science 313:940–943.

Willmott, C. J., C. M. Rowe, and Y. Mintz. 1985. Climatology of the terrestrial seasonal water cycle. Journal of Climatology 5:589–606.

Young, D. J. N., J. T. Stevens, J. M. Earles, J. Moore, A. Ellis, A. L. Jirka, and A. M. Latimer. 2017. Long-term climate and competition explain forest mortality patterns under extreme drought. Ecology Letters 20:78–86.

Zhao, S., N. Pederson, L. D'Orangeville, J. HilleRisLambers, E. Boose, C. Penone, B. Bauer, Y. Jiang, and R. D. Manzanedo. 2019. The International Tree-Ring Data Bank (ITRDB) revisited: Data availability and global ecological representativity. Journal of Biogeography 46:355–368.

Table 4.1. List of drought metrics compared including resolution, method of ET calculation (both potential/reference ET [ET_0] and actual evapotranspiration, AET), and source of raw climate data. PPT = precipitation data source, T = temperature data source. Note that CMD has no resolution as it is a point estimate. N/A = not applicable or included in given modeling approach.

Model	Metric	Resolution (m)	PET or ET_0	AET	PPT	T	Reference
Climate WNA	CMD	N/A	Hargreaves	N/A	PRISM (BI[1])	PRISM (BI)	(Wang *et al.*, 2011)
CalBCM	CWD	270	Thornthwaite	Output from CalBCM	PRISM (GIDS[2])	PRISM (GIDS)	(Flint *et al.*, 2013b)
P-ET	P-ET	30	N/A	Flux~NDVI	PRISM (BI)	PRISM (BI)	(Goulden *et al.*, 2012a)
TerraClim	DEF	~4000	Penman-Montieth	Dobrowski (Thornthwaite-Mather)	WorldClim	WorldClim	(Abatzoglou *et al.*, 2018)
TerraClim	PDSI	~4000			WorldClim	WorldClim	(Abatzoglou *et al.*, 2018)

[1]Downscaled from 800 m using bilinear interpolation.
[2]Downscaled from 800 m using Gradient-Inverse Distance Squared interpolation

Table 4.2. Model posterior credible intervals for each drought metric. All models used only the RWI as a response, and drought metric and drought metric nested by tree as predictors. B_0 = intercept (i.e. mean expected annual RWI), B_1= effect of drought metric on RWI (i.e. slope of relationship), σ = variance. Bold values represent three best fit models and largest effect sizes (most negative posterior).

Metric	Parameter	Mean Posterior	Credible Interval
P-ET	B_0	1.01	1.00,1.01
	B_1	**-0.08**	-0.07,-0.08
	σ	0.23	0.23,0.23
CMD	B_0	0.99	0.99,0.99
	B_1	-0.03	-0.02,-0.03
	σ	0.24	0.24,0.24
CWD	B_0	0.99	0.99,0.99
	B_1	**-0.05**	-0.05,-0.06
	σ	0.24	0.23,0.24
DEF	B_0	0.99	0.99,0.99
	B_1	-0.04	-0.04,-0.05
	σ	0.24	0.24,0.24
PDSI	B_0	0.98	0.98,0.99
	B_1	**-0.08**	-0.08,-0.08
	σ	0.22	0.22,0.23

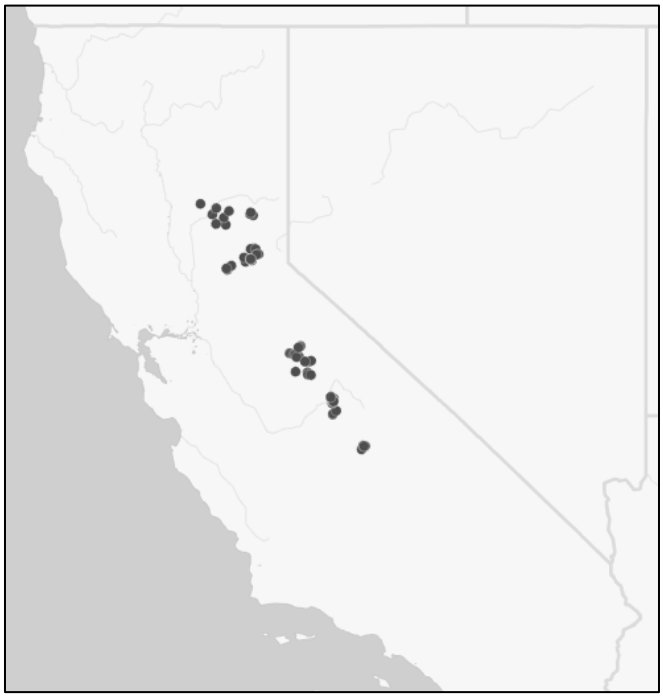

Figure 4.1. Location of tree core samples used for comparison of drought metrics. Increment cores were taken at breast height from selected trees at all shown locations. See text for description of tree selection and core extraction and processing.

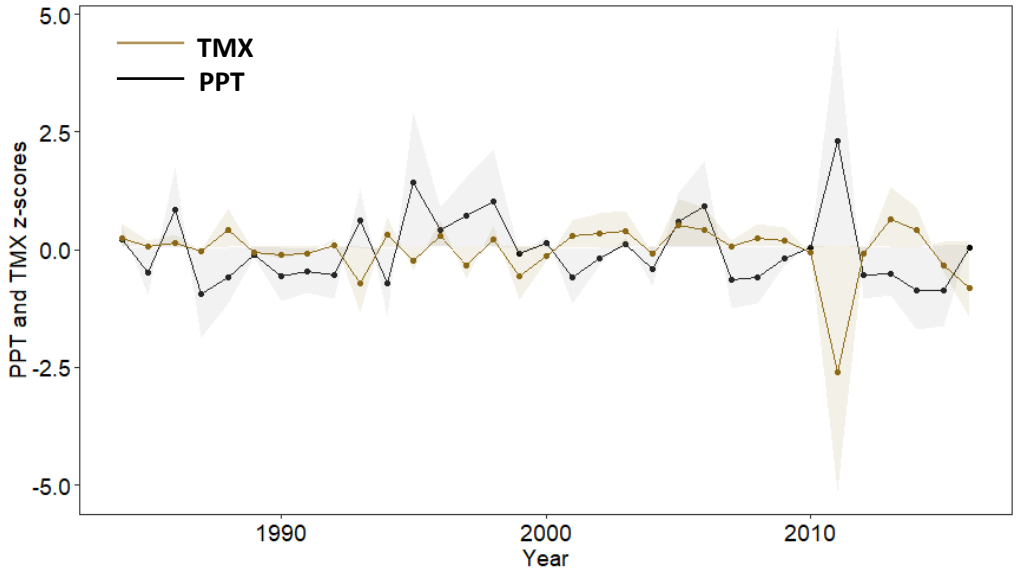

Figure 4.2. Precipitation (PPT) and maximum temperature (TMX) from 1986-2016 across all sampled sites in the Sierra Nevada, California. Values are scaled by subtracting the mean and dividing by the standard deviation (i.e., converted to z-scores) to put them on comparable scales. Note 2011 was anomalously wet and cold. Shaded areas represent 95% confidence intervals.

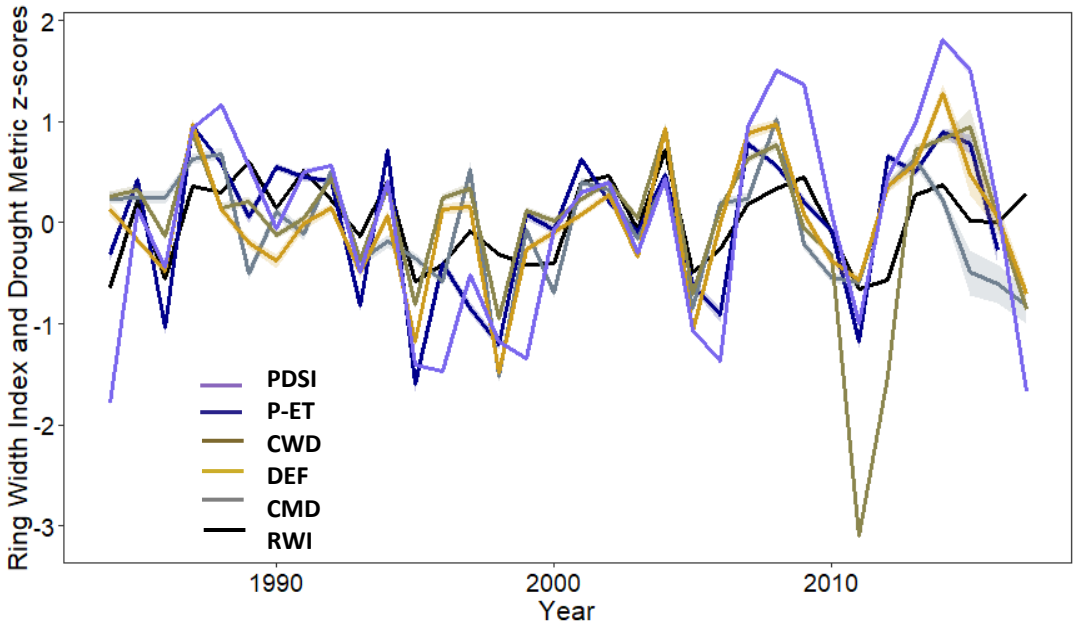

Figure 4.3. Z-scores of each climate metric and the inverse of ring width index (RWI). Positive values represent high drought and low ring width, while negative values represent low drought and high relative ring width. PDSI = Palmer Drought Severity Index, P-ET = Precipitation minus NDVI-derived ET, CWD = Climatic Water Deficit (Cal-BCM), DEF = Climate Water Deficit (TerraClim), CMD = Climatic Moisture Deficit (ClimateNA), and RWI = average ring width index, a detrended chronology from 866 trees in the Sierra Nevada mountains. Note that both PDSI and P-ET were also inverted, with raw values converted to negative values before being converted to z-scores.

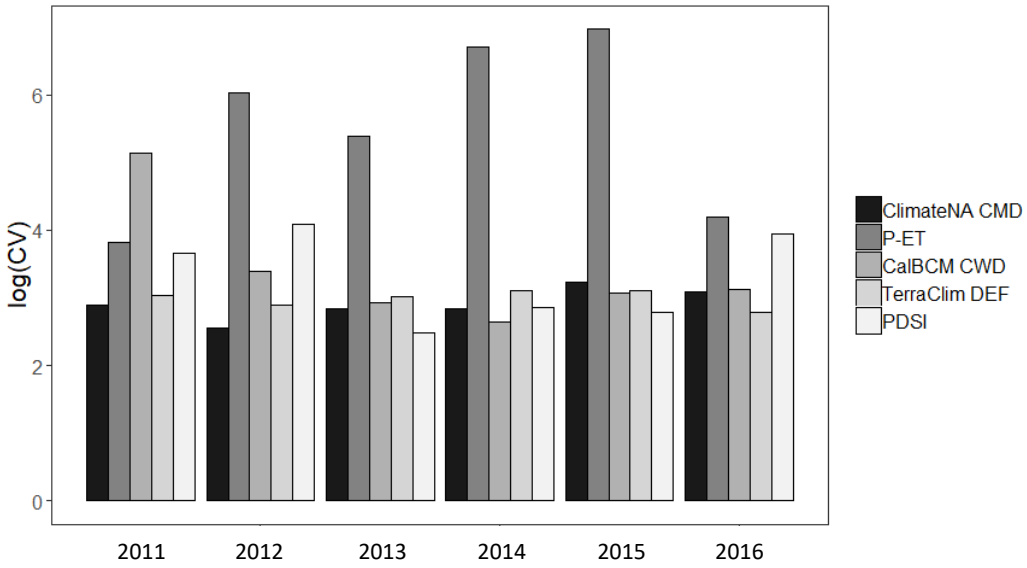

Figure 4.4. Average within-year coefficient of variation of degree of drought as estimated by all measured drought metrics. CV is used here as a measure of spatial variability; higher within-year CV represents higher between-location variance. See Figure 4.3 and text for description of each drought metric.

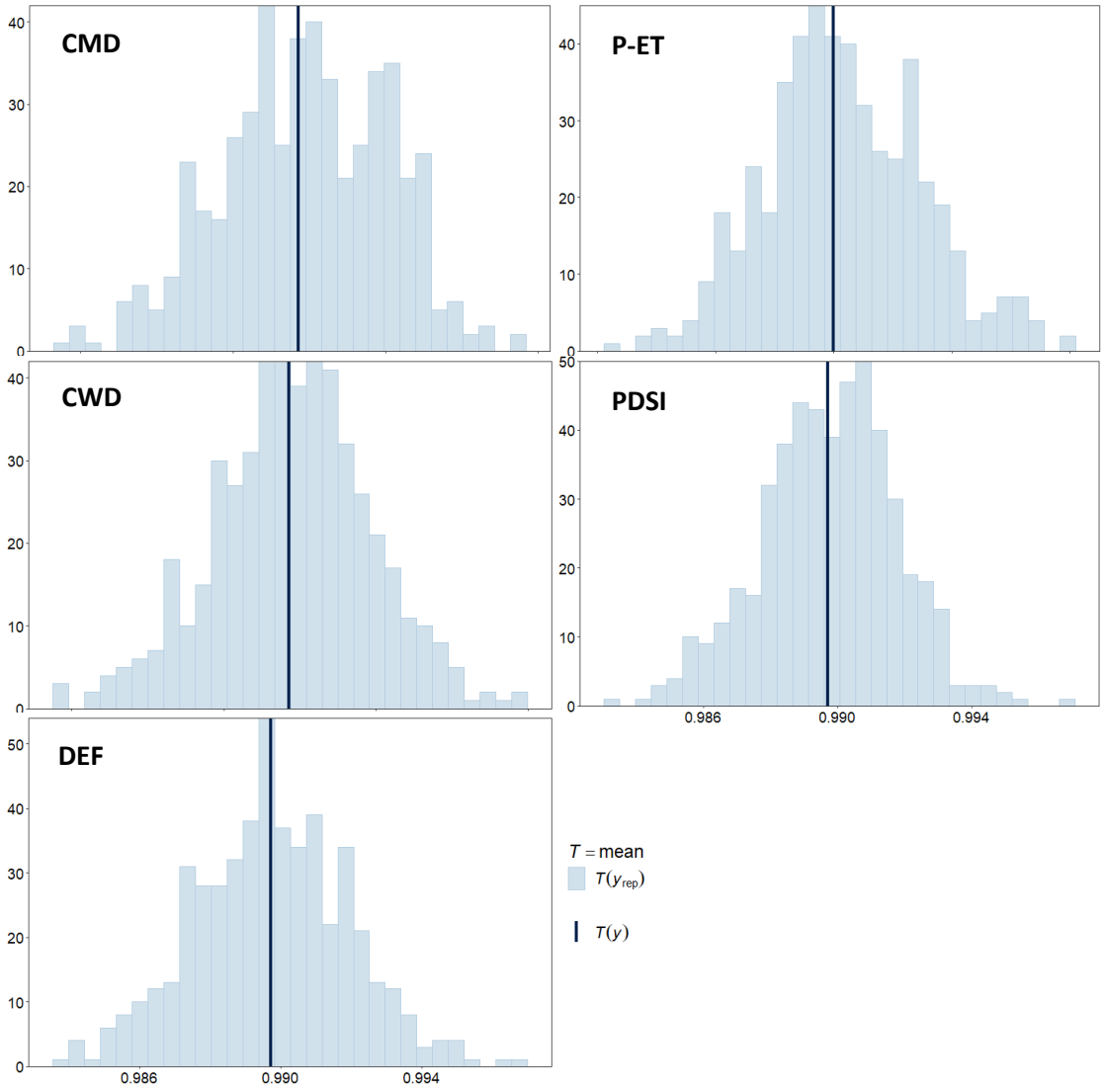

Figure 4.5. Posterior predictive checks of Bayesian linear models for each drought metric. T(y) = mean RWI in observed dataset, T(yrep) = 500 random subsamples of posterior predicted RWI. Results show that PDSI and CWD models have the smallest ranges of posterior predictions (less variance), while the P-ET model has the largest number of predicted values closes to the mean. The DEF model had the highest total number of random draws that matched mean RWI, but also had a wide distribution of mean RWI, while CMD had mean predicted RWI that were lower than observed RWI. See Figure 4.3 caption and text for description of drought metric abbreviations.

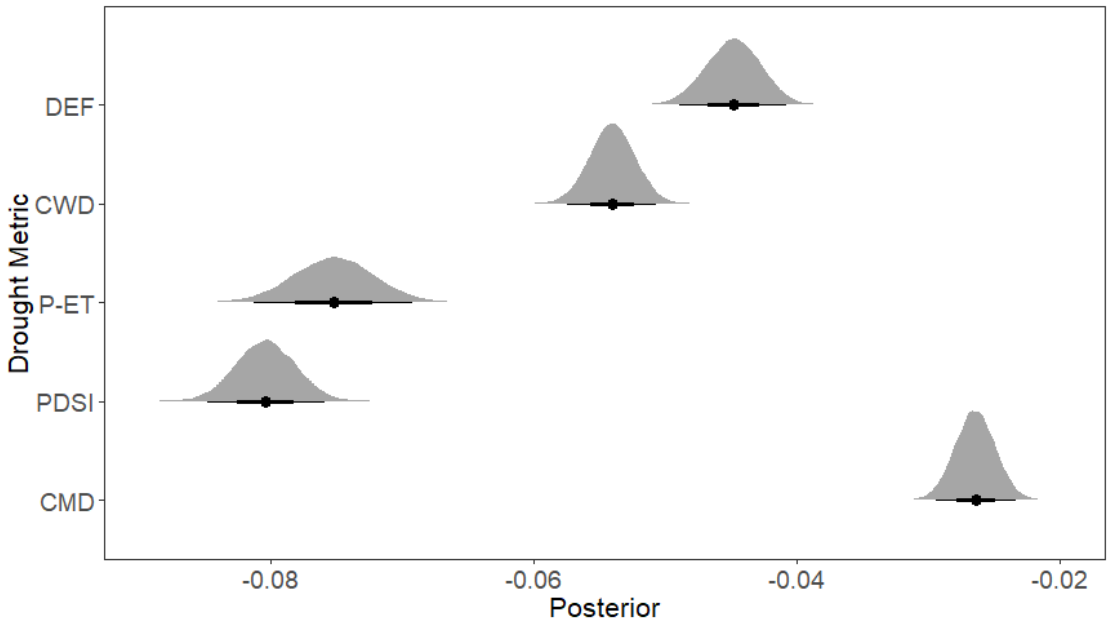

Figure 4.6. Model posterior credible intervals for the effect (β) of each drought metric on tree ring width. Shaded areas represent posterior distributions, lines represent 60% (thick line) and 95% (thin line) credible intervals, and black dots represent mean posterior vales. More negative values represent a more negative effect of drought—as modeled by each respective drought metric—on ring width index. See Figure 4.3 caption and text for description of drought metric abbreviations.

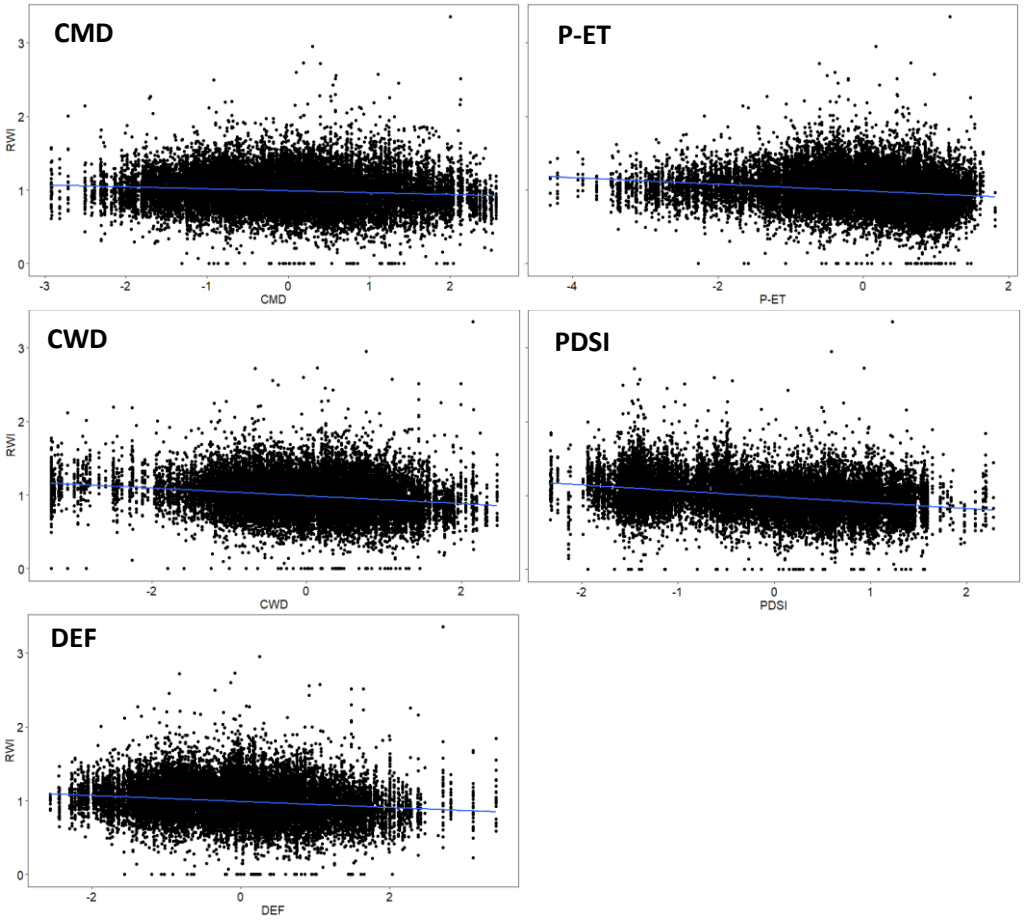

Figure 4.7. Marginal effects from each drought metric model. Line represents modeled RWI as a function of each drought metric while controlling for variation across individual trees. Points represent ring width index (RWI) values. Drought metrics are scaled by subtracting the mean and dividing by the standard deviation (i.e., converted to z-scores) to place them on comparable scales. See Figure 4.3 caption and text for description of drought metric abbreviations. Note that P-ET and PDSI here are inverted (-[P-ET] and -PDSI) to make them comparable to other drought metrics, where high values = high degree of drought.

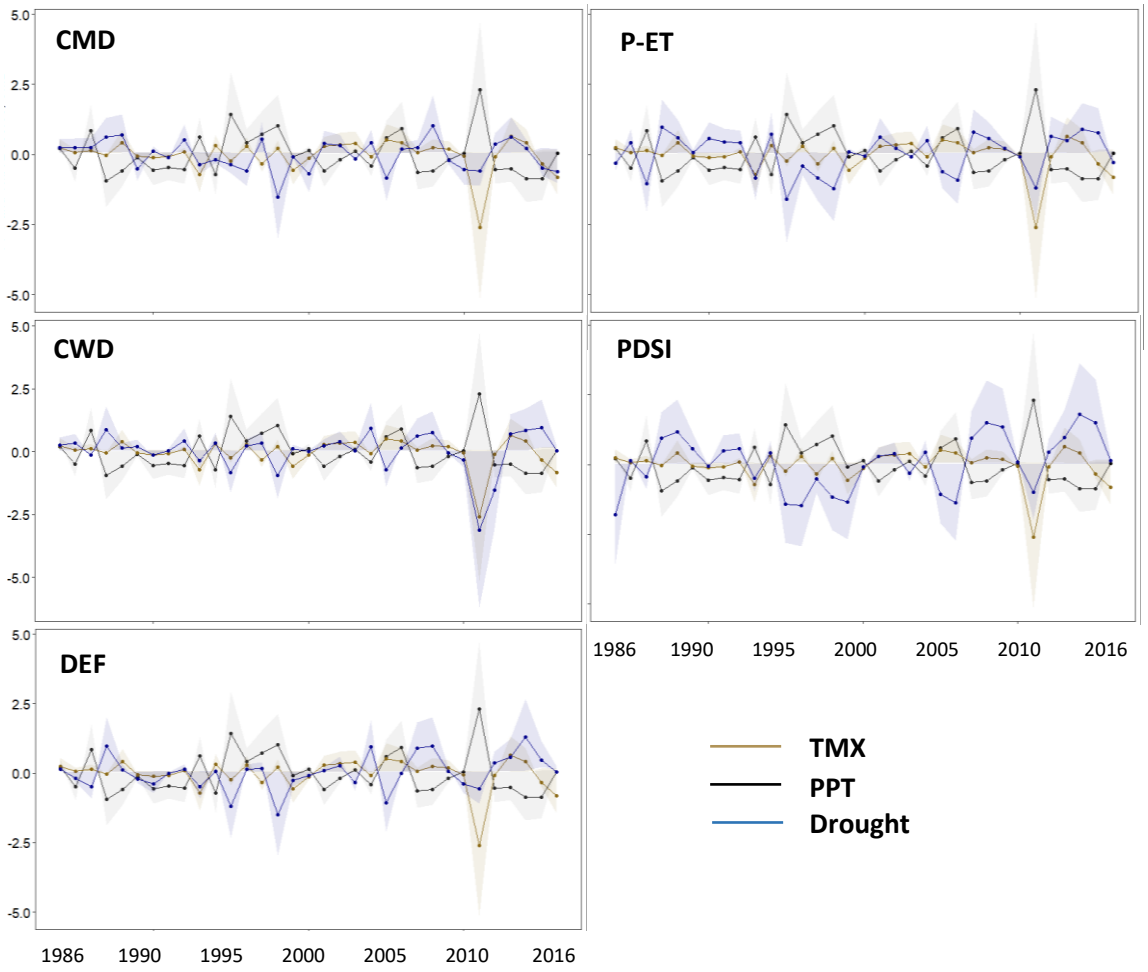

Figure 4.8. Direct comparisons of each drought metric to raw maximum temperature (TMX) and precipitation (PPT). Drought metrics are scaled by subtracting the mean and dividing by the standard deviation (i.e., converted to z-scores) to place them on comparable scales. Shaded areas represent 95% confidence intervals. See Figure 4.3 caption and text for description of drought metric abbreviations.

Supplementary Materials

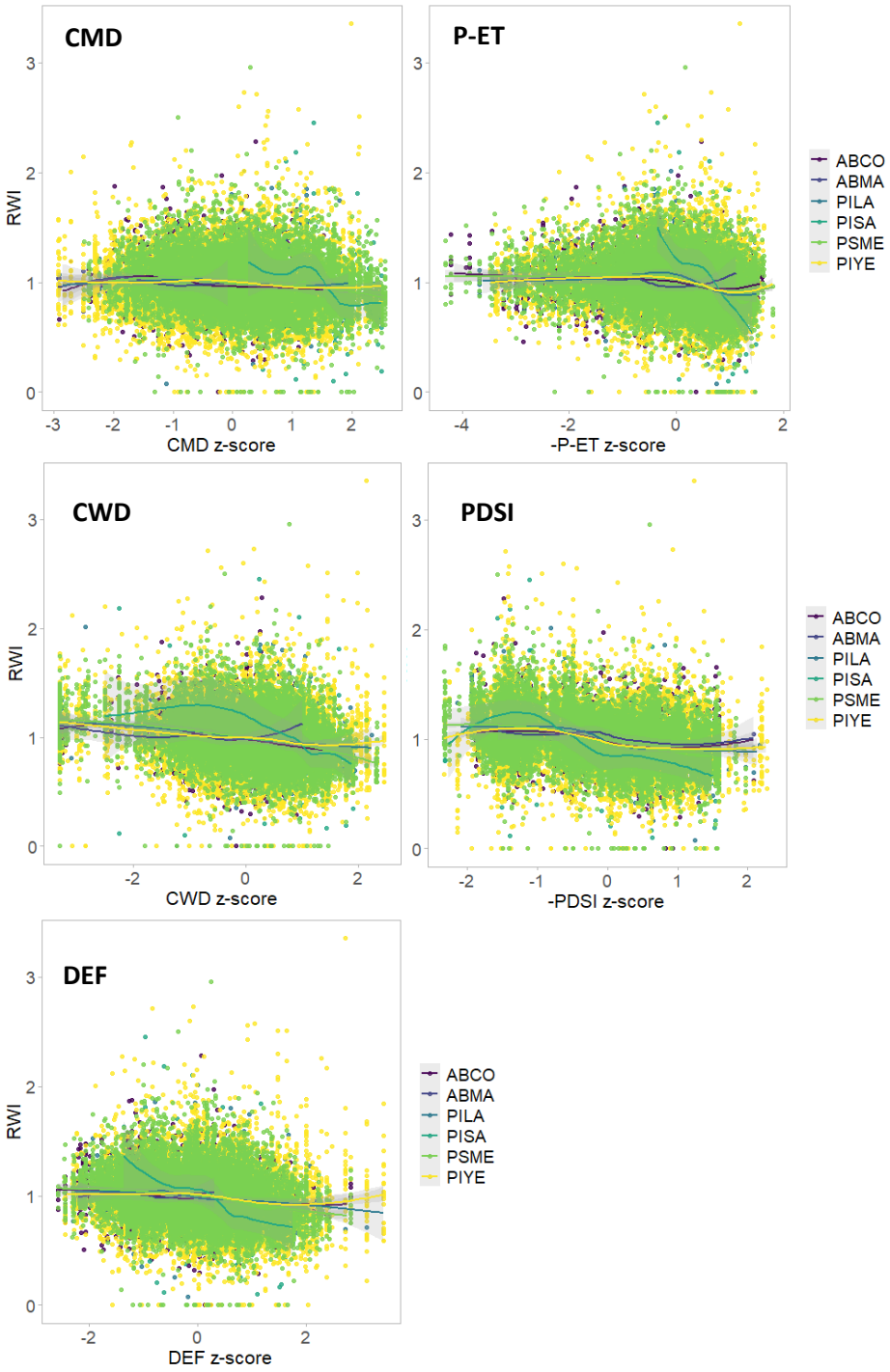

Figure S4.1. Species-specific responses in ring width index (RWI) to drought for drought metrics. Sample size differences between species were too large for

incorporation of a species effect directly in the model, but species effects were still explored visually to account for any dramatic differences. Only *Pinus sabiniana* (PISA) showed different responses to climate from other species. Drought metrics are scaled by subtracting the mean and dividing by the standard deviation (i.e., converted to z-scores) to place them on comparable scales. See Figure 4.3 caption and text for description of drought metric abbreviations. ABCO = *Abies concolor*, ABMA = *A. magnifica*, PILA = *Pinus lambertiana*, PISA = *P. sabiniana*, PSME = *Pseudotsuga menziesii*, PIYE = *P. jeffreyi* and *P. ponderosa*, which were lumped into "yellow pine" category for classification of species range boundaries, due to diffuse range boundaries between these two species.

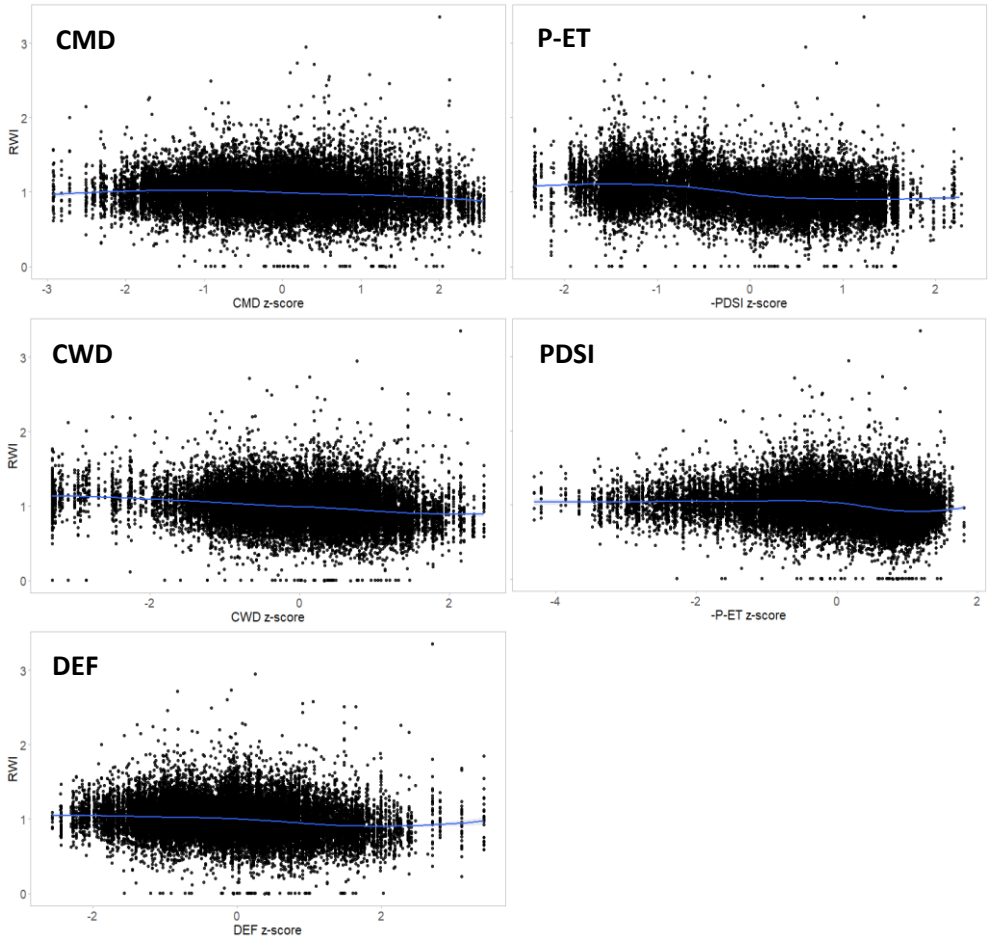

Figure S4.2. Relationship between ring width index (RWI) and drought metrics. Blue line represents best-fit line (spline regression) for each metric. Drought metrics are scaled by subtracting the mean and dividing by the standard deviation (i.e., converted to z-scores) to place them on comparable scales. See Figure 4.3 caption and text for description of drought metric abbreviations.

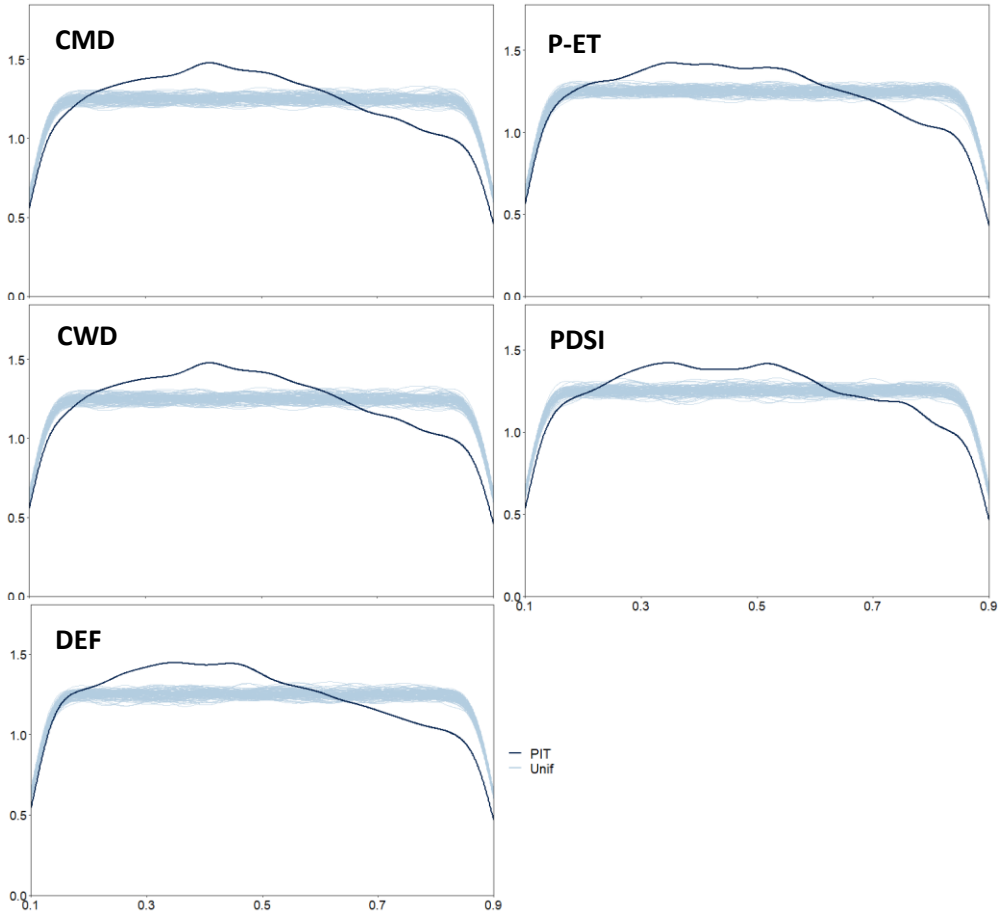

Figure S4.3. Leave-one-out Posterior Integral Transformed (LOO-PIT) model comparisons. Light blue lines represent integral-transformed ring width index (RWI) (i.e., distribution of RWI values transformed to lay along a uniform distribution). Dark blue lines represent PI-transformed model output. Departures of the PIT values from the uniform values represent model fit departures. Best fit, determined visually, is seen in PDSI and P-ET.

Chapter 5:
Growth variability and xylem traits as predictors of tree mortality during drought

5.0 Abstract

Tree response to drought is theoretically a function of tree size, growth, competitive environment, and the interaction between tree physiology and drought intensity. Few studies, however, have combined cellular-scale physiological measurements with tree-ring and forest-scale measurements to examine cross-scale predictors of drought-induced mortality. Here, we combine measurements of xylem anatomical variation with tree ring records, forest inventory data, and multiple drought metrics at various scales to identify determinants of drought-induced mortality in response to the 2012-2016 megadrought in California's Sierra Nevada. We found that trees with high average hydraulic safety (ratio of xylem cell wall thickness to cell diameter), high hydraulic safety plasticity (annual variation), and high plasticity in diameter growth were more likely to die during the 2012-2016 drought. As the sampled trees were also exposed to a bark beetle (*Dendroctonus* spp.) outbreak, we hypothesize that the mechanism of mortality is likely C depletion. We then explore the impacts of this C depletion effect on surviving trees by comparing cone production to measured hydraulic safety and ring width. We found that cone production is loosely positively correlated with ring width, but that no one trait predicts reproductive output. Our results demonstrate the importance of both cellular and forest-scale traits in predicting forest response to climate change.

5.1 Introduction

Western North American forests have been experiencing decreased moisture availability and increased temperatures, driving dramatic shifts in forest density and composition (McIntyre et al. 2015), and widespread drought-induced mortality (van Mantgem and Stephenson 2007, Clyatt et al. 2016). For example, the California drought of 2012-2016 was more severe than any observed in the previous 1200 years (Griffin and Anchukaitis 2014), and left an estimated 130 million standing dead trees in the Sierra Nevada (Moore et al. 2020). Globally, instances of drought-induced forest mortality have increased in frequency in the last two decades (Allen et al. 2010), and are predicted to rise as temperatures increase (IPCC 2014, Allen et al. 2015). This mass tree mortality may have myriad implications for water resources (Flint et al. 2013, Goulden and Bales 2014, Grossiord et al. 2014), fire prevalence (Dale et al. 2001), and land management (Clark et al. 2016). However, it also provides a unique opportunity to test hypotheses regarding drivers of tree mortality in a natural setting.

Current understanding of drought impacts on forests stems from either experimental application of drought to seedlings and saplings in a controlled greenhouse environment, or observations of whole-forest die-off. Greenhouse and experimental studies allow direct measurement of ecophysiological drivers of mortality in seedlings and young trees including wood anatomy (Anfodillo et al. 2012, Anderegg and Anderegg 2013, Aaltonen et al. 2016), water potential, and stem water conductivity (Mitchell et al. 2013, Anderegg and Anderegg 2013). Such measurements can reveal lethal threshold levels of water stress. Field observation studies allow exploration of climate and forest structure metrics that predict mortality (Das et al. 2013, 2016, Young et al. 2017), and

how biotic stressors such as pests interact with and alter likelihood of tree mortality (Stephenson et al. 2019). Few studies, however, consider interactions across these scales, and fewer still examine consequences of drought on components of fitness beyond survival.

Under climate change, tree species must either adapt to changing conditions, migrate to track their environmental niche, or both, if they are to avoid a shrinking geographic range (Aitken et al. 2008). After a major drought, which represents a strong selective pressure (Eveno et al. 2008, Alberto et al. 2013), surviving trees may be expected to exhibit more drought-resilient physiological traits than dead trees. However, which traits will be favored is not entirely clear. In isohydric species like pines that respond to drought stress by closing stomata to control stem water potential, drought induces closure of leaf stomata, reducing water loss comes at the expense of carbon (C) assimilation and photosynthesis (Tardieu and Simonneau 1998, Klein 2014). Physiological responses to drought include building of C-expensive drought-resistant xylem (Bryukhanova and Fonti 2012, Bouche et al. 2014), increased allocation of C to root growth (Hagedorn et al. 2016), and changes in C storage dynamics (Chapin et al. 1990, Sala et al. 2012, Adams et al. 2013). Thus, reduced C assimilation under drought coupled with enhanced allocation of remaining C to drought resilience traits may lead to tradeoffs among drought defense, radial growth, and other C-intensive processes such as reproduction (Lauder et al. 2019). These tradeoffs may then be associated with drought-induced selection of trees with high reproductive effort at the expense of drought defense or growth.

The record of not only how a tree grows, but the mechanisms underlying observed growth patterns and C allocation to growth, is maintained in the growth rings of a tree (Martínez-Vilalta 2018). Conifer growth rings are made up almost entirely of xylem cells called tracheids, the primary water-conducting cells of a plant. Wider tree rings are associated with larger or more numerous tracheids; larger tracheids can move more water, but potentially at a higher risk of cavitation (via air embolism of the water column) or wall collapse (Pittermann et al. 2006). Drought stress, at both seasonal and long-term scales, is known to induce smaller tracheid diameters and thicker walls in conifers (Bryukhanova and Fonti 2012, Cuny et al. 2014, Fonti and Babushkina 2016). This change in tracheid anatomy may be both a response to and a defense against drought conditions. Drought induces smaller cell diameters via means of turgor-limited cell expansion; decreased water availability leads to decreased outward pressure from within the xylem cell and thus limited cell expansion and subsequent diameter (Woodruff et al. 2004, Anfodillo et al. 2012). This decreased cell expansion time, however, may increase both cavitation resistance and mechanical damage resistance by means of higher water potentials and increased wall thickening times (Cuny et al. 2014).

"Thickness to span" (also referred to as Mork's index, Hacke et al. 2001) is a ratio of xylem cell wall thickness to tracheid cell lumen diameter. Trees vary both within and between species in their threshold thickness to span ratio beyond which hydraulic failure occurs, with higher ratios being correlated with higher drought survival (Bouche et al. 2014). Evidence is mixed, however, for this relationship across different species. Intermediate ratios of wall thickness to diameter were associated with higher resistance to cavitation in Douglas-fir (*Pseudotsuga menziesii*), and large ratios were least resistant

(Dalla-Salda et al. 2014). Extension of this intra-annual observation to inter-annual measurements of tracheid anatomy would improve understanding of the relationships between anatomy and drought-induced mortality over time. Inter-annual variation in wall thickness may be particularly significant in multi-year droughts, as previously grown tree rings are used for water transport for many years (Pallardy et al. 1995).

Inter-annual variation in tree ring traits may influence reproductive effort. Cone production in conifers typically takes two to three years (Guo et al. 2016). Trees that are highly sensitive to drought may develop higher thickness-to-span ratios than less drought-sensitive neighbors. This higher thickness-to-span ratio is associated with a higher total C cost per unit volume of wood (Lauder et al. *in review*, Chapter 3), resulting in less C left to allocate toward reproduction. Tradeoffs between growth and reproduction are well studied, but the impacts of drought on the degree of tradeoff remain largely unknown. Under mesic conditions, conifers typically demonstrate a positive relationship between growth and reproduction overall (Woodward and Silsbee 1994, Despland and Houle 1997, Santos et al. 2010, Ayari et al. 2012, Ayari and Khouja 2014, Hisamoto and Goto 2017). Masting, the synchronous production of large seed crops across a population (Kelly et al. 2013), has been shown to induce negative correlations between growth and reproduction both during and after mast years (Eis et al. 1965, Woodward and Silsbee 1994, Hacket-Pain et al. 2017, Hacket-Pain et al. 2018). Drought appears to be associated with increased reproductive output overall, likely due to the positive effects of warm and dry climate on resource priming, cone primordia formation, and pollen dispersal (Lauder et al. 2019). Few studies have explored the impact of drought on growth-reproduction tradeoffs, however, and even fewer have examined the direct mechanism of potential drought-induced changes in degree of tradeoff. Changes in total stored non-structural carbohydrates (NSC) are implicated in changes in C allocation during drought (Sala et al. 2012, Aaltonen et al. 2016, Adams et al. 2017). Whether these changes are driven by increased allocation to drought defenses and growth ("Fight" behaviors, Lauder et al. 2019), or reproductive output ("Flight" behavior) remains unexplored. Such an analysis is necessary in order to understand not only how trees die under extreme drought, but also how traits that confer survival influence overall tree fitness.

Here, we examine tracheid anatomy and its relation to tree diameter, ring width, competitive pressure and climate before, during, and after drought in widely distributed conifer species, ponderosa pine (*Pinus ponderosa*), and Jeffrey pine (*P. jeffreyi*), along an elevation gradient. We ask: which physiological traits influence likelihood of mortality in these species, and how do these traits influence likelihood of successful reproduction in surviving trees? We scale drought response of these species from the individual cell to the forest stand by incorporating data at the levels of the tracheid (anatomy), the whole tree (growth and survival), and the forest (climate, competition). This scaling fills a significant gap in our ability to connect ecophysiological and experimental responses to landscape-scale efforts to understand and predict climate change impacts on forests.

5.2 Methods

5.2.1 Plot locations

Three elevational transects were established: one each in the Southern, Central, and Northern Sierra Nevada (Figure 5.1), in Sequoia National Park (S), Sierra National Forest on both private property and in conjunction with Southern Sierra Critical Zone Observatory (R), and Tahoe National Forest (T), respectively. Sites were located at the lowest elevation boundary of *P. ponderosa*, the zone of overlap between *P. ponderosa* and *P. jeffreyi*¸ the mid to upper elevation range of *P. jeffreyi,* and the zone of overlap between *P. jeffreyi* and *P. monticola*. Plots were placed at locations that were accessible and contained target species. At each site, we established a 0.8 ha plot in which we identified and measured diameter at breast height (DBH) of all species, and mapped individual tree locations. Mapped tree locations and diameters were used to calculate the Hegyi index of competition for all trees. The Hegyi index is a size-weighted measure of competition experienced by target trees (Hegyi 1974).

5.2.2 Core measurements

We sampled a minimum of 10 individuals of each target species (*P. ponderosa* and *P. jeffreyi*) present in each site with a 4.37mm Haglof increment borer (Haglof, Sweden) increment borer at breast height. Co-occurring non-target species (*Abies concolor, A. magnifica, Calocedrus decurrens, P. lambertiana,* and *P. contorta*) were also sampled to assist in site-level tree core cross-dating and other plot-scale characteristics, but were not analyzed here due to low sample sizes per species. Cores were taken in two perpendicular directions (parallel and perpendicular to slope) to mediate potential reaction wood in trees growing on slopes and to ensure complete ring detection (Speer 2010). To test how various traits influence likelihood of mortality, we sampled both living and dead trees, with dead trees identified as those completely defoliated or with no green foliage.

Cores were prepared using standard dendrochronology methods (Speer 2010). All extracted cores were stabilized in wooden mounts and surfaced using consecutively finer grades of sandpaper until individual cells were visible. Cores were then scanned at 800 dpi on a flatbed scanner and ring widths were measured in the winDENDRO (Regent Instruments Canada Inc. 2017) tree ring software package. Cores were cross-dated visually within winDENDRO, and final cross-dating accuracy was checked using COFECHA (Grissino-Mayer 2001), and adjusted manually under a stereo microscope if necessary.

After cross-dating, 10-16 µm radial thin sections were made of each core using the GSL-1 tree core microtome (Gärtner et al. 2014). In lieu of stabilization of tree cores in paraffin, we brushed prepared core surfaces with a non-Newtonian starch solution to facilitate non-destructive wood sectioning (von Arx et al. 2016). Thin sections were cleaned of starch and fixed to glass slides, and cross-stained using a 1% safranin and 1% astra blue solution (1:1 v/v) to enhance contrast between lignified tracheid cell walls and cellulosic materials. Slides were permanently fixed using Euparal, and photographed at 100x using a Leica DM microscope at constant light saturation across all images. Images were analyzed in winCELL (Regent Instruments Canada Inc. 2017) following processing to remove artifacts such as areas un-cleaned of starch, or to exclude areas of broken cell walls or warped cells from final analysis. Individual traits analyzed include tracheid diameter, tracheid area, cell wall thickness, total count, and density.

5.2.3 Reproductive effort measures

To quantify reproductive effort, we conducted visual binocular cone counts of sampled trees in the summers of 2017, 2018, and 2019. Not all trees could be sampled in all years, with the highest density of cone counts conducted in 2019. We counted all visible cones using binoculars and a spotting scope where necessary to confirm cone presence and growth stage. Cones on the ground were also counted and categorized as current year, past year, or older based on cone color and degree of decay. Green cones or light brown cones that were unopened were counted as current, light brown cones with seeds still present within bracts were previous year, and gray-brown cones that broke easily in the hand were classified as >1 year old (Redmond et al. 2012). Ground cone counts were only conducted in areas where all ground cones could reasonably be sourced to nearby parent trees.

5.2.4 Climate Data

The degree of drought stress experienced by trees growing in each plot was evaluated using multiple available climate data sources. Models of likelihood of mortality included maximum July temperature, minimum January temperature, and the following measures of water availability:

1. Climatic moisture deficit (CMD) from ClimateNA (Wang et al. 2011, 2016)
2 & 3. Palmer Drought Severity Index (PDSI) and water deficit (DEF) extracted from TerraClim (Abatzoglou et al. 2018)
4.Climatic Water Deficit (CWD) from Cal-BCM (Flint et al. 2013)
5. A metric of precipitation minus ET (P-ET) using ET calculated from LandSat-derived Normalized Differential Vegetation Index (NDVI) and eddy flux tower-measured ET (Goulden et al. 2012, Bales et al. 2018).

We opted to use multiple climate datasets in this analysis due to the different ability of each to track "true drought" with respect to both temperature and soil water availability for tree growth. We used tree ring records from 866 trees throughout the Sierra Nevada to test the ability of each of these drought metrics to predict tree ring growth, and found that PDSI, P-ET, and CWD models had the best fit (Chapter 4). PDSI and P-ET had the highest correlation coefficients with growth, but PDSI had the lowest spatial variability and P-ET had very high spatial variability. This means that P-ET may best predict tree ring growth at local scales and may best track spatial variability in drought. However, because that study (Chapter 4) did not include mortality or wood anatomy, we chose to extend the test of each drought metric to this dataset.

5.2.5 Statistical Analysis

After cross-dating removed cores that were unable to be dated, along with sample loss or an inability to generate thin sections with high enough quality for tracheid measurement, we were left with 156 individual tree ring width chronologies and 57 trees with thin sections from multiple rings. Not all records exist for all individuals, as thin sections may be taken from trees whose entire chronology could not be dated, or cores could be dated on trees whose wood was too brittle for thin sectioning.

In order to fill these gaps, we used multiple imputation using chained equations using the "mice" package in R version 3.6.3 (R Development Core Team 2020). In this method, missing values are imputed based on iterative regressions using all available data. The multiple iterations allow estimates of the likely missing values and error around the estimates of the missing values. We estimated missing values by imputing five new gap-filled datasets with 150 iterations of classification and regression trees using all available data. This led to, for example, missing hydraulic safety factor (HSF) being estimated from climate, species, location, growth, and competition data, and growth being estimated from climate, species, location, competition, and HSF data. Final imputed data was checked against raw values visually, and means and ranges were found to approximate raw data (Figure S5.1), and thus were averaged across all five imputations to create the final dataset. Analyses were conducted using both this imputed dataset and the original measured dataset to evaluate the effects of imputation. Models approximated each other, but did have different results; raw data models did not converge, and were left with less than half of the original dataset due to inherent row-wise deletion of observations with missing values in R. So only imputed datasets (n = 157 final individual tree observations) were used for final analyses.

Ring widths were detrended to remove age-based biases in tree growth estimates. Ring widths were converted to ring width index (RWI) by dividing all ring widths by the mean value for each year of a cubic spline with a 20-year length (Figure S5.2). This length of spline retains 95% of decadal variance but minimized age-biased growth patterns (Speer 2010). We then used these detrended ring widths to calculate the Gini coefficient, a measure of growth variability for which high values represent high year-to-year variation in growth and low values represent "constant" growth (Biondi and Qeadan 2008). All detrending and ring width analyses were conducted in the package "dplR" (Bunn 2008) in R.

Cell traits were used to derive a hydraulic safety factor (HSF), calculated as

$$HSF_i = \frac{S}{0.5(T_{w1}+T_{w2})},$$

where: S = "span," the diameter of the cell lumen, and T = wall thickness for wall 1 (*w1*) and wall 2 (*w2*) of cell i moving from left to right along the direction of growth in the image. Calculating these metrics for all cells for all rings led to an extremely large dataset (>9 million cellular observations). To simplify final analyses, we calculated mean HSF (mHSF) for each ring. We then calculated the Gini coefficient of HSF to estimate variability in mean HSF across multiple years for each tree.

We constructed models of likelihood of mortality as a function of tracheid anatomy, growth, growth plasticity, degree of drought experienced, growth and tracheid anatomical response to drought, and competition. To test the effects of mediating variables and indirect effects, as well as uncertainty in effects, we use two different modeling methods and compared results. We first used Bayesian logistic regression to estimate the effects of all predictors on likelihood of mortality by species and year. We then used path analysis, a form of structural equation model (SEM), to model both direct effects of all predictors on likelihood of morality as well as interactions and indirect effects of predictors on each other and likelihood of mortality. This allowed a nested structure, where, for example, tracheid traits influence likelihood of mortality directly (via changes in physiological drought resistance) and indirectly (via influences on C use and ring width). This approach allowed

us to use multiple lines of evidence to infer final predictors of mortality. Further, the SEMs did not allow incorporation of prior year effects due to multiple collinearity (current year growth is highly correlated with prior year climate and growth), while the Bayesian models did not converge when including a variable representing latewood/earlywood ratios in tree rings.

The Bayesian model was constructed as:

$$
\begin{aligned}
M_{ijt} &\sim Bern(\theta_{ij}) \\
logit(\theta_{ijt}) = \big(&\beta_j + \beta_{ijt}Drought_{ij} + \beta_{ijt}Drought_{ij}^{t-1} + \beta_{ijt}RWI_{ij} + \beta_{ijt}RWI_{ij}^{t-1} \\
&+ \beta_{ijt}HSF_{ij} + \beta_{ijt}HSF_{ij}^{t-1} + \beta_{ijt}TMN_{ij} + \beta_{ijt}TMN_{ij}^{t-1} + \beta_{ijt}gini_{ij} \\
&+ \beta_{ijt}HSFgini_{ij} + \beta_{ijt}Hegyi_{ij} + \beta_{ijt}HSFDrought_{ij} \\
&+ \beta_{ijt}RWIDrought_{ij} + \beta_{ijt}DBH_{ij}, \sigma_y^2\big) \\
&\beta_{ijt} \sim Student\big(\nu_{ijt}, \mu_{ijt}, \sigma_\beta^2\big),
\end{aligned}
$$

where: *M* = likelihood of mortality in tree *i* for species *j* in year *t*, a Bernoulli distributed function of θ; θ is connected to a series of linear predictors via a logit link; *Drought* = the drought metric of choice for that model with all metrics run in their own models; *t*-1 superscripts represent lagged effects (value of each predictor from the prior growth year); *RWI* = ring width index; *HSF* = hydraulic safety factor (i.e. "thickness-to-span"); *TMN* = minimum temperature; *Gini* = growth variability; *HSFgini* = variability in HSF; *Hegyi* = the Hegyi index of competition for tree *i*; *HSFDrought* and *RWIDrought* = the linear correlation between HSF or RWI, respectively, and the chosen drought metrics across all growth years; and *DBH* = last measured diameter at breast height.

Bayesian logistic models were built in the R package "brms" (Bürkner 2017). Predictors were all centered and scaled by subtracting the mean and dividing by the standard deviation. Priors were Student-t-distributed with a mean of zero, three degrees of freedom, and a scale of 2.5. This prior distribution is based on providing vaguely informative priors for logistic regressions when all predictors are scaled (Gelman et al. 2008), and represents a change of 0.50 in the probability of mortality for each 1 s.d. change in a predictor. Prior distribution for all parameters is shown relative to posteriors in Figure 5.2. Model fit was assessed using the leave-one-out information criterion (LOOIC), with smaller values of LOOIC indicating better fit. Cross-validation via LOO is based on evaluation of the log-likelihood of a single data point that was not included in parameter estimation, and then repeating this for each data point. This yields an estimate of overall model out-of-sample predictive accuracy (Vehtari et al. 2017).

Path analysis models were built in the R package "lavaan" (Rosseel 2012), as:

$$
\begin{aligned}
M_{ij} &= logit(RWI_{ij} + Drought_{ij} + HSF_{ij} + HSFgini_{ij} + Gini_{ij} + Hegyi_{ij}) \\
RWI_{ij} &= RWI_{ij}^{t-1} + Drought_{ij} + TMN_{ij} + Hegyi_{ij} \\
HSF_{ij} &= LumenLength_{ij} + WallThickness_{ij} + HSFsl_{ij},
\end{aligned}
$$

where *LumenLength* = tracheid lumen diameter for tree *i* in year *j*; *WallThickness* = wall thickness of tracheids within tree *i* in year *j*; and *HSFsl* = the slope of the relationship between HSF and tree ring position, representing "degree of latewood formation". SEM

model fit was assessed using Akaike's Information Criterion (AIC) and p-values from a χ^2 goodness-of-fit test comparing the model covariance with covariance in the data (in this case a high p-value indicates good model fit).

Finally, reproduction was compared to all other traits measured using a negative binomial regression with cone count on target trees as a response. Negative binomial regression gives the likelihood of reproduction based on zero-inflated count data, and is useful for estimating likelihood of an event given sparse observations (Hoef and Boveng 2007, Lindén and Mäntyniemi 2011). Under the "fight or flight" hypothesis (Lauder et al. 2019), flight is denoted by a mast prior to mortality. However, our reproduction dataset does not cover enough time to assess whether reproductive effort constitutes a mast. Further no trees that died during our observation period had cones observed on them immediately prior to death, so instead we analyzed likelihood of reproduction given other traits in surviving trees. Thus our analysis of reproductive effort is a test of the impact of "fight" behaviors on reproduction.

5.3 Results

We found that drought, growth variability, and variation in xylem anatomy all influenced likelihood of mortality in pines. The Bayesian models all achieved convergence ($1.00 < \hat{R} < 1.01$ for all predictors), with the best-fit models including either P-ET or PDSI as the drought metric predictors. However, the CWD-specific model had only slightly lower fit (Table 5.1). Trees were more likely to die when PDSI was high (Figure 5.2) or when P-ET was low (Figure 5.3); however, effects differed by species, with *P. ponderosa* being more likely to die in general (higher intercept) and being more responsive to both drought metrics. Within the PDSI and P-ET models, the best predictors of mortality were Gini, HSFgini, minimum temperature, the drought metrics, and the interaction between RWI and drought (Figure 5.4). However, only Gini and HSFgini had credible intervals that did not overlap zero across all models, meaning they have a clearly non-zero effect on mortality (Table 5.2).

We identified multiple novel predictors of tree mortality. Gini coefficient, representing growth variability, was both higher and more variable in trees that eventually died than living trees (Figure 5.5). This demonstrates that trees that are able to grow at constant rates may more likely to survive drought stress, regardless of absolute growth increment. Both HSF and inter-annual variability in HSF (HSFgini) were significantly greater in trees that eventually died than in living trees (Figure 5.6). Interestingly, competition had a negative effect on likelihood of mortality in both species, with trees with a high Hegyi index being less likely to die (Figure 5.7).

We found that the best predictors of mortality were remarkably consistent across models, with growth variability (Gini coefficient of RWI) and competition being identified as strong predictors regardless of modeling approach or drought metric used. The path analysis models that included CMD, P-ET, or DEF as the drought metric had the best fits (Table 5.3). The single best-fit SEM included CMD and all predictors included in the Bayesian models (Figure 5.8). The most significant predictors of mortality in the SEMs were HSF (r = -0.19), CMD (r = 0.19), competition (r = -0.16), and Gini coefficient (r = 0.21), with the effect of HSF being driven primarily by lumen diameter (r = -0.89) and less so by tracheid wall thickness (r = 0.49).

Reproductive effort was high in trees with higher annual growth but was not predicted by interactions between growth and other physiological traits or by drought intensity. Negative binomial regressions of cone production did not converge, likely due to a very low number of non-zero observations. While more data is needed to assess model reproductive effort with the "fight or flight" framework, we examined univariate correlations between cone production and predictors. Cone production in living trees was positively correlated with ring width of the current and previous year ($p = 0.013$ and 0.19, $R^2 = 0.214$ and 0.192, respectively, $n = 27$, Figure 5.9).

5.4 Discussion

Tree mortality during drought is thought to be a function of numerous interacting factors including drought intensity (Das et al. 2013, Young et al. 2017), competition, tree growth in current and prior years (Das et al. 2007), and tree physiology (Anderegg et al. 2013, Adams et al. 2017). However, interpretation of models of likelihood of drought-induced mortality depend on the drought metric of choice (Bhuyan et al. 2017; Chapter 4), the degree of interaction between competition and drought (Das et al. 2011, Young et al. 2017), species-specific variation in growth response to climate (Cailleret et al. 2017, Aubry-Kientz and Moran 2017), and biotic interactions (Das et al. 2016, Stephenson et al. 2019).

Significant growth declines between years (Das et al. 2007), as well as increasing departure of variation in ring width from variation in climate (i.e. declining synchrony between growth and climate; Cailleret et al. 2017, 2019) have been found to predict likelihood of mortality. We show that trees with high growth plasticity were more likely to die, consistent with observations of growth variability in the most recent 10-15 years of growth predicting mortality in *P. edulis* (Ogle et al. 2000). This demonstrates that trees that grow more when water is available, and less when water is less available, may be less resilient to drought, or at least to multi-year droughts. Thus, growth amount alone is likely not a sufficient predictor of forest response to climate stress; consistency of growth may be more important.

Our most surprising and significant finding is that trees with both higher HSF and higher variation in HSF (HSFgini) are more likely to die, even though one would expect trees with high HSF to be more resistant to hydraulic failure during drought. We hypothesize multiple mechanisms for the relationship between HSF, HSFgini, and likelihood of mortality. Higher values of HSF are associated with higher C costs per unit volume of wood, due to the positive relationships between HSF, lignin and total C content (Amthor 2003, Lauder et al. 2019). This higher C allocation toward hydraulic safety depletes C reserves that may be necessary for other stress responses.

The trees sampled here were exposed to extensive bark beetle (*Dendroctonus spp.*) outbreak, particularly in the southern and central Sierra Nevada (Hicke et al. 2016). The primary mechanism of tree defense against bark beetle is construction of C-rich resin ducts and resin to prevent successful bark beetle intrusion (Franceschi et al. 2005, Kane and Kolb 2010). Depletion of C reserves via drought-induced stomatal closure, coupled with increased C allocation to drought-resistant xylem, may predispose drought-sensitive trees to bark beetle intrusion. Although we did not include signs of bark beetle stress in this study, recent observations have attributed mortality in *P. ponderosa* and *P. jeffreyi* to bark beetle, with drought being the ultimate cause and bark beetle being the proximate cause

(i.e., drought weakened trees while bark beetle killed them; Hicke et al. 2016, Stephenson et al. 2019). Bark beetles induce mortality in a number of ways, including direct physical girdling of plant vasculature and inoculation with fungal and bacterial pathogens that can either physically block xylem and phloem flow or override tree chemical defenses (Raffa et al. 2008, Huang et al. 2020). We hypothesize that the positive effect of HSF on mortality found here is consistent with bark beetle-induced mortality, with trees with high HSF depleting available resources.

High values of HSFgini being associated with mortality demonstrates the potential hydraulic impacts of variations in HSF. While high HSF is associated with drought resilience, it is also associated with lower total hydraulic conductance. Hydraulic conductance, according to the Hagen-Poiseuille law, is proportional to conduit (i.e., tracheid) diameter to the fourth power (Gooch 2011). In tall conifers, maintenance of conductance up the entire stem is important for maintaining canopy hydration, which itself can influence degree of stomatal response to drought (Loewenstein and Pallardy 1998). Growing xylem cells with high HSF may limit drought-induced cavitation, but at the expense of water transport to the upper canopy (Loewenstein and Pallardy 1998, Pittermann et al. 2006). Xylem continues to be used for water transport for multiple years after growth, and trees that build xylem cells with a high HSF may be using excess C resources to build that xylem, while also lowering total canopy conductance in subsequent years. However, reversing this reduced conductance by building larger xylem cells in wet years may also reduce drought resistance should drought conditions return. Trees that grow rings with fairly constant HSF may thus be less prone to both resource depletion and cavitation.

Another surprising finding in this study was the negative impact of competition on likelihood of mortality. Previous work has demonstrated that competition often amplifies drought-induced mortality (Young et al. 2017). A potential explanation for this discrepancy is scale-dependence of the drought metric used. Quantifying competition at whole-forest scales is often done using long-term forest inventory datasets such as the Forest Inventory and Analysis (FIA) dataset (e.g., Young et al. 2017, Evans et al. 2017). Competition metrics derived from these large inventory datasets, however, are often based on basal area (BA) of trees per unit area. Although this provides a valid estimate of total biomass in an area, it cannot capture small-scale heterogeneity in competitive effects. For example, two 0.8 ha plots can have the same total BA with a high density of small trees or a low density of larger trees, in multiple combinations and spatial configurations. In this vein, basal area alone does not quantify the degree of competition experienced by a single tree. Here, we used a tree-specific index of competition that incorporates target tree DBH and distance-weighted DBH of all surrounding trees. Thus, our competition effect may represent a more spatially explicit impact of competition and likelihood of mortality.

One biological explanation for the negative effect of competition on mortality may be size-dependence of our sampled trees. Examination of the relationship between Hegyi index and tree size in our plots demonstrates that larger trees are subject to less competition (Figure 5.10). This makes theoretical sense given that large trees often dominate and shade out the forest beneath them. Large trees are predicted to experience a higher degree of mortality during drought in the Sierra Nevada, primarily due to bark beetle preferential attack on larger trees (Stephenson et al. 2019). Large trees presumably have thicker phloem

than smaller neighbors, and beetle attack rates are higher on trees with thick phloem layers (Fischer et al. 2010). Further, a DBH effect was included in our models and found not to be significant. Thus, our negative effect of competition on mortality may be an artifact of both loss of large trees with lower Hegyi indices, and surviving trees being smaller and found in more dense plots. Smaller trees are often found in more dense plots until competition leads to self-thinning, which would then manifest a negative effect of competition on mortality. Further research is needed to parse competition effects, potentially by only sampling trees in standardized competitive environments—a sampling scheme not supported by our current dataset.

The SEM approach allowed us to test for indirect effects and mechanisms of relationships between predictors and survival that the Bayesian model did not support. The most strongly mediated variables in our data were lumen length, mediated by HSF, and RWI of the previous year, mediated by current RWI. Interestingly, the SEM did not find that HSFgini was significantly correlated with likelihood of mortality and found that HSF was actually negatively correlated with mortality, counter to both the Bayesian model results and observations. This may be due to the nature of structural models, however; the effect of HSF in this model is part of a "path" of effects from lumen length and wall thickness through HSF to mortality. In this case, it appears that the primary effect of differences in HSF may be due to the highly negative effect of lumen length and highly positive effect of wall thickness on HSF (Figure 8).

The mediating effect of lumen length and wall thickness on HSF may be fully explored by comparing RWI and HSF in living and dead trees (Figure S5.3). Dead trees appear to have produced tracheids with higher HSF in rings that were also larger prior to death, whereas living trees show a negative relationship between ring width and HSF. However, neither relationship was statistically significant (linear regression $p > 0.05$). The positive relationship between HSF and RWI in dead trees shows that as they grew larger rings, they may have grown a higher density of thicker walled cells than living trees in a given year. This also sheds further light on the potential mechanism of mortality due to higher growth plasticity and HSF plasticity. If dead trees are growing larger rings by means of increased cell density with thick walls, both C depletion and decreased hydraulic conductance may play a role. Living trees, meanwhile, appear to grow larger rings by growing cells with larger lumen diameters and thinner walls. This is again counter to expectations of HSF playing a role in drought defense but demonstrates that instead the mechanism of mortality may be associated with altered patterns of C allocation to xylem lignification.

Cone production did not vary relative to measured variables enough for models to converge, and thus few conclusions can be drawn from the cone data. The only physiological variable that appeared to be correlated with reproductive effort was RWI (and RWI of the previous year). A positive relationship between RWI and cone production means trees that grow more produce more cones, counter to the "flight" behavior prediction of a negative correlation between RWI or HSF and cone production or a growth-fecundity tradeoff. Our data primarily includes cone counts conducted in 2017-2019, after the end of the drought. It is worth noting that the majority of observations from early surveys were sparse, with little to no cone production. More data are needed to fully test which variables predict reproductive effort, but our results indicate a potential positive relationship between

growth and cone output in surviving trees after drought, and that this effect may be a post-drought reproductive flush. Recent work in angiosperms in Mediterranean forests has demonstrated that positive relationships between growth and reproduction may simply become less positive (i.e. the slope of the relationship decreases) during simulated drought (Bogdziewicz et al. 2020). We did not measure reproduction prior to the drought in our trees and cannot compare relationships between drought-stressed and vigorous trees. However, future work should consider differences in growth and reproduction in natural populations before and during drought, or degree of drought stress experienced by target trees.

To our knowledge, this study is the first to document positive effects of growth variability and variability in hydraulic safety traits on likelihood of mortality. We show that trees with high growth plasticity and high inter-annual variation in the ratio of tracheid wall thickness to cell diameter are more likely to die during drought. We hypothesize this is likely due to drawdowns of already drought-depleted C resources by increased C allocation to tracheid wall lignification. We further hypothesize that hydraulic stresses are higher in trees that swap between low conductivity/high drought resistance and high conductivity/low drought resistance growth types than those that maintain constant growth strategies. Our data demonstrate trees that employ conservative growth strategies—constant growth that is neither reduced excessively during drought or overzealous during periods of water excess—may best confer drought resistance. Whether this is a genetic characteristic of certain trees, the effect of site characteristics, or an interaction is unknown and is an important future research question. These results have important implications for future projections of forest response to drought. The majority of studies that project forest response to climate change focus on growth, with simple increases in biomass or growth indicative of "positive" responses to climate and declines in growth indicative of negative responses. Our results show that "type" of growth (i.e. xylem anatomy or C cost) as well as plasticity in ring width and tracheid anatomy, should be incorporated into models of forest response to change. Doing so would improve our ability to predict not just forest growth response to changes in climate, but likelihood of mortality. Further, incorporation of growth variability and anatomy in models of forest change would allow inclusion of mechanisms of response, greatly expanding understanding of forest health in a changing climate

5.5 Acknowledgements

Financial support for this research was provided by an NSF IOS grant (1925577). We thank Susan Glasser, Zachary Malone, Patricia Alcala, and Stephanie Ross for assistance with processing thin section samples and photographs, and preliminary analyses and reports that assisted in the development of this manuscript. We also thank Mengjun Shu, Nikole Vannest, and Dean Wu for helpful comments during project development. We thank Adrian Das, Jarmila Pittermann, and Derek Young for helpful discussions about tree mortality, tracheid anatomy, and drought and competition, respectively. We also thank Sequoia National Park, Sierra National Forest, and Tahoe National Forest for permission to establish permanent sampling plots and logistical support. We also thank Julia Morocco, Madisen Hinkley, Aubrey Hayes, Pedro Garcia, and Veronica Magana-Buie for assistance with tree core preparation and analysis.

5.6 References:

Aaltonen, H., A. Lindén, J. Heinonsalo, C. Biasi, and J. Pumpanen. 2016. Effects of prolonged drought stress on Scots pine seedling carbon allocation. Tree Physiology:1–10.

Abatzoglou, J. T., S. Z. Dobrowski, S. A. Parks, and K. C. Hegewisch. 2018. TerraClimate, a high-resolution global dataset of monthly climate and climatic water balance from 1958–2015. Scientific Data 5:170191.

Adams, H. D., M. J. Germino, D. D. Breshears, G. A. Barron-Gafford, M. Guardiola-Claramonte, C. B. Zou, and T. E. Huxman. 2013. Nonstructural leaf carbohydrate dynamics of *Pinus edulis* during drought-induced tree mortality reveal role for carbon metabolism in mortality mechanism. New Phytologist 197:1142–1151.

Adams, H. D., M. J. B. Zeppel, W. R. L. Anderegg, H. Hartmann, S. M. Landhäusser, D. T. Tissue, T. E. Huxman, P. J. Hudson, T. E. Franz, C. D. Allen, L. D. L. Anderegg, G. A. Barron-Gafford, D. J. Beerling, D. D. Breshears, T. J. Brodribb, H. Bugmann, R. C. Cobb, A. D. Collins, L. T. Dickman, H. Duan, B. E. Ewers, L. Galiano, D. A. Galvez, N. Garcia-Forner, M. L. Gaylord, M. J. Germino, A. Gessler, U. G. Hacke, R. Hakamada, A. Hector, M. W. Jenkins, J. M. Kane, T. E. Kolb, D. J. Law, J. D. Lewis, J.-M. Limousin, D. M. Love, A. K. Macalady, J. Martínez-Vilalta, M. Mencuccini, P. J. Mitchell, J. D. Muss, M. J. O'Brien, A. P. O'Grady, R. E. Pangle, E. A. Pinkard, F. I. Piper, J. A. Plaut, W. T. Pockman, J. Quirk, K. Reinhardt, F. Ripullone, M. G. Ryan, A. Sala, S. Sevanto, J. S. Sperry, R. Vargas, M. Vennetier, D. A. Way, C. Xu, E. A. Yepez, and N. G. McDowell. 2017. A multi-species synthesis of physiological mechanisms in drought-induced tree mortality. Nature Ecology & Evolution 1:1285.

Aitken, S., S. Yeaman, J. Holliday, T. Wang, and S. Curtis-McLane. 2008. Adaptation, migration or extirpation: climate change outcomes for tree populations. Evolutionary Applications 1:95–111.

Alberto, F. J., J. Derory, C. Boury, J.-M. Frigerio, N. E. Zimmermann, and A. Kremer. 2013. Imprints of Natural Selection Along Environmental Gradients in Phenology-Related Genes of Quercus petraea. Genetics 195:495–512.

Allen, C. D., D. D. Breshears, and N. G. McDowell. 2015. On underestimation of global vulnerability to tree mortality and forest die-off from hotter drought in the Anthropocene. Ecosphere 6:1–55.

Allen, C. D., A. K. Macalady, H. Chenchouni, D. Bachelet, N. McDowell, M. Vennetier, T. Kitzberger, A. Rigling, D. D. Breshears, E. H. (Ted) Hogg, P. Gonzalez, R. Fensham, Z. Zhang, J. Castro, N. Demidova, J.-H. Lim, G. Allard, S. W. Running, A. Semerci, and N. Cobb. 2010. A global overview of drought and heat-induced tree mortality reveals emerging climate change risks for forests. Forest Ecology and Management 259:660–684.

Alley, W. M. 1984. The Palmer Drought Severity Index: Limitations and Assumptions. Journal of Climate and Applied Meteorology 23:1100–1109.

Amthor, J. S. 2003. Efficiency of lignin biosynthesis: a quantitative analysis. Annals of Botany 91:673–695.

Anderegg, W. R. L., and L. D. L. Anderegg. 2013. Hydraulic and carbohydrate changes in experimental drought-induced mortality of saplings in two conifer species. Tree Physiology 33:252–260.

Anfodillo, T., A. Deslauriers, R. Menardi, L. Tedoldi, G. Petit, and S. Rossi. 2012. Widening of xylem conduits in a conifer tree depends on the longer time of cell expansion downwards along the stem. Journal of Experimental Botany 63:837–845.

von Arx, G., A. Crivellaro, A. L. Prendin, K. Čufar, and M. Carrer. 2016. Quantitative Wood Anatomy—Practical Guidelines. Frontiers in Plant Science 7.

Aubry-Kientz, M., and E. V. Moran. 2017. Climate Impacts on Tree Growth in the Sierra Nevada. Forests 8:414.

Ayari, A., and M. L. Khouja. 2014. Ecophysiological variables influencing Aleppo pine seed and cone production: a review. Tree Physiology 34:426–437.

Ayari, A., A. Zubizarreta-Gerendiain, M. Tome, J. Tome, S. Garchi, and B. Henchi. 2012. Stand, tree and crown variables affecting cone crop and seed yield of Aleppo pine forests in different bioclimatic regions of Tunisia. Forest Systems 21:128–140.

Bales, R. C., M. L. Goulden, C. T. Hunsaker, M. H. Conklin, P. C. Hartsough, A. T. O'Geen, J. W. Hopmans, and M. Safeeq. 2018. Mechanisms controlling the impact of multi-year drought on mountain hydrology. Scientific Reports 8:690.

Bhuyan, U., C. Zang, and A. Menzel. 2017. Different responses of multispecies tree ring growth to various drought indices across Europe. Dendrochronologia 44:1–8.

Biondi, F., and F. Qeadan. 2008. Inequality in Paleorecords. Ecology 89:1056–1067.

Bogdziewicz, M., M. Fernández-Martínez, J. Espelta, R. Ogaya, and J. Penuelas. 2020. Is forest fecundity resistant to drought? Results from an 18-yr rainfall-reduction experiment. New Phytologist.

Bouche, P. S., M. Larter, J.-C. Domec, R. Burlett, P. Gasson, S. Jansen, and S. Delzon. 2014. A broad survey of hydraulic and mechanical safety in the xylem of conifers. Journal of Experimental Botany 65:4419–4431.

Bryukhanova, M., and P. Fonti. 2012. Xylem plasticity allows rapid hydraulic adjustment to annual climatic variability. Trees 27:485–496.

Bunn, A. G. 2008. A dendrochronology program library in R (dplR). Dendrochronologia 26:115–124.

Bürkner, P.-C. 2017. brms: An R Package for Bayesian Multilevel Models Using Stan. Journal of Statistical Software 80:1–28.

Cailleret, M., V. Dakos, S. Jansen, E. M. R. Robert, T. Aakala, M. M. Amoroso, J. A. Antos, C. Bigler, H. Bugmann, M. Caccianaga, J.-J. Camarero, P. Cherubini, M. R. Coyea, K. Čufar, A. J. Das, H. Davi, G. Gea-Izquierdo, S. Gillner, L. J. Haavik, H. Hartmann, A.-M. Hereş, K. R. Hultine, P. Janda, J. M. Kane, V. I. Kharuk, T. Kitzberger, T. Klein, T. Levanic, J.-C. Linares, F. Lombardi, H. Mäkinen, I. Mészáros, J. M. Metsaranta, W. Oberhuber, A. Papadopoulos, A. M. Petritan, B. Rohner, G. Sangüesa-Barreda, J. M. Smith, A. B. Stan, D. B. Stojanovic, M.-L. Suarez, M. Svoboda, V. Trotsiuk, R. Villalba, A. R. Westwood, P. H. Wyckoff, and J. Martínez-Vilalta. 2019. Early-Warning Signals of

Individual Tree Mortality Based on Annual Radial Growth. Frontiers in Plant Science 9.

Cailleret, M., S. Jansen, E. M. R. Robert, L. Desoto, T. Aakala, J. A. Antos, B. Beikircher, C. Bigler, H. Bugmann, M. Caccianiga, V. Čada, J. J. Camarero, P. Cherubini, H. Cochard, M. R. Coyea, K. Čufar, A. J. Das, H. Davi, S. Delzon, M. Dorman, G. Gea-Izquierdo, S. Gillner, L. J. Haavik, H. Hartmann, A.-M. Hereş, K. R. Hultine, P. Janda, J. M. Kane, V. I. Kharuk, T. Kitzberger, T. Klein, K. Kramer, F. Lens, T. Levanic, J. C. L. Calderon, F. Lloret, R. Lobo-Do-Vale, F. Lombardi, R. L. Rodríguez, H. Mäkinen, S. Mayr, I. Mészáros, J. M. Metsaranta, F. Minunno, W. Oberhuber, A. Papadopoulos, M. Peltoniemi, A. M. Petritan, B. Rohner, G. Sangüesa-Barreda, D. Sarris, J. M. Smith, A. B. Stan, F. Sterck, D. B. Stojanović, M. L. Suarez, M. Svoboda, R. Tognetti, J. M. Torres-Ruiz, V. Trotsiuk, R. Villalba, F. Vodde, A. R. Westwood, P. H. Wyckoff, N. Zafirov, and J. Martínez-Vilalta. 2017. A synthesis of radial growth patterns preceding tree mortality. Global Change Biology 23:1675–1690.

Calflora: Information on California plants for education, research and conservation. 2014. . The Calflora Database [a non-profit organization], Berkeley, CA.

Chapin, F. S., E.-D. Schulze, and H. A. Mooney. 1990. The Ecology and Economics of Storage in Plants. Annual Review of Ecology and Systematics 21:423–447.

Clark, J. S., L. Iverson, C. W. Woodall, C. D. Allen, D. M. Bell, D. C. Bragg, A. W. D'Amato, F. W. Davis, M. H. Hersh, I. Ibanez, S. T. Jackson, S. Matthews, N. Pederson, M. Peters, M. W. Schwartz, K. M. Waring, and N. E. Zimmermann. 2016. The impacts of increasing drought on forest dynamics, structure, and biodiversity in the United States. Global Change Biology 22:2329–2352.

Clyatt, K. A., J. S. Crotteau, M. S. Schaedel, H. L. Wiggins, H. Kelley, D. J. Churchill, and A. J. Larson. 2016. Historical spatial patterns and contemporary tree mortality in dry mixed-conifer forests. Forest Ecology and Management 361:23–37.

Cuny, H. E., C. B. K. Rathgeber, D. Frank, P. Fonti, and M. Fournier. 2014. Kinetics of tracheid development explain conifer tree-ring structure. New Phytologist 203:1231–1241.

Dale, V. H., L. A. Joyce, S. McNulty, R. P. Neilson, M. P. Ayres, M. D. Flannigan, P. J. Hanson, L. C. Irland, A. E. Lugo, C. J. Peterson, D. Simberloff, F. J. Swanson, B. J. Stocks, and B. M. Wotton. 2001. Climate Change and Forest Disturbances Climate change can affect forests by altering the frequency, intensity, duration, and timing of fire, drought, introduced species, insect and pathogen outbreaks, hurricanes, windstorms, ice storms, or landslides. BioScience 51:723–734.

Dalla-Salda, G., M. E. Fernández, A.-S. Sergent, P. Rozenberg, E. Badel, and A. Martinez-Meier. 2014. Dynamics of cavitation in a Douglas-fir tree-ring: transition-wood, the lord of the ring? Journal of Plant Hydraulics 1:e005.

Daly, C., R. P. Neilson, and D. L. Phillips. 1994. A Statistical-Topographic Model for Mapping Climatological Precipitation over Mountainous Terrain. Journal of Applied Meteorology 33:140–158.

Das, A., J. Battles, N. L. Stephenson, and P. J. van Mantgem. 2011. The contribution of competition to tree mortality in old-growth coniferous forests. Forest Ecology and Management 261:1203–1213.

Das, A. J., J. J. Battles, N. L. Stephenson, and P. J. van Mantgem. 2007. The relationship between tree growth patterns and likelihood of mortality: a study of two tree species in the Sierra Nevada. Canadian Journal of Forest Research 37:580–597.

Das, A. J., N. L. Stephenson, and K. P. Davis. 2016. Why do trees die? Characterizing the drivers of background tree mortality. Ecology 97:2616–2627.

Das, A. J., N. L. Stephenson, A. Flint, T. Das, and P. J. van Mantgem. 2013. Climatic Correlates of Tree Mortality in Water- and Energy-Limited Forests. PLoS ONE 8.

Despland, E., and G. Houle. 1997. Climate influences on growth and reproduction of *Pinus banksiana* (Pinaceae) at the limit of the species distribution in eastern North America. American Journal of Botany 84:928–928.

Eis, S., E. H. Garman, and L. F. Ebell. 1965. Relation between cone production and diameter increment of Douglas Fir (*Pseudotsuga menziesii* (mirb.) Franco), Grand Fir (*Abies grandis* (dougl.) Lindl.), and Western White Pine (*Pinus monticola* Dougl.). Canadian Journal of Botany 43:1553–1559.

Evans, M. E. K., D. A. Falk, A. Arizpe, T. L. Swetnam, F. Babst, and K. E. Holsinger. 2017. Fusing tree-ring and forest inventory data to infer influences on tree growth. Ecosphere 8:n/a-n/a.

Eveno, E., C. Collada, M. A. Guevara, V. Leger, A. Soto, L. Diaz, P. Leger, S. C. Gonzalez-Martinez, M. T. Cervera, C. Plomion, and P. H. Garnier-Gere. 2008. Contrasting patterns of selection at *Pinus pinaster* Ait. drought stress candidate genes as revealed by genetic differentiation analyses. Molecular Biology and Evolution 25:417–437.

Fischer, M. J., K. M. Waring, R. W. Hofstetter, and T. E. Kolb. 2010. Ponderosa pine characteristics associated with attack by the roundheaded pine beetle. Forest Science 56:473–483.

Flint, L. E., A. L. Flint, J. H. Thorne, and R. Boynton. 2013. Fine-scale hydrologic modeling for regional landscape applications: the California Basin Characterization Model development and performance. Ecological Processes 2:1–21.

Fonti, P., and E. A. Babushkina. 2016. Tracheid anatomical responses to climate in a forest-steppe in Southern Siberia. Dendrochronologia 39:32–41.

Franceschi, V. R., P. Krokene, E. Christiansen, and T. Krekling. 2005. Anatomical and chemical defenses of conifer bark against bark beetles and other pests. New Phytologist 167:353–376.

Gärtner, H., S. Lucchinetti, and F. H. Schweingruber. 2014. New perspectives for wood anatomical analysis in dendrosciences: The GSL1-microtome. Dendrochronologia 32:47–51.

Gelman, A., A. Jakulin, M. G. Pittau, and Y.-S. Su. 2008. A weakly informative default prior distribution for logistic and other regression models. The Annals of Applied Statistics 2:1360–1383.

Gooch, J. W. 2011. Hagen-Poiseuille Equation. Pages 355–355 *in* J. W. Gooch, editor. Encyclopedic Dictionary of Polymers. Springer New York.

Goulden, M. L., R. G. Anderson, R. C. Bales, A. E. Kelly, M. Meadows, and G. C. Winston. 2012. Evapotranspiration along an elevation gradient in California's Sierra Nevada. Journal of Geophysical Research: Biogeosciences 117:G03028.

Goulden, M. L., and R. C. Bales. 2014. Mountain runoff vulnerability to increased evapotranspiration with vegetation expansion. Proceedings of the National Academy of Sciences 111:14071–14075.

Goulden, M. L., and R. C. Bales. 2019. California forest die-off linked to multi-year deep soil drying in 2012–2015 drought. Nature Geoscience 12:632–637.

Griffin, D., and K. J. Anchukaitis. 2014. How unusual is the 2012–2014 California drought? Geophysical Research Letters 41:2014GL062433.

Grissino-Mayer, H. D. 2001. Evaluating Crossdating Accuracy: A Manual and Tutorial for the Computer Program COFECHA. Tree-Ring Research.

Grossiord, C., A. Gessler, A. Granier, S. Berger, C. Bréchet, R. Hentschel, R. Hommel, M. Scherer-Lorenzen, and D. Bonal. 2014. Impact of interspecific interactions on the soil water uptake depth in a young temperate mixed species plantation. Journal of Hydrology 519, Part D:3511–3519.

Guo, Q., S. J. Zarnoch, X. Chen, and D. G. Brockway. 2016. Life cycle and masting of a recovering keystone indicator species under climate fluctuation. Ecosystem Health and Sustainability 2:e01226.

Hacke, U. G., V. Stiller, J. S. Sperry, J. Pittermann, and K. A. McCulloh. 2001. Cavitation Fatigue. Embolism and Refilling Cycles Can Weaken the Cavitation Resistance of Xylem. Plant Physiology 125:779–786.

Hacket-Pain, A. J., D. Ascoli, G. Vacchiano, F. Biondi, L. Cavin, M. Conedera, I. Drobyshev, I. D. Liñán, A. D. Friend, M. Grabner, C. Hartl, J. Kreyling, F. Lebourgeois, T. Levanič, A. Menzel, E. van der Maaten, M. van der Maaten-Theunissen, L. Muffler, R. Motta, C.-C. Roibu, I. Popa, T. Scharnweber, R. Weigel, M. Wilmking, and C. S. Zang. 2018. Climatically controlled reproduction drives interannual growth variability in a temperate tree species. Ecology Letters.

Hacket-Pain, A. J., J. G. A. Lageard, and P. A. Thomas. 2017. Drought and reproductive effort interact to control growth of a temperate broadleaved tree species (*Fagus sylvatica*). Tree Physiology 37:744–754.

Hagedorn, F., J. Joseph, M. Peter, J. Luster, K. Pritsch, U. Geppert, R. Kerner, V. Molinier, S. Egli, M. Schaub, J.-F. Liu, M. Li, K. Sever, M. Weiler, R. T. W. Siegwolf, A. Gessler, and M. Arend. 2016. Recovery of trees from drought depends on belowground sink control. Nature Plants 2:16111.

Hegyi, F. 1974. A simulation model for managing jack pine stands. Pages 74–90 Growth Models for Tree and Stand Simulations.

Hicke, J. A., A. J. H. Meddens, and C. A. Kolden. 2016. Recent Tree Mortality in the Western United States from Bark Beetles and Forest Fires. Forest Science 62:141–153.

Hisamoto, Y., and S. Goto. 2017. Genetic control of altitudinal variation on female reproduction in *Abies sachalinensis* revealed by a crossing experiment. Journal of Forest Research 22:195–198.

Hoef, J. M. V., and P. L. Boveng. 2007. Quasi-Poisson Vs. Negative Binomial Regression: How Should We Model Overdispersed Count Data? Ecology 88:2766–2772.

Huang, J., M. Kautz, A. M. Trowbridge, A. Hammerbacher, K. F. Raffa, H. D. Adams, D. W. Goodsman, C. Xu, A. J. H. Meddens, D. Kandasamy, J. Gershenzon, R.

Seidl, and H. Hartmann. 2020. Tree defence and bark beetles in a drying world: carbon partitioning, functioning and modelling. New Phytologist 225:26–36.

IPCC. 2014. Climate Change 2014: Impacts,Adaptation, and Vulnerability. Part A: Global and Sectoral Aspects. Contribution of Working Group II to the Fifth Assessment Report of the Intergovernmental Panel on Climate Change. Page 1132. Cambridge University Press, Cambridge, UK and New York, USA.

Kane, J. M., and T. E. Kolb. 2010. Importance of resin ducts in reducing ponderosa pine mortality from bark beetle attack. Oecologia 164:601–609.

Kelly, D., A. Geldenhuis, A. James, E. P. Holland, M. J. Plank, R. E. Brockie, P. E. Cowan, G. A. Harper, W. G. Lee, M. J. Maitland, A. F. Mark, J. A. Mills, P. R. Wilson, and A. E. Byrom. 2013. Of mast and mean: differential-temperature cue makes mast seeding insensitive to climate change. Ecology Letters 16:90–98.

Klein, T. 2014. The variability of stomatal sensitivity to leaf water potential across tree species indicates a continuum between isohydric and anisohydric behaviours. Functional Ecology 28:1313–1320.

Lauder, J. D., E. V. Moran, and S. C. Hart. 2019. Fight or Flight? Potential tradeoffs between drought defense and reproduction in conifers. Tree Physiology 39:1071–1085.

Lindén, A., and S. Mäntyniemi. 2011. Using the negative binomial distribution to model overdispersion in ecological count data. Ecology 92:1414–1421.

Loewenstein, N. J., and S. G. Pallardy. 1998. Drought tolerance, xylem sap abscisic acid and stomatal conductance during soil drying: a comparison of canopy trees of three temperate deciduous angiosperms. Tree Physiology 18:431–439.

van Mantgem, P. J., and N. L. Stephenson. 2007. Apparent climatically induced increase of tree mortality rates in a temperate forest. Ecology Letters 10:909–916.

Martínez-Vilalta, J. 2018. The rear window: structural and functional plasticity in tree responses to climate change inferred from growth rings. Tree Physiology 38:155–158.

McIntyre, P. J., J. H. Thorne, C. R. Dolanc, A. L. Flint, L. E. Flint, M. Kelly, and D. D. Ackerly. 2015. Twentieth-century shifts in forest structure in California: Denser forests, smaller trees, and increased dominance of oaks. Proceedings of the National Academy of Sciences of the United States of America 112:1458–1463.

Mitchell, P. J., A. P. O'Grady, D. T. Tissue, D. A. White, M. L. Ottenschlaeger, and E. A. Pinkard. 2013. Drought response strategies define the relative contributions of hydraulic dysfunction and carbohydrate depletion during tree mortality. New Phytologist 197:862–872.

Moore, J., M. Woods, and D. Greenberg. 2020. 2019 Aerial Survey Results: California. USDA Forest Service Region 5 Forest Health Monitoring Aerial Survey Program, Davis, CA.

Ogle, K., T. G. Whitham, and N. S. Cobb. 2000. Tree-Ring Variation in Pinyon Predicts Likelihood of Death following Severe Drought. Ecology 81:3237.

Pallardy, S. G., Čermák J., F. W. Ewers, M. R. Kaufmann, W. C. Parker, and J. S. Sperry. 1995. 9 - Water Transport Dynamics in Trees and Stands. Pages 301–389 *in* W. K. Smith and T. M. Hinckley, editors. Resource Physiology of Conifers. Academic Press, San Diego.

Pittermann, J., J. S. Sperry, J. K. Wheeler, U. G. Hacke, and E. H. Sikkema. 2006. Mechanical reinforcement of tracheids compromises the hydraulic efficiency of conifer xylem. Plant, Cell & Environment 29:1618–1628.

R Development Core Team. 2020. R: A language and environment for statistical computing. R Foundation for Statistical Computing, Vienna, Austria.

Raffa, K. F., B. H. Aukema, B. J. Bentz, A. L. Carroll, J. A. Hicke, M. G. Turner, and W. H. Romme. 2008. Cross-scale Drivers of Natural Disturbances Prone to Anthropogenic Amplification: The Dynamics of Bark Beetle Eruptions. BioScience 58:501–517.

Redmond, M. D., F. Forcella, and N. N. Barger. 2012. Declines in pinyon pine cone production associated with regional warming. Ecosphere 3:1–14.

Regent Instruments Canada Inc. 2017. winDENDRO for Tree-ring Analysis.

Rosseel, Y. 2012. lavaan: An R Package for Structural Equation Modeling. Journal of Statistical Software 48:1–36.

Sala, A., D. R. Woodruff, and F. C. Meinzer. 2012. Carbon dynamics in trees: feast or famine? Tree Physiology 32:764–775.

Santos, L., E. Notivol, R. Zas, M. R. Chambel, J. Majada, and J. Climent. 2010. Variation of early reproductive allocation in multi-site genetic trials of Maritime pine and Aleppo pine. Forest Systems 19:381–392.

Speer, J. 2010. Fundamentals of Tree Ring Research. University of Arizona Press.

Stephenson, N. L., A. J. Das, N. J. Ampersee, B. M. Bulaon, and J. L. Yee. 2019. Which trees die during drought? The key role of insect host-tree selection. Journal of Ecology 107:2383–2401.

Tardieu, F., and T. Simonneau. 1998. Variability among species of stomatal control under fluctuating soil water status and evaporative demand: modelling isohydric and anisohydric behaviours. Journal of Experimental Botany 49:419–432.

Vehtari, A., A. Gelman, and J. Gabry. 2017. Practical Bayesian model evaluation using leave-one-out cross-validation and WAIC. Statistics and Computing 27:1413–1432.

Wang, T., A. Hamann, D. Spittlehouse, and C. Carroll. 2016. Locally Downscaled and Spatially Customizable Climate Data for Historical and Future Periods for North America. PLOS ONE 11:e0156720.

Woodruff, D. R., B. J. Bond, and F. C. Meinzer. 2004. Does turgor limit growth in tall trees? Plant, Cell & Environment 27:229–236.

Woodward, A., and D. Silsbee. 1994. Influence of climate on radial growth and cone production in the subalpine fir (*Abies lasiocarpa*) and mountain hemlock (*Tsuga mertensiana*). Canadian Journal of Forest Research 24:1133–1143.

Young, D. J. N., J. T. Stevens, J. M. Earles, J. Moore, A. Ellis, A. L. Jirka, and A. M. Latimer. 2017. Long-term climate and competition explain forest mortality patterns under extreme drought. Ecology Letters 20:78–86.

Table 5.1. Bayesian logistic regression model fit comparison. All models were the same and included all predictors, with only different drought metrics chosen for each. LOOIC = leave-one-out information criterion, with lower values representing better model fit. Bold values represent top two best fits, n = 156 trees.

Model Drought Metric	**LOOIC**
CMD	138.4
CWD	**126.9**
DEF	144.3
PDSI	**100.2**
P-ET	**125.8**

Table 5.2. Bayesian logistic regression model parameter estimates. Due to the large number of models and parameters, not all tested models are displayed but only significant parameters (where credible intervals do not overlap 0). Drought metrics from each of the top models are also displayed even though they are not significant. Full list of all estimated parameters is available in Appendix B. $\hat{R}$ = indicator of convergence, with values < 1.02 indicating model convergence.

	Estimate	**Est.Error**	**95% CI**		$\hat{R}$	**Model**
Intercept	1.62	4.40	-7.10	10.42	1.00	PDSI
PDSI	1.60	3.65	-4.35	10.22	1.00	PDSI
Gini	0.79	0.51	-0.19	1.86	1.00	PDSI
HSF gini	0.26	0.45	-0.63	1.17	1.00	PDSI
Min. Temp.	4.17	4.08	-2.38	13.37	1.00	PDSI
Hegyi Index	-0.17	0.10	-0.38	-0.01	1.00	PDSI
Intercept	0.55	4.50	-8.70	9.30	1.00	PET
P-ET	-1.52	3.10	-8.54	3.80	1.00	PET
Gini	0.63	0.37	-0.08	1.39	1.00	PET
HSFgini	0.13	0.37	-0.59	0.85	1.00	PET
Min. Temp.	1.39	2.27	-2.21	6.72	1.00	PET
Hegyi Index	-0.23	0.08	-0.40	-0.09	1.00	PET
RWIxP-ET	-2.47	1.77	-6.25	0.71	1.00	PET
Intercept	1.56	4.32	-7.06	10.09	1.00	CWD
CWD	-1.81	3.64	-9.53	3.88	1.00	CWD
HSF	-0.85	1.98	-4.84	3.08	1.00	CWD
Gini	0.68	0.37	-0.03	1.42	1.00	CWD
HSF gini	0.20	0.36	-0.53	0.90	1.00	CWD
Min. Temp.	1.30	2.25	-2.82	6.21	1.00	CWD
Hegyi Index	-0.22	0.08	-0.39	-0.07	1.00	CWD
DBH	-0.85	0.47	-1.81	-0.01	1.00	CWD

Table 5.3. Structural Equation Model (SEM) model fits. P-values are significance from χ^2 tests comparing structural model covariance to data covariance, with values greater than 0.05 representing model covariance that is not significantly different from that observed in the data. Note p-values from χ^2 tests in this case are not comparable between models, and are only used here to confirm non-significant differences in covariances. AIC = Akaike's information criterion, with lower values representing better fit. Bold metrics represent top two values in each fit measure, while Bold and Italic represents the only metric/model combination that was best fit according to both measures.

Model Drought Metric	**p-value**	**AIC**
CWD	0.058	**560.38**
CMD	**0.219**	**543.62**
DEF	0.059	**554.58**
P-ET	**0.193**	561.50
PDSI	**0.122**	563.85

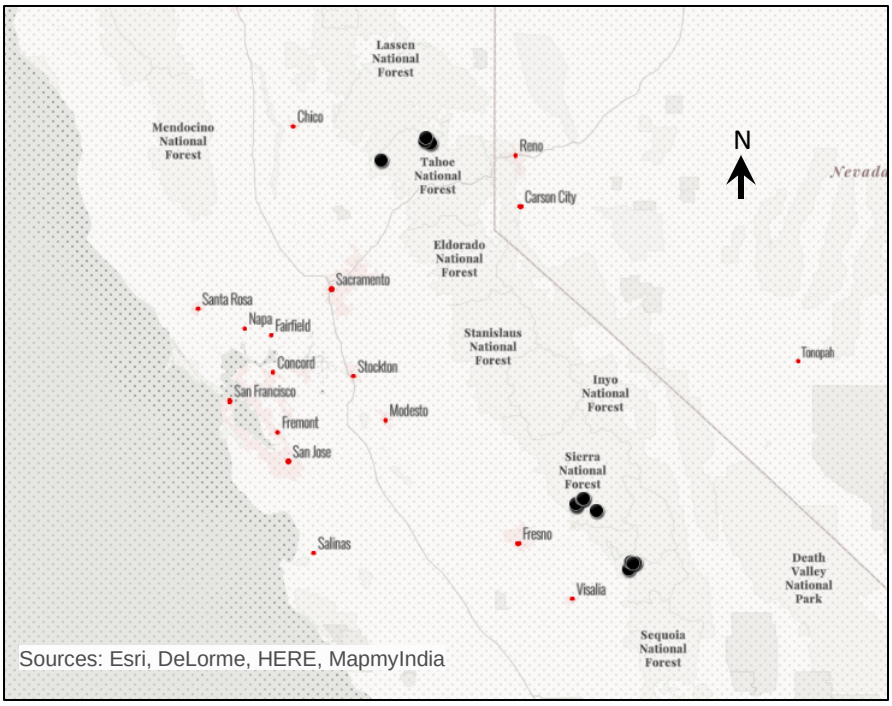

Figure 5.1. Map of sample locations of all cored trees across the Sierra Nevada. Black dots represent sample locations.

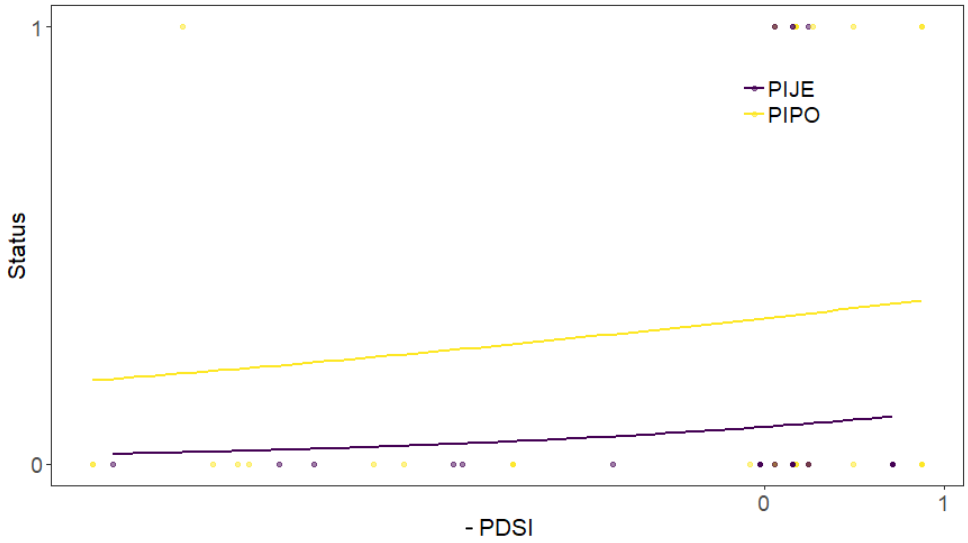

Figure 5.2. Relationship between scaled (mean = 0) -PDSI (higher values represent higher degree of drought) and likelihood of tree mortality (Status = 1) in *P. ponderosa* (PIPO) and *P. jeffreyi* (PIJE). Lines represent likelihood of mortality, while points represent observations.

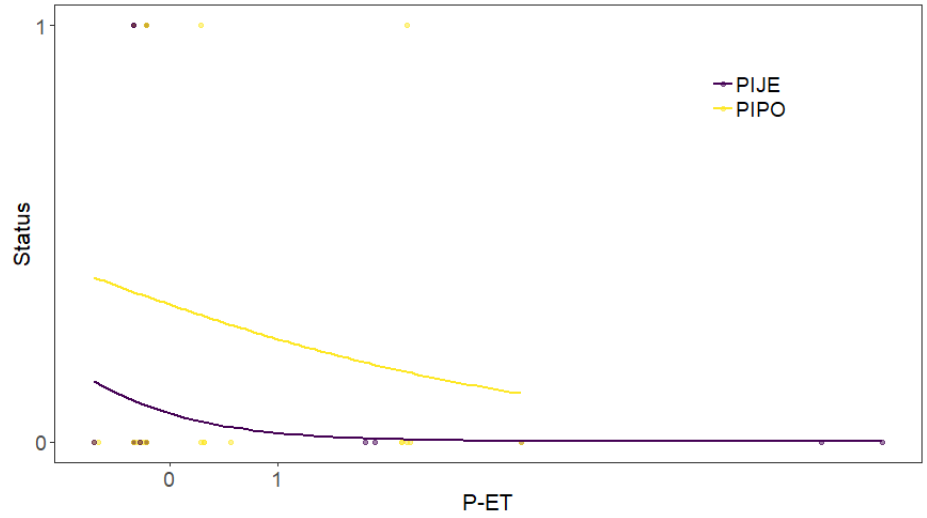

Figure 5.3. Relationship between scaled (mean = 0) P-ET (lower values represent higher degree of drought) and likelihood of tree mortality (Status = 1) in *P. ponderosa* (PIPO) and *P. jeffreyi* (PIJE). Lines represent likelihood of mortality, while points represent observations.

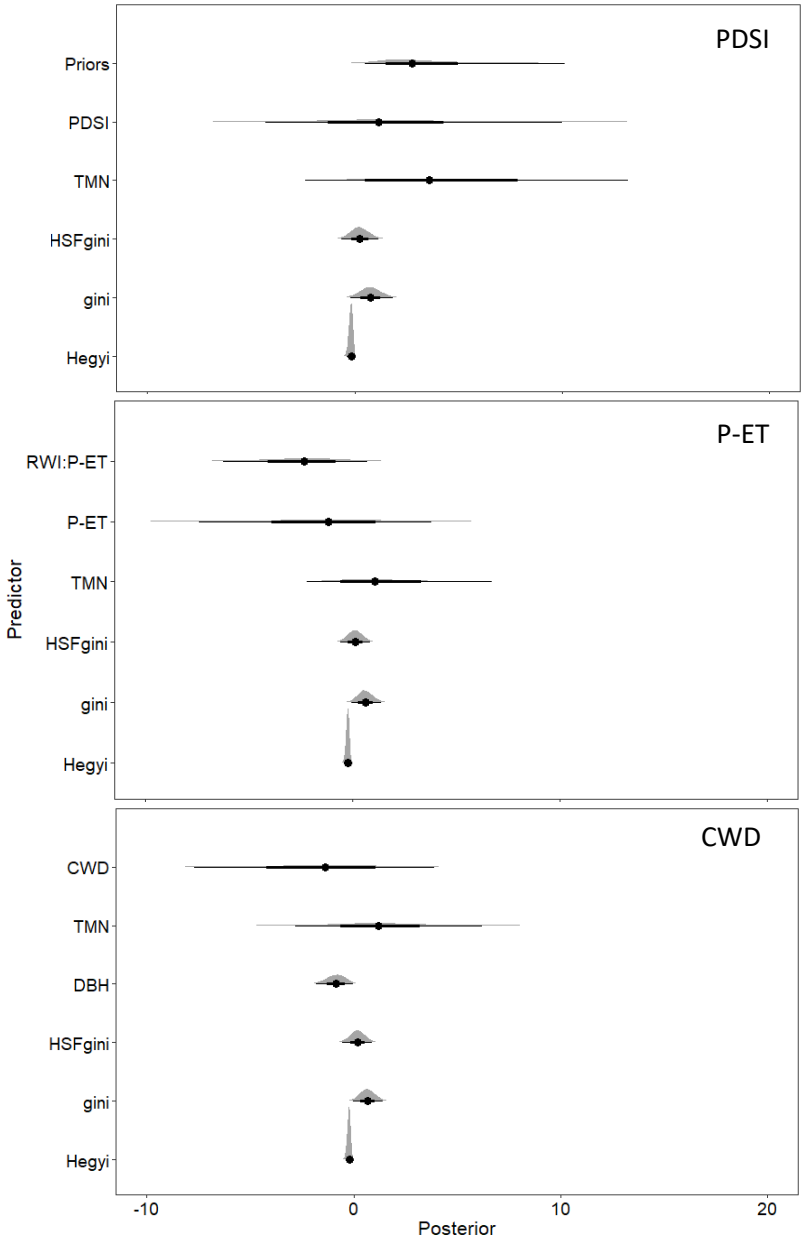

Figure 5.4. Posteriors of predictors with most significant (non-zero) posteriors from top three best-fit Bayesian logistic regressions. Drought metric listed in upper right of each figure represents model (see text for description). Gray density plot represents posterior distribution, circle represents posterior mean, and thick and thin horizontal lines represent 65% and 95% credible intervals, respectively. Priors (in top figure only but constant across all models) = distribution of student-t priors for all variables. PDSI = Palmer Drought Severity Index, TMN = minimum temperature, HSFgini = variability in HSF (wall thickness/lumen diameter), Gini = growth variability, Hegyi = hegyi index of competition, P-ET = precipitation minus evapotranspiration, CWD = Climatic Water Deficit, RWI:P-ET = interaction between ring width index and P-ET.

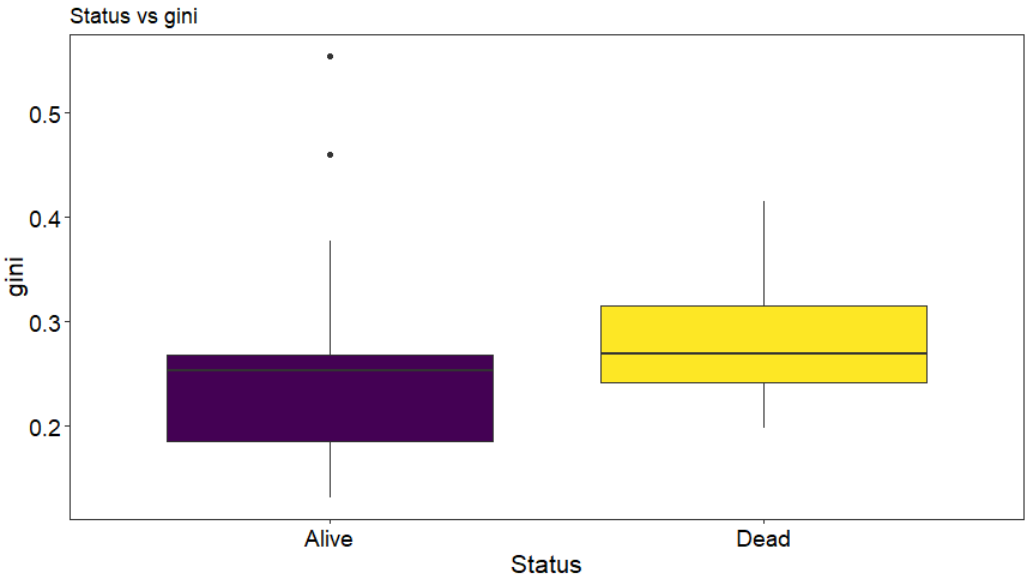

Figure 5.5. Boxplots of observed Gini coefficients (variability in growth) between living and dead trees (ANOVA p = 0.011). Solid line represents median value, boxes define first and third quartiles, whiskers represent range, and dots represent outliers (>1.5 sd from mean).

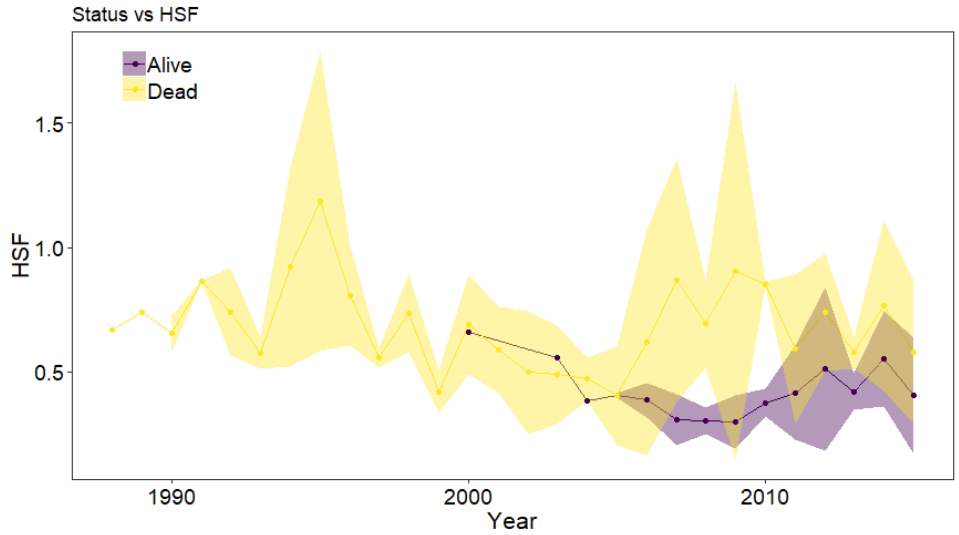

Figure 5.6. Measured HSF (ratio of wall thickness/lumen diameter) in living and dead trees over time. Shaded area represent 95% confidence intervals. *P. ponderosa* (PIPO) and *P. jeffreyi* (PIJE). Lines represent likelihood of mortality, while points represent observations.

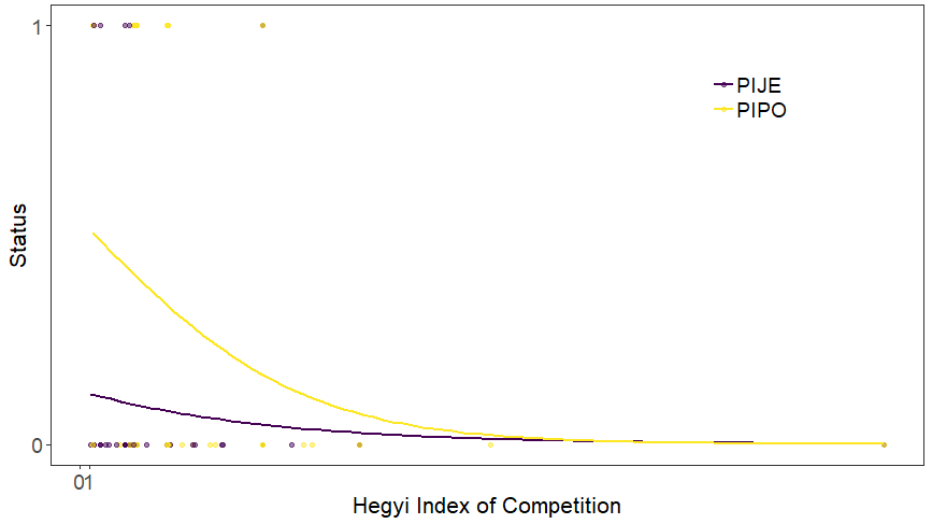

Figure 5.7. Relationship between Hegyi index of competition and likelihood of tree mortality (Status = 1) in *P. ponderosa* (PIPO) and *P. jeffreyi* (PIJE). Lines represent likelihood of mortality, while points represent observations.

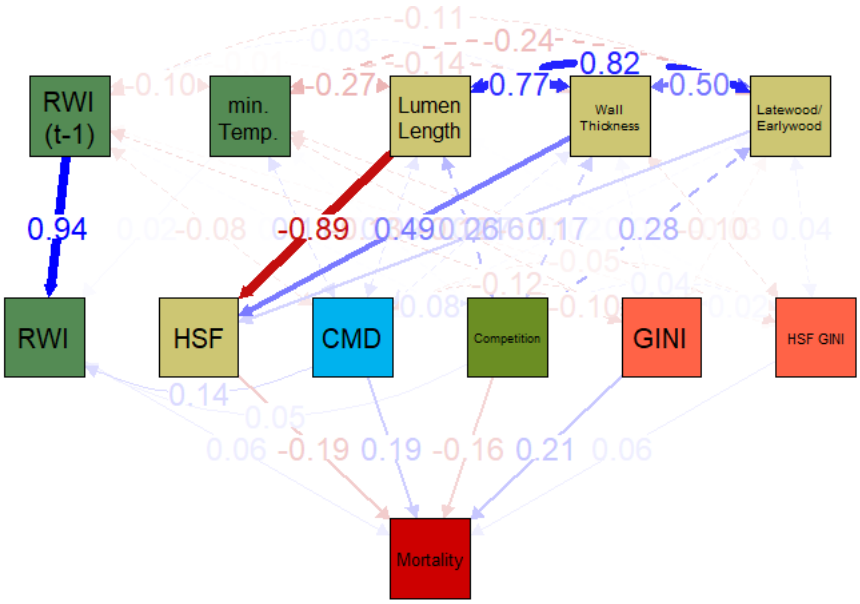

Figure 5.8. Path diagram of results of structural equation model (SEM). Boxes represent input variables, arrows represent correlations, with direction of arrow representing the "direction of influence." Colors of arrows represent positive or negative correlations (red = negative, blue = positive), with color brightness corresponding to degree of correlation (bright colors = higher correlation). Colors of boxes are color-coded to represent predictor "group" in the original structural model: green = growth and temperature that influences growth, tan = hydraulic traits, pink = variability, blue = drought metric, light green = competition/stand characteristics, and red = mortality. RWI = ring width index, RWI (t-1) = RWI in prior year, HSF = hydraulic safety factor (xylem wall thickness/xylem lumen diameter), CMD = climatic moisture deficit from the ClimateNA climate model, Gini = interannual growth variability, HSFgini = interannual variability in HSF.

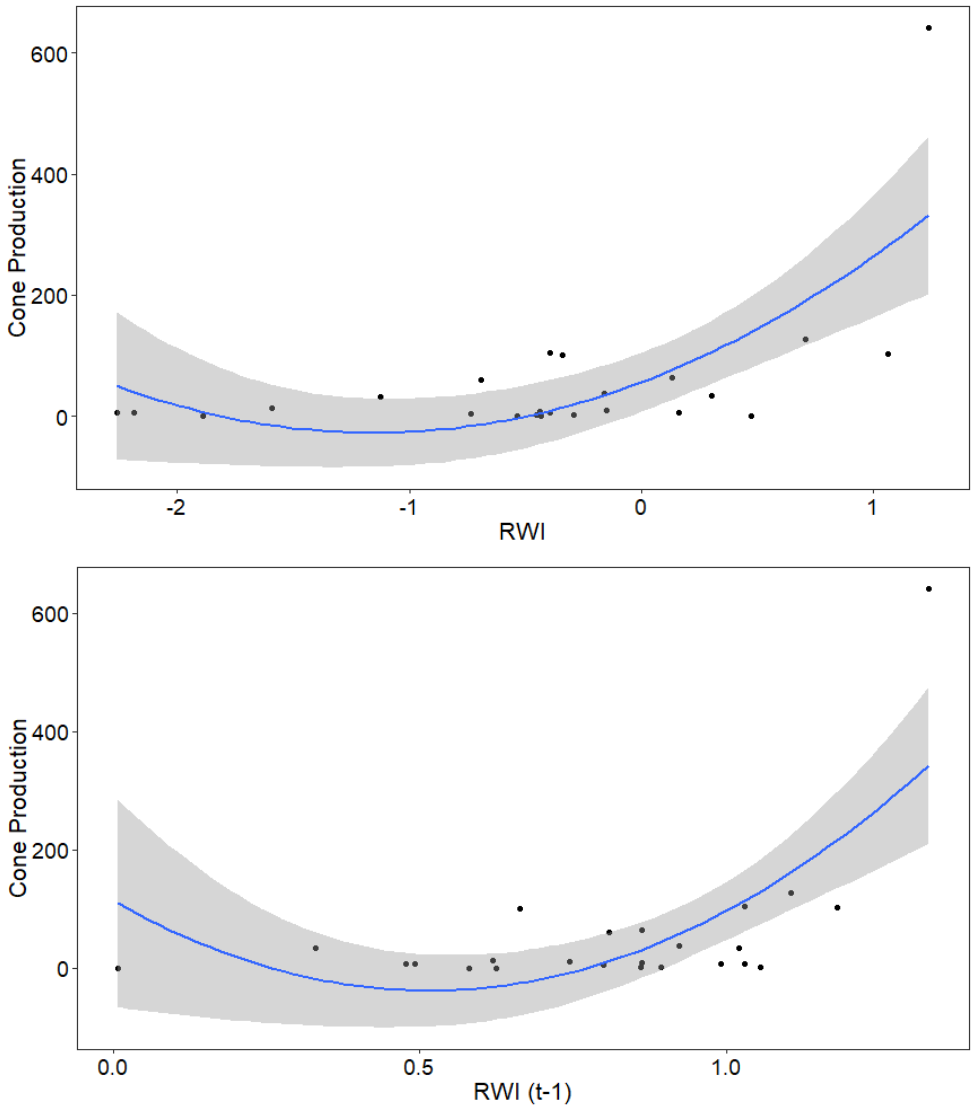

Figure 5.9. Relationship between total cone production (mature cone presence on trees and on ground that are attributable to a target tree) and ring width (RWI, $p = 0.013$ $R^2 = 0.214$, $n = 27$) in the current and prior (t-1, $p = 0.19$, $R^2 = 0.192$, $n = 27$) year. Lines represent best fit (local spline regression) lines, with shaded areas representing 95% confidence intervals of the best fit spline.

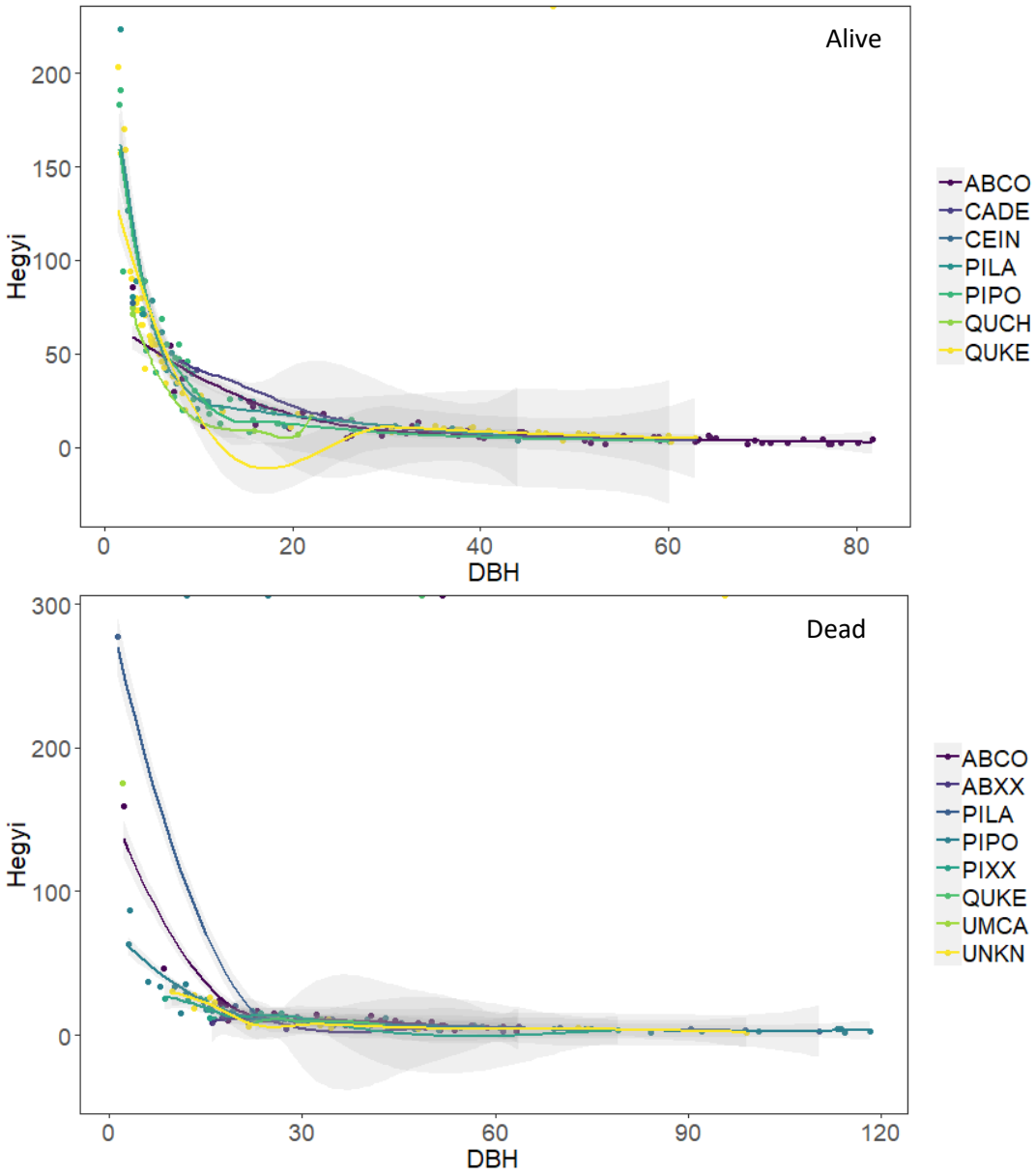

Figure 5.10. Relationship between Hegyi index and tree diameter at breast height (DBH). Hegyi index is a DBH-weighted measure of competition. Larger trees experience lower levels of competition in both living (top panel) and dead (bottom panel) trees. ABCO = *Abies concolor*, ABXX = unknown *Abies* sp., CADE = *Calocedrus decurrens*, CEIN = *Ceanothus integerrimus* (not included in analysis but marked here due to larger size), PILA = *Pinus lambertiana*, PIPO = *P. ponderosa*, PIXX = unknown *Pinus* sp., QUCH = *Quercus chrysolepis*, QUKE = *Quercus kelloggii*, UMCA = *Umbellularia californica*, UNKN = unknown (standing snag).

Supplemental Figures

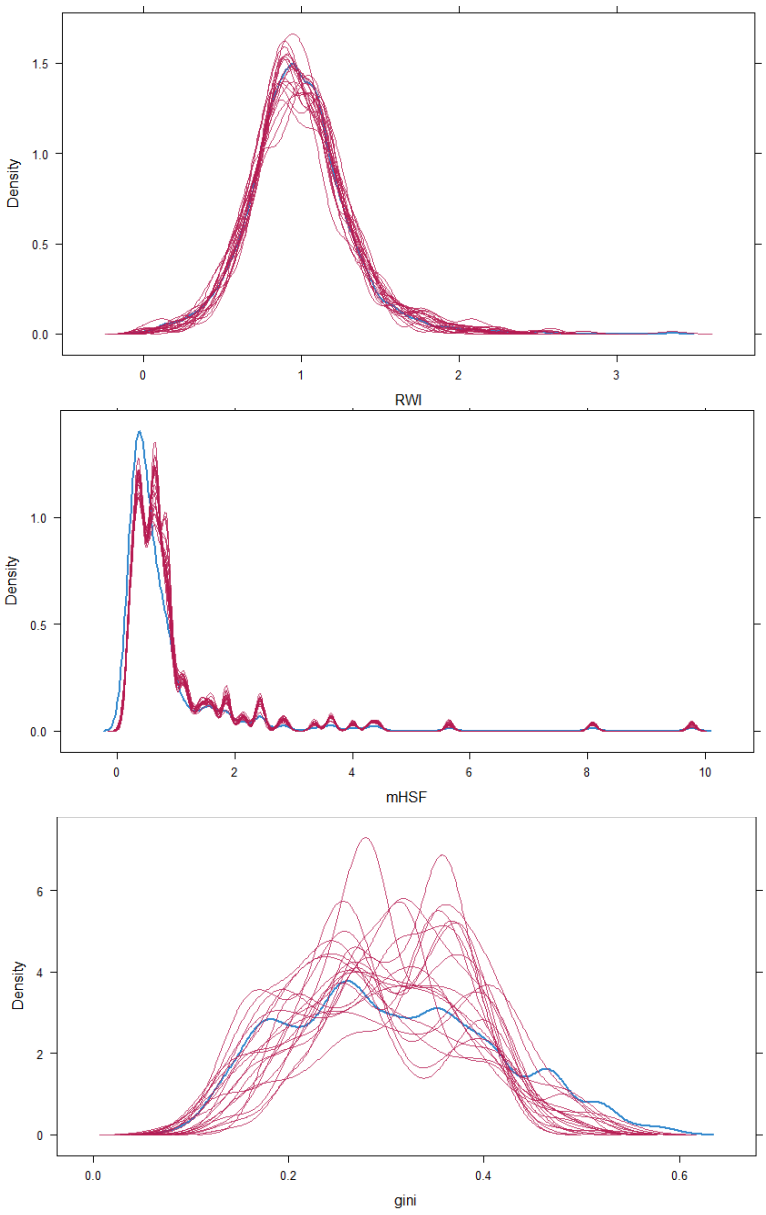

Figure S5.1. Results of multiple imputation for the three primary values imputed to fill data gaps: RWI (top), mean HSF (mHSF, middle), and Gini coefficient (bottom). Blue lines represent frequency distributions of raw data. Red lines represent density distributions of results of 20 imputations, where each variable is estimated based on all other variables iteratively. Ring width index (RWI) and mean hydraulic safety factor (mHSF) imputations appear to match observations almost perfectly. Gini coefficient imputations are more variable, but imputed datasets with high densities of some values (peaks) appear to not be generating outliers, but instead high densities of intermediate Gini values.

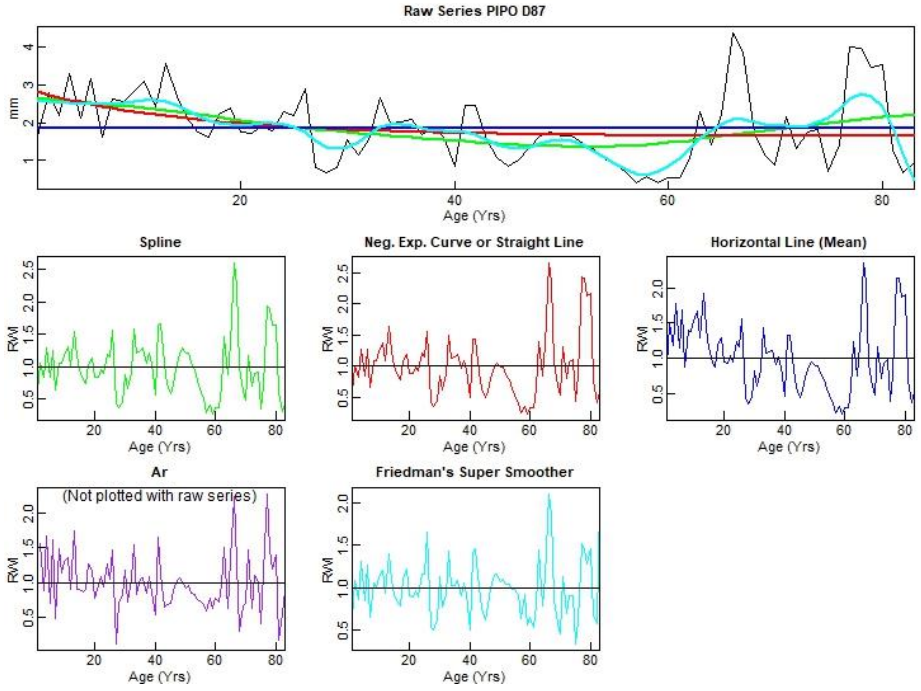

Figure S5.2. Example of detrending methods for ring widths, using the i.detrend function in R package "dplR" (Bunn, 2008). Top image is raw ring width (black line), with the detrending line for each method shown by a different color. To calculate ring width index (RWI), raw ring width is divided by the value of the line at each time point. Resulting RWI chronologies for each method are displayed below. We chose a cubic spline (green) with a 20-year length (i.e., 20 years between inflection points) to retain variation at decadal scales but minimize age-based effects and high-frequency variation (Speer 2010). Cubic splines are considered more aggressive than dividing by a negative exponential function (red line, which represents strictly age-based growth), an autoregressive model (purple), or dividing by the mean ring width (dark blue), and more conservative than a smoothing function (light blue, which only removes inter-annual variation).

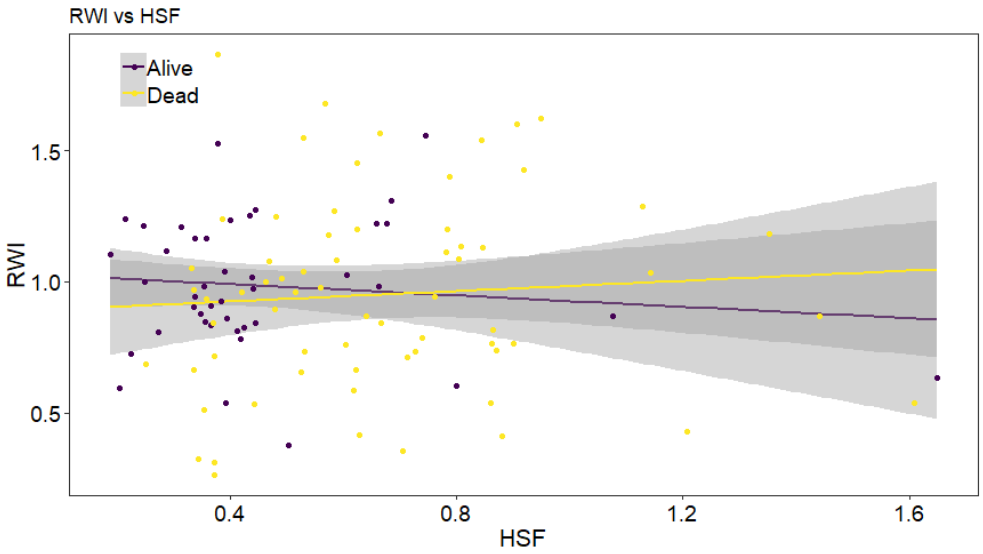

Figure S5.3. Relationship between hydraulic safety factor (HSF) and ring width index (RWI) in living and dead trees. Dead trees show a positive but not statistically significant (linear regression p = 0.61) relationship between HSF and RWI, indicating higher HSF in larger rings, and smaller HSF in smaller rings. Living trees show the opposite (also not statistically significant (p = 0.60) relationship, with HSF declining in larger rings. Shaded areas represent 95% confidence intervals of the regression lines.

Chapter 6:
Conclusion

6.1 Introduction

Forest response to climate change is a function of tree survival, growth, and fecundity. As climate continues to change and forests are exposed to both increasing aridity in general (IPCC 2014) and increased drought frequency and intensity (Cook et al. 2010, Allen et al. 2010), forests may shift in density, composition, and distribution (Allen et al. 2015). The degree of these shifts will be mediated by variation in individual and species-level traits that confer fitness. In long-lived species like trees, fitness is enhanced via growth and survival as well as increased fecundity (Moran et al. 2017, Lauder et al. 2019). Little work to date has explored interactions across these traits, such as how mechanisms of drought survival interact with growth and reproduction. Fewer studies still have examined how cellular traits scale to influence whole-forest response to climate. In this dissertation, I showed that variation in tree carbon (C) allocation strategies may be expected to significantly influence drought response through trade-offs among growth, drought defense (via increased allocation to C-expensive lignin in xylem cell walls), pest defense, and reproductive output. I then identified novel predictors of tree mortality in Sierra Nevada conifers during the 2012-2016 drought and identified variation in metrics used to quantify that drought. These novel predictors of mortality included high hydraulic safety, counter to theoretical expectations, and inter-annual variability in growth and hydraulic safety.

Theory predicts that increased thickening of xylem cell walls via lignification increases resistance to drought (Sperry 2003, Sperry et al. 2006). This increased resistance is thought to stem from enhanced mechanical resistance to implosion (Hacke et al. 2001, Pittermann et al. 2006b) or decreased likelihood of inter-tracheid air seeding and embolism formation (Pittermann et al. 2006a). However, lignification of xylem cell walls is C-expensive (Amthor 2003, Pittermann et al. 2006b, Lauder et al. 2019). Here I demonstrated that trees that died during extreme drought had thicker cell walls and more total lignin and C per annual ring. Coupled with the observation that bark beetle outbreak coincided with the extreme 2012-2016 drought, this finding extends prior theory and research on C depletion in drought stressed trees (McDowell et al. 2008, McDowell 2011, Adams et al. 2017) to identify the trade-off between drought defense and pest defense as a potential mechanism of that depletion and its influence on drought survival.

The influence of C allocation to growth and hydraulic safety on tree mortality under drought may also depend on how one defines drought. Drought metrics attempt to quantify drought via calculation of some biologically meaningful measure of water availability, typically in the soil. The methods used to calculate this water availability vary widely, however, in both their theoretical assumptions and their methods of calibration. Thus, choosing one metric of drought over another for inclusion in models of forest response to drought without consideration of these differences may alter model outcomes. I demonstrated that five popular drought metrics vary in their ability to predict tree growth according to a set of tree ring chronologies from across the Sierra Nevada. I further showed that these differences may stem from both varied underlying calculations

and different sensitivities to wet and dry years that not always vary across the landscape in accordance with their respective spatial resolutions. These results build on prior research examining how not all droughts are equal in their impacts (Anderegg et al. 2013) by demonstrating that there is further uncertainty in understanding tree response to drought that stems from our methods of quantifying drought. These results underline the complex interactions among tree physiology, drought stress, landscape scale drought measurement, and pest stress, and lay out a clear path for future research.

6.2 Implications for Future Study

Current models of forest response to climate change typically examine either individual tree ring growth (Charney et al. 2016) or change in total biomass as a proxy for growth. However, there is increasing evidence that growth variability (Ogle et al. 2000) or departure between tree growth and climate (Das et al. 2007, Cailleret et al. 2017, 2019) are better predictors of forest mortality than growth alone, and our results identify variation in hydraulic safety and the C cost of that safety as a potential mechanism of this discrepancy. This frames an important avenue for future research: the sensitivity of models of forest response to change to variance in tree physiology.

Models of forest response to change that only incorporate growth do not account for what that growth means for resistance to extreme stress. For example, our finding that growth variability outweighs absolute growth in predicting mortality demonstrates that a model based on growth alone will predict positive forest response to change if average growth is high. But two forests can have the same level of average growth rate, while one forest contains trees with high inter-annual variation in growth and the other contains trees with low inter-annual variation. In the case of a growth-only model, both forests would be identified as responding positively to change, while we demonstrate here that the forest with a high degree of inter-annual variation may be expected to be less resilient to increased drought stress. Future work should examine inclusion of a growth variability term and sensitivity to that growth variability.

The C cost of hydraulic safety also represents a significant target for future study. The role of C dynamics in tree physiological response to stress has a rich literature (Mooney 1972, Körner 2003, Hoch et al. 2003, Sala et al. 2012, Aaltonen et al. 2016), but few studies have connected C dynamics, cellular physiology, and drought response at the stand level. Two novel questions arise from our observations of high hydraulic safety and lignification in dead trees: 1) are there significant trade-offs between hydraulic safety and reproduction under drought that can influence fitness of surviving trees? And 2) can these traits be mapped to allow a true scaling of hydraulic safety and drought resilience to the entire landscape?

In this dissertation I outline the potential mechanisms for a tradeoff between growth and reproduction, and between hydraulic safety and reproduction. However, I was unable to find sufficient evidence for or against this tradeoff in our sampled trees. Recent work demonstrating a lack of direct tradeoff between growth and reproduction in trees subjected to experimental drought shows instead that the relationship between growth and reproduction is altered, but not inverted, by drought. This shows that more work is needed to explore the relationships between reproduction and hydraulic safety in trees sampled here.

The observation of high lignification and hydraulic safety in dead trees provides an interesting target for applications to forest management. Mapping these physiological traits would provide valuable insights into total tree C content (as a function of lignin), as well as an ability to predict drought response at the forest population level. An interesting future direction for scaling of drought resilience traits is remote sensing of canopy chemistry and modeling of relationships between stem and canopy chemistry and physiology. On-going work is identifying hyperspectral bandwidths that can detect canopy water content (Asner et al. 2016) and canopy lignin content (Serrano et al. 2002). No work to date has scaled stem lignin and C to canopy traits using remote sensing, and this represents a potentially exciting application of my findings to landscape-scale forest drought planning.

6.3 Concluding Remarks

This dissertation constitutes an important contribution to the field of drought physiology and forest response to climate change. Our findings outline newly identified traits that confer drought resilience or susceptibility during a complex and extreme real-world drought. Interactions among pest stress, drought stress, tree physiology, and stand dynamics all influence forest drought resilience. The findings in this dissertation pave the way for new explorations of not only how trees survive drought, but what survival or mortality means in terms of reproductive capacity and C dynamics in a changing world.

6.4 References

Aaltonen, H., A. Lindén, J. Heinonsalo, C. Biasi, and J. Pumpanen. 2016. Effects of prolonged drought stress on Scots pine seedling carbon allocation. Tree Physiology:1–10.

Adams, H. D., M. J. B. Zeppel, W. R. L. Anderegg, H. Hartmann, S. M. Landhäusser, D. T. Tissue, T. E. Huxman, P. J. Hudson, T. E. Franz, C. D. Allen, L. D. L. Anderegg, G. A. Barron-Gafford, D. J. Beerling, D. D. Breshears, T. J. Brodribb, H. Bugmann, R. C. Cobb, A. D. Collins, L. T. Dickman, H. Duan, B. E. Ewers, L. Galiano, D. A. Galvez, N. Garcia-Forner, M. L. Gaylord, M. J. Germino, A. Gessler, U. G. Hacke, R. Hakamada, A. Hector, M. W. Jenkins, J. M. Kane, T. E. Kolb, D. J. Law, J. D. Lewis, J.-M. Limousin, D. M. Love, A. K. Macalady, J. Martínez-Vilalta, M. Mencuccini, P. J. Mitchell, J. D. Muss, M. J. O'Brien, A. P. O'Grady, R. E. Pangle, E. A. Pinkard, F. I. Piper, J. A. Plaut, W. T. Pockman, J. Quirk, K. Reinhardt, F. Ripullone, M. G. Ryan, A. Sala, S. Sevanto, J. S. Sperry, R. Vargas, M. Vennetier, D. A. Way, C. Xu, E. A. Yepez, and N. G. McDowell. 2017. A multi-species synthesis of physiological mechanisms in drought-induced tree mortality. Nature Ecology & Evolution 1:1285.

Allen, C. D., D. D. Breshears, and N. G. McDowell. 2015. On underestimation of global vulnerability to tree mortality and forest die-off from hotter drought in the Anthropocene. Ecosphere 6:art129.

Allen, C. D., A. K. Macalady, H. Chenchouni, D. Bachelet, N. McDowell, M. Vennetier, T. Kitzberger, A. Rigling, D. D. Breshears, E. H. (Ted) Hogg, P. Gonzalez, R. Fensham, Z. Zhang, J. Castro, N. Demidova, J.-H. Lim, G. Allard, S. W. Running, A. Semerci, and N. Cobb. 2010. A global overview of drought and heat-induced

tree mortality reveals emerging climate change risks for forests. Forest Ecology and Management 259:660–684.

Amthor, J. S. 2003. Efficiency of lignin biosynthesis: a quantitative analysis. Annals of Botany 91:673–695.

Anderegg, L. D. L., W. R. L. Anderegg, and J. A. Berry. 2013. Not all droughts are created equal: translating meteorological drought into woody plant mortality. Tree Physiology 33:672–683.

Asner, G. P., P. G. Brodrick, C. B. Anderson, N. Vaughn, D. E. Knapp, and R. E. Martin. 2016. Progressive forest canopy water loss during the 2012–2015 California drought. Proceedings of the National Academy of Sciences 113:E249–E255.

Cailleret, M., V. Dakos, S. Jansen, E. M. R. Robert, T. Aakala, M. M. Amoroso, J. A. Antos, C. Bigler, H. Bugmann, M. Caccianaga, J.-J. Camarero, P. Cherubini, M. R. Coyea, K. Čufar, A. J. Das, H. Davi, G. Gea-Izquierdo, S. Gillner, L. J. Haavik, H. Hartmann, A.-M. Hereş, K. R. Hultine, P. Janda, J. M. Kane, V. I. Kharuk, T. Kitzberger, T. Klein, T. Levanic, J.-C. Linares, F. Lombardi, H. Mäkinen, I. Mészáros, J. M. Metsaranta, W. Oberhuber, A. Papadopoulos, A. M. Petritan, B. Rohner, G. Sangüesa-Barreda, J. M. Smith, A. B. Stan, D. B. Stojanovic, M.-L. Suarez, M. Svoboda, V. Trotsiuk, R. Villalba, A. R. Westwood, P. H. Wyckoff, and J. Martínez-Vilalta. 2019. Early-Warning Signals of Individual Tree Mortality Based on Annual Radial Growth. Frontiers in Plant Science 9.

Cailleret, M., S. Jansen, E. M. R. Robert, L. Desoto, T. Aakala, J. A. Antos, B. Beikircher, C. Bigler, H. Bugmann, M. Caccianiga, V. Čada, J. J. Camarero, P. Cherubini, H. Cochard, M. R. Coyea, K. Čufar, A. J. Das, H. Davi, S. Delzon, M. Dorman, G. Gea-Izquierdo, S. Gillner, L. J. Haavik, H. Hartmann, A.-M. Hereş, K. R. Hultine, P. Janda, J. M. Kane, V. I. Kharuk, T. Kitzberger, T. Klein, K. Kramer, F. Lens, T. Levanic, J. C. L. Calderon, F. Lloret, R. Lobo-Do-Vale, F. Lombardi, R. L. Rodríguez, H. Mäkinen, S. Mayr, I. Mészáros, J. M. Metsaranta, F. Minunno, W. Oberhuber, A. Papadopoulos, M. Peltoniemi, A. M. Petritan, B. Rohner, G. Sangüesa-Barreda, D. Sarris, J. M. Smith, A. B. Stan, F. Sterck, D. B. Stojanović, M. L. Suarez, M. Svoboda, R. Tognetti, J. M. Torres-Ruiz, V. Trotsiuk, R. Villalba, F. Vodde, A. R. Westwood, P. H. Wyckoff, N. Zafirov, and J. Martínez-Vilalta. 2017. A synthesis of radial growth patterns preceding tree mortality. Global Change Biology 23:1675–1690.

Charney, N. D., F. Babst, B. Poulter, S. Record, V. M. Trouet, D. Frank, B. J. Enquist, and M. E. K. Evans. 2016. Observed forest sensitivity to climate implies large changes in 21st century North American forest growth. Ecology Letters 19:1119–1128.

Cook, E. R., R. Seager, R. R. Heim, R. S. Vose, C. Herweijer, and C. Woodhouse. 2010. Megadroughts in North America: placing IPCC projections of hydroclimatic change in a long-term palaeoclimate context. Journal of Quaternary Science 25:48–61.

Das, A. J., J. J. Battles, N. L. Stephenson, and P. J. van Mantgem. 2007. The relationship between tree growth patterns and likelihood of mortality: a study of two tree species in the Sierra Nevada. Canadian Journal of Forest Research 37:580–597.

Hacke, U. G., J. S. Sperry, W. T. Pockman, S. D. Davis, and K. A. McCulloh. 2001. Trends in wood density and structure are linked to prevention of xylem implosion by negative pressure. Oecologia 126:457–461.

Hoch, G., A. Richter, and Ch. Körner. 2003. Non-structural carbon compounds in temperate forest trees. Plant, Cell & Environment 26:1067–1081.

IPCC. 2014. Climate Change 2014: Impacts,Adaptation, and Vulnerability. Part A: Global and Sectoral Aspects. Contribution of Working Group II to the Fifth Assessment Report of the Intergovernmental Panel on Climate Change. Page 1132. Cambridge University Press, Cambridge, UK and New York, USA.

Körner, C. 2003. Carbon limitation in trees. Journal of Ecology 91:4–17.

Lauder, J. D., E. V. Moran, and S. C. Hart. 2019. Fight or Flight? Potential tradeoffs between drought defense and reproduction in conifers. Tree Physiology 39:1071–1085.

McDowell, N. G. 2011. Mechanisms linking drought, hydraulics, carbon metabolism, and vegetation mortality. Plant Physiology 155:1051–1059.

McDowell, N., W. T. Pockman, C. D. Allen, D. D. Breshears, N. Cobb, T. Kolb, J. Plaut, J. Sperry, A. West, D. G. Williams, and E. A. Yepez. 2008. Mechanisms of plant survival and mortality during drought: why do some plants survive while others succumb to drought? New Phytologist 178:719–739.

Mooney, H. A. 1972. The Carbon Balance of Plants. Annual Review of Ecology and Systematics 3:315–346.

Moran, E., J. Lauder, C. Musser, A. Stathos, and M. Shu. 2017. The genetics of drought tolerance in conifers. New Phytologist:n/a-n/a.

Ogle, K., T. G. Whitham, and N. S. Cobb. 2000. Tree-Ring Variation in Pinyon Predicts Likelihood of Death following Severe Drought. Ecology 81:3237.

Pittermann, J., J. S. Sperry, U. G. Hacke, J. K. Wheeler, and E. H. Sikkema. 2006a. Inter-tracheid pitting and the hydraulic efficiency of conifer wood: the role of tracheid allometry and cavitation protection. American Journal of Botany 93:1265–1273.

Pittermann, J., J. S. Sperry, J. K. Wheeler, U. G. Hacke, and E. H. Sikkema. 2006b. Mechanical reinforcement of tracheids compromises the hydraulic efficiency of conifer xylem. Plant, Cell & Environment 29:1618–1628.

Sala, A., D. R. Woodruff, and F. C. Meinzer. 2012. Carbon dynamics in trees: feast or famine? Tree Physiology 32:764–775.

Serrano, L., J. Peñuelas, and S. L. Ustin. 2002. Remote sensing of nitrogen and lignin in Mediterranean vegetation from AVIRIS data: Decomposing biochemical from structural signals. Remote Sensing of Environment 81:355–364.

Sperry, J. S. 2003. Evolution of water transport and xylem structure. International Journal of Plant Sciences 164:s115–s127.

Sperry, J. S., U. G. Hacke, and J. Pittermann. 2006. Size and function in conifer tracheids and angiosperm vessels. American Journal of Botany 93:1490–1500.

Appendix A. ImageJ **s**cript for automatically batch analyzing images for total lignin via stain quantification.

Change “\\YourPathHere\\” to the path location of all of your photos to be analyzed.

```
//Script for analyzing Red Stain Intensity

//Note that ImageJ scripting language uses “//” for comments, and “\\” instead of “\” in all

//path names

//To Use: Open ImageJ, Plugins -> Macros -> Record

//Copy and paste this entire script into the blank field

//Save as whatever you want to call it to your ImageJ/Macros/ directory

//Must be saved as .ijm file

//Then to run, close ImageJ, reopen, Plugins -> Macros -> Run

//Select saved macro

run("Input/Output...", "jpeg=85 gif=-1 file=.csv use_file copy_row save_column");


//Set image path to folder with all processed images

PATH = "C:\\YourPathHere\\";

list = getFileList(PATH);


//Set measurements to default measures plus integrated density

run("Set Measurements...", "area mean standard min integrated stack display

redirect=None decimal=3");
```

```
//Open background correction image
open("C:\\YourPathHere\\BackgroundImage");


//Loop for all images -> open, split color channels, delete blue and green channel, run
//background correction draw area, run measure, close
for (i=0; i<list.length; i++) {
        setTool(3);  // Choose freehand tool
        open(PATH+list[i]); // Open next image in folder
        run("Split Channels"); // Split color channels
        selectWindow(list[i]+" (blue)"); // Close blue
        run("Close");
        selectWindow(list[i]+" (green)"); // Close green
        run("Close");
        selectWindow(list[i]+" (red)"); //Select Red
        //imageId = getImageId()
        //run("Calculator Plus", "i1=[imageId] i2=[ref 3 SR1705.jpg] operation=[Scale: i2
                = i1 x k1 + k2], k1=1, k2=0, create"); //Perform background correction
        //selectWindow(list[i]+" (red)");
        //run("Close");
        //selectWindow("Result"); //Select background correction result
                waitForUser("Draw a polygon around your chosen analysis area.");
                //Prompt for measurement area
        getSelectionCoordinates(xpoints,ypoints);
```

```
makeSelection("freehand",xpoints,ypoints);
run("Measure"); //Conduct measurements
selectWindow(list[i]+" (red)");
run("Close"); //Close window before opening next image
}
```

//Export results: select measurement results table (will be open in background). Select all and //copy and paste into a.csv file or preferred spreadsheet. Note that this code can easily be //modified to add an “export results function” as the user sees fit. Simply place the export //function after the final closing “}” bracket.

Appendix B. All estimated model parameters from models of mortality likelihood (Chapter 5). All models were the same; "Model" represents primary drought metric, which is the only predictor that changed between models. $\widehat{R}$ = indicator of model convergence, with values <1.02 indicating convergence of all model chains.

Predictor	Estimate	Est.Error	l-95% CI	u-95% CI	$\widehat{R}$	Model
Intercept	0.55	4.50	-8.70	9.30	1.00	PET
RWI	0.28	1.77	-3.19	3.78	1.00	PET
PmET	-1.52	3.10	-8.54	3.80	1.00	PET
mHSF	-1.22	2.07	-5.43	2.86	1.00	PET
gini	0.63	0.37	-0.08	1.39	1.00	PET
HSFgini	0.13	0.37	-0.59	0.85	1.00	PET
mTMN	1.39	2.27	-2.21	6.72	1.00	PET
cindex	-0.23	0.08	-0.40	-0.09	1.00	PET
RWI1	-0.36	3.12	-6.87	5.79	1.00	PET
PmET1	-1.53	3.10	-8.73	3.88	1.00	PET
mHSF1	-0.74	3.38	-8.12	5.64	1.00	PET
RWIPET	-2.47	1.77	-6.25	0.71	1.00	PET
mHSFPET	-0.68	1.61	-3.93	2.43	1.00	PET
LastDBH	-0.69	0.42	-1.58	0.07	1.00	PET
RWI:PmET	-1.32	2.80	-7.56	3.70	1.00	PET
RWI:mHSF	0.00	1.63	-3.45	3.12	1.00	PET
PmET:mHSF	-1.08	2.51	-6.43	3.67	1.00	PET
RWI:PmET:mHSF	0.35	2.82	-5.07	6.16	1.00	PET
sd(Intercept)	5.01	4.48	0.15	16.60	1.00	PET
sd(RWI)	3.05	3.25	0.09	11.70	1.00	PET
sd(PmET)	6.69	5.90	0.25	21.62	1.00	PET
sd(mHSF)	3.24	3.27	0.10	12.01	1.00	PET
sd(mTMN)	5.51	4.43	0.27	16.51	1.00	PET
sd(RWI1)	4.29	4.01	0.13	14.61	1.00	PET
sd(PmET1)	6.65	5.97	0.27	21.88	1.00	PET
sd(mHSF1)	5.31	5.10	0.20	18.64	1.00	PET
sd(RWI:PmET)	4.91	4.55	0.16	16.70	1.00	PET
sd(RWI:mHSF)	2.92	3.33	0.07	12.06	1.00	PET
sd(PmET:mHSF)	5.70	4.65	0.20	17.25	1.00	PET
sd(RWI:PmET:mHSF)	5.18	4.92	0.16	17.96	1.00	PET
Intercept1	1.62	4.40	-7.10	10.42	1.00	PDSI
RWI2	0.59	2.09	-3.93	4.49	1.00	PDSI
PDSI	1.60	3.65	-4.35	10.22	1.00	PDSI
mHSF2	-1.27	1.98	-5.41	2.54	1.00	PDSI
gini1	0.79	0.51	-0.19	1.86	1.00	PDSI
HSFgini1	0.26	0.45	-0.63	1.17	1.00	PDSI
mTMN1	4.17	4.08	-2.38	13.37	1.00	PDSI
cindex1	-0.17	0.10	-0.38	-0.01	1.00	PDSI
RWI11	-0.42	3.41	-7.53	6.29	1.00	PDSI
PDSI1	1.64	3.63	-4.25	10.44	1.00	PDSI
mHSF11	-0.78	3.27	-7.90	5.16	1.00	PDSI
RWIPDSI	-2.75	2.29	-7.75	1.24	1.00	PDSI

Predictor	Estimate	Est.Error	l-95% CI	u-95% CI	Rhat	Mod
mHSFPDSI	-1.63	1.92	-5.70	1.86	1.00	PDSI
LastDBH1	-0.39	0.49	-1.42	0.51	1.00	PDSI
RWI:PDSI	0.36	2.47	-4.67	5.23	1.00	PDSI
RWI:mHSF1	0.67	1.70	-2.82	4.06	1.00	PDSI
PDSI:mHSF	-0.43	2.21	-5.07	3.83	1.00	PDSI
RWI:PDSI:mHSF	0.11	2.95	-5.64	6.28	1.00	PDSI
sd(Intercept)1	4.44	4.26	0.14	15.60	1.00	PDSI
sd(RWI)1	3.90	3.76	0.15	13.83	1.00	PDSI
sd(PDSI)	12.76	9.73	0.54	36.12	1.00	PDSI
sd(mHSF)1	3.17	3.40	0.09	12.59	1.00	PDSI
sd(mTMN)1	9.01	5.97	0.79	23.31	1.00	PDSI
sd(RWI1)1	4.58	4.35	0.16	16.26	1.00	PDSI
sd(PDSI1)	12.98	11.87	0.61	36.42	1.00	PDSI
sd(mHSF1)1	5.05	4.84	0.18	17.73	1.00	PDSI
sd(RWI:PDSI)	5.90	5.13	0.25	18.95	1.00	PDSI
sd(RWI:mHSF)1	3.06	3.40	0.09	12.38	1.00	PDSI
sd(PDSI:mHSF)	4.00	3.61	0.13	13.26	1.00	PDSI
sd(RWI:PDSI:mHSF)	12.57	8.32	1.69	33.00	1.00	PDSI
Intercept2	1.76	4.64	-7.76	10.86	1.00	CMD
RWI3	0.42	1.99	-3.46	4.54	1.00	CMD
CMD	-0.57	2.72	-6.41	4.53	1.00	CMD
mHSF3	-1.56	2.33	-6.56	2.88	1.00	CMD
gini2	0.50	0.42	-0.32	1.34	1.00	CMD
HSFgini2	0.12	0.38	-0.64	0.85	1.00	CMD
mTMN2	1.27	2.75	-3.57	7.48	1.00	CMD
cindex2	-0.18	0.08	-0.36	-0.03	1.00	CMD
RWI12	-0.50	3.37	-7.72	6.04	1.00	CMD
CMD1	-0.52	2.75	-6.35	4.72	1.00	CMD
mHSF12	-0.97	3.60	-8.99	5.35	1.00	CMD
RWICMD	0.62	1.63	-2.51	3.94	1.00	CMD
mHSFCMD	1.44	1.60	-1.58	4.74	1.00	CMD
LastDBH2	-0.55	0.46	-1.51	0.29	1.00	CMD
RWI:CMD	0.25	1.86	-3.74	3.79	1.00	CMD
RWI:mHSF2	-0.32	1.62	-3.80	2.83	1.00	CMD
CMD:mHSF	0.47	1.44	-2.53	3.34	1.00	CMD
RWI:CMD:mHSF	-1.18	1.77	-4.69	2.40	1.00	CMD
sd(Intercept)2	5.41	4.80	0.21	17.41	1.00	CMD
sd(RWI)2	3.99	3.75	0.18	13.73	1.00	CMD
sd(CMD)	6.39	5.09	0.28	19.19	1.00	CMD
sd(mHSF)2	5.13	4.70	0.17	17.36	1.00	CMD
sd(mTMN)2	12.04	6.54	2.84	28.41	1.00	CMD
sd(RWI1)2	5.10	4.73	0.18	17.29	1.00	CMD
sd(CMD1)	6.38	5.17	0.27	19.06	1.00	CMD
sd(mHSF1)2	6.34	5.77	0.24	21.14	1.00	CMD

Predictor	Estimate	Est.Error	l-95% CI	u-95% CI	Rhat	Mod
sd(RWI:CMD)	4.05	4.25	0.13	15.08	1.00	CMD
sd(RWI:mHSF)2	3.08	3.40	0.09	12.15	1.00	CMD
sd(CMD:mHSF)	2.32	2.28	0.07	8.49	1.00	CMD
sd(RWI:CMD:mHSF)	3.31	3.61	0.09	12.94	1.00	CMD
Intercept3	1.56	4.32	-7.06	10.09	1.00	CWD
RWI4	0.56	1.96	-3.50	4.35	1.00	CWD
tCWD	-1.81	3.64	-9.53	3.88	1.00	CWD
mHSF4	-0.85	1.98	-4.84	3.08	1.00	CWD
gini3	0.68	0.37	-0.03	1.42	1.00	CWD
HSFgini3	0.20	0.36	-0.53	0.90	1.00	CWD
mTMN3	1.30	2.25	-2.82	6.21	1.00	CWD
cindex3	-0.22	0.08	-0.39	-0.07	1.00	CWD
RWI13	-0.47	3.18	-7.25	5.54	1.00	CWD
tCWD1	-1.75	3.32	-9.32	3.95	1.00	CWD
mHSF13	-0.58	3.26	-7.55	5.68	1.00	CWD
RWICWD	0.85	1.35	-1.72	3.58	1.00	CWD
mHSFCWD	-0.96	1.71	-4.49	2.32	1.00	CWD
LastDBH3	-0.85	0.47	-1.81	-0.01	1.00	CWD
RWI:tCWD	1.06	2.12	-3.11	5.35	1.00	CWD
RWI:mHSF3	-0.08	1.62	-3.15	3.59	1.00	CWD
tCWD:mHSF	0.57	1.88	-3.05	4.48	1.00	CWD
RWI:tCWD:mHSF	-1.74	2.40	-6.86	2.64	1.00	CWD
sd(Intercept)3	5.09	4.76	0.16	17.56	1.00	CWD
sd(RWI)3	3.88	3.92	0.13	14.01	1.00	CWD
sd(tCWD)	8.50	7.44	0.33	27.48	1.00	CWD
sd(mHSF)3	3.51	3.71	0.09	13.73	1.00	CWD
sd(mTMN)3	6.57	5.58	0.26	20.64	1.00	CWD
sd(RWI1)3	5.00	4.79	0.17	17.58	1.00	CWD
sd(tCWD1)	8.67	7.65	0.36	28.10	1.00	CWD
sd(mHSF1)3	5.16	4.95	0.16	17.95	1.00	CWD
sd(RWI:tCWD)	4.00	3.80	0.14	14.30	1.00	CWD
sd(RWI:mHSF)3	3.19	3.67	0.08	13.12	1.00	CWD
sd(tCWD:mHSF)	2.96	2.75	0.11	10.25	1.00	CWD
sd(RWI:tCWD:mHSF)	4.52	4.15	0.14	15.10	1.00	CWD
Intercept4	1.86	4.48	-7.01	10.99	1.00	DEF
RWI5	0.55	2.06	-3.68	4.66	1.00	DEF
DEF	-1.78	2.87	-8.18	3.13	1.00	DEF
mHSF5	-1.28	2.07	-5.46	2.88	1.00	DEF
gini4	0.76	0.41	-0.01	1.58	1.00	DEF
HSFgini4	0.07	0.38	-0.70	0.81	1.00	DEF
mTMN4	1.31	2.05	-2.46	5.77	1.00	DEF
cindex4	-0.27	0.09	-0.45	-0.12	1.00	DEF
RWI14	-0.66	3.34	-7.88	5.63	1.00	DEF
DEF1	-1.78	2.84	-8.10	3.12	1.00	DEF

Predictor	Estimate	Est.Error	l-95% CI	u-95% CI	Rhat	Mod
mHSF14	-0.81	3.45	-8.44	5.49	1.00	DEF
RWIDEF	0.49	1.54	-2.49	3.62	1.00	DEF
mHSFDEF	2.08	1.82	-1.27	5.95	1.00	DEF
LastDBH4	-1.07	0.50	-2.13	-0.19	1.00	DEF
RWI:DEF	1.28	1.86	-2.55	4.95	1.00	DEF
RWI:mHSF4	0.24	1.47	-2.76	3.38	1.00	DEF
DEF:mHSF	-0.07	1.61	-3.23	3.21	1.00	DEF
RWI:DEF:mHSF	-0.78	1.66	-4.23	2.44	1.00	DEF
sd(Intercept)4	5.17	4.63	0.19	17.26	1.00	DEF
sd(RWI)4	4.17	3.68	0.18	13.78	1.00	DEF
sd(DEF)	3.88	3.70	0.11	13.57	1.00	DEF
sd(mHSF)4	4.08	3.95	0.12	14.55	1.00	DEF
sd(mTMN)4	5.40	4.77	0.18	17.70	1.00	DEF
sd(RWI1)4	4.74	4.37	0.16	15.88	1.00	DEF
sd(DEF1)	3.86	3.65	0.13	13.37	1.00	DEF
sd(mHSF1)4	5.23	4.81	0.17	17.80	1.00	DEF
sd(RWI:DEF)	3.57	3.40	0.12	12.52	1.00	DEF
sd(RWI:mHSF)4	2.71	3.06	0.07	10.82	1.00	DEF
sd(DEF:mHSF)	2.72	2.52	0.09	9.37	1.00	DEF
sd(RWI:DEF:mHSF)	2.96	3.16	0.07	11.35	1.00	DEF